

NCHRP

REPORT 556

**NATIONAL
COOPERATIVE
HIGHWAY
RESEARCH
PROGRAM**

Design and Construction Guidelines for Geosynthetic- Reinforced Soil Bridge Abutments with a Flexible Facing

TRANSPORTATION RESEARCH BOARD
OF THE NATIONAL ACADEMIES

TRANSPORTATION RESEARCH BOARD EXECUTIVE COMMITTEE 2006 (Membership as of November 2005)

OFFICERS

Chair: *John R. Njord, Executive Director, Utah DOT*

Vice Chair: *Michael D. Meyer, Professor, School of Civil and Environmental Engineering, Georgia Institute of Technology*

Executive Director: *Robert E. Skinner, Jr., Transportation Research Board*

MEMBERS

MICHAEL W. BEHRENS, *Executive Director, Texas DOT*

ALLEN D. BIEHLER, *Secretary, Pennsylvania DOT*

LARRY L. BROWN, SR., *Executive Director, Mississippi DOT*

DEBORAH H. BUTLER, *Vice President, Customer Service, Norfolk Southern Corporation and Subsidiaries, Atlanta, GA*

ANNE P. CANBY, *President, Surface Transportation Policy Project, Washington, DC*

JOHN L. CRAIG, *Director, Nebraska Department of Roads*

DOUGLAS G. DUNCAN, *President and CEO, FedEx Freight, Memphis, TN*

NICHOLAS J. GARBER, *Professor of Civil Engineering, University of Virginia*

ANGELA GITTENS, *Vice President, Airport Business Services, HNTB Corporation, Miami, FL*

GENEVIEVE GIULIANO, *Director, Metrans Transportation Center, and Professor, School of Policy, Planning, and Development, USC, Los Angeles*

BERNARD S. GROSECLOSE, JR., *President and CEO, South Carolina State Ports Authority*

SUSAN HANSON, *Landry University Professor of Geography, Graduate School of Geography, Clark University*

JAMES R. HERTWIG, *President, CSX Intermodal, Jacksonville, FL*

GLORIA JEAN JEFF, *Director, Michigan DOT*

ADIB K. KANAFANI, *Cahill Professor of Civil Engineering, University of California, Berkeley*

HERBERT S. LEVINSON, *Principal, Herbert S. Levinson Transportation Consultant, New Haven, CT*

SUE MCNEIL, *Professor, Department of Civil and Environmental Engineering, University of Delaware*

MICHAEL R. MORRIS, *Director of Transportation, North Central Texas Council of Governments*

CAROL A. MURRAY, *Commissioner, New Hampshire DOT*

MICHAEL S. TOWNES, *President and CEO, Hampton Roads Transit, Hampton, VA*

C. MICHAEL WALTON, *Ernest H. Cockrell Centennial Chair in Engineering, University of Texas, Austin*

LINDA S. WATSON, *Executive Director, LYNX—Central Florida Regional Transportation Authority*

MARION C. BLAKEY, *Federal Aviation Administrator, U.S.DOT (ex officio)*

JOSEPH H. BOARDMAN, *Federal Railroad Administrator, U.S.DOT (ex officio)*

REBECCA M. BREWSTER, *President and COO, American Transportation Research Institute, Smyrna, GA (ex officio)*

GEORGE BUGLIARELLO, *Chancellor, Polytechnic University, and Foreign Secretary, National Academy of Engineering (ex officio)*

J. RICHARD CAPKA, *Acting Administrator, Federal Highway Administration, U.S.DOT (ex officio)*

THOMAS H. COLLINS (Adm., U.S. Coast Guard), *Commandant, U.S. Coast Guard (ex officio)*

JAMES J. EBERHARDT, *Chief Scientist, Office of FreedomCAR and Vehicle Technologies, U.S. Department of Energy (ex officio)*

JACQUELINE GLASSMAN, *Deputy Administrator, National Highway Traffic Safety Administration, U.S.DOT (ex officio)*

EDWARD R. HAMBERGER, *President and CEO, Association of American Railroads (ex officio)*

DAVID B. HORNER, *Acting Deputy Administrator, Federal Transit Administration, U.S.DOT (ex officio)*

JOHN C. HORSLEY, *Executive Director, American Association of State Highway and Transportation Officials (ex officio)*

JOHN E. JAMIAN, *Acting Administrator, Maritime Administration, U.S.DOT (ex officio)*

EDWARD JOHNSON, *Director, Applied Science Directorate, National Aeronautics and Space Administration (ex officio)*

ASHOK G. KAVEESHWAR, *Research and Innovative Technology Administrator, U.S.DOT (ex officio)*

BRIGHAM MCCOWN, *Deputy Administrator, Pipeline and Hazardous Materials Safety Administration, U.S.DOT (ex officio)*

WILLIAM W. MILLAR, *President, American Public Transportation Association (ex officio)*

SUZANNE RUDZINSKI, *Director, Transportation and Regional Programs, U.S. Environmental Protection Agency (ex officio)*

ANNETTE M. SANDBERG, *Federal Motor Carrier Safety Administrator, U.S.DOT (ex officio)*

JEFFREY N. SHANE, *Under Secretary for Policy, U.S.DOT (ex officio)*

CARL A. STROCK (Maj. Gen., U.S. Army), *Chief of Engineers and Commanding General, U.S. Army Corps of Engineers (ex officio)*

NATIONAL COOPERATIVE HIGHWAY RESEARCH PROGRAM

Transportation Research Board Executive Committee Subcommittee for NCHRP

JOHN R. NJORD, *Utah DOT (Chair)*

J. RICHARD CAPKA, *Federal Highway Administration*

JOHN C. HORSLEY, *American Association of State Highway
and Transportation Officials*

MICHAEL D. MEYER, *Georgia Institute of Technology*

ROBERT E. SKINNER, JR., *Transportation Research Board*

MICHAEL S. TOWNES, *Hampton Roads Transit, Hampton, VA*

C. MICHAEL WALTON, *University of Texas, Austin*

NATIONAL COOPERATIVE HIGHWAY RESEARCH PROGRAM

NCHRP REPORT 556

**Design and Construction Guidelines
for Geosynthetic-Reinforced Soil Bridge
Abutments with a Flexible Facing**

JONATHAN T. H. WU

KEVIN Z. Z. LEE

SAM B. HELWANY

KANOP KETCHART

University of Colorado at Denver
Denver, CO

SUBJECT AREAS

Highway and Facility Design • Bridges, Other Structures, and Hydraulics and Hydrology • Soils, Geology, and Foundations

Research Sponsored by the American Association of State Highway and Transportation Officials
in Cooperation with the Federal Highway Administration

TRANSPORTATION RESEARCH BOARD

WASHINGTON, D.C.

2006

www.TRB.org

NATIONAL COOPERATIVE HIGHWAY RESEARCH PROGRAM

Systematic, well-designed research provides the most effective approach to the solution of many problems facing highway administrators and engineers. Often, highway problems are of local interest and can best be studied by highway departments individually or in cooperation with their state universities and others. However, the accelerating growth of highway transportation develops increasingly complex problems of wide interest to highway authorities. These problems are best studied through a coordinated program of cooperative research.

In recognition of these needs, the highway administrators of the American Association of State Highway and Transportation Officials initiated in 1962 an objective national highway research program employing modern scientific techniques. This program is supported on a continuing basis by funds from participating member states of the Association and it receives the full cooperation and support of the Federal Highway Administration, United States Department of Transportation.

The Transportation Research Board of the National Academies was requested by the Association to administer the research program because of the Board's recognized objectivity and understanding of modern research practices. The Board is uniquely suited for this purpose as it maintains an extensive committee structure from which authorities on any highway transportation subject may be drawn; it possesses avenues of communications and cooperation with federal, state and local governmental agencies, universities, and industry; its relationship to the National Research Council is an insurance of objectivity; it maintains a full-time research correlation staff of specialists in highway transportation matters to bring the findings of research directly to those who are in a position to use them.

The program is developed on the basis of research needs identified by chief administrators of the highway and transportation departments and by committees of AASHTO. Each year, specific areas of research needs to be included in the program are proposed to the National Research Council and the Board by the American Association of State Highway and Transportation Officials. Research projects to fulfill these needs are defined by the Board, and qualified research agencies are selected from those that have submitted proposals. Administration and surveillance of research contracts are the responsibilities of the National Research Council and the Transportation Research Board.

The needs for highway research are many, and the National Cooperative Highway Research Program can make significant contributions to the solution of highway transportation problems of mutual concern to many responsible groups. The program, however, is intended to complement rather than to substitute for or duplicate other highway research programs.

NOTE: The Transportation Research Board of the National Academies, the National Research Council, the Federal Highway Administration, the American Association of State Highway and Transportation Officials, and the individual states participating in the National Cooperative Highway Research Program do not endorse products or manufacturers. Trade or manufacturers' names appear herein solely because they are considered essential to the object of this report.

NCHRP REPORT 556

Price \$25.00

Project 12-59

ISSN 0077-5614

ISBN 0-309-09845-9

Library of Congress Control Number 2006921471

© 2006 Transportation Research Board

COPYRIGHT PERMISSION

Authors herein are responsible for the authenticity of their materials and for obtaining written permissions from publishers or persons who own the copyright to any previously published or copyrighted material used herein.

Cooperative Research Programs (CRP) grants permission to reproduce material in this publication for classroom and not-for-profit purposes. Permission is given with the understanding that none of the material will be used to imply TRB, AASHTO, FAA, FHWA, FMCSA, FTA, or Transit Development Corporation endorsement of a particular product, method, or practice. It is expected that those reproducing the material in this document for educational and not-for-profit uses will give appropriate acknowledgment of the source of any reprinted or reproduced material. For other uses of the material, request permission from CRP.

NOTICE

The project that is the subject of this report was a part of the National Cooperative Highway Research Program conducted by the Transportation Research Board with the approval of the Governing Board of the National Research Council. Such approval reflects the Governing Board's judgment that the program concerned is of national importance and appropriate with respect to both the purposes and resources of the National Research Council.

The members of the technical committee selected to monitor this project and to review this report were chosen for recognized scholarly competence and with due consideration for the balance of disciplines appropriate to the project. The opinions and conclusions expressed or implied are those of the research agency that performed the research, and, while they have been accepted as appropriate by the technical committee, they are not necessarily those of the Transportation Research Board, the National Research Council, the American Association of State Highway and Transportation Officials, or the Federal Highway Administration, U.S. Department of Transportation.

Each report is reviewed and accepted for publication by the technical committee according to procedures established and monitored by the Transportation Research Board Executive Committee and the Governing Board of the National Research Council.

Published reports of the

NATIONAL COOPERATIVE HIGHWAY RESEARCH PROGRAM

are available from:

Transportation Research Board
Business Office
500 Fifth Street, NW
Washington, DC 20001

and can be ordered through the Internet at:
<http://www.national-academies.org/trb/bookstore>

Printed in the United States of America

THE NATIONAL ACADEMIES

Advisers to the Nation on Science, Engineering, and Medicine

The **National Academy of Sciences** is a private, nonprofit, self-perpetuating society of distinguished scholars engaged in scientific and engineering research, dedicated to the furtherance of science and technology and to their use for the general welfare. On the authority of the charter granted to it by the Congress in 1863, the Academy has a mandate that requires it to advise the federal government on scientific and technical matters. Dr. Ralph J. Cicerone is president of the National Academy of Sciences.

The **National Academy of Engineering** was established in 1964, under the charter of the National Academy of Sciences, as a parallel organization of outstanding engineers. It is autonomous in its administration and in the selection of its members, sharing with the National Academy of Sciences the responsibility for advising the federal government. The National Academy of Engineering also sponsors engineering programs aimed at meeting national needs, encourages education and research, and recognizes the superior achievements of engineers. Dr. William A. Wulf is president of the National Academy of Engineering.

The **Institute of Medicine** was established in 1970 by the National Academy of Sciences to secure the services of eminent members of appropriate professions in the examination of policy matters pertaining to the health of the public. The Institute acts under the responsibility given to the National Academy of Sciences by its congressional charter to be an adviser to the federal government and, on its own initiative, to identify issues of medical care, research, and education. Dr. Harvey V. Fineberg is president of the Institute of Medicine.

The **National Research Council** was organized by the National Academy of Sciences in 1916 to associate the broad community of science and technology with the Academy's purposes of furthering knowledge and advising the federal government. Functioning in accordance with general policies determined by the Academy, the Council has become the principal operating agency of both the National Academy of Sciences and the National Academy of Engineering in providing services to the government, the public, and the scientific and engineering communities. The Council is administered jointly by both the Academies and the Institute of Medicine. Dr. Ralph J. Cicerone and Dr. William A. Wulf are chair and vice chair, respectively, of the National Research Council.

The **Transportation Research Board** is a division of the National Research Council, which serves the National Academy of Sciences and the National Academy of Engineering. The Board's mission is to promote innovation and progress in transportation through research. In an objective and interdisciplinary setting, the Board facilitates the sharing of information on transportation practice and policy by researchers and practitioners; stimulates research and offers research management services that promote technical excellence; provides expert advice on transportation policy and programs; and disseminates research results broadly and encourages their implementation. The Board's varied activities annually engage more than 5,000 engineers, scientists, and other transportation researchers and practitioners from the public and private sectors and academia, all of whom contribute their expertise in the public interest. The program is supported by state transportation departments, federal agencies including the component administrations of the U.S. Department of Transportation, and other organizations and individuals interested in the development of transportation. www.TRB.org

www.national-academies.org

COOPERATIVE RESEARCH PROGRAMS STAFF FOR NCHRP REPORT 556

ROBERT J. REILLY, *Director, Cooperative Research Programs*
CRAWFORD F. JENCKS, *Manager, NCHRP*
TIMOTHY G. HESS, *Senior Program Officer*
EILEEN P. DELANEY, *Director of Publications*
HILARY FREER, *Senior Editor*
ELLEN CHAFEE, *Assistant Editor*

NCHRP PROJECT 12-59 PANEL Field of Design—Area of Bridges

ROBERT K. BARRETT, *Yenter Companies, Grand Junction, CO (Chair)*
NASER ABU-HEJLEH, *Colorado DOT*
TIMOTHY ADAMS, *South Carolina DOT*
BRUCE E. BRUNETTE, *Alaska DOT*
JERRY A. DIMAGGIO, *Federal Highway Administration*
JAMES B. HIGBEE, *Utah DOT*
GORDON KELLER, *USDA Forest Service*
LAURA KRUSINSKI, *Maine DOT*
JAWDAT SIDDIQI, *Ohio DOT*
MICHAEL ADAMS, *FHWA Liaison*
G.P. JAYAPRAKASH, *TRB Liaison*

FOREWORD

*By Timothy G. Hess
Staff Officer
Transportation Research
Board*

This report presents the findings of research undertaken to develop a rational design method and construction guidelines for using geosynthetic-reinforced soil (GRS) systems in bridge abutments. This report will be of immediate interest to professionals responsible for designing and constructing GRS structures.

The use of geosynthetic-reinforced soil (GRS) systems as the foundation for or as integral structural components of bridge abutments and piers is receiving increased attention and interest. The soil mass of GRS systems is reinforced in layers with a polymeric geosynthetic (e.g., geogrids or geotextiles), and the layered reinforcement is attached to facing elements that constitute the outer wall. Because the facing elements are commonly composed of articulated units that are not rigidly attached to each other, the wall is deemed flexible. Various materials, including natural rock, concrete block, gabion, or timber, may be used for the flexible facing. GRS structures are more forgiving to differential foundation settlement thus minimizing the bump that commonly develops between the roadway and bridge. GRS structures are more adaptable to low-quality backfill, easier to construct, and more economical than their conventional counterparts. GRS structures can be put into service quickly, can be built by maintenance personnel, and are especially well suited to projects constructed in areas that are difficult to access with heavy equipment. GRS structures are an economical alternative for temporary structures, because of their easy demolition and the recyclable nature of their components, and for emergency work, because of reduced lead time and lower equipment requirements.

Full-scale tests conducted by the FHWA and by the Colorado DOT on GRS bridge abutments and piers with segmental modular block facing have demonstrated excellent performance characteristics and very high load-carrying capacity. Even with the significant advantages of GRS systems, the use of GRS structures in routine highway bridge construction has not been widely adopted. The primary obstacles to adoption of GRS systems in bridge construction are threefold. The first obstacle is the lack of a rational and reliable design method for such bridge-supporting structures. For example, although the vertical spacing of the reinforcement has been found to affect the performance of the structure, current design methods fail to reflect this important fact. Also, field-measured strains are known to be drastically smaller than those predicted by current design methods. Clearly, the current design methods are not sufficient. The second obstacle is the lack of well-developed guidelines and specifications for constructing the structures. Such guidelines and specifications are critical to the successful application of this technology. The third obstacle is the perception that polymeric geosynthetics may not be strong enough to meet the high service loads expected during the design life of large bridge structures.

Under NCHRP Project 12-59, "Design and Construction of Segmental Geosynthetic-Reinforced Soil (GRS) Bridge Abutments for Bridge Support," the University of

Colorado at Denver developed a rational design method and construction guidelines for GRS bridge abutments and approaches with flexible facing elements. After an extensive literature review, the researchers conducted full-scale experiments and a thorough analytical study. Based on the research results, a rational design method and construction guidelines were developed and design examples illustrating the design computation procedure were conducted and documented.

NCHRP Report 556 consists of the project final report and two appendixes. A third appendix, "Verification of DYNA3D/LS-DYNA" is not included in this report, but is available as *NCHRP Web-Only Document 81* and can be found at <http://www4.trb.org/trb/crp.nsf>.

CONTENTS

1	SUMMARY
8	CHAPTER 1 Introduction and Research Approach Problem Statement, 8 Research Objective, 9 Research Approach, 10
11	CHAPTER 2 Findings Findings from Literature Study, 11 The NCHRP Full-Scale Experiments, 25 Findings from the Analytical Study, 41
96	CHAPTER 3 Interpretation, Appraisal, and Applications Assessment of the NCHRP Test Abutments, 96 Limitations of the Design and Construction Guidelines, 98 Recommended Design Method, 98 Recommended Construction Guidelines, 111 Design Examples, 115
129	CHAPTER 4 Conclusions and Suggested Research Conclusions, 129 Suggested Research, 130
131	REFERENCES
A-1	APPENDIX A Review of Construction Guidelines for GRS Walls
B-1	APPENDIX B A Brief Description of DYNA3D and LS-DYNA
C-1	APPENDIX C Verification of DYNA3D/LS-DYNA—See <i>NCHRP Web-Only Document 81</i>

DESIGN AND CONSTRUCTION GUIDELINES FOR GEOSYNTHETIC-REINFORCED SOIL BRIDGE ABUTMENTS WITH A FLEXIBLE FACING

SUMMARY A rational design method and construction guidelines for geosynthetic-reinforced soil (GRS) bridge abutments with a flexible facing have been developed in this study. The design method and construction guidelines were established based on the findings of (1) a literature study, (2) full-scale experiments, and (3) an analytical study. Each study and the major findings are summarized below.

Literature Study

The literature study included reviewing and synthesizing the measured behavior and lessons learned from case histories of GRS bridge-supporting structures with flexible facings, including six in-service GRS bridge abutments and six full-scale field experiments of GRS bridge piers and abutments. The following were observed about the performance, design, and construction of the GRS bridge-supporting structures:

- GRS bridge abutments with a flexible facing are a viable alternative to conventional bridge abutments. All six in-service GRS abutments performed satisfactorily under service loads. The maximum settlements and maximum lateral displacements for all the abutments met the tolerable movement criteria based on experience with real bridges—100 mm (4 in.) for settlement and 50 mm (2 in.) for lateral displacement.
- With a well-graded and well-compacted granular backfill and closely spaced reinforcement (e.g., 0.2 m of vertical spacing), the load-carrying capacity of a GRS bridge-supporting structure can be as high as 900 kPa. The load-carrying capacity will be significantly smaller (down to 120 to 140 kPa) when the backfill is of a low density or the reinforcement is not of sufficient length or strength.
- With a well-graded and well-compacted granular backfill, the maximum settlement of the loading slab (sill) and the maximum lateral movement of the wall face can be very small under service loads. With a lower quality backfill, the movements will be significantly larger.
- Fill placement density plays a major role in the performance of the GRS structures.
- Preloading can significantly reduce post-construction settlement of a GRS abutment by a factor of 2 to 6, depending on the initial placement density. If there is a

significant difference in the height of the two abutments supporting a bridge, preloading is an effective way to reduce differential settlement.

- With a well-graded and well-compacted granular backfill, long-term creep under service loads can be negligibly small.
- For all the bridge-supporting structures, the maximum tensile strains in the reinforcement were in the range of 0.1 percent to 1.6 percent under service loads, with larger maximum strains being associated with lower strength backfill.
- Reinforcement length and reinforcement type appear to have only a secondary effect on the performance characteristics.
- The “sill clear distance” (i.e., the distance between front edge of sill and back face of wall facing) used in the cases varies widely, from 0.2 m to 2.2 m. A small sill clear distance can only be used with well-compacted backfill, especially near the wall face. A larger sill clear distance may result in a longer bridge deck (thus higher costs) and may compromise stability if the reinforcement is not of sufficient length.

Full-Scale Experiments

The full-scale experiments, referred to as the NCHRP test abutments, consisted of two test sections: the Amoco test section and the Mirafi test section, in a back-to-back configuration. The two test sections differed only in the type of reinforcement. The main features of the test sections were as follows:

- Abutment height: 4.65 m (15.25 ft)
- Sill: 0.9 m × 4.5 m (3 ft x 15 ft)
- Clear distance: 0.15 m (6 in.)
- Reinforcement type: Amoco test section: Amoco 2044 ($T_{ult} = 70$ kN/m)
Mirafi test section: Mirafi 500x ($T_{ult} = 21$ kN/m)
- Reinforcement length: 3.5 m (10 ft)
- Reinforcement spacing: 0.2 m (8 in.)
- Facing: Cinder blocks, without mechanical connection between blocks
- Backfill: A non-plastic silty sand (SP-SM), with internal friction angle = 34.8° from standard direct shear tests; field placement density = 100 percent of T-99.
- Loading: Vertical loads applied to sill in 50 kPa increments. The loading was terminated at 814 kPa for the Amoco test section (as the loading rams reached their maximum extension) and 414 kPa for the Mirafi test section (because of “excessive” deformation).

The measured performance and observed behavior of the NCHRP test abutments are presented in Chapter 2. Highlights of the measured performance and observed behavior follow.

Load-Carrying Capacity and Ductility

- As the loading was being terminated, 814 kPa applied pressure for the Amoco test section and 414 kPa for the Mirafi test section, the Mirafi test section had approached a bearing failure condition while the Amoco test section appeared to

be still sufficiently stable. For a typical design pressure of 200 kPa, the safety margin in terms of load-carrying capacity is considered “acceptable” for the Amoco test section and “marginally acceptable” for the Mirafi test section.

- With a sufficiently strong reinforcement, the Amoco test section was still exhibiting a near-linear load-settlement relationship at 814 kPa, about four times the typical design pressure of 200 kPa, although the deformation had become fairly large—a clear indication of a high ductility of the abutment system. With a weak reinforcement, however, the ductility was significantly compromised. As the applied pressure increased beyond 200 kPa, the rate of settlement continued to increase with increasing applied pressure.

Sill Settlement and Angular Distortion

- The settlement of the sill in the Mirafi test section was about 80 percent greater than in the Amoco test section under an applied pressure of 200 kPa. As the loading was terminated, 814 kPa for the Amoco test section and 414 kPa for the Mirafi test section, the average sill settlement of the two test sections was comparable.
- The sill settlement of the Amoco test section under 200 kPa met the typical settlement criterion of 100 mm (4 in.); while in the Mirafi test section, the sill settlement was likely to compromise ride quality, but would still be considered “tolerable.”
- For an 18-m (60-ft)-long single-span bridge, the “maximum possible” angular distortions for both test sections were below the typical acceptable criterion of 1:200.

Lateral Movement of Abutment Wall

- For both test sections, the abutment wall moved outward with the maximum movement occurring near the top of the wall. The maximum lateral displacements at 200 kPa were somewhat below the typical maximum lateral movement criterion of 50 mm (2 in.).

Contact Pressure on Foundation Level

- The measured contact pressure was the highest beneath the wall face and decreased nearly linearly with the distance from the wall face.
- The 2V:1H pyramidal distribution method suggested by the NHI manual yielded approximately the “average” measured contact pressure, although the calculated pressures were somewhat higher than the measured average values at higher applied pressures.

Observed Behavior

- A tension crack was observed on the wall crest in both load test sections. The tension crack was first observed near where the reinforcement ended at an applied pressure of 150 to 200 kPa. The location of the tension crack suggested that the assumption of a rigid reinforced soil mass in the existing design methods for evaluating external stability is a sound assumption. If an upper wall had been constructed over the test abutment, as in the case of typical bridge abutments, the tension crack would not have been visible and would perhaps be less likely to occur.

- Under higher applied loads, the facing blocks in the top three courses were pushed outward as the sill tilted counter-clockwise toward the wall face. This suggests that (1) a sill clear distance of 0.15 m, a minimum value stipulated by the NHI manual, may be too small, and (2) it may be beneficial to increase the connection strength in the top three to four courses of the facing during construction.

Analytical Study

The Analytical Tool

A finite element software program, DYNA3D, written by Hallquist and Whirley in 1989 (along with its PC version, LS-DYNA), was selected as the analytical tool for the study. The capability of DYNA3D/LS-DYNA for analyzing the performance of segmental facing GRS bridge abutments was evaluated critically. The evaluation included comparing the analytical results with measured data of five well-instrumented full-scale experiments. The comparisons are presented in *NCHRP Web-Only Document 81*. Very good agreements between the analytical results and all the measured quantities (including failure loads, when applicable) were obtained.

Parametric Analysis

An extensive parametric analysis was conducted by using the analytical tool. For the parametric analysis, a bridge abutment configuration and a set of material properties were selected as the base case. The performance characteristics of the base case as affected by soil density (i.e., soil stiffness and friction angle), reinforcement stiffness, reinforcement spacing, reinforcement truncation, and the sill clear distance were investigated. The results of the performance analysis (presented fully in Chapter 2) are summarized below.

- Effect of reinforcement spacing: For a fill with $\phi = 34^\circ$, the effect of reinforcement spacing on the abutment performance was very small when the applied pressure was less than 100 kPa. At 200 kPa, there was a 25 percent increase in sill settlement as the spacing increased from 0.2 m to 0.4 m, and another 25 percent increase as the spacing increased from 0.4 m to 0.6 m. The increase in settlement because of an increase in reinforcement spacing was higher at 400 kPa than at 200 kPa.
- Effect of soil stiffness and strength: At reinforcement spacing of 0.2 m, the sill settlement of an abutment with 34° soil friction angle was 23 percent and 35 percent higher than those with 37° and 40° friction angles, respectively. The effect was more pronounced for reinforcement spacing of 0.4 m. The performance of an abutment with $\phi = 34^\circ$ and reinforcement spacing = 0.2 m was very similar to an abutment with $\phi = 37^\circ$ and reinforcement spacing = 0.4 m, suggesting that more closely spaced reinforcement had an effect similar to denser fill compaction.
- Effect of reinforcement stiffness: For a soil with $\phi = 34^\circ$ and reinforcement spacing = 0.2 m, the sill settlement decreased 43 percent at 200 kPa as the reinforcement stiffness increased from 530 kN/m to 5,300 kN/m. The sill settlement increased about 250 percent as the reinforcement stiffness decreased from 530 kN/m to 53 kN/m.
- Effect of sill clear distance: The sill settlement increased about 20 percent when the sill clear distance increased from 0 to 0.15 m and increased another 10 percent when the sill clear distance increased from 0.15 to 0.3 m.

- Effect of truncated reinforcement at base: For a soil with $\phi = 34^\circ$ and reinforcement spacing = 0.4 m, the effect was insignificant.

Load-Carrying Capacity Analysis

To determine the allowable sill pressures for the recommended design method, 72 additional analyses were performed using the LS-DYNA code. The effects of the following parameters were investigated: sill type (integrated sill and isolated sill), sill width (0.8 m, 1.5 m, and 2.5 m), reinforcement spacing (0.2 m and 0.4 m), soil friction angle (34° , 37° , and 40°), and foundation (6-m thick medium sand foundation and rigid foundation).

The results of the load-carrying analysis (presented more fully in Chapter 2 of this report) are summarized below.

- For reinforcement spacing of 0.2 m, none of the abutments suffered from any stability problems up to an applied pressure of 1,000 kPa.
- For reinforcement spacing of 0.4 m, most of the abutments encountered facing failure (i.e., the top two to three courses of facing blocks “fell off” the wall face) when the applied pressure exceeded 500 kPa to 970 kPa (depending on the geometric condition and material properties of the abutment). Only those abutments with sill width = 0.8 m and soil friction angle = 37° and 40° did not encounter facing failure up to an applied pressure of 1,000 kPa. Nonetheless, there was no catastrophic failure in any of the abutments up to 1,000 kPa applied pressure.
- The differences in the magnitude of the performance characteristics for ϕ between 34° and 37° were generally greater than those between 37° and 40° . This suggests that increasing the soil friction angle (by selecting a better fill type and/or with better compaction efforts) to improve the performance characteristics will be more efficient for soils with a lower friction angle than for soils with a higher friction angle.
- The effect of reinforcement spacing on sill settlement and maximum lateral displacement of wall face was significant, especially at higher applied pressure (i.e., greater than 200 kPa).
- A glaring difference between an integrated sill and an isolated sill was in the rotation of the sill. The integrated sills experienced counter-clockwise tilting; while the isolated sills generally experienced clockwise rotation, except for a larger sill width (2.5 m) where the rotations were clockwise.
- Over a rigid foundation, the abutments tend to have significantly smaller sill settlements, smaller maximum lateral wall displacements, smaller sill lateral movements, and smaller sill rotations (except for isolated sills) than the abutments situated over a medium sand foundation.

The allowable bearing pressures of GRS abutments were evaluated using the results of the 36 analyses with a medium sand foundation, because GRS abutments offered more conservative allowable bearing pressures than those abutments with a rigid foundation. Two performance criteria were examined. One criterion involves a limiting sill settlement, where the allowable bearing pressure is corresponding to a sill settlement of 1 percent of the lower wall height (i.e., 1%H). The other criterion involves the distribution of the critical shear strain in the reinforced soil mass, where the allowable bearing pressure corresponds to a limiting condition in which a triangular critical shear strain distribution reaches the back edge of the sill (i.e., the heel of the sill).

The bearing pressures obtained from the two performance criteria formed the basis for the recommended allowable bearing pressures in the recommended design method presented in Chapter 3.

Major Refinements and Revisions to the NHI Design Method

The recommended design method adopted the format and basic methodology of the NHI design method for mechanically stabilized earth (MSE) abutments. Fourteen specific refinements and revisions to the NHI design method are stipulated in the recommended design method. The refinements and revisions and the basis for each refinement and revision are presented in Chapter 3. The major refinements and revisions to the NHI design method are as follows:

- The allowable bearing pressure of the bridge sill on a load-bearing wall (the lower wall) of a GRS abutment is determined as a function of the friction angle of the fill, reinforcement vertical spacing, sill width, and sill type (isolated sill or integrated sill). A simple three-step procedure is provided for determining the allowable bearing pressures under various design conditions.
- The default value for reinforcement vertical spacing is set as 0.2 m. To ensure satisfactory performance and an adequate margin of stability, reinforcement spacing greater than 0.4 m is not recommended for GRS abutments under any conditions.
- To provide improved appearance and greater flexibility in construction, a front batter of 1/35 to 1/40 from the vertical is recommended for a segmental abutment wall facing. A typical setback of 5 to 6 mm between successive courses of facing blocks is recommended for blocks 200 mm (8 in.) high.
- The reinforcement length may be “truncated” in the bottom part of the wall if the foundation is “competent.” The recommended configuration of the truncation is reinforcement length = 0.35 H at the foundation level (H = total height of the abutment wall) and increases upward at a 45° angle. The allowable bearing pressure of the sill, as determined by the three-step procedure, should be reduced by 10 percent for truncated-base walls. Permitting truncated reinforcement typically will produce significant savings when excavation is involved in the construction of the load-bearing wall of a bridge abutment.
- A recommended sill clear distance between the back face of the facing and the front edge of the sill is 0.3 m (12 in.). The recommended clear distance is a result of finite element analysis with the consideration that the soil immediately behind the facing is usually of a lower compacted density because a heavy compactor is not permitted close to the wall face.
- For most bridge abutments, a relatively high-intensity load is applied close to the wall face. To ensure that the foundation soil beneath the abutment will have a sufficient safety margin against bearing failure, a revision is made to check the contact pressure over a more critical region—within the “influence length” D_1 (as defined in Chapter 3) behind the wall face or the reinforcement length in the lower wall, whichever is smaller. In the current NHI manual, the contact pressure is the average pressure over the entire reinforced zone (with eccentricity correction).
- If the bearing capacity of the foundation soil supporting the bridge abutment is found only marginally acceptable or slightly unacceptable, it is recommended that a reinforced soil foundation (RSF) be employed to increase its bearing capacity and reduce potential settlement. A typical RSF is formed by excavating a pit that is $0.5 * L$ deep (L = reinforcement length in the load-bearing wall) and replacing it with compacted road base material reinforced by the same reinforcement to be

used in the load-bearing wall at 0.3 m vertical spacing. The lateral extent of the RSF should at least cover the vertical projection of the reinforced soil area and should extend no less than $0.25 * L$ in front of the wall face.

- Both a minimum ultimate tensile strength and a minimum tensile stiffness of the reinforcement should be specified to ensure sufficient tensile resistance at the service loads, to provide adequate ductility, and to ensure a sufficient safety margin against rupture failure. A recommended procedure for determining the required minimum tensile stiffness (at 1.0% strain) and the minimum ultimate tensile strength has been stipulated.
- It is recommended to extend the reinforcement lengths in both the upper and lower walls—at least the top three layers in each wall—to approximately 1.5 m beyond the end of the approach slab to enhance the integration effect of the abutment walls with the approach embankment, so as to eliminate the bridge “bumps”—a chronic problem in many bridges.
- Connection strength is not a design concern as long as (1) the reinforcement spacing is kept no greater than 0.2 m, (2) the selected fill is compacted to meet the specification stipulated in the recommended construction guidelines, and (3) the applied pressure does not exceed the recommended design pressures in the recommended design method.

Recommended Construction Guidelines

The recommended construction guidelines were established based on the guidelines for segmental GRS walls as provided by various agencies (including AASHTO, NCMA, FHWA, CTI, SAGP, and JR) as well as the authors’ observations and experiences with the construction of GRS walls and abutments. The construction guidelines focus on GRS abutments with a segmental concrete block facing. Only the basic construction guidelines for three types of flexible facing (i.e., geotextile-wrapped, timber, and natural rock facing) are presented.

CHAPTER 1

INTRODUCTION AND RESEARCH APPROACH

PROBLEM STATEMENT

Soil is generally weak in tension and relatively strong in compression and shear. The concept of reinforcing a soil mass by incorporating a material that is strong in tensile resistance is similar to that of reinforced concrete. The reinforcing mechanisms of reinforced soil and reinforced concrete, however, are somewhat different. In reinforced soil, the bonding between the soil and the reinforcement is derived from soil-geosynthetic interface friction, and in some cases also from adhesion and passive resistance. Through the interface friction, the reinforcement restrains lateral deformation of the soil next to the reinforcement and therefore increases the stiffness and strength of the soil mass.

Over the past two decades, geosynthetic-reinforced soil (GRS), a reinforced soil mass that uses layers of geosynthetics as reinforcement, has been employed in the construction of many earth structures, including retaining walls, embankments, slopes, and shallow foundations. In actual construction, GRS structures have demonstrated many distinct advantages over their conventional counterparts. GRS structures are typically more ductile, more flexible (hence more tolerant to differential settlement), more adaptable to low-quality backfill, easier to construct, and more economical. They also require less overexcavation.

In recent years, applications of the GRS technology to bridge-supporting structures have gained increasing attention. Depending on the facing rigidity, GRS bridge-supporting structures can be grouped into two types: “rigid” facing and “flexible” facing structures. A “rigid” facing is typically a continuous reinforced concrete panel, either precast or cast-in-place. A “flexible” facing, on the other hand, typically takes the form of wrapped geosynthetic sheets, dry-stacked concrete modular blocks, timbers, natural rocks, or gabions. In contrast to a “flexible” facing, a “rigid” facing offers a significant degree of “global” bending resistance along the entire height of the facing panel, and thus offers greater resistance to “global” flexural deformation caused by lateral earth pressure exerted on the facing.

Since 1994, the Japan Railway has constructed a large number of full-height concrete facing GRS bridge abutments and piers (Tateyama et al., 1994; Kanazawa et al., 1994; Tatsuoka et al., 1997) using a rigid wall GRS system

developed by Tatsuoka and his associates at the University of Tokyo. These GRS bridge-supporting structures were constructed in two stages. The first stage involves constructing a wrapped-faced GRS wall with the aid of gabions, and the second stage involves casting in-place a full-height reinforced concrete facing over the wrapped face. Field measurement has shown that these structures experienced little deformation under service loads and have performed far better than conventional reinforced concrete retaining walls and abutments in the 1995 Japan Great Hanshin earthquake that measured 7.2 on the Richter scale (Tatsuoka et al., 1997). Most recently, Tatsuoka and his associates developed a pre-load-prestress technique to improve the performance of the GRS bridge-supporting structures (Tatsuoka et al., 1997; Uchimura et al., 1998). Despite their success, the “rigid” facing GRS bridge-supporting structures have only found applications in Japan, mostly because of their cost and longer construction time compared to GRS walls with a “flexible” facing.

GRS bridge-supporting structures with a flexible facing have been the subject of several studies (e.g., Gotteland et al., 1997; Adams, 1997; Ketchart and Wu, 1997; Miyata and Kawasaki, 1994; Werner and Resl, 1986; and Benigni et al., 1996), and recently have seen actual applications in the United State and abroad, including the Vienna railroad embankment in Austria (Mannsbart and Kropik, 1996), the New South Wales GRS bridge abutments in Australia (Won et al., 1996), the Black Hawk bridge abutments in Colorado (Wu et al., 2001), and the Founders/Meadows bridge abutments in Colorado (Abu-Hejleh et al., 2000). These structures have shown great promise in terms of ductility, flexibility, constructability, and costs.

Figure 1-1 shows the schematic diagram of a typical GRS bridge abutment with a segmental concrete block facing. The abutment has four major components: (1) a GRS load-bearing wall (the lower wall), (2) a back wall (the upper wall), which may or may not be a reinforced soil wall, (3) a bridge sill, i.e., a footing to support bridge loads, and (4) a segmental concrete block wall facing. The bridge sill can be either integrated with the upper wall face (referred to as an “integrated sill”) or isolated from the upper wall as a separate footing (referred to as an “isolated sill”). The bridge sill shown in Figure 1-1 is an integrated sill.

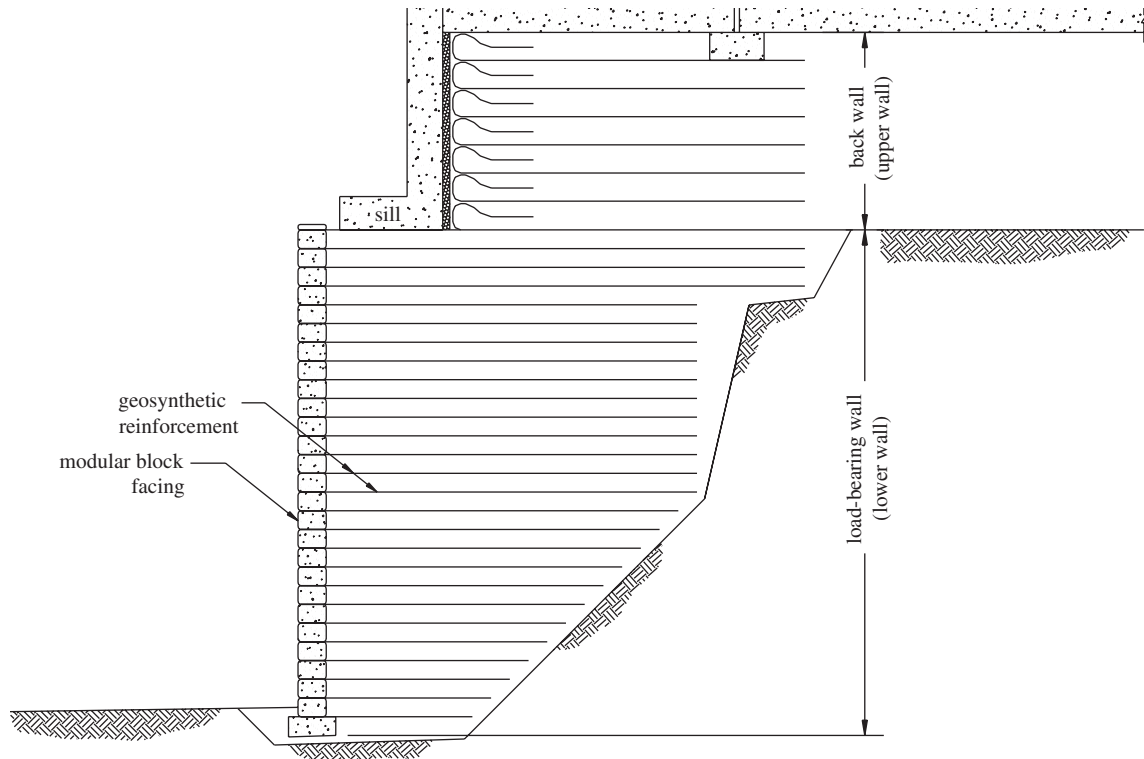


Figure 1-1. Typical GRS bridge abutment with a segmental concrete block facing.

GRS abutments with a flexible facing have some distinct advantages over the conventional reinforced concrete abutments. The advantages include the following:

- GRS abutments are more flexible, hence more tolerant to foundation settlement and to seismic loading.
- When properly designed and constructed, GRS abutments are remarkably stable. GRS abutments also have higher ductility (i.e., are less likely to experience a sudden catastrophic collapse) than conventional reinforced concrete abutments.
- When properly designed and constructed, GRS abutments can alleviate the bridge “bumps” commonly occurring at the two ends of a bridge supported by conventional reinforced concrete abutments, especially when they are on piles.
- GRS abutments do not require embedment into the foundation soil for stability. This advantage is especially important when an environmental problem, such as excavation into previously contaminated soil, is involved.
- The lateral earth pressure behind a GRS abutment wall is much smaller than that in a conventional reinforced concrete abutment.
- Construction of GRS abutments is rapid and requires only “ordinary” construction equipment.

- GRS abutments are generally much less expensive to construct than their conventional counterparts.

It has generally been assumed that the design methods and construction guidelines of GRS retaining walls are readily applicable to GRS bridge abutments. The approach has raised concerns as GRS abutments are generally subjected to a relatively high-intensity load that is fairly close to the wall face. Basic design guidelines for Mechanically Stabilized Earth (MSE) bridge abutments have been provided by the National Highway Institute (NHI) reference manual, entitled *Mechanically Stabilized Earth Walls and Reinforced Soil Slopes Design and Construction Guidelines*, (Elias et al., 2001). The NHI manual also gives a design example for an abutment reinforced with steel strips. Design and construction guidelines for GRS abutments with a flexible facing that are based on sound engineering research are not available.

RESEARCH OBJECTIVE

The objective of this study was to develop rational design and construction guidelines for GRS bridge abutments with a flexible facing. The objective has been successfully achieved.

RESEARCH APPROACH

The following tasks and the associated research approach were undertaken to achieve the objective of this study:

- Task 1: Perform Literature Study

An extensive literature study was performed to synthesize the measured performance and observed behavior from case histories of well-instrumented GRS bridge-supporting structures. Both in-service structures and full-scale experiments from around the world were included in the literature study. In addition, a literature study on construction guidelines and specifications of GRS walls used in the United States and abroad was conducted. The findings of the study were used as the framework of the recommended construction guidelines.

- Task 2: Conduct Analytical Study

A finite element computer code, DYNA3D, written by Hallquist and Whirley in 1989 (along with LS-DYNA, a PC version of DYNA3D) was selected for this study. The code was selected primarily because of its capability to predict different failure modes of GRS abutments with a segmental concrete block facing. The analytical study includes the following:

- Extensive verification of the capability of DYNA3D and LS-DYNA to analyze performance and failure conditions of GRS bridge-supporting structures with a segmental concrete block facing was conducted. The structures analyzed include the spread footing tests by Briaud and Gibbens (1994), the spread footing tests on reinforced sands by Adams and Collin (1997), the FHWA Turner-Fairbank GRS bridge pier in Virginia (Adams, 1997), the Garden experimental embankment in France (Gotteland et al., 1997), and the two full-scale GRS bridge abutment loading experiments conducted as part of this study.
- A parametric study on the performance characteristics of GRS bridge abutments as affected by (a) soil placement condition, (b) reinforcement stiffness/strength, (c) reinforcement spacing, (d) truncation of reinforcement near wall base, (e) sill width, and (f) the clear distance between the front edge of sill and back face of wall facing.

- A series of load-carrying capacity analyses of GRS abutments with a segmental concrete block facing were also conducted to determine the allowable bearing pressures of sills under various design conditions.

- Task 3: Conduct Full-Scale Loading Experiments

Two full-scale experiments of GRS abutments with a segmental concrete block facing were performed at the Turner-Fairbank Highway Research Center in McLean, Virginia, under the supervision of Michael Adams. The test abutments were instrumented to monitor their performance in response to increasing loads applied to the sill. The measured results of the experiments were analyzed by the finite element analysis code, DYNA3D, for further verification of the analytical model. The full-scale experiments were also evaluated by the MSEW program, an analysis/design computer program based on the design method presented in the NHI manual.

- Task 4: Develop Design and Construction Guidelines

A design method for GRS abutments with a flexible facing was developed in the course of this study. The design method adopted the format and methodology of the design method for MSE bridge abutments in the NHI manual. Fourteen refinements and revisions of the NHI design methods were proposed. The refinements and revisions were based on measured performance of case histories, findings of the analytical study, and the authors' experience with GRS walls and abutments.

Construction guidelines for GRS abutments with different forms of flexible facing were also developed. The construction guidelines were based primarily on the guidelines provided by provided by: the American Association of State Highway and Transportation Officials, AASHTO (1998), the National Concrete Masonry Association, NCMA (1997), the Federal Highway Administration, FHWA (Elias and Christopher, 1997), the Colorado Transportation Institute, CTI (Wu, 1994), the Swiss Association of Geotextile Professionals, SAGP (1981), and the Japan Railways, JR (1998), as well as the authors' experience with GRS walls and abutments. The recommended construction guidelines addressed site and foundation preparation, reinforcement selection and placement, backfill selection and placement, facing selection and placement, drainage, and construction sequence.

CHAPTER 2

FINDINGS

FINDINGS FROM LITERATURE STUDY

Over the past two decades, GRS has been used in the construction of various earth structures, including retaining walls, embankments, slopes, and shallow foundations. In actual construction, GRS structures have demonstrated many distinct advantages over their conventional counterparts. GRS structures typically are more ductile, more flexible (hence more tolerant to differential settlement), more adaptable to low quality backfill, easier to construct, and more economical. They also require less overexcavation.

In recent years, applications of the GRS technology to bridge-supporting structures have gained increasing attention. The facing of GRS bridge-supporting structures can be grouped into two types: rigid and flexible. A rigid facing is a continuous reinforced concrete facing, either precast or cast-in-place. A flexible facing, on the other hand, typically takes the form of wrapped geosynthetic sheets, dry-stacked concrete modular blocks, natural rocks, or gabions. In contrast to a flexible facing, a rigid facing offers a certain degree of global bending resistance along the entire height of the facing, thus offering greater constraint to lateral earth pressure-induced “global” bending deformation.

Since 1994, the Japan Railway has constructed many full-height facing GRS bridge abutments and piers (e.g., Tateyama et al., 1994; Kanazawa et al., 1994; Tatsuoka et al., 1997) using a rigid facing GRS wall system developed by Tatsuoka and his associates at the University of Tokyo. These GRS bridge-supporting structures have been constructed in two stages. The first stage involves constructing a wrapped-faced GRS wall with the aid of gabions, and the second stage involves casting in place a full-height reinforced concrete facing over the wrapped face. Field measurement has shown that these structures experienced little deformation under service loads and have performed far better than conventional reinforced concrete retaining walls and abutments in the 1995 Japan Great Hansin earthquake that measured 7.2 on the Richter scale (Tatsuoka et al., 1997). Most recently, Tatsuoka and his associates developed a preload-prestress method for improved performance of the GRS bridge-supporting structures (Tatsuoka et al., 1997; Uchimura et al., 1998). Despite their success, the rigid facing GRS bridge-supporting structures have found applications only in Japan, mostly because of their higher cost and longer construction time compared with GRS walls with flexible facings.

GRS bridge-supporting structures with flexible facings have been the subject of many studies and recently have seen some actual applications, in the United States and abroad. This study synthesizes the measured behavior and experiences gained from case histories of flexible facing GRS bridge-supporting structures from around the world. Observations were made in relation to performance, design, and construction of flexible facing GRS bridge-supporting structures. The case histories were organized into two groups: in-service structures and field experiments. Most of these studies were on bridge abutments, with a few on bridge piers. The design and construction of GRS bridge abutments are similar in principle to GRS walls, except the former typically are subject to a rather high surface load close to the wall face. Also, some U.S. states do not permit the use of segmental concrete facing in GRS bridge-supporting structures because of concerns with the durability of masonry units when exposed to chemical agents such as de-icing fluids. Based on the measured performance of the case histories, observations were made in relation to performance, design, and construction of GRS bridge-supporting structures. Some of the material properties and the methods for determining the properties are not reported because they are not available in the source materials.

In-Service Bridge-Supporting Structures

The construction-related information and measured performance of six in-service GRS bridge abutments are described below. The six abutments are the Vienna railroad embankment in Austria (Mannsbart and Kropik, 1996), the New South Wales GRS bridge abutments in Australia (Won et al., 1996), the Black Hawk bridge abutments in Colorado (Wu et al., 2001), the Founders/Meadows bridge abutments in Colorado (Abu-Hejleh et al., 2000), the Feather Falls Trail bridge abutments in California (Keller and Devin, 2003), and the Alaska bridge abutments in Alaska (Keller and Devin, 2003).

Case A1: Vienna Railroad Embankment, Austria (Mannsbart and Kropik, 1996)

A temporary GRS embankment was constructed in Vienna, Austria, to support a railroad track. The railroad embankment had a height of 2.1 m and a slope inclination of

63 deg from the horizontal. A needle-punched nonwoven geotextile was used as the reinforcement. The geotextile had a tensile strength of 23 kN/m with elongation at break of 45 percent. The reinforcement spacing and length were 0.3 m and 1.7 m, respectively. The backfill was a compacted gravelly sand. Its placement unit weight was 21 kN/m³, and the design internal friction angle was 35 deg.

The individual layers of the structure were built using a removable formwork consisting of steel angles and wooden bars. To get adequate friction between the adjacent geotextile layers, a thin layer of sandy gravel was placed on each lift before the installation of the next layer. Given that the structure had to fulfill only a temporary function, a wrapped-around wall face was used and the surface protection was omitted.

Above the reinforced structure, a 0.9-m-high unreinforced embankment with a slope of 45 deg was built as a buffer for the traffic. The design traffic load was 60 kPa, exerted at 1.45 m from the top edge of the unreinforced embankment. The cross-section of the temporary embankment is shown in Figure 2-1. Weekly settlement measurement was carried out on 6 points along the 100-m-long embankment. The results indicated that under traffic load, the measured settlement was nil at four of the six points, and at the other two points the settlement was less than 1 mm.

Case A2: New South Wales GRS Bridge Abutments, Australia (Won et al., 1996)

Geogrid reinforced bridge abutments with a segmental block facing were constructed to support end spans directly for a major bridge in New South Wales, Australia, in 1994. The bridge consisted of a nine-span superstructure over the Tweed River. The abutments were up to 10 m high, constructed in a terraced arrangement, as shown in Figure 2-2.

The facing comprised “Keystone” segmental concrete blocks that were partially voided internally, and aggregates were used to fill the block during construction. High-strength

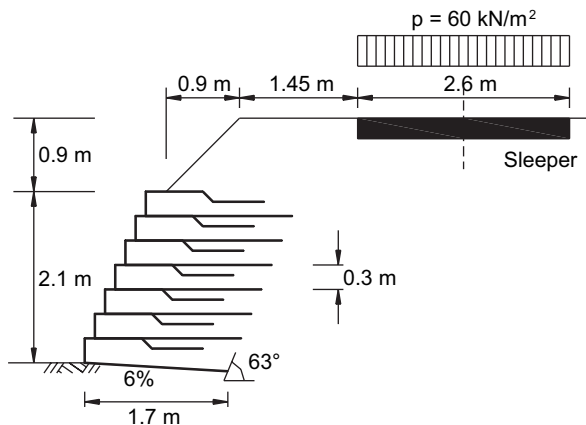


Figure 2-1. Cross-section of the Vienna railroad embankment, Austria (Mannsbart and Kropik, 1996).

fiberglass dowels were used to interlock block layers vertically. Foundation conditions at the site consisted of a 1- to 3-m-thick layer of loose silty sand containing thin discontinuous silty clay layers overlying a medium dense silty sand layer varying in thickness from 7 m to 10 m. Sandstone bedrock was present at 13 m depth.

The two abutments are referred to as Abutment A and Abutment B. Abutment A consisted of three terraced segmental block walls with 12 layers of a Tensar HDPE geogrid, SR 110, beneath the sill beam. The tensile strength of the geogrid was 110 kN/m at 11.2 percent strain. Total tiered height was 6.5 m. Abutment B consisted of four terraced segmental block walls with 17 layers of SR110 geogrid beneath the sill beam. Total tiered height was 9.5 m. To account for creep, temperature variation, and construction damage, the allowable long-term design strength for the SR110 geogrid was taken as 27 kN/m. The vertical spacing of geogrid layers was 40 cm or 60 cm. The maximum reinforcement length was 15 m. The backfill material, a fine sand, was compacted to at least 95 percent Standard Relative Density to have a design friction angle of 32 deg. Additional layers of geogrid, 5 m long with a wrap-around face, were used to reduce active earth pressure behind the sill beam. The unreinforced concrete sill beam was 20 cm thick and 2.5 m wide. It was set back 2.5 m from the edge of the top wall to reduce the effects of horizontal pressure because of sill beam load distribution through the reinforced soil. In view of the loose nature of the foundation soil, the top 1 m was excavated and compacted in the vicinity of the lowest-tiered wall.

A comprehensive monitoring program was implemented to evaluate the performance of Abutment B. Sill beam loading occurred during January 1994. The maximum reinforcement tension at Level 1 approached 33 kN/m and occurred toward the back of the reinforced soil block. The maximum reinforcement tension at Level 2 was 21 kN/m and occurred toward the back of the reinforced soil block. At Level 3 reinforcement, the effect of sill beam loading was evident with a maximum reinforcement tension of 22 kN/m occurring under the sill beam region. The maximum strain in the geogrid was 1.6 percent, occurring at Level 1. The maximum settlement was 80 mm. Lateral movements of the reinforced soil structure deduced from wall survey and inclinometers I1 and I2 (see Figure 2-2) were 10 mm up to the completion of the abutment and 26 mm post construction movements for the lowest-tiered wall. Subsequent site investigations of the loose upper silty sand layer indicated the presence of thin discontinuous seams of medium stiff silty clay, which could have contributed to the deformation response at the base of the structure.

Case A3: Black Hawk Bridge Abutments, Colorado (Wu et al., 2001)

Two rock-faced GRS abutments were constructed to support the Bobtail Road Bridge, a 36-m-span steel arched bridge in Black Hawk, Colorado (see Figures 2-3 and 2-4).

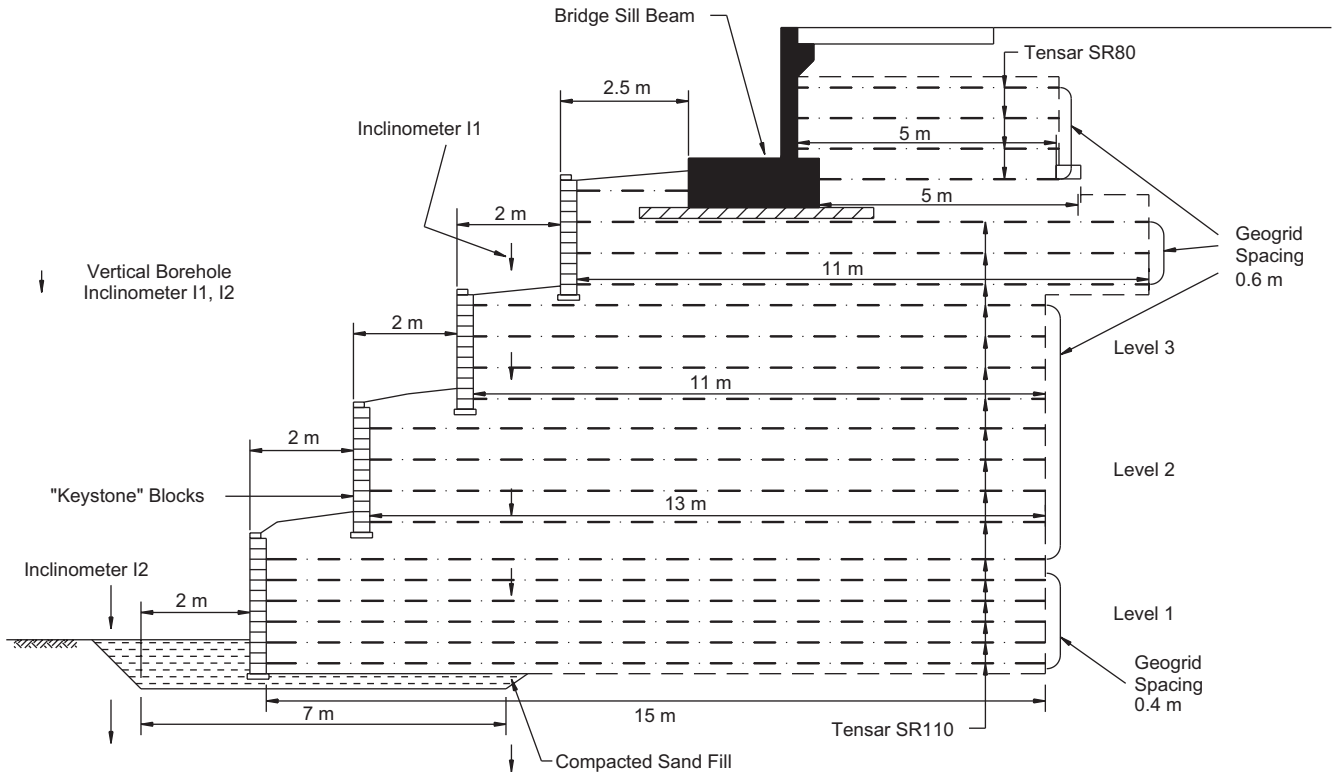


Figure 2-2. Cross-section of the New South Wales GRS bridge abutments, Australia (Won et al., 1996).

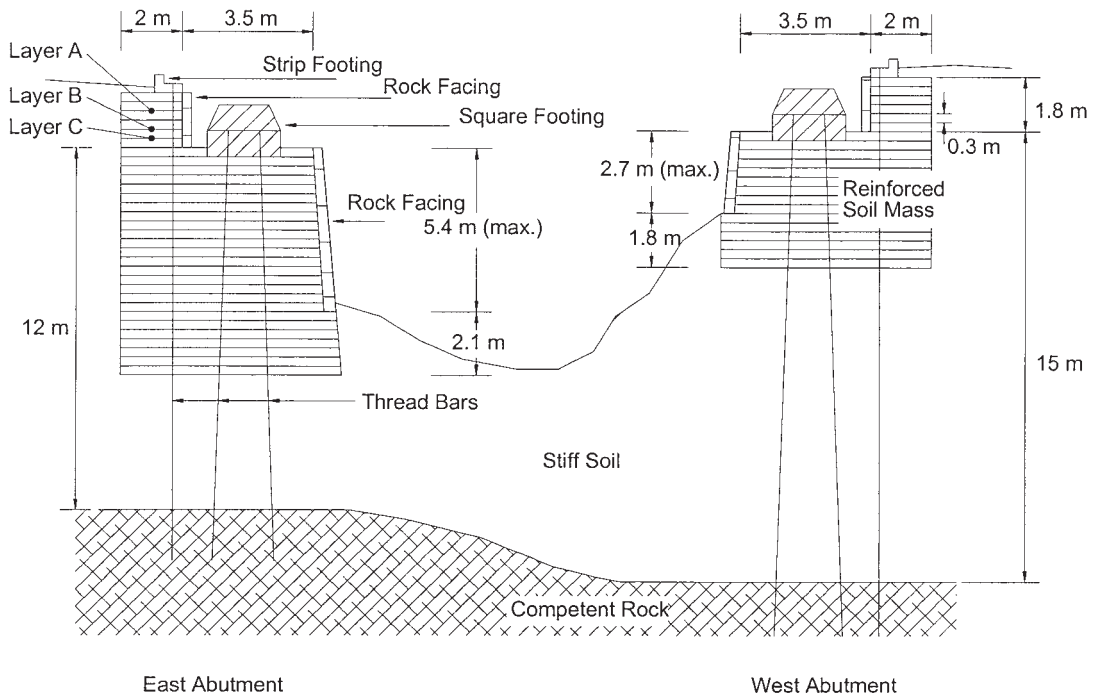


Figure 2-3. Cross-section of the Black Hawk bridge abutments (Wu et al., 2001).

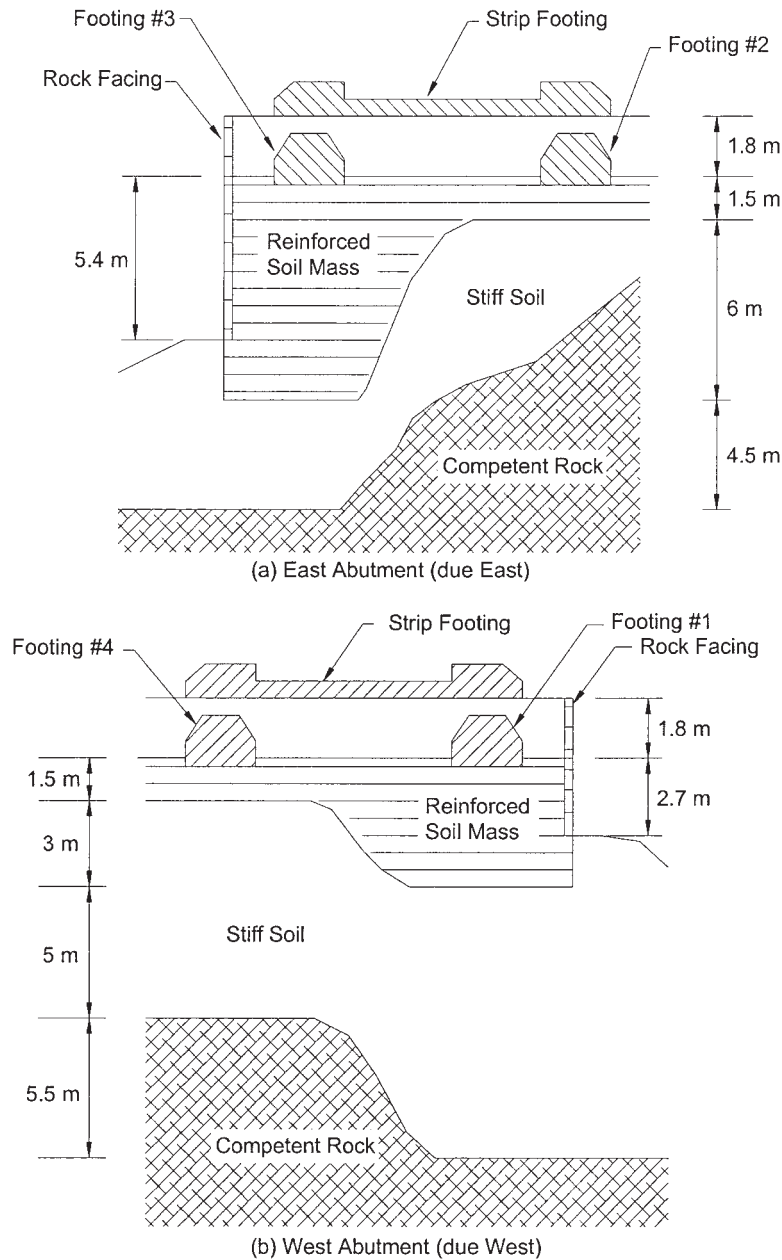


Figure 2-4. Footings and foundations of the Black Hawk bridge abutments (Wu et al., 2001).

Each GRS abutment comprised a two-tier GRS mass with two square footings on the lower tier and a strip footing on the upper tier. The square footings on the West abutment are referred to as Footings #1 and #4, and the square footings on the East abutment are referred to as Footings #2 and #3. The GRS bridge abutments were constructed on a stiff soil. The thicknesses of the lower tier reinforced soil mass under Footings #1 and #4 were, respectively, 4.5 m and 1.5 m; and 7.5 m and 1.5 m under Footings #2 and #3, respectively. The lower part of the GRS abutment was embedded in the ground, while the upper part was above ground. Only the part above ground was constructed with rock facing. The above

ground portion of the abutment had different heights, varying from 1.0 m to 2.7 m for the West abutment; and from 1.0 m to 5.4 m for the East abutment. The thickness of the upper tier reinforced soil mass was 1.8 m for both abutments. The upper tier reinforced soil mass was built to support the strip footing and the approach ramp.

The abutments were constructed with the onsite soil, classified as SM-SC per ASTM D2487, and reinforced with layers of a woven geotextile at vertical spacing of 0.3 m. The polypropylene woven geotextile (Amoco 2044) had a wide-width tensile strength of 70 kN/m in both machine and cross-machine directions at 18 percent strain, per ASTM D4595

(the wide-width strip method). The backfill had 12 percent of fines (passing sieve No. 200). The backfill material was compacted to 91 percent relative compaction per AASHTO T-99 (the moisture-density relation of soil was determined by using a 2.5 kg rammer with a 305 mm drop), having a dry unit weight of 15.8 kN/m³ at a water content of 12.2 percent. The measured friction angle and cohesion, as determined from the CD triaxial compression tests, were 31 deg and 34 kPa, respectively.

For each square footing, a vertical pressure of 245 kPa (1.6 times the design load of 150 kPa) was applied and sustained for 100 minutes, then unloaded to zero. Three loading-unloading cycles were applied following the first loading-unloading cycle. In the reloading cycles, the typical applied pressure was the design load (150 kPa). For the strip footing, the vertical load was increased incrementally to 80 kPa (2 times the design load of 40 kPa), sustained for 120 minutes, and then unloaded to zero. The vertical load applied in the reloading cycle was 40 kPa (the design load). The load was maintained for 120 minutes before unloading. At the design load of 150 kPa in the preloading cycle, the average settlements were 13.3 mm, 6.4 mm, 28 mm, and 4.9 mm for Footings #1 through #4, respectively. At 150 kPa in the first reloading cycle, the average settlements were reduced to 2.5 mm, 3.8 mm, 4.5 mm, and 3.3 mm for Footings #1 through #4 respectively. Further reduction in the settlement was negligible in the subsequent reloading cycle. Preloading reduced the maximum lateral movement at 150 kPa loading pressure from 1.5 mm to 0.6 mm in Footing #1, and from 13.2 mm to 4.5 mm in Footing #3.

In the preloading cycle, under a load of 245 kPa sustained for 60 minutes, the vertical creep displacements of Footings #1 to #4 were, respectively, 6.7 mm, 4.0 mm, 7.2 mm, and 2.1 mm. In the reloading cycle, under the sustained load of 150 kPa, the vertical and lateral creep deformations were insignificant.

At 80 kPa in the preloading cycle, the maximum strains in layers A, B, and C were 0.18 percent, 0.04 percent, and 0.06 percent, respectively. At a sustained load of 80 kPa in the preloading cycle, the creep strains in layers A, B, and C were 0.032 percent, 0.009 percent, and 0.003 percent, respectively. Locations of layers A, B, and C are shown in Figure 2-3. The creep strains were negligible at the sustained load of 40 kPa in the reloading cycle.

Based on the measured data, the following findings and conclusions were made:

- By preloading the reinforced soil mass to 245kPa, the settlement at the design load of 150 kPa was reduced by a factor of 1.5 to 6 for the four square footings.
- Preloading also reduced the lateral movement of the GRS abutments. The lateral movement was reduced by a factor of 2.5 to 3 at 150 kPa.
- After the first reloading cycles, there was no significant reduction of lateral and vertical displacements of GRS abutments in the subsequent reloading cycles.

- The maximum strain mobilized in the reinforcement was very small (less than 0.2 percent at 80 kPa).
- Preloading reduced creep strains in the reinforced structure and the geotextile reinforcement.

Case A4: Founders/Meadows Bridge Abutments, Colorado (Abu-Hejleh et al., 2000)

A replacement bridge was constructed over Interstate Highway 25 at Founders/Meadows Parkways near Castle Rock, Colorado, in 1999. In this bridge abutment, both the bridge and the approaching roadway were supported by a system of GRS segmental retaining walls. The front GRS wall supports the bridge superstructure, which extends around a 90-deg curve into a lower GRS wall supporting the wing wall and a second tier, the upper GRS wall. The GRS abutment was constructed on the native claystone or sandstone bedrock. The plan view of the structure is shown in Figure 2-5. Each span of the bridge was 34.5 m long and 34.5 m wide. The design of the abutment followed the AASHTO (1997) guidelines.

Figure 2-6 shows the typical cross-section of the abutment. For the reinforced soil zone behind and below the bridge abutment, a trapezoid-shaped reinforcement was adopted, in which reinforcement increased linearly from 8.0 m at the bottom with 1H:1V slope toward the top. The reinforcement length for the abutment wall was 11 m to 13 m. The centerline of the bridge abutment wall and edge of the foundation were 3.1 m and 1.35 m from the front of the wall face. Dry-stacked hollow-cored concrete blocks were used as the facing. The lower wall had a maximum height of 4.5 m to 5.9 m and the upper wall had a maximum height of 3.0 m for the West abutment and 3.2 m for the East abutment. The lower wall had a minimum embedment of 0.45 m. The abutment was constructed in two phases to accommodate traffic needs.

Three grades of geogrid reinforcement were used: UX6 with an ultimate strength of 157.3 kN/m used below the foundation, UX3 and UX2 with ultimate strengths of 64.2 kN/m and 39.3 kN/m, respectively, per ASTM D4595, used behind the abutment wall. The ultimate strength of the geogrids was measured in accordance with the ASTM D4595 test method. The reinforcement spacing was 0.4 m. The backfill soil was a mixture of gravel (35 percent), sand (54 percent) and fines (11 percent). The average unit weight and dry unit weight of the compacted fill were 22.1 kN/m³ and 21 kN/m³ (95 percent of AASHTO T-180, the moisture-density relation being determined by using a 4.54 kg rammer with a 457 mm drop), respectively. The average placement moisture content was 5.6 percent.

Field monitoring was performed with various instruments during and after the construction of the structure. The measured vertical stresses did not differ significantly from the static states calculated as $\sigma_z = \gamma z + q + \Delta\sigma_z$, where q is the uniform surcharge and $\Delta\sigma_z$ is the increase in vertical stress caused by concentrated surcharge loads assuming 2V:1H

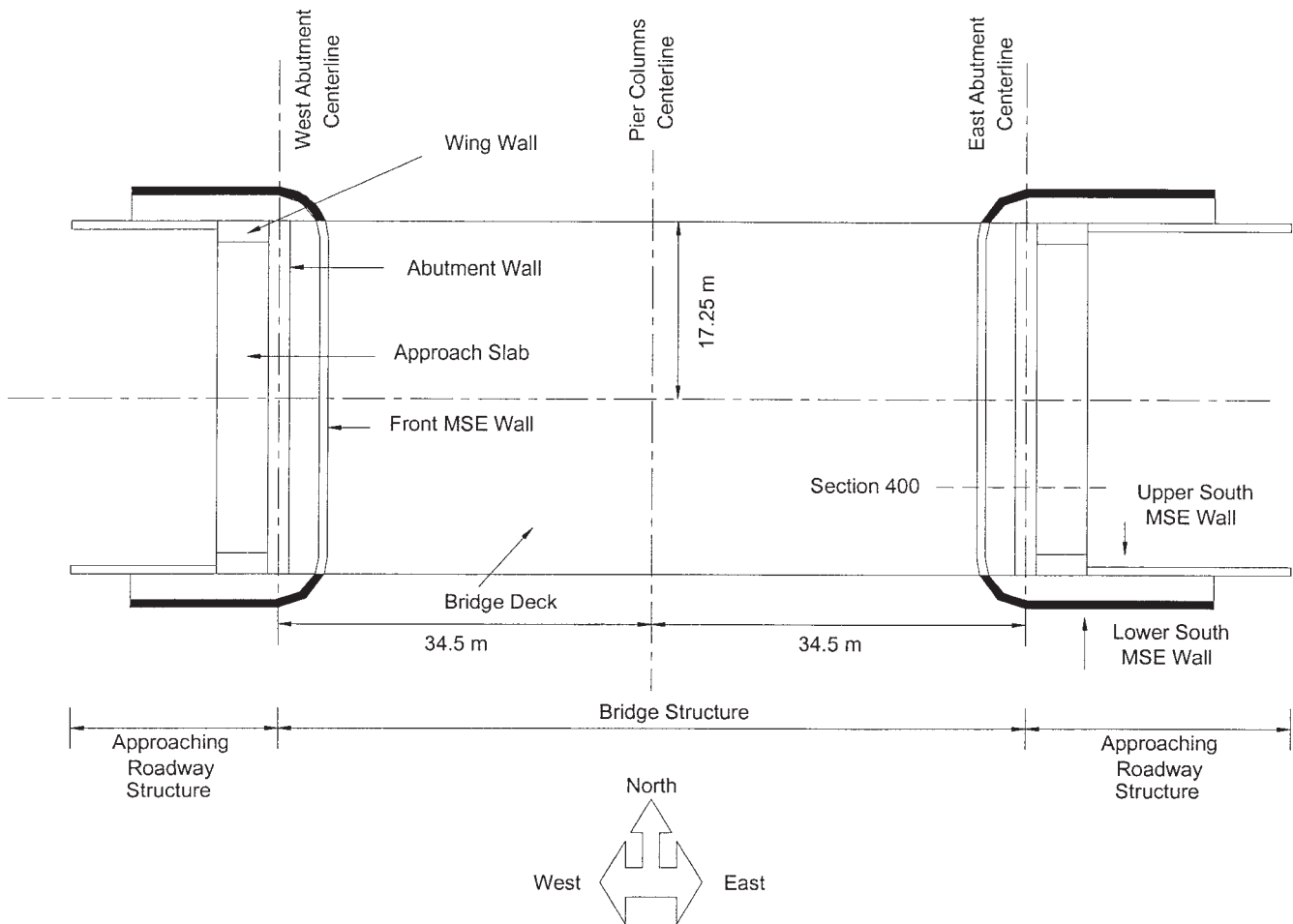


Figure 2-5. Plan view of the Founders/Meadows bridge-supporting structure (Abu-Hejleh et al., 2000).

pressure distribution. The horizontal stresses measured on the facing at the end of construction, however, were much smaller than the Rankine active earth pressures. The measured geogrid strains at the end of construction were very low, on the order of 0.1 percent.

The measured outward movement of the GRS wall face was also very small. The maximum outward movement experienced along Section 400 during the construction of the front GRS wall up to the bridge foundation elevation was about 9 mm. The maximum outward movements experienced during placement of the bridge superstructure were on the order of 7 mm to 9 mm. The field measurements also indicated the sill settled about 13 mm because of the loads of the bridge and the approaching roadway structures. Along Section 400 (see Figure 2-5), the leveling pad settled vertically almost 5 mm during the construction of the front GRS wall up to the bridge foundation elevation and settled another 6 mm when the bridge and approaching roadway structures were placed.

Post-construction performance of the Founders/Meadows bridge abutment was evaluated by Abu-Hejleh et al. (2002), with the following findings:

- Eighteen months after opening to traffic, the maximum outward displacement of the front wall facing and the maximum settlement of the bridge abutment footing were 13 mm (0.22 percent of wall height) and 11 mm (0.18 percent of wall height), respectively. The maximum outward displacement of the front wall facing occurred at the elevation directly below the bridge sill.
- Movement of the leveling pad (located at the base of the GRS structure) was negligible, and the outward wall displacement tended to decrease toward the leveling pad.
- Both the rates of wall movements and the strain of geogrid reinforcements decreased with time.
- Outward wall displacement as inferred by the integration of the strain distribution curve with respect to the reinforcement length matched closely with that determined from surveying. This implies that little slippage between the soil and reinforcement had occurred.
- Probable causes for post-construction movements were traffic load, deformation under sustained load (creep), and seasonal variation.
- The GRS bridge abutment shows no sign of the “bridge bump” problem. The Founders/Meadows GRS bridge

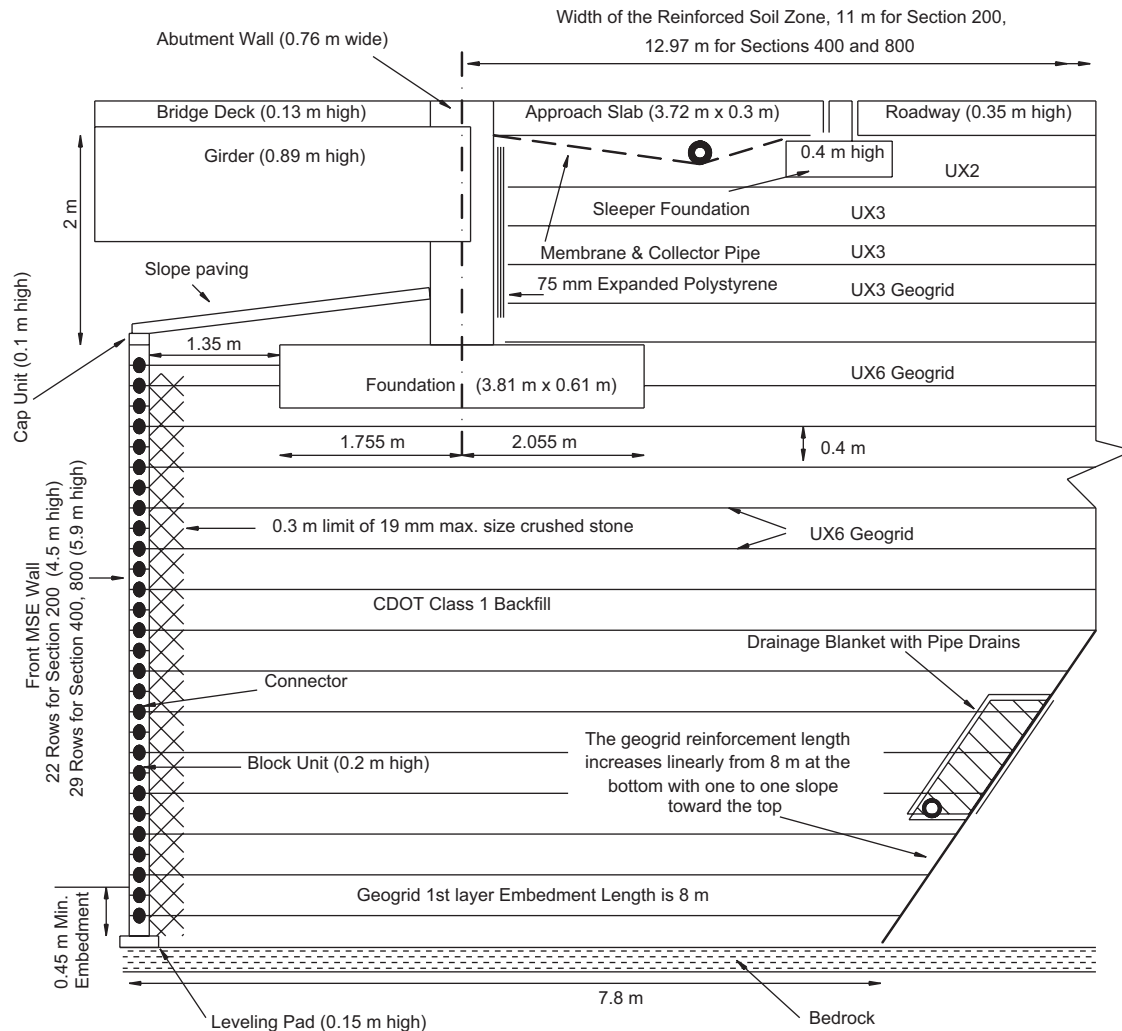


Figure 2-6. Typical cross-section of front and abutment walls, the Founders/Meadows bridge abutments (Abu-Hejleh et al., 2000).

abutment has exhibited excellent short- and long-term performance characteristics.

Abu-Hejleh et al. (2003) also indicated that the rate of creep reinforcement strain under service load decreased with time: a maximum increase of strain of 0.09 percent during the first year, a maximum increase of strain of 0.04 percent during the second year, and a maximum increase of strain of 0.02 percent during the third year in service. The largest reinforcement strain occurred directly beneath the bridge sill. The maximum reinforcement strain after about 33 months in service was 0.27 percent.

The Colorado DOT concluded that the general layout and design of future GRS abutments should follow those in the Founders/Meadows abutment. The GRS abutments work well for multiple span bridges, have the potential for eliminating the “bump at the bridge” problem, avoid disadvantages associated with the use of deep foundations, and allow for construction in stages and within a smaller working area.

The Colorado DOT provided the following guidelines for design and construction of GRS abutments:

1. The foundation soil for these abutments should be firm enough to limit the post-construction settlement of the bridge sill to 75 mm.
2. The designer should plan for a bridge sill settlement of at least 25 mm caused by the bridge superstructure loads.
3. The maximum tension line needed in the internal stability analysis should be assumed bilinear, starting at the toe of the wall and extending through a straight line to the back edge of the bridge sill at the mid height of the wall, and from there extending vertically to the back edge of the bridge sill.
4. Ideally, construction should take place during the warm and dry seasons.
5. The backfill behind the abutment wall should be placed before the girders.

Case A5: Feather Falls Trail Bridge Abutments, California (Keller and Devin, 2003)

A 12-m-long trail bridge was constructed in 1999 on the Feather Falls Trail in the Plumas National Forest in northern California. Because the project site was remote and without road access, the bridge materials had to be flown in with a helicopter. Because of the deeply incised and narrow channel, the abutments were placed well above the channel high-water level. GRS abutments were selected for this project because they use small, lightweight materials and are easy to construct.

Figure 2-7 shows the cross-section of the GRS abutments. The two abutments were 1.5 and 2.4 m high, and the wall facing comprised 0.15 m by 0.15 m treated timbers. Two polyester woven geotextiles of different strengths were used for the reinforcement. The top four layers of the reinforcements had an ultimate strength of 70 kN/m, while the remaining reinforcements had an ultimate strength of 52 kN/m, per ASTM D4595. The vertical reinforcement spacing was 0.15 m, and the average reinforcement length was 2.0 m. Most of the reinforcements were sandwiched and nailed between the facing timbers, but the top four reinforcements were wrapped around the outside of the facing timbers and covered with timber boards to ensure maximum connection strength and to protect the geotextiles.

Onsite rocky soil was used as the backfill and was compacted to 95 percent of its maximum dry density per AASHTO T-99. A geocomposite drain was placed behind each GRS

abutment, and each abutment had an embedment depth of 0.6 m to offer scour protection against a possible debris slide in the drainage.

The entire construction of the bridge took about 2 weeks with a crew of two people. The GRS abutments have performed well since the bridge was put in service.

Case A6: Alaska Bridge Abutments, Alaska (Keller and Devin, 2003)

Two GRS abutments, constructed in 1992, support a 15.1-m-long precast, double-tee concrete bridge in the Tongass National Forest in southeast Alaska. Because transportation and construction costs are high in this area, the bridge and abutment designs had to be economical and easy to construct, without the need for specialized equipment. Because the bridge is located in the tidal-influence zone, there were concerns about corrosion loss, so GRS abutments were selected over hot-dipped galvanized welded-wire walls, which commonly had been adopted in the area. The GRS abutments were 3.7 m high and had three vertical faces: a front wall paralleled to the stream alignment and two wing walls oriented at 90 deg and 77 deg relative to the front-face wall. The distance between the front wall face to the toe of the sill was 0.9 m, and the distance between the centerline of the bearing of the bridge to the front wall face was 1.5 m. The combination of dead and live design loads caused by bridge superstructure was limited to 240 kPa.

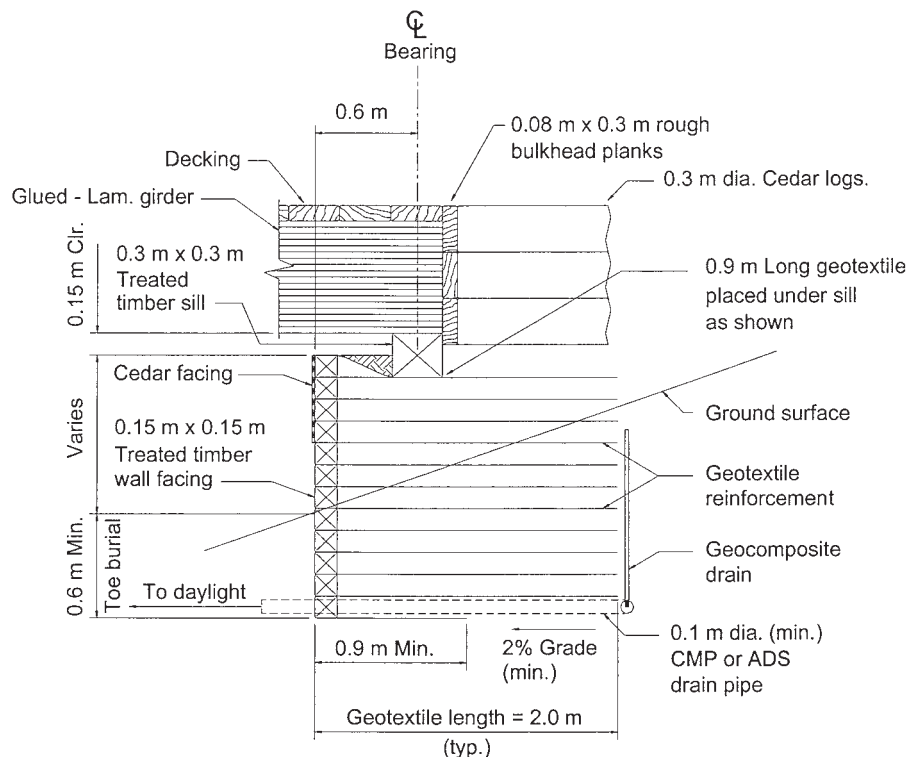


Figure 2-7. Cross-section of the Feather Falls Trail bridge abutments, California (Keller and Devin, 2003).

HDPE geogrids were used as the reinforcements. The base-to-height ratio for the front facing wall was 1:1 and was 0.7:1 for the two adjoining wing walls. The vertical spacing for the geogrid was 0.3 m near the base of the wall and 0.15 m near the top of the wall. Geogrids were wrapped around the timber facing, and 19 mm rebar drift pins were driven into pre-bored holes to hold the timber facing together. The full height of the wall was covered with 50-mm-thick treated timber board to protect the geogrids against UV degradation and floating debris. A free-draining granular material with maximum particle size of 25 mm was used as the backfill. The GRS abutments have performed well since construction.

Field Experiments of Bridge-Supporting Structures

The test conditions and measured performance of six field experiments of GRS bridge abutments and piers are described below. The six field experiments are the Garden experimental embankment in France (Gotteland et al., 1997), the FHWA Turner-Fairbank GRS bridge pier in Virginia (Adams, 1997), the Havana Yard GRS bridge pier and abutment in Colorado (Ketchart and Wu, 1997), the Fiber Reinforced Plastic (FRP) geogrid-reinforced retaining wall in Japan (Miyata and Kawasaki, 1994), the Chemie Linz full-scale GRS embankment in Austria (Werner and Resl, 1986), and the Trento test wall in Italy (Benigni et al., 1996).

Case B1: Garden Experimental Embankment, France (Gotteland et al., 1997)

A full-scale experiment was conducted in 1994 to investigate the failure behavior of GRS structures as bridge abutments, referred to as the “Garden” program (*Geotextile: Application en Reinforcement, experimentation et Normalisation*). A 4.35-m-high embankment was constructed for the experiment, as shown in Figure 2-8. The test embankment was divided into two symmetrical parts corresponding to two different embankment profiles: the NW wall and the W wall. A fine sand used as backfill was compacted at its maximum standard Proctor density. The backfill had a dry unit weight of 16.6 kN/m³, friction angle of 30 deg, and cohesion of 2 kPa. Segmental concrete blocks were used as the facing. The NW wall was reinforced by a nonwoven geotextile with a tensile strength of 25 kN/m at 30 percent strain. The W wall was reinforced with a knitted woven geotextile with a tensile strength of 44 kN/m at 15 percent strain. The reinforcement spacing was 29 cm.

The reinforced embankment was loaded in the same way as a bridge deck through a foundation slab. The 1.0-m-wide foundation was 1.5 m from the edge of facing. The embankment was loaded by a beam acted on by two thrust rams, each restrained by four tie-bars anchored into the embankment foundation.

The test embankment was instrumented to monitor the performance of the embankment during loading. Two months

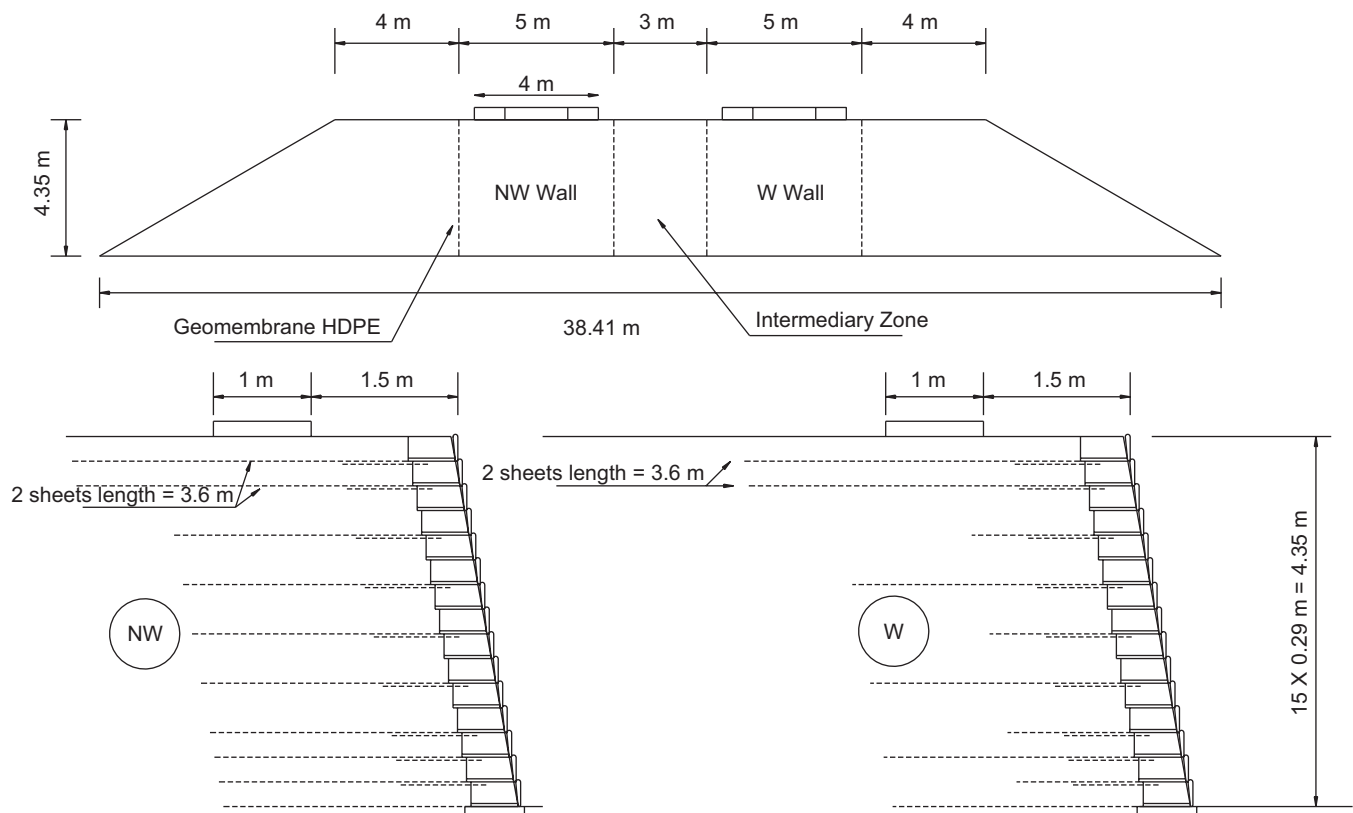


Figure 2-8. The Garden experimental embankment, France (Gotteland et al., 1997).

after the construction of the reinforced embankment, a load was applied to the foundation on the top of the structure until failure occurred. The load was applied over 2 days. The experiment was terminated when a permissible facing displacement was reached (0.20 m maximum horizontal displacement for the NW wall and 0.15 m for the W wall). The structure was examined layer by layer by careful excavation at the end of the experiment.

A localized failure was noted to have occurred at the upper layers of the NW wall (with a nonwoven geotextile), whereas the W wall (with woven geotextile) experienced a deeper failure with a downstream tilting effect giving rise to a wide surface crack at the upstream end of the geotextile sheets. However, the main deformation occurred at the upper layers for both walls. The load-settlement curves for two walls showed a distinct break point that corresponds to two distinct slopes of the curves. The “critical loads” at the break point for the NW wall and the W wall were quite large, 140 kN/m and 123 kN/m respectively. The corresponding settlements were 36 mm and 33 mm, respectively. The lower “critical load” of the W wall can be attributed to its shorter “intermediate” reinforcement (see Figure 2-8), even though the reinforcement had higher strength than that of the NW wall.

Case B2: FHWA Turner-Fairbank GRS Bridge Pier, Virginia (Adams, 1997)

A full-scale bridge pier was constructed and load tested at the Turner-Fairbank Highway Research Center, FHWA, in McLean, Virginia. The pier was 5.4 m high and 3.6 m by 4.8 m at its base. The pier was supported on a reinforced soil foundation (RSF). The RSF comprised compacted road

base and three layers of biaxial geogrid reinforcement, spaced 0.3 m apart. The RSF was 1.2 m deep, over an area of 7.3 m by 7.5 m. Figure 2-9 shows the cross-section of the GRS bridge pier.

The pier was constructed with modular concrete blocks as the facing and was reinforced with a polypropylene woven geotextile, Amoco 2044, at vertical spacing of 0.2 m. Because the geotextile was stronger in the cross-machine direction (38 kN/m at 5 percent strain) than in the machine direction (21 kN/m at 5 percent strain), the width and length directions were alternated between layers. The backfill was classified as a well-graded gravel. The maximum dry unit weight was 24 kN/m³, per AASHTO T-99, with the optimum moisture content being 5.0 percent. The average compaction in the field was about 95 percent of the maximum dry density.

The FHWA Turner-Fairbank pier was load-tested by applying vertical loads on top of the backfill in two loading cycles. The first loading cycle was performed when the pier height was 3.0 m. The 3.0-m-high pier was loaded to about 600 kPa. The settlement varied roughly linearly with the applied load. At 200 kPa, the settlement was about 13 mm, and at 600 kPa, the settlement was about 34 mm. The maximum lateral displacements at 200 kPa and 600 kPa were about 6 mm and 20 mm, respectively.

The second loading cycle was performed when the pier was at its full height. The second loading cycle was conducted in three parts:

1. The pier was incrementally loaded to 415 kPa and then held for 100 minutes;
2. The load was then ramped up to 900 kPa and held for 150 minutes and unloaded; and

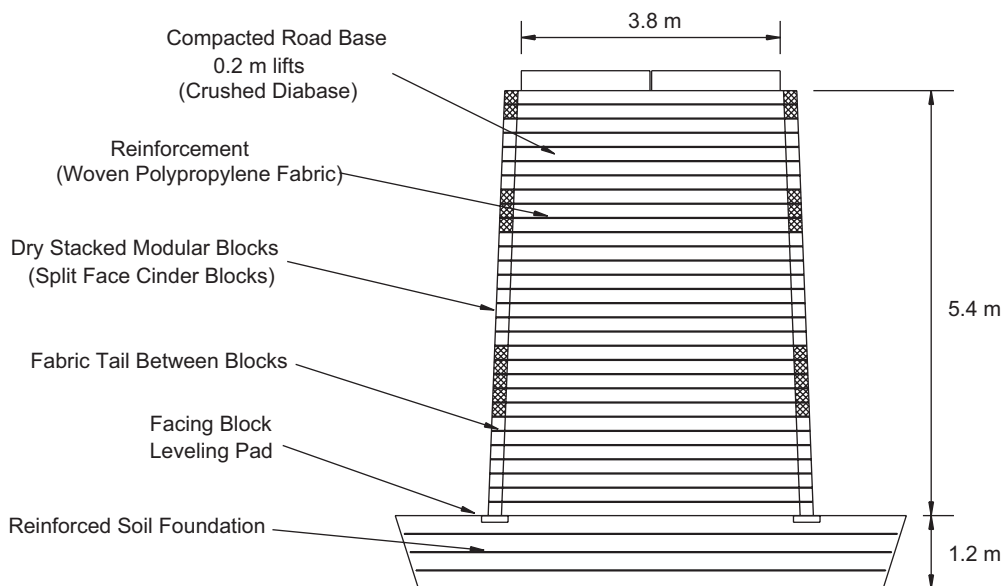


Figure 2-9. Cross-section of the FHWA Turner-Fairbank GRS bridge pier (Adams, 1997).

- The pier was reloaded to 415 kPa and then held for 100 minutes.

At 415 kPa pressure, the pier settled about 25 mm; at 900 kPa, the settlement was about 70 mm. During the reload cycle, settlement was roughly reduced by a factor of two. At 200 kPa, the pier deformed laterally less than 3 mm. The maximum strain in the reinforcement was recorded near the middle of the pier and was about 2.3 percent. The reinforcement strain in the first loading cycle at 400 kPa was about 0.5 percent.

Based on the measured results, the following conclusions were made:

- At 200 kPa of loading, the GRS pier performed very satisfactorily. The maximum strain in the reinforcement was 0.25 percent. The maximum lateral displacement was 3 mm, yet no cracks occurred in the facing blocks. For the full-height load tests, the vertical settlement was about 15 mm in the initial load cycles and about 5 mm during the reload cycles.
- Preloading reduced vertical settlement by about 50 percent and limited the vertical creep deformation. Preloading did not reduce lateral deformation.

- At 200 kPa, creep was not a concern in a closely spaced reinforced soil system with a well-compacted granular backfill.

Case B3: Havana Yard GRS Bridge Pier and Abutment, Denver, Colorado (Ketchart and Wu, 1997)

The Havana Yard GRS bridge supporting structures, consisting of two piers and one abutment, were constructed inside a 3.5-m-deep pit. The outer pier and the abutment were 7.6 m tall, and the center pier was 7.3 m tall. The center pier and the abutment were of a rectangular shape, and the outer pier was of an oval shape. The base of the outer pier, the center pier, and the abutment were, respectively, 2.4 m by 5.2 m (major and minor axes), 2.1 m by 4.8 m, and 3.6 m by 5.2 m. Segmental concrete blocks, each 0.2 m in height, were used as the facing element for all three structures. On the east face of the abutment, the facing assumed a 13 percent “negative batter” up to a height of 3.5 m. From 3.5 m to the top of the abutment were walking steps. Figure 2-10 shows the cross-section of the Havana Yard GRS bridge pier and abutment.

The backfill was a “road base” material containing 13 percent of fines. The maximum dry unit weight was 21.2 kN/m³,

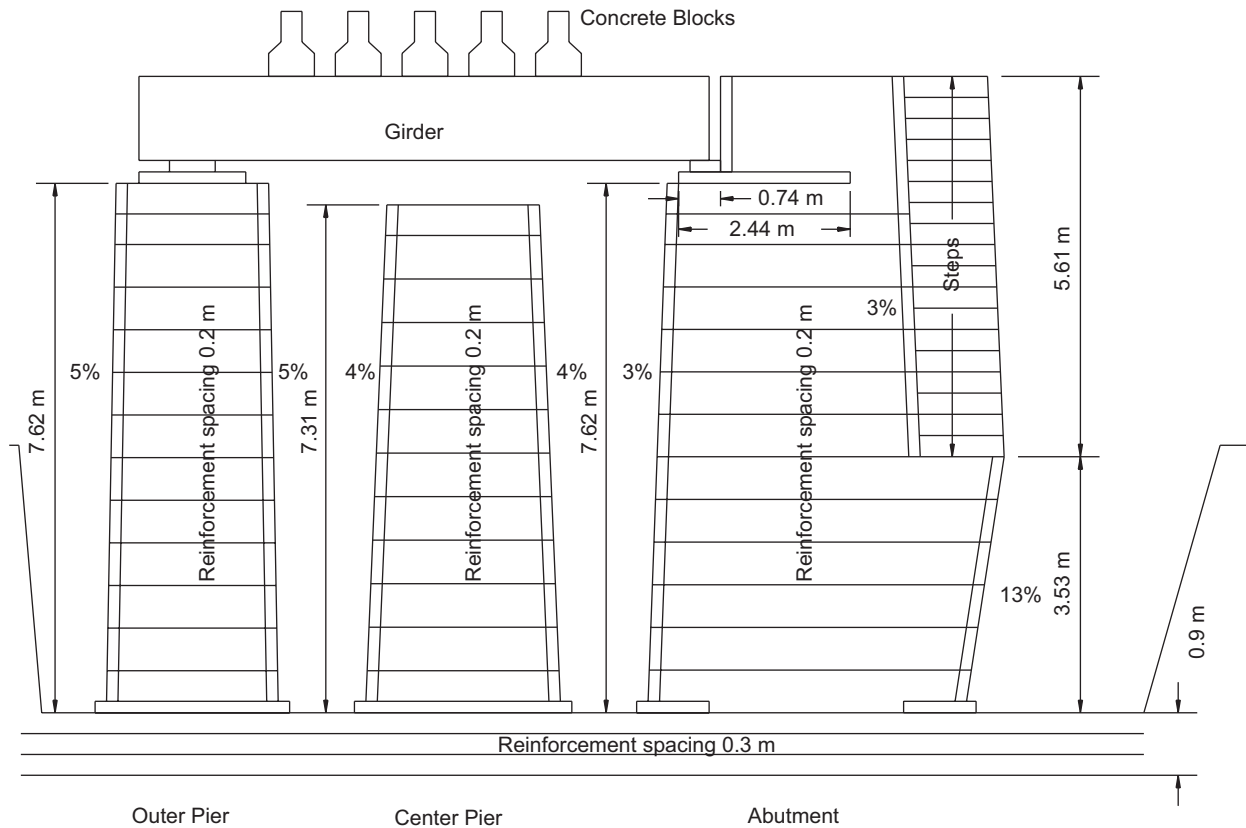


Figure 2-10. Cross-section of the Havana Yard GRS bridge pier and abutment, Denver, Colorado, (Ketchart and Wu, 1997).

and the optimum moisture content was 6.7 percent, per AASHTO T-180. The field measured average dry unit weight was 19.1 kN/m³ (or 90 percent relative compaction) in the center pier and the abutment. The average placement moisture was 2.5 percent for the center pier and 1.6 percent for the abutment. The fill density of the outer pier was believed to be significantly lower than these measured values because a lighter compaction plant was employed for the outer pier because of its size and shape.

The reinforcement for all three structures was a woven polypropylene geotextile (Amoco 2044) with a wide width tensile resistance at 5 percent strain in the machine and cross-machine directions of 38 kN/m and 21 kN/m, respectively. The vertical spacing of the geotextile reinforcement was 0.2 m. The top four layers of the reinforcement in the abutment employed a wrapped-around procedure behind the facing block. A center geotextile “tail,” 1.2 m in length, was placed between each of these four layers to connect the backfill to the facing blocks.

On top of the outer pier and the abutment were 0.3-m-thick concrete pads to support steel bridge girders. The concrete pads were 0.9 m wide and 3.1 m long for the piers and 2.4 m wide and 3.7 m long for the abutment. The clearance distance of the concrete pad was 0.2 m from the back face of the facing blocks.

For loading tests, three steel bridge girders were placed over the top concrete pads of the outer pier and the abutment. Each girder was supported by steel bearing plates resting on the concrete pads. The steel bearing plates were located along the centerline of the top concrete pads. The span of the girders was 10.4 m. A total of 124 concrete blocks was placed on the girders. The total load was 2,340 kN, corresponding to an applied pressure of 232 kPa and 130 kPa on the outer pier and abutment, respectively.

The findings and conclusions of this project as summarized by the authors are as follows:

- The displacements of the pier and the abutment were comparable at applied load of 2,340 kN. The maximum vertical displacement was slightly higher in the outer pier than in the abutment. The maximum vertical displacements were 27.1 mm in the abutment and 36.6 mm in the outer pier, corresponding to 0.35 percent and 0.48 percent of the structure height. The maximum lateral displacement in the abutment was somewhat higher than that in the outer pier. The maximum lateral elongation of the perimeter was 4.3 mm in the abutment and 12.7 mm in the outer pier.
- The ratio of the vertical movement to the structure height at 232 kPa of the outer pier (0.48 percent) was higher than that of the FHWA Turner-Fairbank pier (0.30 percent). This may be attributed to the much lower compaction effort on the outer pier. The reinforcement strains in the fill direction of the outer pier and the FHWA Turner-Fairbank pier, however, were of similar magnitude (0.2 percent to 0.4 percent). This suggests that the lateral movements of these piers are comparable.
- Under a sustained load of 2,340 kN for 70 days, the creep displacements in both vertical and lateral directions of the outer pier were about 4 times larger than those in the abutment because of lower compaction effort of the outer pier. The maximum vertical creep displacement was 61.6 mm in the outer pier and 18.3 mm in the abutment. The maximum lateral creep displacement was 59.5 mm in the outer pier and 14.3 mm in the abutment.
- A significant part of the maximum vertical and lateral creep displacements of the pier and the abutment occurred in the first 15 days. At 15 days, the maximum vertical and lateral creep displacements were about 70 percent to 75 percent of the creep displacements at 70 days in respective directions.
- Creep deformation of the structures decreased with time. The vertical creep rates reduced nearly linearly (on log-log scale) with time. The creep rate of the outer pier (7.5 mm/day after 3 days and 0.1 mm/day after 70 days) was higher than that of the abutment (2.2 mm/day after 3 days and 0.03 mm/day after 70 days).
- Hairline cracks of the facing blocks occurred in the outer pier and the abutment because of the lateral bulging and the down-drag force because of the friction between the backfill and the facing blocks. Installing flexible material (i.e., cushion) between vertically adjacent blocks may have alleviated this problem.
- The maximum strains in the reinforcement were less than 1.0 percent. Compared with the rupture strain of the reinforcement of 18 percent, the safety margin against rupture of reinforcement appeared to be very high.
- The calculated lateral displacements from the reinforcement strain distribution were in very good agreement with the measured lateral displacements.
- With the less stringent construction condition (using a lightweight vibrating compaction plate), the outer pier showed about 1.5 times larger vertical displacement-to-height ratio than the Turner-Fairbank pier; whereas the lateral displacements were similar.

Case B4: FRP Geogrid-Reinforced Retaining Wall, Japan (Miyata and Kawasaki, 1994)

The FRP geogrid-reinforced test embankment consisted of three types of GRS retaining walls, referred to as Types A, B, and C (see Figure 2-11). The test embankment had a height of 5.0 m with a 0.3H:1V slope. Type A had a soft wall face with gabions only, Type B had a cement-treated wall face, and Type C was a gravity retaining wall made of cement-treated soil. An FRP geogrid, having a tensile strength of 49 kN/m at 2 percent strain, was used as reinforcement.

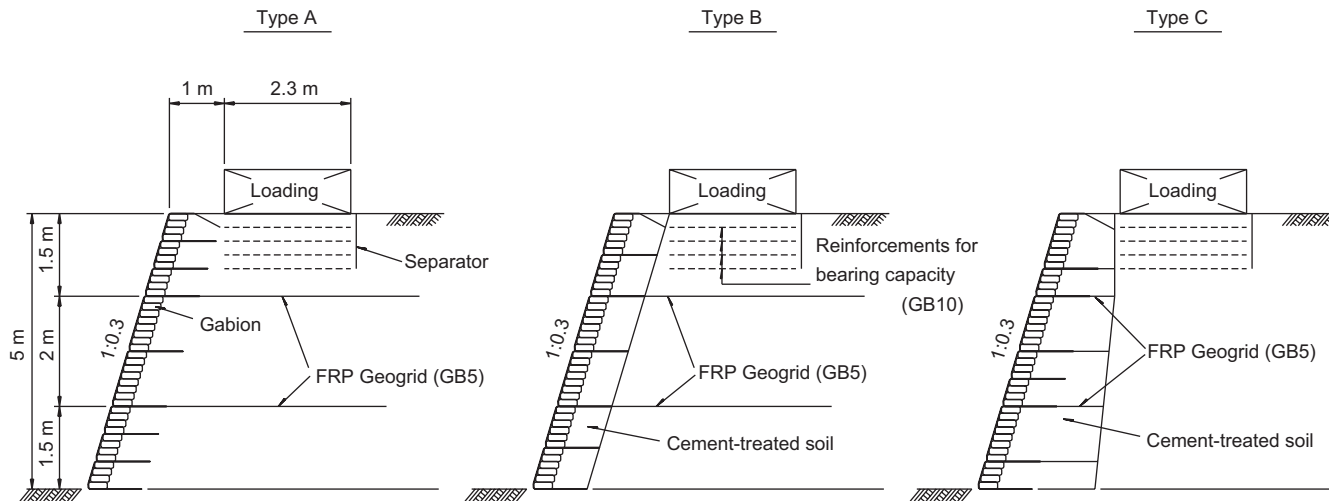


Figure 2-11. Cross-section of the FRP geogrid-reinforced retaining wall, Japan (Miyata and Kawasaki, 1994).

To perform the load test, a 2.3-m-wide loading frame was first placed on the top of the embankment at 1.0 m from the front wall face. Loads were then applied by inserting loading steel plates into the loading frame in steps up to a total weight of 590 kN ($q = 127$ kPa). The lateral displacement of Type A was much larger than those of Types B and C. The maximum values were about 40 mm, 25 mm, and 20 mm for Types A, B, and C, respectively. In addition, the deformation mode of Type A differed from Types B and C. Type A, with a soft wall face, showed a swell-out mode with the maximum lateral movement occurring at about the mid-height of the wall. Types B and C, with a rigid wall surface, showed a forward fall-down mode with the maximum movement occurring at the top of the wall.

Case B5: Chemie Linz Full-Scale GRS Embankment, Austria (Werner and Resl, 1986)

A multi-layered geotextile reinforced embankment was built in 1981 and had been exposed to 3 years of extreme climatic fluctuations and environmental influences by the time it was loaded in 1984. The height of the embankment was 2.4 m. Figure 2-12 shows the geometry and loading scheme of the Chemie Linz full-scale GRS embankment. A silty gravelly sand was used as backfill. The design shear strength parameters of the backfill were $\phi = 21^\circ$, $c = 20$ kN/m², and the bulk unit weight was 19.3 kN/m³. A polypropylene needle-punched nonwoven geotextile, with tear strength = 16 kN/m, grab strength = 1,200 N, and elongation at failure = 80 percent, as determined with DIN 53815 (German Standards: testing of textiles) was used as reinforcement. The vertical reinforcement spacing was 0.35 m. Wrapped facing was adopted for the structure.

Seven steel slabs, each measuring 3 m by 1.3 m by 0.2 m, and two steel cylinders of 0.8 m in diameter were used to load the GRS embankment, which produced a total load of

510 kN or 130 kN/m². Without rupture or critical deformation occurring, the load of 130 kN/m² corresponded to 1.7 times the theoretical breaking load, as determined from Bishop's lamella circular sliding surfaces method. The measured maximum vertical settlement and lateral displacement of the embankment face were about 16 cm and 11 cm, respectively.

Case B6: Trento Test Wall, Italy (Benigni et al., 1996)

A 5-m-high test wall, referred to as the Trento test wall, was constructed in Northern Italy. A well-graded cohesionless sandy gravelly soil, with shear strength parameters $c' = 100$ kPa and $\phi' = 40^\circ$ determined from the CD triaxial tests, was used as backfill. It had a dry unit weight of 19.6 to 20.4 kN/m³ with in situ water content of 2.4 to 5.5 percent. Wrapped wall face was adopted for the wall. A geocomposite, with tensile strength of 27 kN/m at 16 percent strain per DIN EN ISO 10319 (German Standards: geotextiles wide-width tensile test), was used as reinforcement. The reinforced section of the wall was constructed in lifts separated by geocomposite layers and with the final spacing being 0.5 m. The reinforcement length was 2.0 m (40 percent of the wall height). Figure 2-13 shows the cross-section of the test wall.

During construction, the wall face was supported by 1-m-high wooden forms, assembled with wide long boards nailed to brackets, which were wedged against a temporary scaffold. On completion of each lift, the underlying geosynthetic was wrapped around at the face and extended 2 m inside the backfill. A new reinforced layer was then unrolled parallel to the wall face and positioned so that a 0.5-m-long tail rested on top of the one already wrapped around, while the remaining 2.5-m-long part draped over the wooden form. No windrows were used to anchor the reinforcement in the backfill.

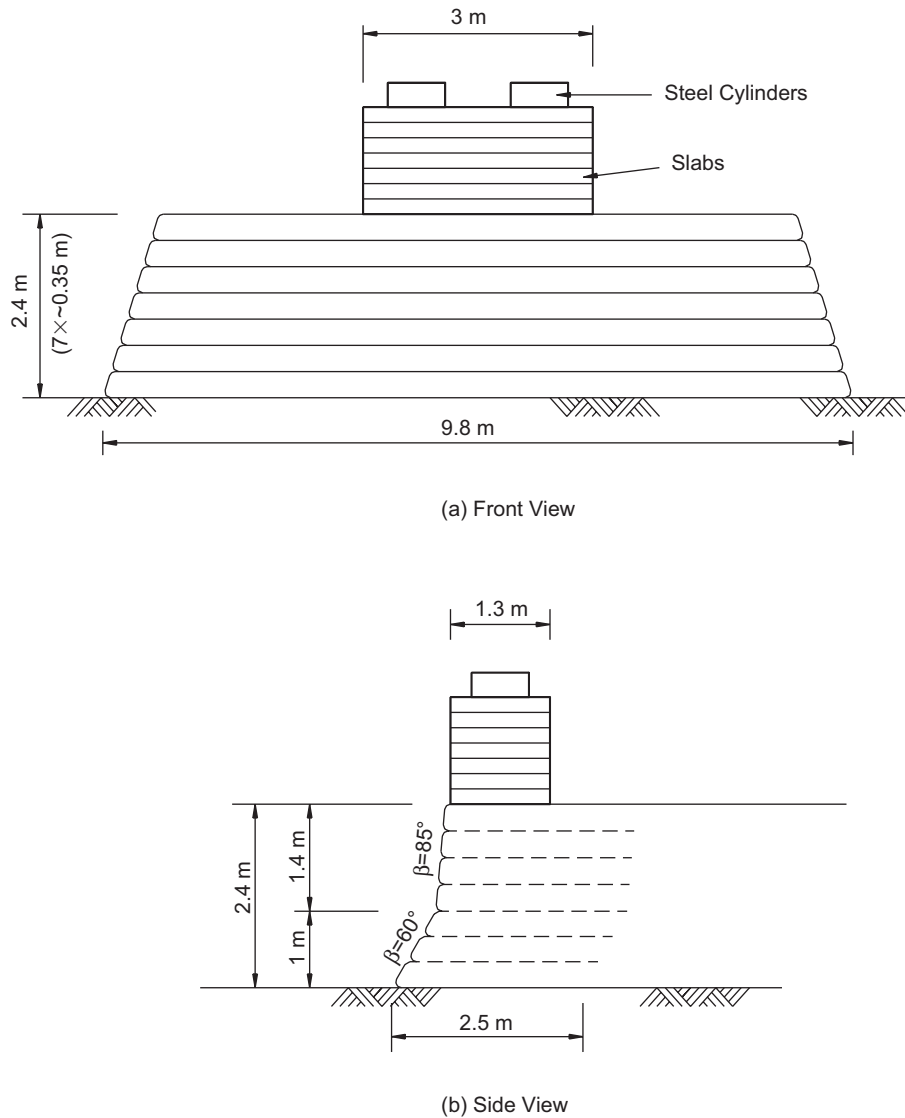


Figure 2-12. Geometry and loading scheme of the Chemie Linz full-scale GRS embankment, Austria (Werner and Resl, 1986).

The loading test was performed by the weight of the stacked iron ingots evenly distributed over two 3 m by 3 m wide loading platforms placed on top of the wall. The maximum surcharge loading, reached after 51 hours, was estimated at 84 kPa. The wall did not collapse under the applied load, although somewhat large movements were recorded. In addition, although most of the horizontal and vertical displacements were not recovered on unloading, it appeared that the wall had sustained almost no damage.

Synthesis of Performance Characteristics

The main performance characteristics of the 12 case histories reviewed in this study, including six in-service GRS bridge abutments and six full-scale field experiments, are

summarized in Table 2-1. The performance characteristics include wall height, backfill, reinforcement type, reinforcement spacing, facing type and connection, ratio of reinforcement length to wall height, maximum settlement of loading slab, maximum lateral movement of the wall face, maximum reinforcement strain, and failure pressure.

Based on the measured performance, the following observations are made in relation to performance, design, and construction of GRS bridge-supporting structures:

- GRS bridge abutments with flexible facings are indeed a viable alternative to conventional bridge abutments. All six in-service GRS bridge abutments (Cases A1 through A6) exhibited satisfactory performance characteristics under service loads. The maximum settlements and maximum lateral displacements for all the abutments were

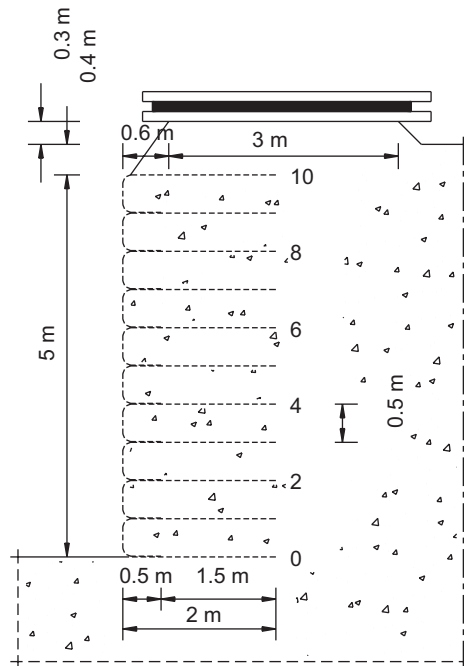


Figure 2-13. Cross-section of the Trento test wall, Italy (Benigni et al., 1996).

under the tolerable movement criteria that were based on experience with real bridges—102 mm for settlement and 51 mm for lateral displacement (Grover, 1978; Bozozuk, 1978; Walkinshaw, 1978; Wahls, 1990).

- With a well-graded and well-compacted granular backfill and with closely spaced reinforcement (e.g., 0.2 m vertical spacing), the load carrying capacity of a GRS bridge supporting structure is very high (as high as 900 kPa in Case B2). The load-carrying capacity would be significantly smaller (e.g., 120 to 140 kPa in Case B1) if the backfill is of lower strength and the reinforcement is not of sufficient length (e.g., Case B1 where reinforcement extended only 0.3 m beyond the back edge of the sill).
- With a well-graded and well-compacted granular backfill, the maximum settlement of the loading slab and the maximum lateral movement of the wall face are very small under service loads (e.g., Cases A1, A4, and B2). With a lower quality backfill (as in Case B5, where the backfill was a silty gravelly sand with $c = 20$ kPa and $\phi = 21$ deg and in Case A2, where the backfill was a fine sand with $\phi = 32$ deg), the displacements would be significantly larger.
- Fill placement density seems to play a major role in the performance of the GRS structures. For instance, Case B3 experienced 50 percent larger settlement than Case B2, even though the two GRS piers used the same reinforcement and the same reinforcement spacing. The difference in settlement resulted primarily from the difference in fill placement density and fill type.
- Preloading can significantly reduce post-construction settlement of a GRS abutment (as in Cases A3 and B2)

by a factor of 2 to 6, depending on the initial placement density. In situations where the foundation soil is of different thickness, preloading is an effective means to reduce differential settlement (as in Case A3).

- With a well-graded and well-compacted granular backfill, long-term creep under service loads can be negligibly small, as evidenced by Cases A4 and B2.
- The maximum tensile strains in the reinforcement were in the range of 0.1 percent to 1.6 percent under service loads, with larger maximum strains being associated with lower strength backfill (e.g., 1.6 percent maximum strain in Case A2).
- Reinforcement length and reinforcement type appeared to have only secondary effect on the performance characteristics.
- The “sill clearance distance” (i.e., the distance between front edge of sill and back face of wall facing) employed in the cases vary fairly widely, from 0.2 m in Case B3 to 2.2 m in Case A2. A larger sill clearance will result in a longer bridge deck, thus higher costs, and may compromise stability if the reinforcement is not sufficiently long (e.g., Case B1).

THE NCHRP FULL-SCALE EXPERIMENTS

Two full-scale experiments of segmental GRS bridge abutments, as shown in Figure 2-14, were conducted at the Turner-Fairbank Highway Research Center in McLean, Virginia. The purposes of the full-scale experiments were to (1) examine the behavior of segmental GRS abutments subject to various load levels and (2) furnish a complete set of data (including material properties, material placement conditions, loading history, and measured and observed behavior) for verification of the analytical model employed in this study.

Description of Test Sections

The full-scale bridge abutments in the experiments consisted of two test sections. The two test sections were in a back-to-back configuration, as shown in Figure 2-15. The abutments were 4.65 m tall. Each test section had four components: (1) an abutment wall, (2) two wing walls, (3) a GRS mass, and (4) a sill on the top surface of the GRS mass near the edge of the wall facing. The geometry of the back-to-back test sections and the loading mechanism are shown in Figure 2-15. The back-to-back configuration had some advantages: (a) it eliminated the need to construct an approach fill or a retaining wall behind the abutment, thus reducing the amount of earthwork involved in the experiments; (b) it resulted in more consistent compaction of the fill across the two test sections—a key feature to the success of the experiments; (c) it allowed the behavior of wing walls to be examined; (d) it avoided interferences

(text continued on page 30)

TABLE 2-1 Case studies of GRS bridge-supporting structures with a flexible facing

Case	Height	Backfill	Reinf. Type	Reinf. Spacing	Facing Type and Facing Connection	Reinf. Length to (Lower) Wall Height Ratio	Maximum Settlement of Loading Slab	Maximum Lateral Movement of Wall Face	Maximum Reinf. Strain	Failure Pressure	Note
Vienna Railroad Embankment (Case A1)	2.1 m	$c = 0$ $\phi = 35^\circ$ $\gamma = 21 \text{ kN/m}^3$	Needle-punched nonwoven geotextile with $T_{ult} = 23 \text{ kN/m}$ @ $\epsilon = 45\%$	0.3 m	Wrapped face	0.8	1 mm under traffic load (60 kPa)	Not reported	Not reported	Not loaded to failure	
New South Wales GRS Bridge Abutments (Case A2)	6.5 m and 9.5 m	Compacted fine sand $\phi = 32^\circ$ $\gamma_{dry(max)} = 1.6 \text{ t/m}^3$ (95% "standard relative density")	Tensar HDPE geogrid SR 110 with $T_{ult} = 110 \text{ kN/m}$ @ $\epsilon = 11.2\%$	0.4 m and 0.5 m	Keystone blocks, with fiberglass dowels	1.2 to 1.6	80 mm @ service load	26 mm @ service load	1.6% @ service load	Not loaded to failure	Tiered (terraced) construction; sill clearance distance = 2.2 m
Black Hawk Bridge Abutments (Case A3)	4.5 m and 7.5 m (lower wall)	Silty clayey sand $c = 34 \text{ kPa}$ $\phi = 31^\circ$ $\gamma_{dry} = 15.8 \text{ kN/m}^3$ (91% of T-99) $w = 12\%$ (2% dry of optimum)	Amoco 2044, polypropylene woven geotextile with $T_{ult} = 70 \text{ kN/m}$ @ $\epsilon = 18\%$	0.3 m	Natural rocks, with friction connection	0.7 to 1.2	Initial Loading: 4.9 to 28 mm @ 150 kPa; Reloading: 2.5 to 4.5 mm @ 150 kPa	Initial Loading: 1.5 to 13 mm @ 150 kPa; Reloading: 0.6 to 4.5 mm @ 150 kPa	0.2% @ 80 kPa	Not loaded to failure	Preloading reduced differential settlements from 21.6 mm to less than 1.0 mm; sill clearance distance = 1.5 m
Founders / Meadows Bridge Abutments (Case A4)	4.5 m and 5.9 m (lower wall)	Gravelly sand $\gamma_{dry} = 21 \text{ kN/m}^3$ (95% of T-180) $w = 5.6\%$ (3.2% dry of optimum w/o gravels)	Tensar HDPE geogrid UX6, UX3, & UX2, with $T_{ult} = 157, 64, \& 39 \text{ kN/m}$, respectively	0.4 m	Mesa concrete block, with plastic Mesa connectors	2.7 and 3.5	11 mm @ service load (150 kPa) after 18 months in service	13 mm @ service load (150 kPa) after 18 months in service	0.27 % after 33 months in service	Not loaded to failure	Small creep under service load; sill clearance distance = 1.35 m

TABLE 2-1 (Continued)

Case	Height	Backfill	Reinf. Type	Reinf. Spacing	Facing Type and Facing Connection	Reinf. Length to (Lower) Wall Height Ratio	Maximum Settlement of Loading Slab	Maximum Lateral Movement of Wall Face	Maximum Reinf. Strain	Failure Pressure	Note
Feather Falls Trail Bridge Abutments (Case A5)	1.5 m and 2.4 m	On-site rocky soil (95% of T-99)	Polyester woven geotextiles with $T_{ult} = 52$ and 70 kN/m	0.15 m	Treated timber	1.3 and 0.8	Not reported	Not reported	Not reported	Note loaded to failure	Total cost = $\$320/m^2$ of wall face; no "bridge bump"
Alaska Bridge Abutments (Case A6)	3.7 m	Free-draining granular material with maximum particle size of 25 mm	HDPE geogrid	0.3 m and 0.15 m	Treated timber, with 19 mm rebar drift pins	1.0 and 0.7	Not reported	Not reported	Not reported	Not loaded to failure	Total cost = $\$452/m^2$ of wall face; no "bridge bump"; sill clearance distance = 0.9 m
Garden Experimental Embankment (Case B1)	4.35 m	Compacted fine sand $c = 2$ kPa $\phi = 30^\circ$ $\gamma_{dry} = 16.6$ kN/m ³	Nonwoven geotextile ($T_{ult} = 25$ kN/m @ $\epsilon = 30\%$) and woven geotextile ($T_{ult} = 44$ kN/m @ $\epsilon = 15\%$)	0.54 m (with "tails" for woven reinf.); 0.29 m below sill	Concrete cells, with transverse synthetic bars	0.6	36 mm @ 140 kPa for nonwoven section; 33 mm @ 123 kPa for woven section	Not reported	0.15% for nonwoven geotextile; 0.06% for woven geotextile	Critical load = 140 kPa for nonwoven section (localized failure near the top); critical load = 123 kPa for woven section (deeper failure)	Sill clearance distance = 1 m; other than the top two sheets, reinforcement only extended 0.3 m beyond the edge of sill

TABLE 2-1 (Continued)

Case	Height	Backfill	Reinf. Type	Reinf. Spacing	Facing Type and Facing Connection	Reinf. Length to (Lower) Wall Height Ratio	Maximum Settlement of Loading Slab	Maximum Lateral Movement of Wall Face	Maximum Reinf. Strain	Failure Pressure	Note
FHWA Turner-Fairbank GRS Bridge Pier (Case B2)	5.4 m	Well-graded gravel $\gamma_{dry} = 23 \text{ kN/m}^3$ (95% of T-99) $w = 3$ to 7% ($\pm 2\%$ of optimum)	Amoco 2044, polypropylene woven geotextile with $T_{ult} = 70 \text{ kN/m}$ $@\epsilon = 18\%$	0.2 m	Cinder blocks, with friction connection	0.7 to 0.9	Initial Loading: 15 mm @ 200 kPa; 27 mm @ 415 kPa; 70 mm @ 900 kPa; Reloading: 8 mm @ 200 kPa; 13 mm @ 415 kPa	Initial Loading: 3 mm @ 200 kPa; 9 mm @ 415 kPa; 35 mm @ 900 kPa; Reloading: 3 mm @ 200 kPa; 9 mm @ 415 kPa	2.3% @ 900 kPa	Not loaded to failure	Constructed with a well-compacted granular fill and small reinforcement spacing, the pier was loaded to 900 kPa without failure
Havana Yard GRS Bridge Pier and Abutment (Case B3)	7.6 m	Road base material For abutment: $\gamma_{dry} = 19 \text{ kN/m}^3$ (90% of T-180) $w = 1.6\%$ (5% of dry optimum) For pier: lower density than abutment	Amoco 2044, polypropylene woven geotextile with $T_{ult} = 70 \text{ kN/m}$ $@\epsilon = 18\%$	0.2 m	Cinder blocks, with friction connection	Abutment: 0.6 (typ.) Pier: 0.3 to 0.7	Abutment: 27 mm @ 130 kPa Pier: 37 mm @ 230 kPa	Abutment: 14 mm @ 130 kPa Pier: 13 mm @ 230 kPa	Abutment: 0.2% @ 130 kPa Pier: 0.4% @ 230 kPa	Not loaded to failure	Due to lower placement density, the pier experienced 50% larger settlement than the FHWA pier; sill clearance distance = 0.2 m

TABLE 2-1 (Continued)

Case	Height	Backfill	Reinf. Type	Reinf. Spacing	Facing Type and Facing Connection	Reinf. Length to (Lower) Wall Height Ratio	Maximum Settlement of Loading Slab	Maximum Lateral Movement of Wall Face	Maximum Reinf. Strain	Failure Pressure	Note
FRP Geogrid-Reinforced Retaining Wall (Case B4)	5.0 m (H:V = 3:10)	Not reported	FRP (Fiberglass Reinforced Plastic) geogrid, with $T_{fail} = 49$ kN/m @ $\epsilon = 2\%$	FRP spacing = 1.5 to 2.0 m; tail spacing = 0.5 to 1.0 m; spacing below sill = 0.25 m	Gabions (plastic bags filled with gravel)	0.9	Not reported	40 mm @ 130 kPa	Not reported	Not loaded to failure	Very large reinforcement spacing (except directly beneath sill, with separate reinforcement for bearing capacity)
Chemie Linz Full-Scale GRS Embankment (Case B5)	2.4 m	Silty gravelly sand $c = 20$ kPa $\phi = 21^\circ$ $\gamma = 19.3$ kN/m ³	Polyfelt TS 400, polypropylene needle-punched nonwoven geotextile ($T_{ult} = 16$ kN/m @ $\epsilon = 80\%$, weight = 350 g/m ²)	0.35 m	Wrapped face	1.0	160 mm @ 130 kPa	110 mm @ 130 kPa	Not reported	Not loaded to failure	Structure loaded to 1.7 times the theoretical failure load; little creep
Trento Test Wall (Case B6)	5.0 m	Sandy gravelly soil $c = 100$ kPa $\phi = 40^\circ$ 96 to 100% of T-99 $w = 2.2$ to 5.3% dry of optimum	Polyfelt PEC 50/25, a geocomposite with $T_{ult} = 27$ kN/m @ $\epsilon = 16\%$	0.5 m	Wrapped face	0.35	50 mm @ 84 kPa	90 mm @ 130 kPa	Not reported	Not loaded to failure	

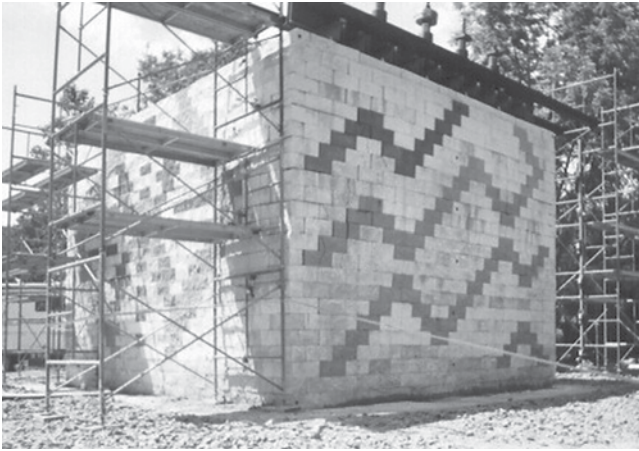


Figure 2-14. The NCHRP full-scale test abutment.

from test sections to its right or left; and (e) it allowed the sill to be loaded without rotating in the longitudinal direction of the abutment because of uneven loading (if the test sections had been in a side-by-side configuration).

The test abutments were constructed over a rigid floor. The rigid floor was a reinforced concrete mat measuring 9.1 m long, 7.3 m wide, and 0.9 m thick. The vertical spacing of the geosynthetic reinforcement for both test sections was 0.2 m in all layers. A concrete “cinder” block of dimensions 194 mm by 194 mm by 397 mm and with a split-face was used as a facing element. The front of each reinforcement sheet was placed between vertically adjacent facing blocks. No pins or any mechanical connectors were used between facing blocks. There was only frictional connection between the facing blocks and the reinforcement sheets. The length of all the reinforcements (“primary reinforcements”) was 3.15 m. In addition to the primary reinforcements, short “intermediate reinforcements” (1.3 m long) were placed at

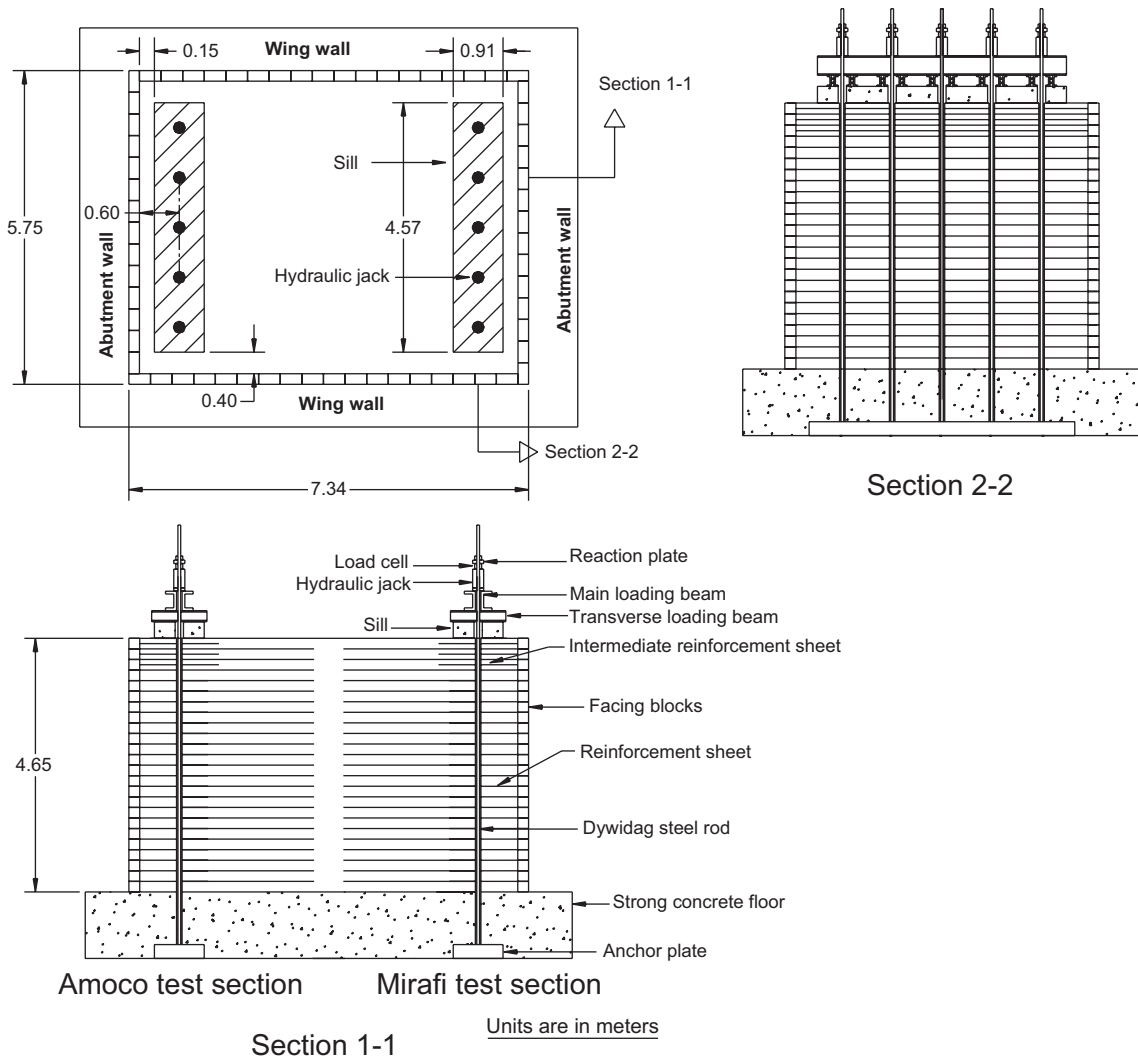


Figure 2-15. Configuration of the NCHRP full-scale test abutments.

the mid-height of the top three facing blocks. These intermediate reinforcements were placed immediately behind the facing block without connection to the facing.

Placed on the top surface of each test section was a 0.3-m-thick concrete sill. The sill was 0.91 m wide and 4.57 m long, with its centerline aligned with the centerline of the abutment. The sill clear distance, measured from the back face of the abutment facing blocks to the front edge of the sill, was 0.15 m. The left and right edges of the sill were 0.40 m away from the back face of the wing walls.

After the test abutment was constructed, a loading assembly was installed over the test section under the supervision of Michael Adams of the TFHRC. The loading assembly comprised a rigid floor (at the bottom of the assembly), hydraulic jacks (directly above the sill), steel rods (through the GRS mass), and reaction plates (at the top of the assembly). The rigid floor can accommodate up to 63 steel rods, each with a diameter of 44.5 mm (1.75 in.) with an allowable tensile load of 1,300 kN. Each steel rod was tied to an anchor base plate embedded in the rigid floor. Five steel rods were used for each test section. Vertical loads were applied on the sill through hydraulic jacks installed between the reaction plate and the sill. On applying hydraulic pressure to the jacks, the sill was pushed downward against the reaction plates and exerted vertical loads to the sill, hence the bridge abutment. A load cell was mounted between each hydraulic jack and the sill to monitor the applied loads.

Construction Material and Placement Conditions

Backfill

The backfill was a non-plastic silty sand classified as SP-SM soil per USC system. The soil was considered representative of a “marginally acceptable” backfill for construction of GRS abutments. The soil has 8.5 percent of fine particles (passing the No. 200 sieve). The maximum dry unit weight of the soil was determined to be 18.3 kN/m³ with the optimum water content being 11.5 percent, per AASHTO T-99. The internal friction angle (ϕ') of the soil was 34.8 deg with a shear stress intercept (c') of 13.8 kPa. The shear strength parameters were determined by standard direct shear tests conducted on the part finer than the No. 10 sieve and prepared at 95 percent maximum dry unit weight, per AASHTO T-99.

In the load tests, the target placement conditions were 100 percent compaction and ± 2 percent of the optimum moisture, per AASHTO T-99. Measurement taken after the load test showed that the compaction was 99.0 percent and the moisture was at 1.7 percent wet of optimum. With the information of the placement conditions of the fill, a series of large-size triaxial tests (with 150-mm-diameter, 300-mm-high specimens) in the “as-constructed” condition were conducted. The tests showed that the soil had $\phi = 37.3^\circ$ and $c = 20$ kPa at the

density and moisture mimicking the actual placement conditions. Large-size direct shear tests (with 300 mm by 300 mm specimens) conducted at the University of Massachusetts showed that the soil had $\phi = 36.5^\circ$ and $c = 0$ kPa, tested in conditions mimicking the actual placement density and moisture. These soil property tests indicate that the fill is deemed acceptable by the current backfill selection criteria.

Geotextile Reinforcement

Everything was essentially the same for the two test sections except for the geotextile reinforcement: one test section used Amoco 2044 (referred to as the Amoco test section) and the other used Mirafi 500x (referred to as the Mirafi test section). The wide-width tensile strength of Amoco 2044 and Mirafi 500x are $T_{ult} = 70$ kN/m and $T_{ult} = 21$ kN/m, respectively, in their cross-machine direction, per ASTM D 4595. Amoco 2044 was selected to represent a “lower bound” high-strength reinforcement, whereas Mirafi 500x represents a low- to medium-strength reinforcement. Both reinforcements are woven polypropylene geotextiles.

Table 2-2 summarizes the main features of the two test sections with information on the test abutments’ configuration and the backfill and geotextile reinforcement properties.

Construction of the NCHRP Test Abutments

The construction procedure of the test abutments can be described by the following steps:

1. Level the surface of the rigid floor with a bedding sand;
2. Lay the first course of facing blocks to form a rectangular external dimension of 5.75 m by 7.34 m;
3. Place and compact backfill at the target density of 100 percent relative compaction using vibratory plate tampers;
4. Examine the field density by a nuclear density gauge;
5. Place two sheets of reinforcement, one in each test section, covering the top surface of the compacted backfill and the facing blocks; and
6. Lay the next course of facing blocks. Repeat Steps 3 to 5 until completion.

Two different sizes of vibratory plate tampers were used in the construction. A lighter weight tamper (MBW AP-2000, weighs 73 kg with a plate size of 48 cm by 53 cm) was used near the facing, whereas a heavier weight tamper (Mikasa MVH-304, weighs 315 kg with a plate size of 45 cm by 86 cm) was used in all other areas. Four to five passes were needed to achieve the targeted compaction.

The construction of the two test sections began in mid-October 2002. On reaching a height of 1.2 m (i.e., with six courses of facing blocks), the construction had to be halted because of weather condition as described below.

TABLE 2-2 Main features of the NCHRP test abutments

	Amoco Test Section	Mirafi Test Section
Abutment height	4.65 m (15.25 ft)	4.65 m (15.25 ft)
Sill	0.9 m × 4.5 m (3 ft × 15 ft)	0.9 m × 4.5 m (3 ft × 15 ft)
Sill clear distance	0.15 m (6 in.)	0.15 m (6 in.)
Reinforcement length	3.15 m (10 ft)	3.15 m (10 ft)
Facing blocks (concrete)	194 mm × 194 mm × 397 mm (7.625 in. × 7.625 in. × 15.625 in.)	194 mm × 194 mm × 397 mm (7.625 in. × 7.625 in. × 15.625 in.)
Vertical reinforcement spacing	0.2 m (8 in.)	0.2 m (8 in.)
Reinforcements	Amoco 2044: a woven polypropylene geotextile with $T_{@e=1.0\%} = 12.3$ kN/m (70 lb/in.) and $T_{ult} = 70$ kN/m (400 lb/in.), per ASTM D4595, in the cross-machine direction.	Mirafi 500x: a woven polypropylene geotextile with $T_{ult} = 21$ kN/m (120 lb/in.), per ASTM D4595, in the cross-machine direction.
Backfill	<p>For both test sections: a non-plastic silty sand (SP-SM, per USC System)</p> <p><u>Gradation:</u></p> <p>Percent passing 0.75-in. sieve = 100% Percent passing No.40 sieve = 59% Percent passing No.200 sieve = 8.5%</p> <p><u>Compaction Test</u>, per AASHTO T-99: Maximum dry unit weight = 18.3 kN/m³ (116.5 lb/ft³) Optimum moisture content = 11.5%</p> <p><u>Standard Direct Shear Test</u> (on the portion passing No. 10 or 2 mm sieve, at 95% maximum dry unit weight per AASHTO T-99; specimen size: 60 mm by 60 mm) Cohesion = 14 kPa (2 psi) Internal friction angle = 34.8°</p> <p><u>Large-size Direct Shear Test</u> (at 99% maximum dry unit weight & 1.5% wet of optimum, per AASHTO T-99; specimen size: 300 mm by 300 mm) Cohesion = 0 kPa Internal friction angle = 36.5°</p> <p><u>Drained Triaxial Test</u> (on the portion passing 9.5 mm or 3/8 in. sieve; at 99% maximum dry unit weight & 1.5% wet of optimum, per AASHTO T-99; specimen size: 150 mm diameter, 300 mm high) Cohesion = 20 kPa (3 psi) Internal friction angle = 37.3°</p>	

The backfill of the test sections was placed at the prescribed density and moisture conditions, except for the last lift (wall elevation from 0.9 m to 1.2 m above base) wherein difficulties were encountered during fill compaction. The lift was emplaced following a prolonged rainy day. The moisture content of the lift was in the range of 12.7 percent to 15.1 percent (i.e., 1.2 percent to 3.6 percent wet of optimum). In areas with high moisture contents (around 15 percent), the measured relative compaction was 95 percent per AASHTO T-99. Numerous attempts were made to increase the density by increasing the compaction passes of the vibrating tamper. Water, however, emerged from the top surface during the additional passes, and the measured density remained practically unchanged (relative compaction increased from 95.3 percent to 95.7 percent). Because of the weather, the construction had to be halted after some extended high-intensity precipitation at the con-

struction site. Draining and drying of water from the backfill did not appear possible absent an extended period of dry weather.

In light of the difficulties with the placement density and moisture encountered in the 1.2-m-high abutments and the relatively “wet” winter experienced on the test site, it was judged necessary to remove the abutment and reconstruct two new test sections. The backfill on removal was found to be in a rather wet condition. There was also significant water accumulation near the base of the fill.

Construction of the new GRS abutment test sections began in April 2003. The new test sections were constructed with the same backfill. There were concerns as to whether difficulties with placement density might be encountered as in the previous case. However, a decision was made to employ the same backfill so that the desired condition of using a “marginally acceptable” backfill could be fulfilled. The top surface

of the fill was to be completely covered whenever there was any appreciable rainfall to better control the moisture.

Backfill placement density and moisture were measured at the end of each construction lift to ensure that the specified values were met. Four density tests were conducted for each lift. The average placement density and moisture were 99.0 percent compaction and 13.2 percent moisture for the Amoco test section and 98.4 percent compaction and 13.1 percent moisture for the Mirafli test section. Construction of the new test sections was completed near the end of May 2003.

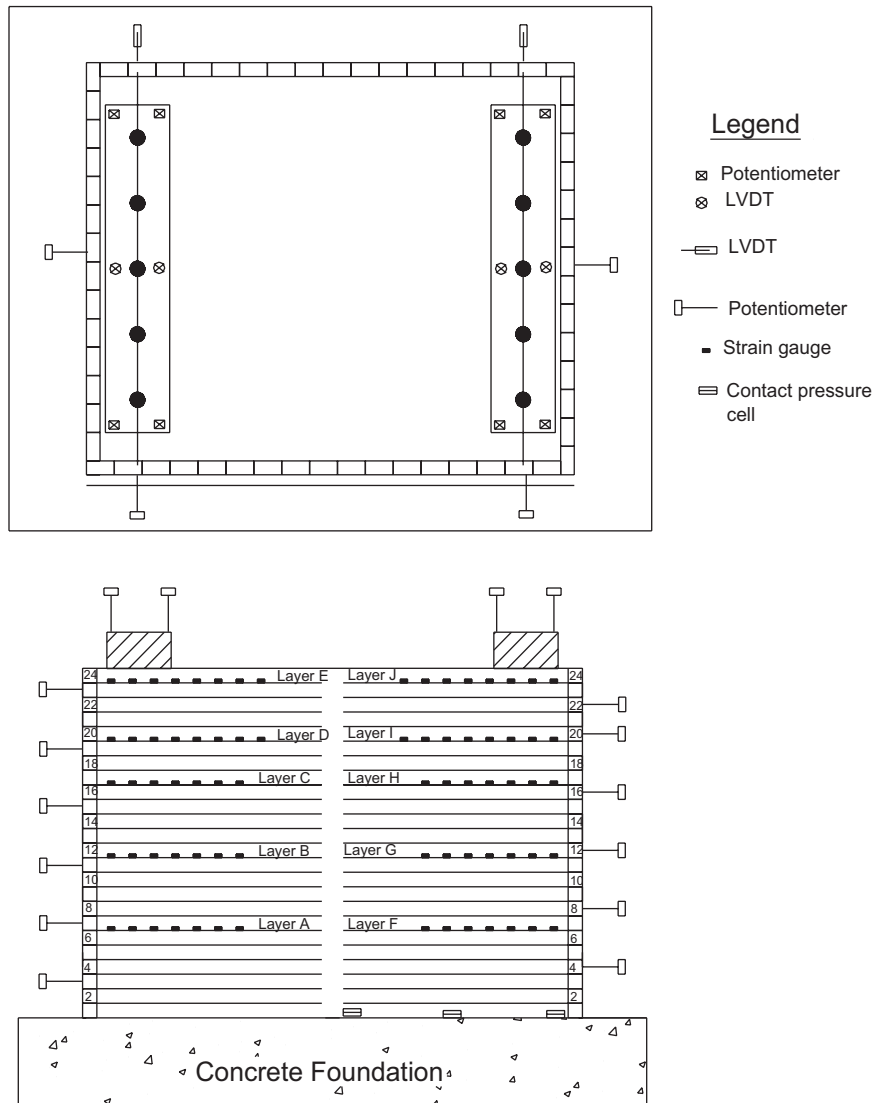
Instrumentation

The instruments employed in the experiment included linear voltage displacement transducers (LVDTs), displacement

potentiometers, a laser displacement measurement device, strain gauges (for geotextile reinforcement), and contact pressure cells. Figure 2-16 shows the instrumentation layout for the experiments.

For each test section, four displacement potentiometers and two LVDTs were used to measure settlements of the sill. Six displacement potentiometers were used to measure lateral movement of the abutment wall. In addition, six potentiometers and six LVDTs were used to measure lateral movements of the two wing walls. Three-dimensional movement of the abutment wall and one of the wing walls for each test section were traced by using a laser displacement measurement device.

A total of 74 high-elongation strain gauges (Micro-Measurement Type EP-08-250BG-120) were mounted on five sheets of Amoco 2044 geotextile for the Amoco test section



Instrumentation Layout of GRS Abutments
 Figure 2-16. Layout of instrumentation.

and five sheets of Mirafi 500x geotextile for the Mirafi test section. The strain gauges were mounted along the centerline of the reinforcement sheets perpendicular to the abutment walls of the test sections. The locations of the strain gauges and reinforcement sheets with strain gauges are shown in Figure 2-16. Three contact pressure cells (Geokon vibrating wire pressure transducer model 4810-25) were mounted on top of the rigid concrete foundation of the Mirafi test section.

Loading

The bridge sill was loaded along its centerline in equal increments of 50 kPa average vertical pressure. Each load increment was maintained for 30 minutes to allow the stress to be transferred to the entire soil mass. The first load test was carried out successfully on the Amoco test section on May 26, 2003. The loading was terminated at an average vertical pressure of 814 kPa, at which time the strokes of the loading rams had reached their maximum extension. The second load test was carried out successfully on the Mirafi test section on June 6, 2003. The loading was terminated at an average vertical pressure of 414 kPa, at which time the abutment experienced “excessive” deformation.

Measured Test Results and Discussions

The results of loading tests on the Amoco and Mirafi test sections and the discussions of the test results are presented in this section. The test results reported include settlement of

sill, lateral movement of abutment wall, tension crack in the soil mass, contact pressure on rigid foundation, and strains in geosynthetic reinforcements.

Sill Settlement

The sill settlements at six measured points including four corner points (with a legend “Pot”) and two mid-length points (with a legend “LVDT”) are shown in Figure 2-17 for the Amoco test section and in Figure 2-18 for the Mirafi test section. The measured data indicated that the front of the sill settled more than the back of the sill, while the left and right sides of the sill settled about the same. The average forward tilting of the Amoco and Mirafi test sections at 200 kPa pressure were about B/90 and B/50 (B = width of sill = 0.91 m), respectively.

The average sill settlements of the six measurement points versus applied loads for both test sections are shown in Figure 2-19. As expected, the settlement increased as the applied load increased. At a pressure of 200 kPa (the limiting bearing capacity of reinforced soil mass of an MSE abutment as recommended by the NHI manual, Elias et al., 2001), the average sill settlement in the Amoco test section was 40 mm, whereas the average sill settlement in the Mirafi test section was 72 mm. As the loading was terminated, 814 kPa for the Amoco test section and 414 kPa for the Mirafi test section, the average sill settlements were 163 mm and 175 mm, respectively. The Mirafi test section at 414 kPa had approached a bearing failure condition while the Amoco test

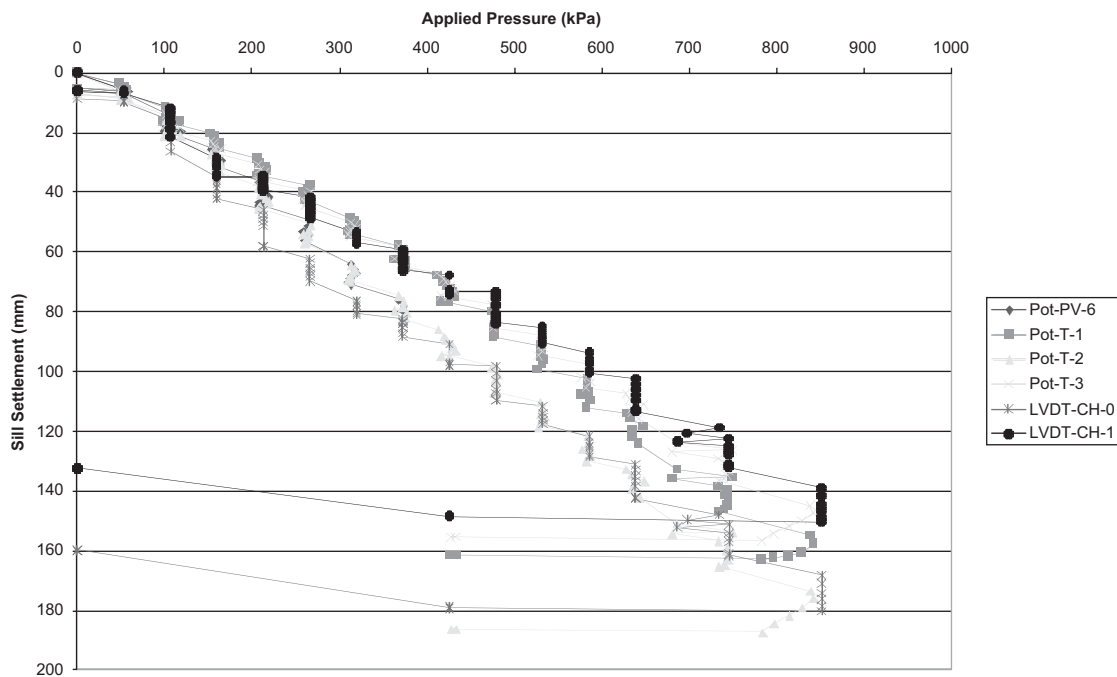


Figure 2-17. Sill settlement versus applied pressure relationships of the Amoco test section.

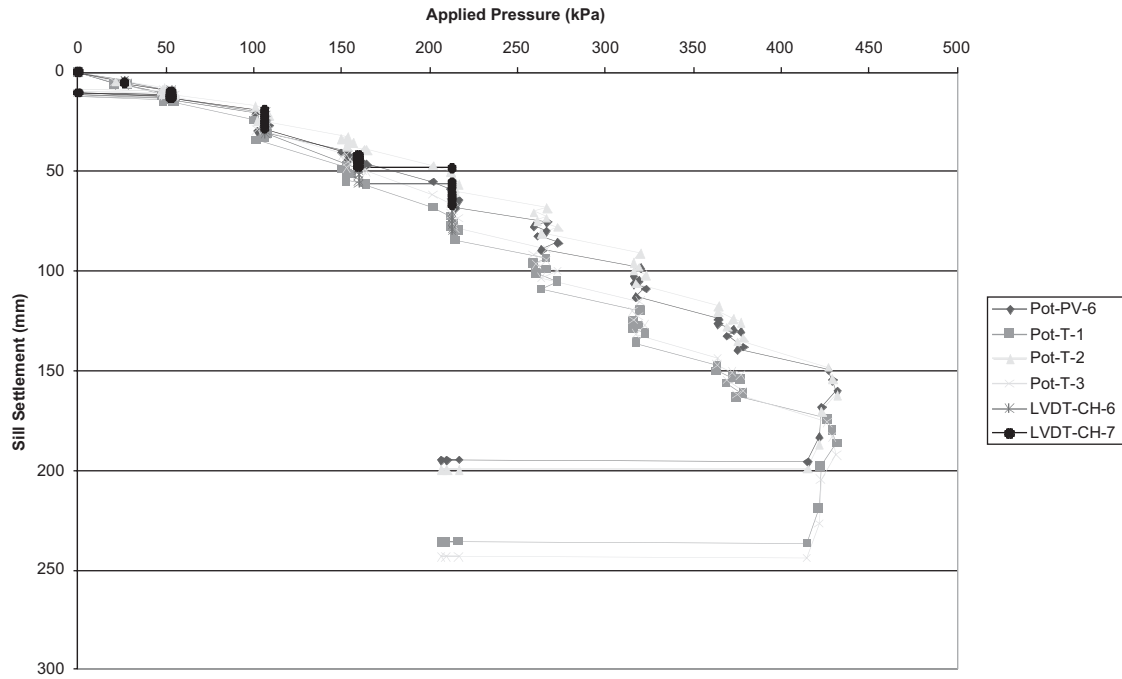


Figure 2-18. Sill settlement versus applied pressure relationships of the Mirafi test section.

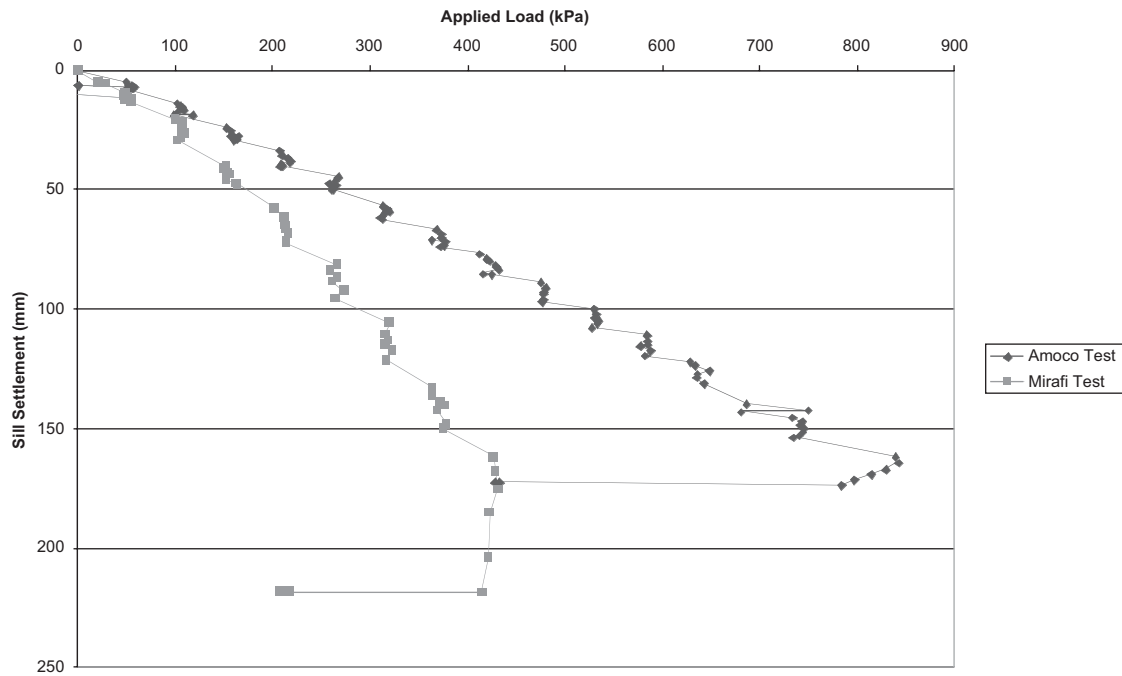


Figure 2-19. Average sill settlement versus applied pressure relationships of the Amoco and Mirafi test sections.

section appeared to be sufficiently stable at 814 kPa. The Amoco and Mirafi test sections are essentially the same in all aspects except the reinforcement type. The difference in the sill settlement can be considered as a result of the difference in reinforcement stiffness and strength, $T_{ult} = 70 \text{ kN/m}$ versus $T_{ult} = 21 \text{ kN/m}$.

Lateral Wall Movement

Figures 2-20 and 2-21 show the lateral movements of the abutment wall and wing-wall, respectively, of the Amoco test section. For the abutment wall, the maximum lateral movement occurred near the top of the wall (the top measurement point was not at the very top of the wall). The top one-third of the wall deformed at a much greater rate than the lower two-thirds of the wall. The maximum lateral movement was 24 mm and 82 mm at 200 kPa and 814 kPa, respectively. For the wing-wall, the lateral movements were much smaller than those of the abutment wall, with the maximum movement occurring at about H/6 (H = wall height) from the top of the wall for all the loads. The maximum lateral movement was 18 mm and 33 mm at 200 kPa and 814 kPa, respectively.

Figures 2-22 and 2-23 show the lateral movements of the abutment and wing-walls, respectively, of the Mirafi test section. For the abutment wall, the maximum lateral movement also occurred near the top of the wall under smaller

loads. As the applied pressure exceeded about 300 kPa, the point of maximum wall movement shifted to H/6 from the top. Contrary to what was observed in the Amoco test section, the upper one-third of the Mirafi test section deformed at a slower rate than the lower two-thirds of the wall. At 200 kPa and 414 kPa, the maximum lateral movements were 36 mm and 115 mm, respectively. For the wing wall, the maximum lateral movement also occurred at about H/6 from the top of the wall. At 200 kPa and 413 kPa, the maximum lateral movements were 30 mm and 86 mm, respectively.

The facing blocks in the top three courses were pushed outward as the sill tilted forward toward to wall face under higher applied loads. This suggests that (1) the sill clear distance of 0.15 m, a minimum value stipulated by the NHI manual, may be too small; and (2) it might be beneficial to increase the connection strength in the top three to four courses of the facing. The authors believe that it would be most effective to inter-connect the top three to four courses of the facing blocks after the construction is completed (i.e., after the deformation because of soil self-weight has occurred).

Tension Cracks

A tension crack on the wall crest was detected in both load tests when the average applied pressure on the sill was about 150 to 200 kPa. For both test sections, the tension crack was

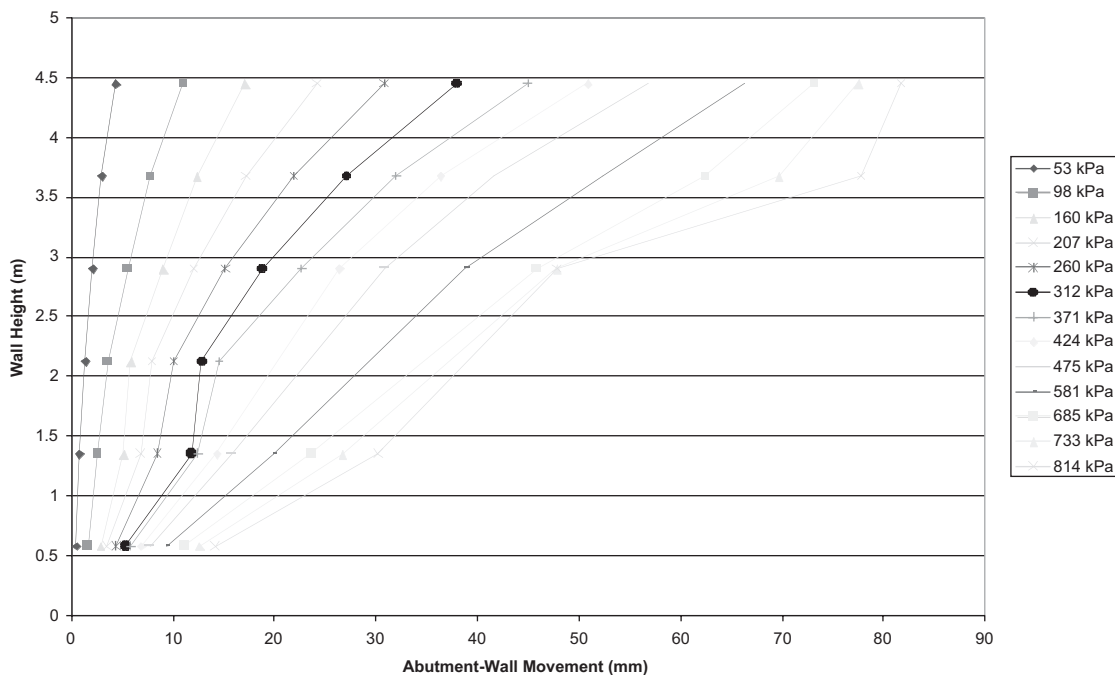


Figure 2-20. Lateral movement of abutment wall: Amoco test section.

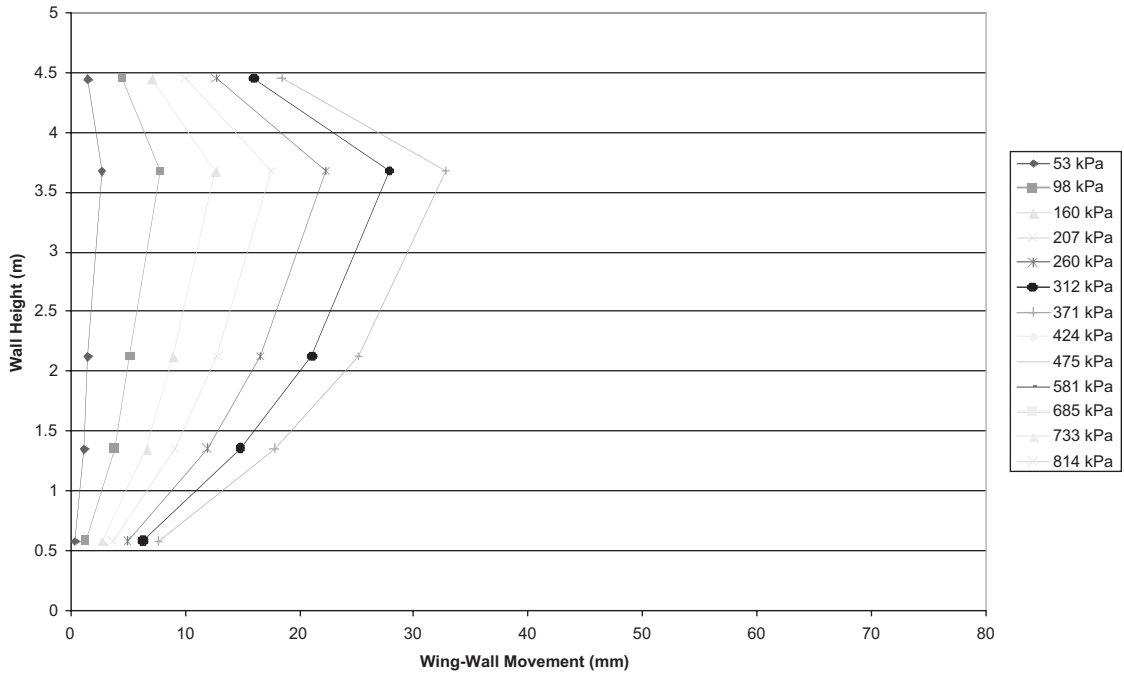


Figure 2-21. Lateral movement of wing wall: Amoco test section.

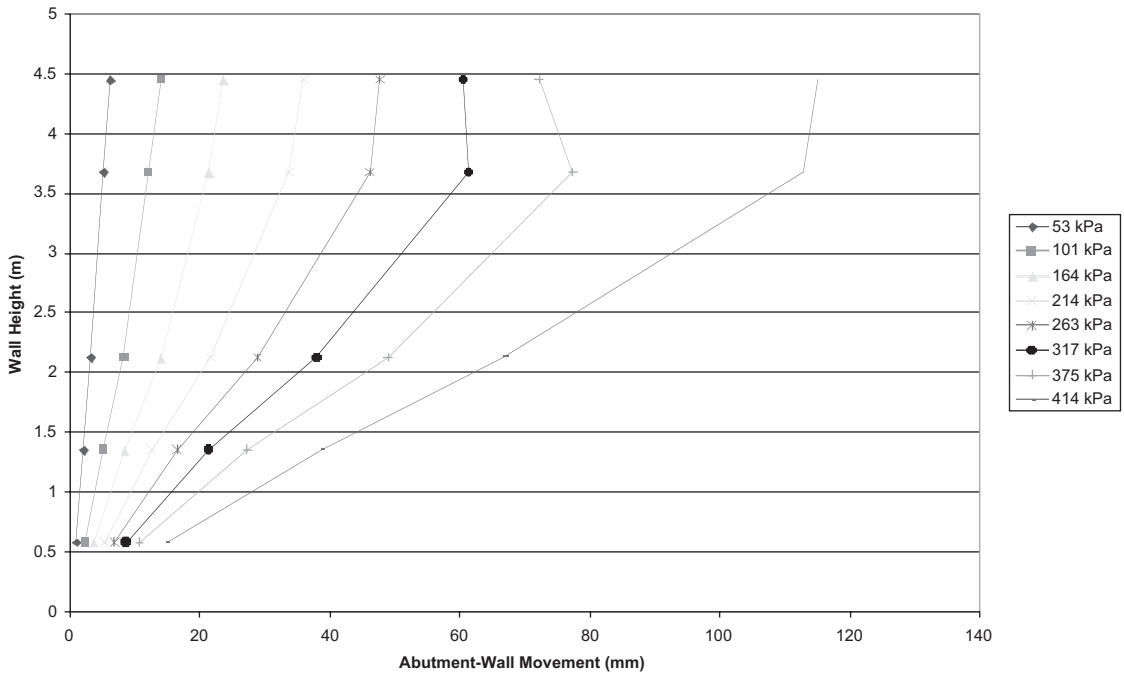


Figure 2-22. Lateral movement of abutment wall: Mirafi test section.

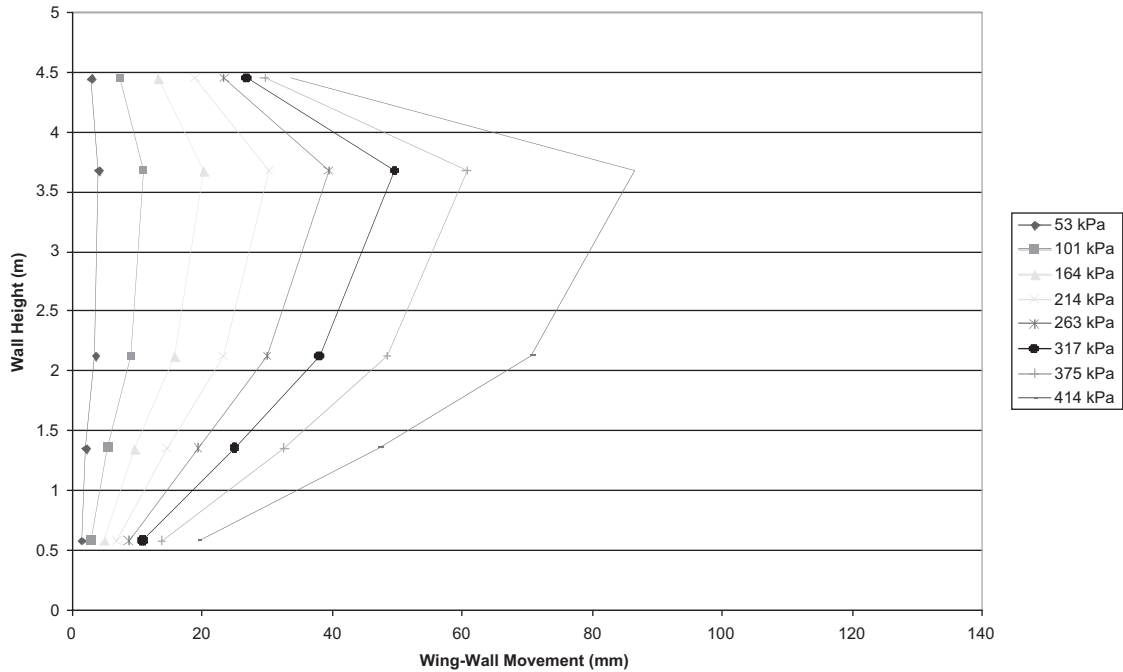


Figure 2-23. Lateral movement of wing wall: Mirafi test section.

about 11 m from the wall face, the location where the geosynthetic reinforcement ended. The cracks were parallel to the abutment wall face and extended through the entire width of the abutment. If an upper wall had been constructed over the test abutment, as in the case of typical bridge abutments, these tension cracks would not have been visible and perhaps less likely to occur. Hairline cracks of the facing blocks were also observed under higher loads in both test sections.

Strains in Reinforcement

A total of 74 strain gauges were mounted on five sheets of Amoco 2044 woven geotextile and five sheets of Mirafi 500x woven geotextile. The strain gauges were mounted by a “patch” technique. A strain gauge was first glued on the surface of a 25 mm by 76 mm patch. The patch was a low-strength heat-bonded nonwoven geotextile. To avoid inconsistent local stiffening of the patch because of the adhesive (given that the adhesive is much stiffer than the geotextile), the glue was applied only around the two ends of the strain gauge. The patch with a strain gauge already mounted was then glued on the reinforcement used in the experiments at a prescribed location, again with the glue applied only at the two ends. To protect the strain gauges from soil moisture and from possible mechanical damage during soil compaction, a microcrystalline wax was applied over the gauge and

covered with a Neoprene rubber patch. This “patch” technique for mounting strain gauges on nonwoven geotextiles has been used successfully in several projects including an FHWA pier (Adams, 1997), a Havana Yard pier and abutment (Ketchart and Wu, 1997), and a Black Hawk abutment (Wu et al., 2001).

Because of the presence of the geotextile patch, calibration of the strain gauges was needed. A wide-width tensile test was performed to correlate the recorded strain (local strain from strain gauges) with actual strain (average strain from the MTS machine) of the reinforcement. Figure 2-24 shows the calibration curve of Amoco 2044 and Mirafi 500x specimens.

Because of the very long time lapse (about 8 months) between strain gauge installation and actual loading experiments, only 13 out of the 74 gauges worked properly. The most likely cause was that the gauges were damaged by the lengthy delay between mounting of strain gauges and actual loading experiments. Figures 2-25 and 2-26 show the measured reinforcement strain versus applied pressure of the Amoco test section and Mirafi test section, respectively. Because of the limited number of operable strain gauges, distributions of strain along any reinforcement sheet cannot be reliably deduced. The operable gauges, however, indicated that the maximum strains at 200 kPa were about 2.0 percent and 1.7 percent in the Amoco and Mirafi test sections, respectively.

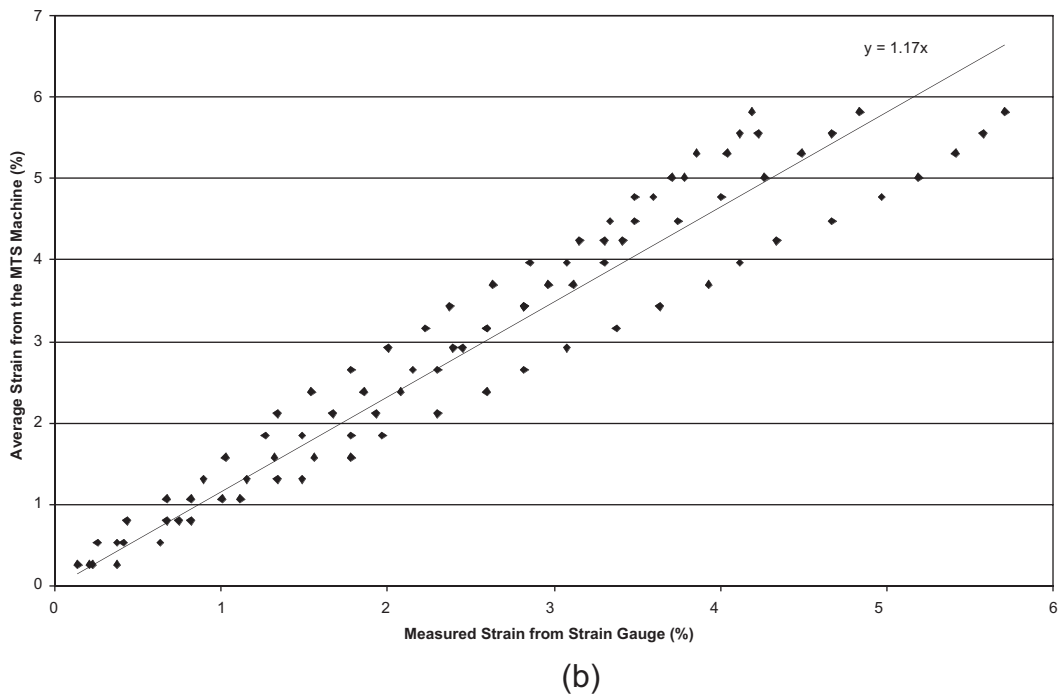
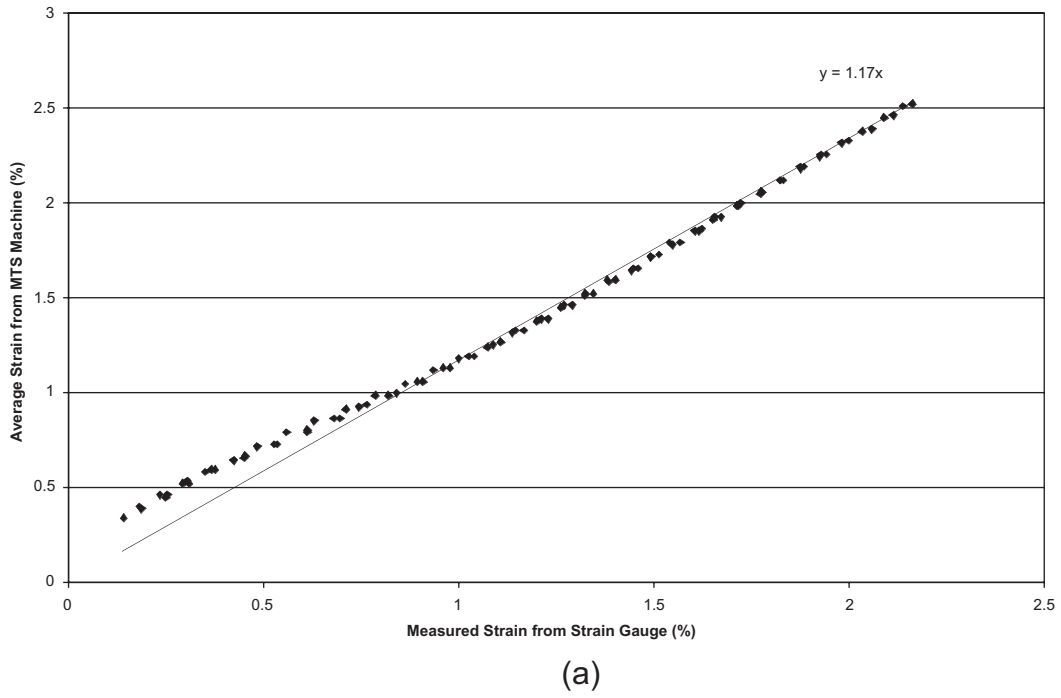


Figure 2-24. Calibration curve for (a) Mirafi 500x and (b) Amoco 2044.

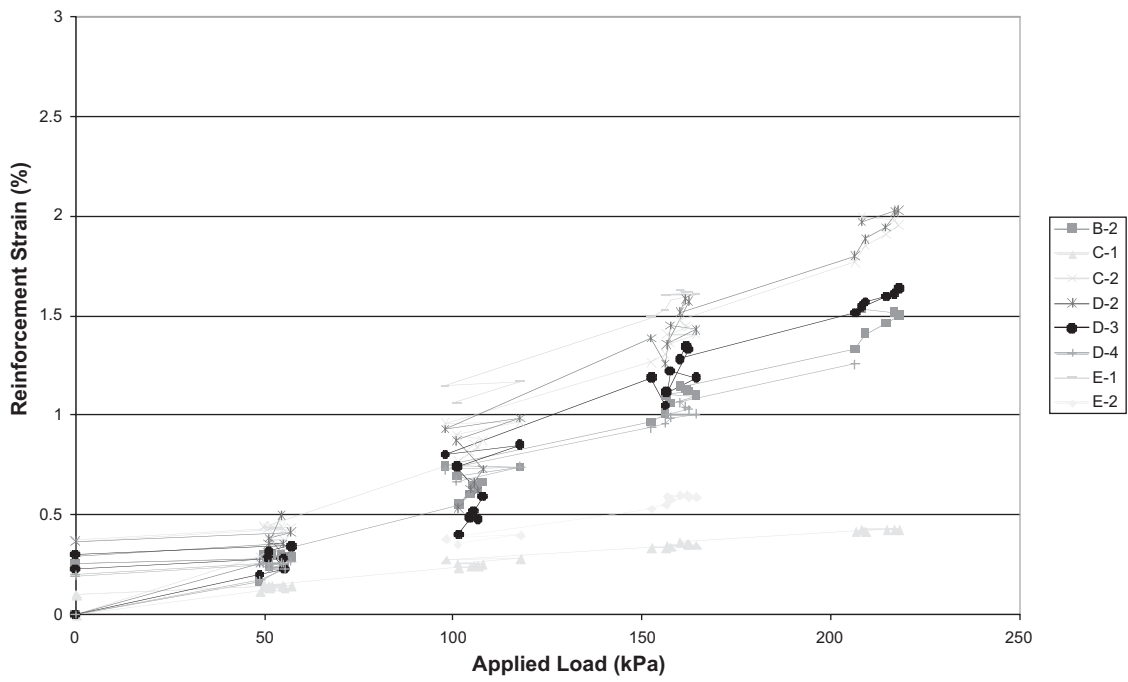


Figure 2-25. Reinforcement strains in the Amoco test section.

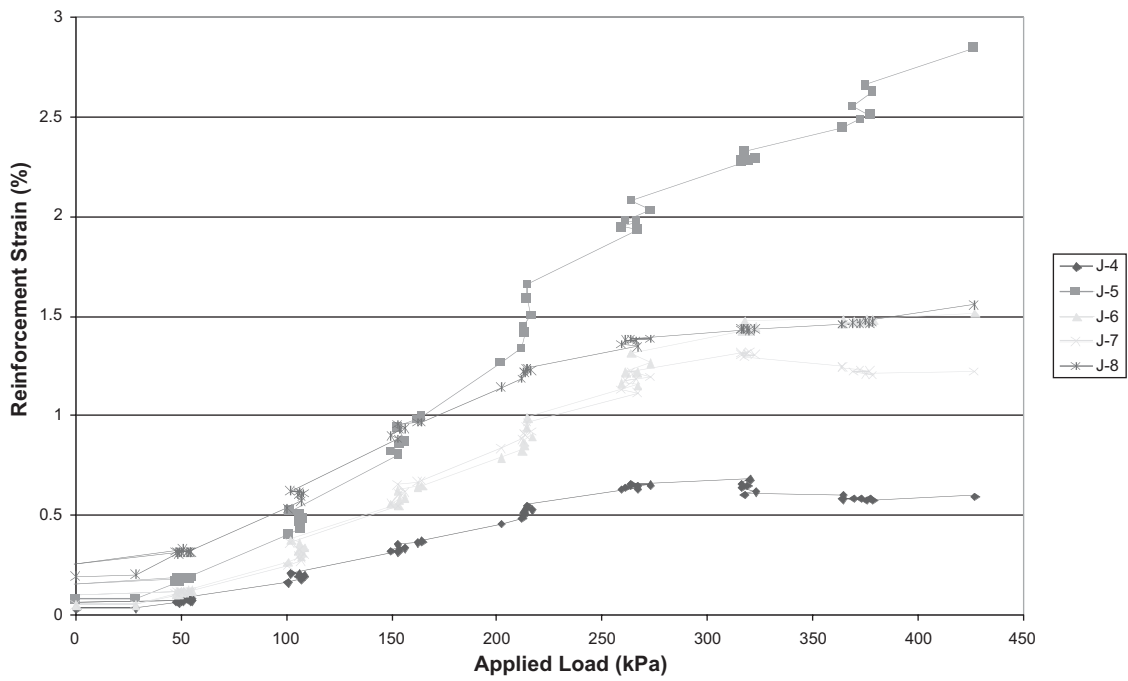


Figure 2-26. Reinforcement strains in the Mirafi test section.

Contact Pressures on the Rigid Foundation

Figure 2-27 shows the measured contact pressures under different applied pressures at three selected points on the rigid floor of the Mirafi test section. The three points are located along the centerline of the abutment and are 0.25 m, 1.72 m, and 3.13 m from the wall face. The largest contact pressure occurred at 0.25 m from the wall face, which is roughly underneath the front of the sill. As expected, the contact pressure reduced with increasing distance from the wall face. At an average applied pressure of 200 kPa, the contact pressures at the three points were 77 kPa, 40 kPa, and 12 kPa.

The NHI manual (Elias et al., 2001) recommends a method based on the 2:1 distribution with a cutoff at wall face to calculate vertical stress in a soil mass because of a concentrated vertical load applied on a footing for external and internal stability assessment. The contact pressure on the rigid foundation as calculated by the method is uniform at any given depth. The calculated contact pressures at the base were 23 kPa, 46 kPa, 69 kPa, and 92 kPa at applied pressures of 100 kPa, 200 kPa, 300 kPa, and 400 kPa, respectively. The corresponding measured average contact pressures are 24 kPa, 45 kPa, 59 kPa, and 77 kPa. A comparison of these contact pressures suggests that (1) the actual contact pressure is higher near the wall face and decreases nearly linearly with the distance from the wall face, and (2) the computation method in the NHI manual yields roughly the “average”

measured contact pressure although the calculated pressures are somewhat higher than the measured average values at higher applied pressures.

Summary of Measured Results of the NCHRP Test Abutments

A summary of the measured performance and observed behavior of the two full-scale test abutments is presented in Table 2-3.

FINDINGS FROM THE ANALYTICAL STUDY

The analytical study was conducted by using a finite element code, DYNA3D (Hallquist and Whirley, 1989), and its PC version, LS-DYNA. The use of DYNA3D requires a workstation (such as CRAY, VAX/VMS, SUN, SILICON GRAPHICS, or IBM RS/6000), while LS-DYNA requires only a personal computer. The two computer codes give essentially the same results although LS-DYNA offers more user-friendly interfaces and greater flexibility in preparing the input file. The analytical model is briefly described in Appendix B.

The capability of DYNA3D/LS-DYNA for analyzing the performance of segmental facing GRS bridge abutments was evaluated. The evaluation included comparing the analytical results with measured data of five full-scale experiments,

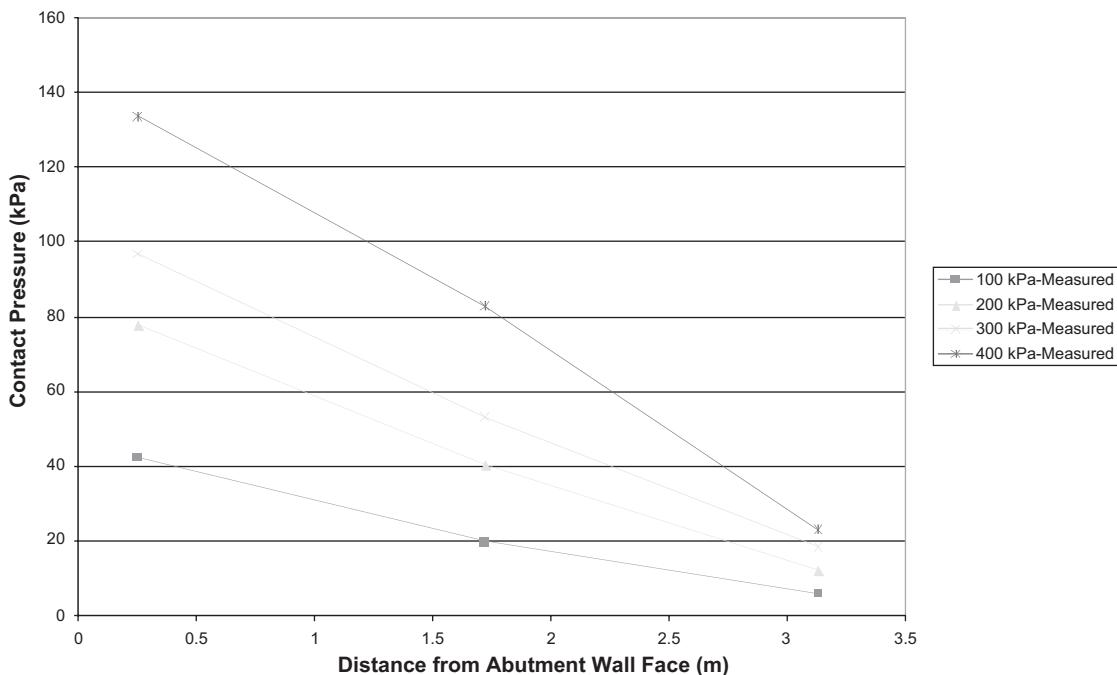


Figure 2-27. Measured contact pressure distribution on rigid foundation.

TABLE 2-3 Summary of measured performance and observed behavior of the NCHRP test abutments

	Amoco Test Section	Mirafi Test Section
Reinforcement	Amoco 2044, $T_{ult} = 70$ kN/m	Mirafi 500x, $T_{ult} = 21$ kN/m
<i>Upon termination of loading:</i>		
Average Applied Pressure	814 kPa	414 kPa
Sill Settlement (front)	175 mm (6.9 in.)	189 mm (7.4 in.)
Sill Settlement (back)	152 mm (6.0 in.)	160 mm (6.3 in.)
Max. lateral movement in abutment wall	82 mm @ 4.5 m from base	115 mm @ 4.5 m from base
Max. lateral movement in wing wall	33 mm @ 3.8 m from base	86 mm @ 3.8 m from base
<i>At 200 kPa (limiting bearing capacity, per NHI manual)</i>		
Applied Pressure (average)	207 kPa	214 kPa
Sill Settlement (front)	45 mm (1.8 in.)	81 mm (3.2 in.)
Sill Settlement (back)	35 mm (1.4 in.)	64 mm (2.5 in.)
Max. lateral movement in abutment wall	24 mm @ 4.5 m from base	36 mm @ 4.5 m from base
Max. lateral movement in wing wall	18 mm @ 3.8 m from base	30 mm @ 3.8 m from base
<i>Observed Behavior:</i>		
<ul style="list-style-type: none"> • The sills in both tests tilted toward the abutment wall face (i.e. the front of the sill settled more than the back; Left and right sides of the sill settled evenly). • The abutment wall leaned forward with the maximum movement occurring near the top of the wall. The top three courses of facing blocks were pushed outward at higher loads. • The wing wall also leaned forward with the maximum movement occurring at approximately 1/6H from the top of the wall. • In both tests, tension cracks occurred parallel to the wall face and were located at end of the reinforcement. Tension cracks initiated around 150–200 kPa average applied pressure. • Most strain gauges were damaged by moisture due to the long delay of actual loading experiments; maximum strain at 200 kPa was about 2.0% • The measured contact pressure on the rigid foundation was larger in front and decreased linearly toward the back. The computation procedure in the NHI Manual yielded about the average value of the contact pressures at a given applied load. 		

including (1) the spread footing experiments by Briaud and Gibbens (1994), (2) the spread footing experiments on reinforced sands by Adams and Collin (1997), (3) the FHWA Turner-Fairbank GRS bridge pier by Adams (1997), (4) the “Garden” experimental embankment in France (Gotteland et al., 1997), and (5) the two full-scale GRS bridge abutment loading experiments conducted as part of this study (referred to as the NCHRP GRS abutment experiment). Very good agreements between the analytical results and the measured data (including measured performance and failure loads) were obtained.

The analyses of the five full-scale experiments are presented in Appendix C, available as *NCHRP Web-Only Document 81*. The findings of a parametric study and findings of performance analysis, all obtained by using the analytical model, are presented in this chapter. The findings of performance analysis were used as the basis for the allowable sill pressures in the recommended design procedure.

Parametric Study

Base Case Geometry, Material Properties, and Loading

After the finite element code, DYNA3D, was satisfactorily verified, a parametric study was conducted to investigate performance characteristics of GRS bridge abutments and the approach fill. The performance characteristics, as affected by soil placement condition, reinforcement stiffness/strength, reinforcement spacing (varying from 20 to 60 cm), reinforcement truncation, footing (sill) width, and the clearance between the front edge of the footing and the back face of the wall facing were investigated. When analyzing the results, the settlement of footing, rotation of the footing, lateral deformation of abutment wall, maximum shear stress levels in the GRS soil mass, ultimate load carrying capacity of the abutment, and potential failure mechanisms were emphasized.

The analytical results obtained from the parametric study served as the basis for establishing preliminary design guidelines of GRS abutments. The maximum tolerable settlement and horizontal movement of bridges, as suggested by Moulton et al. (1985) and by others (as summarized in *NCHRP Report 343*), may be used as the performance limits when establishing the design guidelines.

The “Base Case” geometry used in the parametric analysis is shown schematically in Figures 2-28 and 2-29. The dimensions and parameters of the base case, listed below, were kept constant for all cases of the parametric study unless otherwise stated.

Base Case Dimensions (see Figure 2-28):

- Segmental wall height: 4.6 m
- Total GRS abutment height: 7.1 m
- Concrete block dimensions: 28 cm wide (toe to heel), 20 cm high, 50 cm long
- Sill width: 1.5 m
- Sill clearance: 15 cm
- Loading pad width: 80 cm
- Geosynthetic spacing: 20 cm
- Geosynthetic length: 5 m

Base Case Parameters:

- Geosynthetic stiffness: 530 kN/m
- Soil internal friction angle: 34 deg (See Figure 2-30)

Base Case Loading:

- Uniformly distributed vertical load was applied to the 80-cm-wide loading pad and increased monotonically until failure or until 1000 kPa was reached, whichever occurred first.

Effects of Geosynthetic Spacing

To investigate the effect of vertical spacing between geosynthetic layers on the GRS bridge abutment, three different spacings were used: 20 cm (Base Case), 40 cm, and 60 cm. Four parameters were thought important in describing the performance of a GRS abutment when subjected to superstructure loads. These parameters, termed herein “performance parameters,” are the vertical displacement at the abutment seat (where the girder load is applied), the horizontal displacement at the abutment seat, the maximum displacement of the segmental facing, and sill distortion.

Figure 2-31 shows the effects of increasing spacing on the selected performance parameters. Figure 2-31a shows that the vertical displacement at the abutment seat increases with spacing increase. The increase in displacement becomes more significant as the applied pressure increases. At 200 kPa of applied pressure (moderate pressure), there is a 24 percent increase in vertical displacement at 40 cm spacing as compared with the base case with 20 cm spacing. An increase

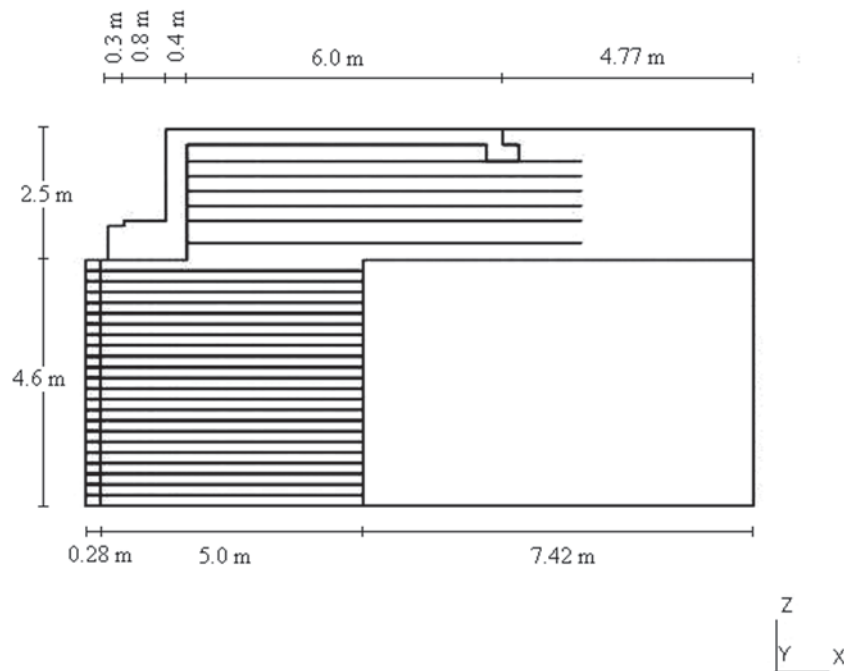
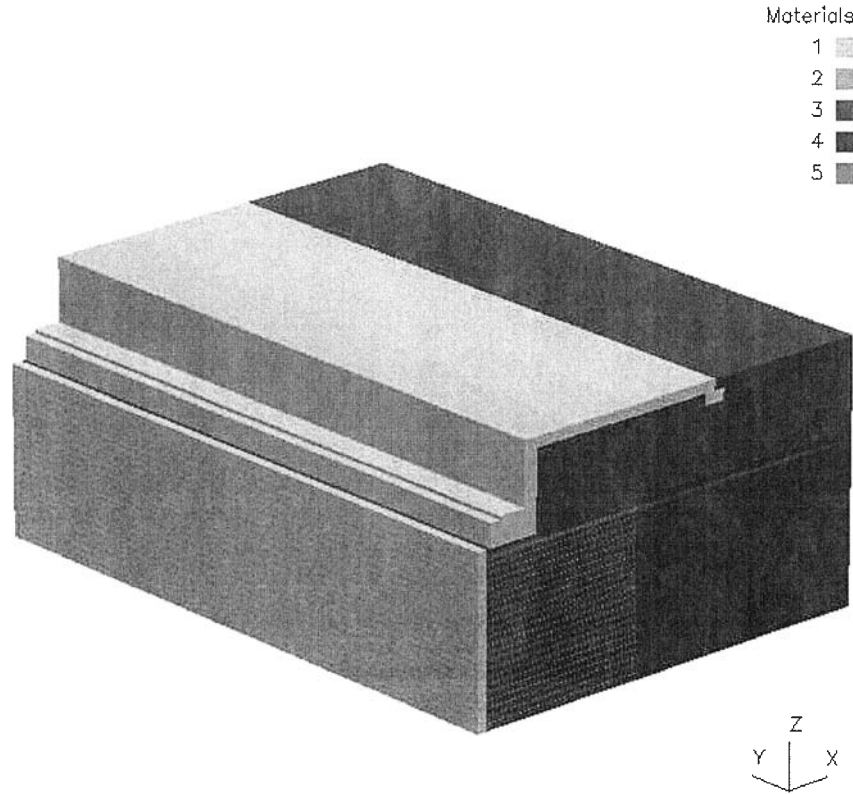


Figure 2-28. Configuration of the base case for the parametric analysis.



Parametric analysis for GRS ab
 t = 0.00000e+00

Figure 2-29. Three-dimensional representation of the base case.

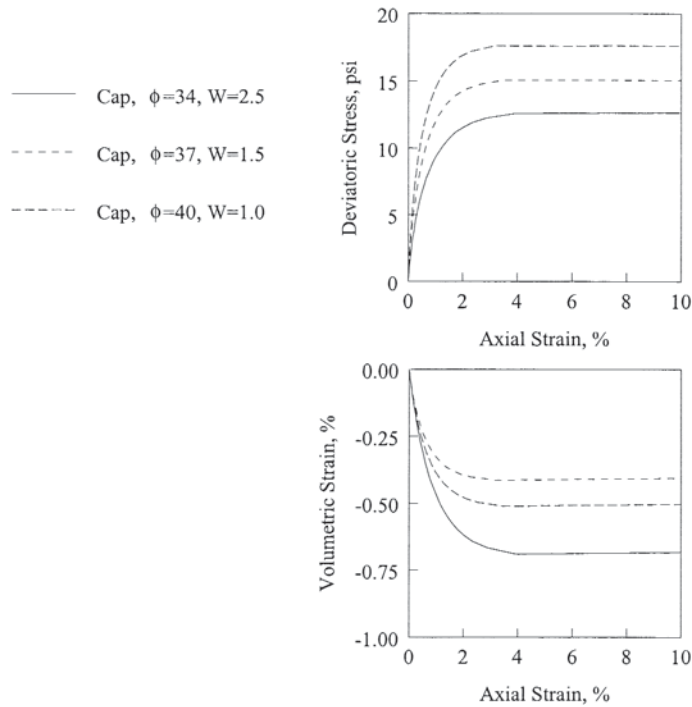


Figure 2-30. Stress-strain-volume change characteristics of soils used in the parametric analysis.

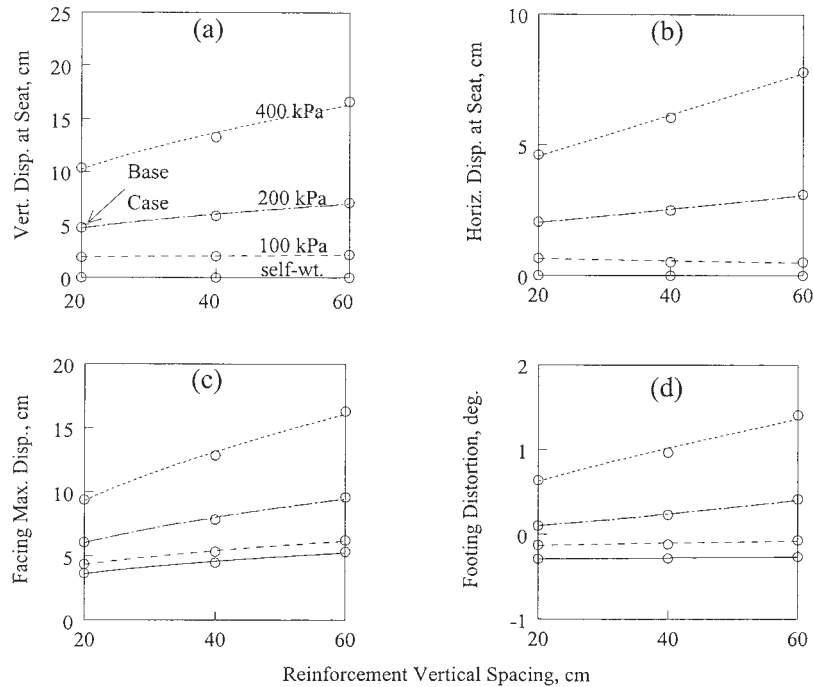


Figure 2-31. Effects of geosynthetic spacing.

of 50 percent in vertical displacement was observed at 60 cm spacing as compared with the base case. Similar trends with similar increases were noted for the horizontal displacement at abutment seat (Figure 2-31b) and for the maximum lateral displacement of the segmental facing (Figure 2-31c). The distortion of the sill, as shown in Figure 2-31d, ranged from +0.1 degree at 20 cm spacing to +0.41 degree at 60 cm spacing (positive distortion = forward tilt).

At an applied pressure of 200 kPa, the vertical and horizontal displacements of the abutment seat for the base case were 4.7 cm and 2.1 cm, respectively (Figure 2-31). Judging from the criteria that the vertical movement should not exceed 100 mm and the horizontal movement should not exceed 50 mm (Wahls, 1990), the values of vertical and horizontal movements associated with the base case at 200 kPa pressure were deemed acceptable. This suggests that the displacements of the abutment are unlikely to cause any damage to the bridge superstructures. Judging from the same criteria, the vertical and horizontal displacements of the abutment seat for the base case at 400 kPa are unacceptable (barely acceptable): the vertical displacement is 10.3 cm, and the horizontal displacement is 4.6 cm (Figure 2-31).

The maximum displacement criterion suggested by Wahls (1990) was based on a comprehensive study of bridge movements reported by Moulton et al. (1985). In the study, measured movements were evaluated for 439 abutments of which most were perched abutments. The study included assessment of which movements were regarded as tolerable and

which were intolerable. The tolerability of the movement was judged qualitatively by the agency responsible for each bridge in accordance with the following criterion: "Movement is not tolerable if damage requires costly maintenance and/or repairs and a more expensive construction to avoid this would have been preferable."

Effects of Backfill Soil Type

Three backfill soils with internal friction angles of $\phi = 34^\circ$, 37° , and 40° and relative compactions (RC) of 95 percent, 100 percent, and 105 percent, respectively, are used in the analysis to investigate the effects of backfill soil type on the performance of the GRS abutment. The soil parameters used in the analysis were deduced from triaxial test results conducted on numerous backfill materials (Duncan et al., 1980). Figure 2-30 shows the stress-strain behavior and the volumetric strain-axial strain behavior of the three soils. The study by Duncan et al. (1980) presented estimates of stress-strain-strength parameters and volumetric strain-axial strain parameters for various soil types and degrees of compaction. These estimates were made using the compilations of data taken from 135 different soil parameters. Using these data, conservative parameter values have been interpreted for the soils under various types and degrees of compaction. The values of stress-strain-strength parameters and volumetric strain-axial strain parameters of 16 materials averaged from the aforementioned 135 materials were presented in the study. These parameters

are called conservative in that they are typical of the lower values of strength and modulus and the higher values of unit weight for each soil type.

Figure 2-32 shows the effects of backfill soil type, as signified by ϕ , on the performance parameters for geosynthetic spacings of 20 cm. More favorable response is attained when using soil types that have higher stiffness and strength and lower deformations. At 200 kPa of applied pressure, the vertical displacement at the abutment seat decreased 23 percent when ϕ increased from 34° (base case) to 37° as indicated in Figure 2-32a. The vertical displacement decreased 35 percent when ϕ was increased from 34° to 40°. The effect of increasing ϕ on the horizontal displacement of the abutment seat was similar in trend but with smaller magnitudes as shown in Figure 2-32b. As shown in Figure 2-32c, at 200 kPa of applied pressure, the maximum lateral displacement of the segmental facing decreased roughly linearly with increasing ϕ , with a total reduction of 45 percent at $\phi = 40^\circ$ as compared with the base case. The distortion of sill changed from +0.1° at $\phi = 34^\circ$ to +0.04° at $\phi = 40^\circ$ as shown in Figure 2-32d.

Figure 2-33 shows the effects of backfill soil type on the performance parameters for geosynthetic spacing $s = 40$ cm. As shown in Figure 2-33a, for $\phi = 34^\circ$, $s = 40$ cm, and at an applied pressure of 200 kPa, the vertical displacement of the abutment seat is 5.8 cm, which is 24 percent greater than that corresponding to the base case ($\phi = 34^\circ$, $s = 20$ cm, Figure 2-32a). For $\phi = 37^\circ$ and $s = 40$ cm, the vertical displacement at the abutment seat is 9 percent smaller than the base case. For $\phi = 40^\circ$ and $s = 40$ cm, the vertical displacement at the abutment seat is 28 percent smaller than that of the base case.

The horizontal displacement at the abutment seat (Figure 2-33b) and the maximum lateral displacement of the segmental wall (Figure 2-33c) closely follow the trend of the vertical displacement at the abutment seat. The distortion of sill changed from +0.23° at $\phi = 34^\circ$ to +0.035° at $\phi = 40^\circ$ as shown in Figure 2-33d. The response of the base case ($\phi = 34^\circ$, $s = 20$ cm, Figure 2-32) is very similar to the case of $\phi = 37^\circ$ and $s = 40$ cm, indicating that a better soil compaction may substitute for closer spacing (to a certain extent).

Effects of Geosynthetic Stiffness

The effects of geosynthetic stiffness ($E * t$) on the performance of the GRS abutment is shown in Figure 2-34 for geosynthetic spacings of 20 cm, and in Figure 2-35 for $s = 40$ cm. The stiffness of the base case was assumed to be 530 kN/m. A lower stiffness of 53 kN/m and a higher stiffness of 5300 kN/m were used to investigate the effects of geosynthetic stiffness on performance parameters.

Figure 2-34a shows that the vertical displacement of the abutment seat of the base case is 4.7 cm for an applied pressure of 200 kPa. This displacement is reduced 43 percent when the geosynthetic stiffness is increased to 5300 kN/m. On the other hand, a drastic increase of 252 percent in displacement is noted when the geosynthetic stiffness is reduced to 53 kN/m. The same trend is noted for the horizontal displacement of the abutment seat (Figure 2-34b) and for the maximum lateral displacement of the segmental wall (Figure 2-34c). The distortion of the sill for the base case is +0.1°

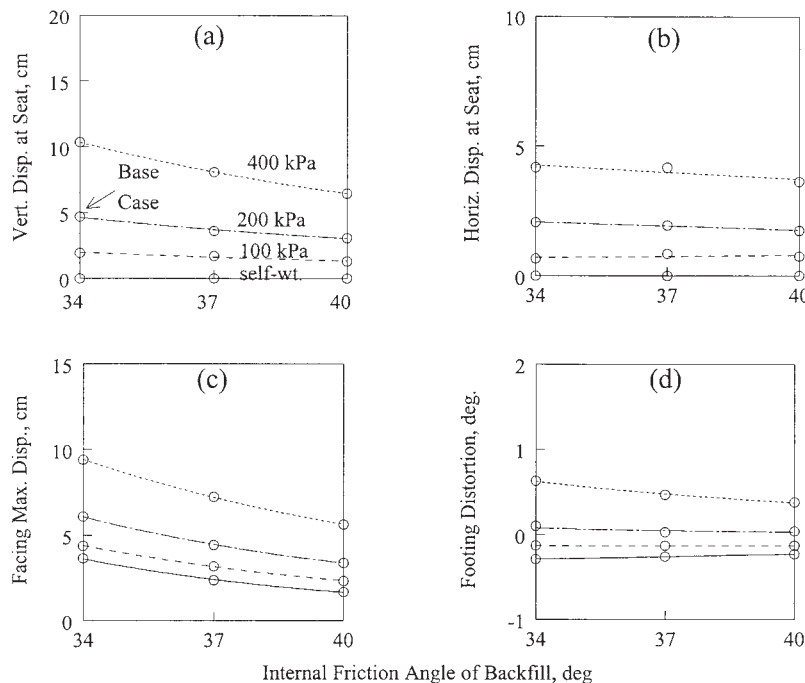


Figure 2-32. Effects of backfill internal friction angle for $s = 20$ cm.

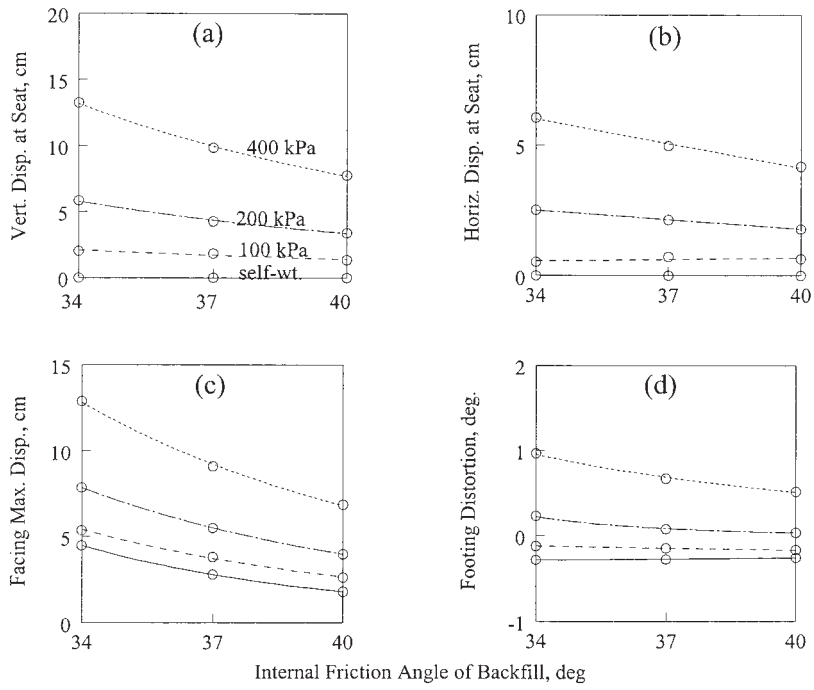


Figure 2-33. Effects of backfill internal friction angle for $s = 40$ cm.

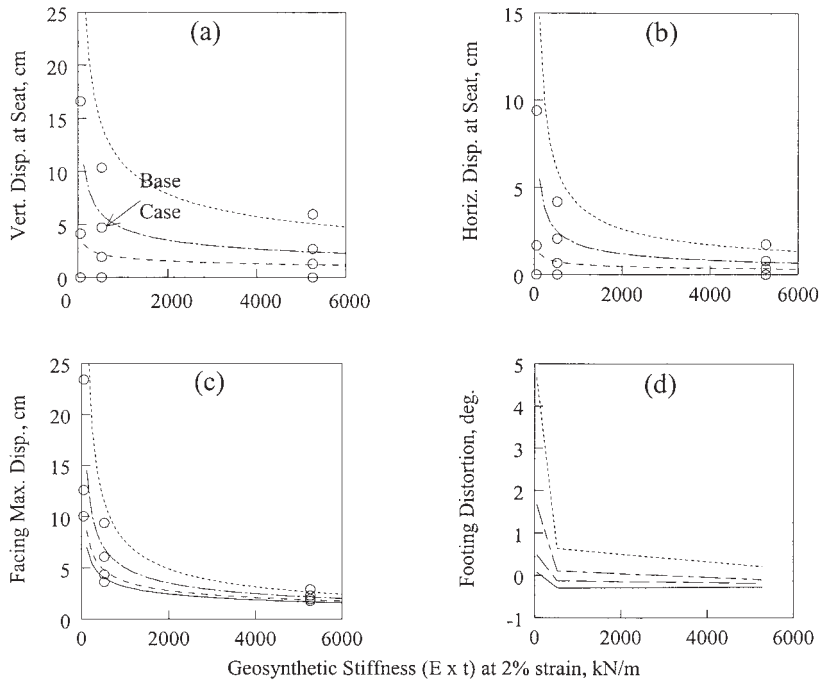


Figure 2-34. Effects of geosynthetic stiffness for $s = 20$ cm.

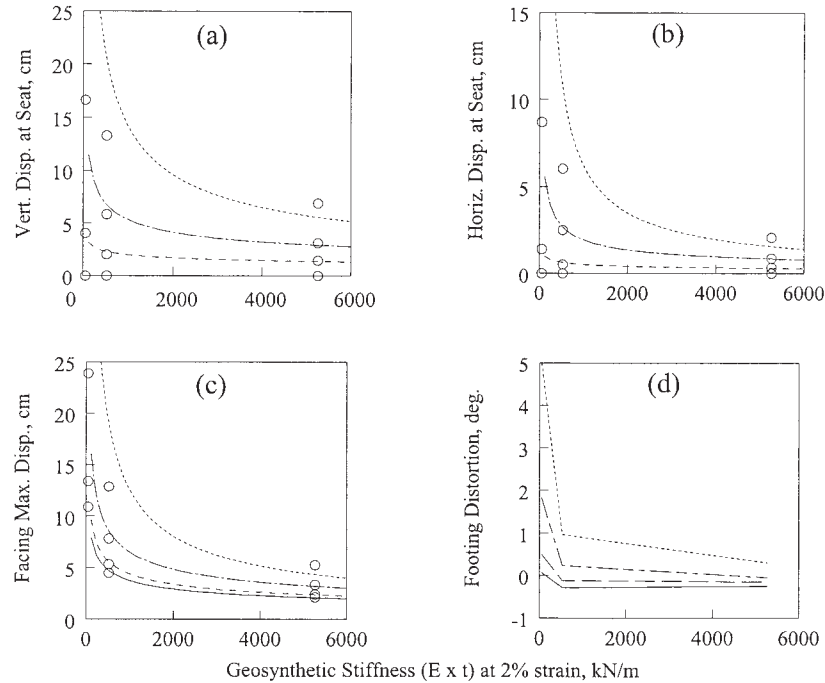


Figure 2-35. Effects of geosynthetic stiffness for $s = 40$ cm.

(forward tilt) as shown in Figure 2-34d. This distortion becomes -0.1° (backward tilt) when the stiffness is increased to 5300 kN/m. The distortion corresponding to a geosynthetic stiffness of 53 kN/m is $+1.67^\circ$.

Figure 2-35a indicates that at an applied pressure of 200 kPa, $s = 40$ cm, and $E * t = 530$ kN/m, there is a 24 percent increase in vertical displacement of the abutment seat as compared with the base case (Figure 2-34a). For $E * t = 5300$ kN/m and $s = 40$ cm, there is a 34 percent reduction in the magnitude of the vertical displacement at the abutment seat as compared with the base case (Figure 2-34a). Similar trends, but with greater changes, are noted in Figure 2-35b for the horizontal displacement of the abutment seat and in Figure 2-35c for the maximum lateral displacement of the segmental wall. The distortion of the sill ranged from $+1.8^\circ$ at $E * t = 53$ kN/m to -0.05° at $E * t = 5300$ kN/m as shown in Figure 2-35d.

Effects of Sill Clear Distance

Sill clear distances of 0 cm, 15 cm (base case), and 30 cm were used to investigate the effects of clearance on the GRS abutment. The effects of sill clear distance on the performance of the GRS abutment is shown in Figure 2-36 for geosynthetic spacing $s = 20$ cm and in Figure 2-37 for $s = 40$ cm.

Figure 2-36a shows that the vertical displacement of the abutment seat of the base case is 4.7 cm for an applied pressure of 200 kPa. This displacement is reduced 20 percent when the clearance is reduced to 0 cm. On the other hand, an

increase of 11 percent in displacement is noted when the clearance is increased to 30 cm. The same trend and magnitude is noted for the horizontal displacement of the abutment seat (Figure 2-36b). For the maximum lateral displacement of the segmental wall (Figure 2-36c), the trend was similar but with smaller magnitudes. The distortion of the sill for the base case is $+0.1^\circ$ (forward tilt) as shown in Figure 2-36d. This distortion becomes -0.1° (backward tilt) when the clearance is reduced to 0 cm. The distortion corresponding to a clearance of 30 cm is $+0.22^\circ$.

Figure 2-37a indicates that at an applied pressure of 200 kPa, $s = 40$ cm and a clear distance of 0 cm, there is a 4 percent increase in vertical displacement of the abutment seat as compared with the base case (Figure 2-36a). For a clear distance of 30 cm and $s = 40$ cm, there is a 37 percent increase in the magnitude of the vertical displacement at the abutment seat as compared with the base case (Figure 2-36a). Similar trends with comparable magnitudes are noted in Figure 2-37b for the horizontal displacement of the abutment seat and in Figure 2-37c for the maximum lateral displacement of the segmental wall. The distortion of the sill ranged from -0.02° at a clear distance of 0 cm to $+0.33^\circ$ at a clear distance of 30 cm as shown in Figure 2-37d.

Figures 2-36 and 2-37 show that the performance of the GRS abutment caused by decreasing sill clear distance is counter-intuitive. Decreasing clear distance indicates that the applied pressure is closer to the segmental facing, thus, greater displacements of the segmental facing, and therefore greater displacements at the abutment seat are expected. This discrepancy may be attributed to the fact that when the clear

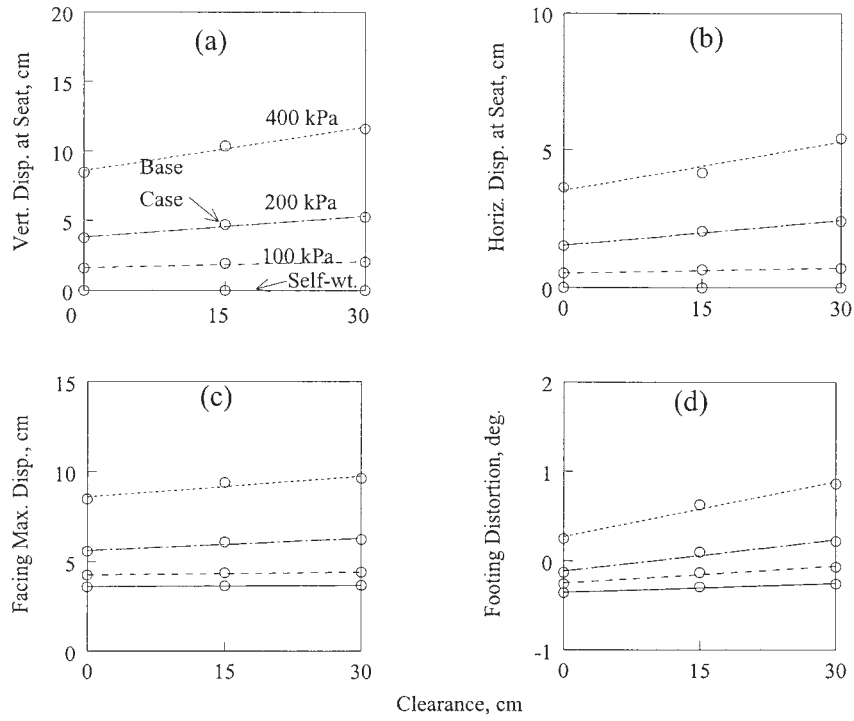


Figure 2-36. Effects of sill clear distance for $s = 20$ cm.

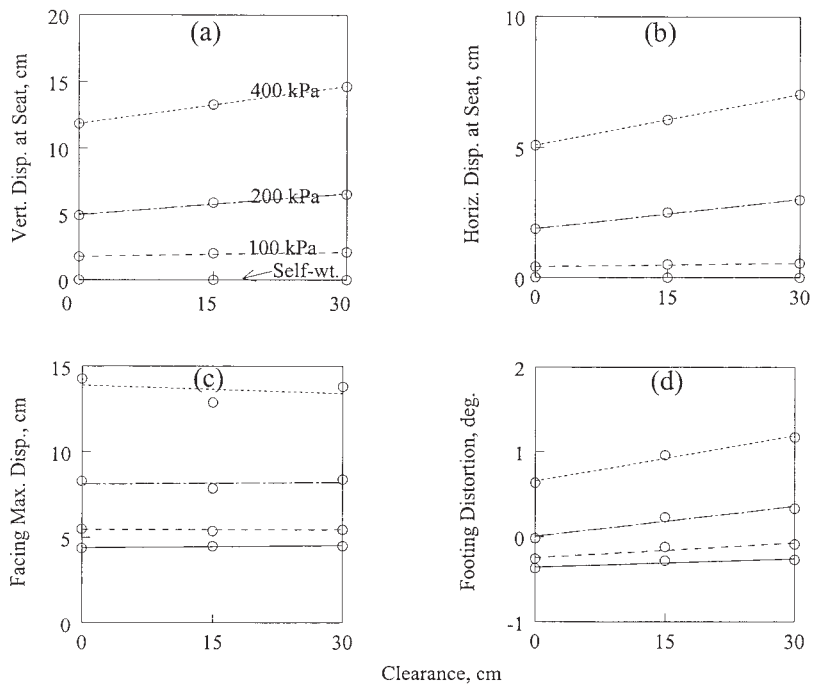


Figure 2-37. Effects of sill clear distance for $s = 40$ cm.

distance is small, there will be more contribution, in terms of stiffness, from the segmental facing. Nevertheless, this counter-intuitive response can be ascertained via large-scale testing of a GRS bridge abutment with small and large sill clearances.

Effects of Sill Width

To investigate the effect of sill width on the GRS bridge abutment, two sill widths were used: 150 cm (Base Case), and 100 cm. The effects of sill width on the performance of the GRS abutment is shown in Figure 2-38 for $s = 20$ cm and in Figure 2-39 for $s = 40$ cm.

At 300 kN/m of applied load (corresponding to 200 kPa of applied pressure for the 150-cm-wide sill, and 300 kPa for the 100-cm-wide sill), the vertical displacement at the abutment seat increased 21 percent when the width decreased from 150 cm (base case) to 100 cm, as indicated in Figure 2-38a. The effect of decreasing sill width on the horizontal displacement of the abutment seat was similar in trend and magnitude as shown in Figure 2-38b. As shown in Figure 2-38c, at 300 kN/m of applied load, the maximum lateral displacement of the segmental facing increased roughly 11 percent when sill width decreased to 100 cm. The distortion of sill changed from $+0.1^\circ$ at sill width of 150 cm to $+0.18^\circ$ at sill width of 100 cm as shown in Figure 2-38d.

As shown in Figure 2-39a, for a sill width of 150 cm, $s = 40$ cm, and an applied load of 300 kN/m, the vertical dis-

placement of the abutment seat is 5.8 cm, which is 24 percent greater than that corresponding to the base case (sill width = 150 cm, $s = 20$ cm, Figure 2-38a). For a sill width of 100 cm and $s = 40$ cm, the vertical displacement at the abutment seat is 67 percent greater than the base case. The horizontal displacement at the abutment seat (Figure 2-39b) and the maximum lateral displacement of the segmental wall (Figure 2-39c) follow the same trend of the vertical displacement at the abutment seat. The distortion of sill changed from $+0.4^\circ$ at sill width of 150 cm to $+0.28^\circ$ at sill width of 100 cm, as shown in Figure 2-39d. Figures 2-38 and 2-39 show that the performance parameters increased at a higher rate under higher applied loads.

Effects of Reinforcement Truncation

To study the effects of truncated reinforcement on the performance of the GRS abutment, the GRS abutment was modified so that the reinforcement length is truncated at the base. The truncated base was assumed to be $H/4$ and increases upward at 45° angle (H is the height of the segmental wall).

Figure 2-40 shows the effect of truncated reinforcement on the performance parameters for $s = 40$ cm. The figure compares the truncated and non-truncated reinforcement cases and indicates that the effect of truncated reinforcement is insignificant in terms of displacements. Figure 2-40d shows that there is a small decrease in sill distortion in the case of truncated reinforcement.

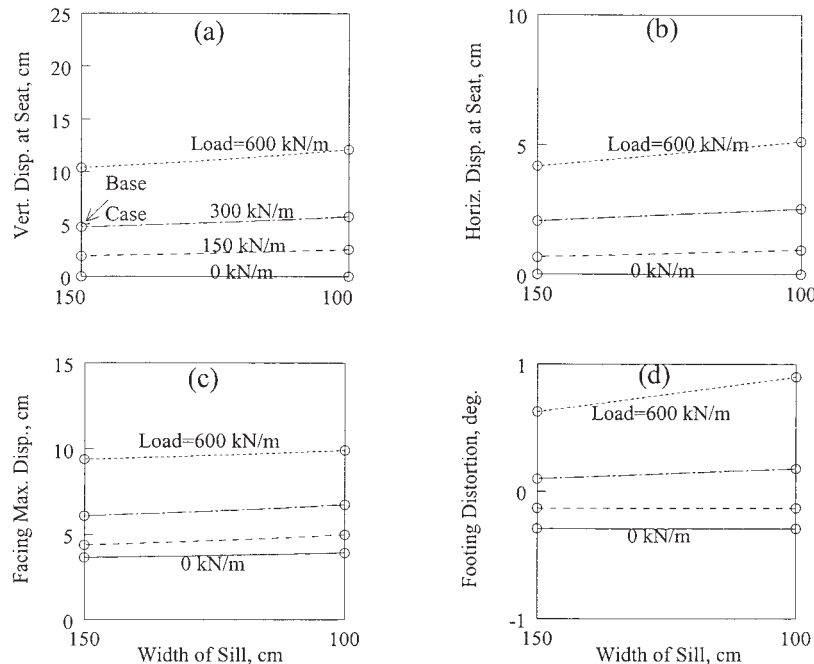


Figure 2-38. Effects of sill width for $s = 20$ cm.

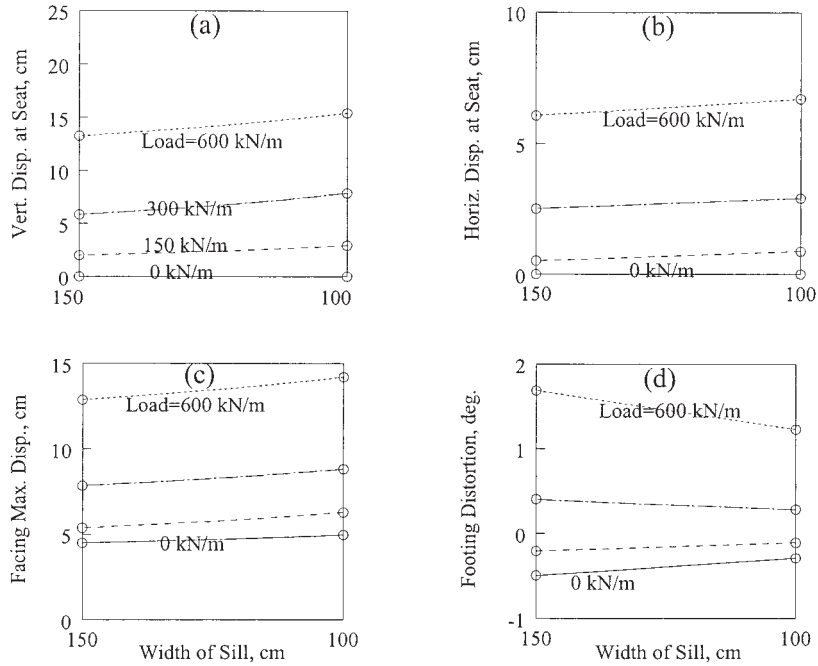


Figure 2-39. Effects of sill width for $s = 40$ cm.

Predicting Failure Loads

In the parametric study, none of the GRS bridge abutments failed “catastrophically” as in the Garden experiment and the Garden test analysis described in Appendix C (*NCHRP Web-Only Document 81*). All abutments withstood the 1000 kPa

load but suffered very significant displacements and distresses without sudden failure. It is suitable to think about shear strain in the soil mass as a measure of distress in a GRS abutment. Thus, a simple failure criterion based on the maximum shear strain is proposed herein in order to estimate the allowable bearing pressure of a spread footing.

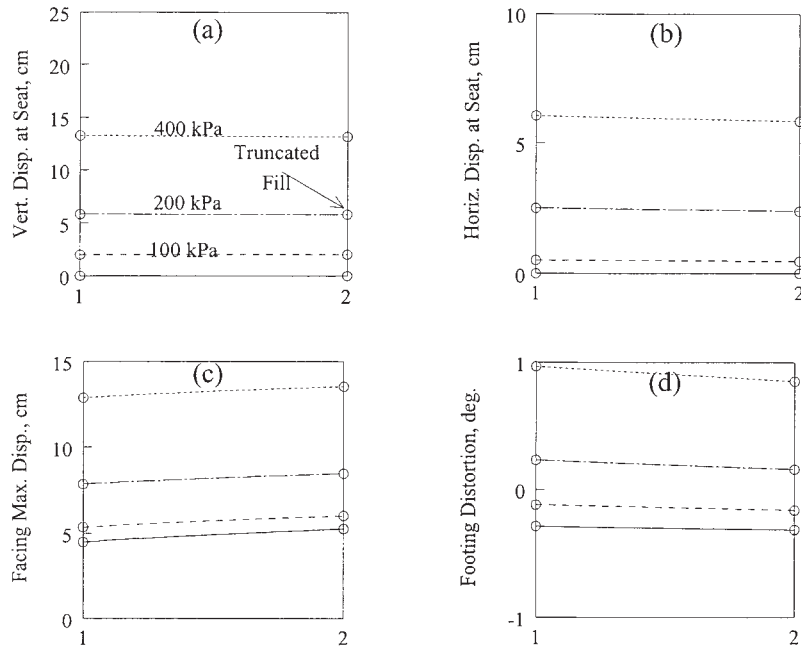


Figure 2-40. Effects of reinforcement truncation for $s = 40$ cm.

From the parametric analysis, it was noted in most cases that there exists a triangular failure zone initiating near the soil-facing interface and propagating into the backfill as the load is increased. This failure zone sustained greater shear strains than the rest of the backfill. The proposed failure criterion suggests that failure occurs when (1) the triangular shear zone propagates all the way to the back edge of the spread footing as shown in Figure 2-41, and (2) the triangular shear zone sustains shear strains that exceed a critical value, $\gamma_{(critical)}$, defined as:

$$\gamma_{(critical)} = 2/3 [(\epsilon_1)_{failure} - (\epsilon_3)_{failure}]$$

where $(\epsilon_1)_{failure}$ is the axial strain at failure, $(\epsilon_3)_{failure}$ is the radial strain at failure, and $2/3$ is a reduction factor (equivalent to a safety factor of 1.5). Both $(\epsilon_1)_{failure}$ and $(\epsilon_3)_{failure}$ can be obtained from triaxial test results. For the soils used in the parametric analysis with $\phi = 34^\circ$, 37° , and 40° , the critical shear strain, $\gamma_{(critical)}$, is determined as 3.2 percent with the help of the triaxial test results presented in Figure 2-30. This critical shear strain value was then used to estimate the allowable bearing pressure under different conditions as shown in Table 2-4.

Load-Carrying Capacity Analysis

A series of load-carrying capacity analyses, as an extension of the Parametric Study presented in the previous section, was conducted to examine the effect of sill type, sill width, soil stiffness/strength, reinforcement spacing, and

foundation stiffness on the allowable load-carrying capacity of GRS abutment sills. Seventy-two analyses were performed using the LS-DYNA code. The variables in the analyses included the following:

- Sill type: integrated sill and isolated sill;
- Sill width: 0.8 m, 1.5 m, and 2.5 m;
- Reinforcement spacing: 0.2 m and 0.4 m;
- Soil friction angle: 34° , 37° , and 40° ; and
- Foundation: 6-m-thick medium sand foundation and rigid foundation.

Of the 72 analyses, one-half were for a GRS abutment situated over a medium sand foundation (with its stiffness representing a lower-bound “competent” foundation), and the other half were for a GRS abutment situated over a rigid foundation.

Geometry and Material Properties

Figures 2-42 through 2-47 show the configuration of the abutments investigated in this study. Sill widths of 0.8 m, 1.5 m, and 2.5 m, and two sill types (integrated and isolated sills) were investigated. The abutments share the following common features:

- Lower wall height = 4.67 m (15.3 ft); upper wall height = 2.44 m (8 ft);

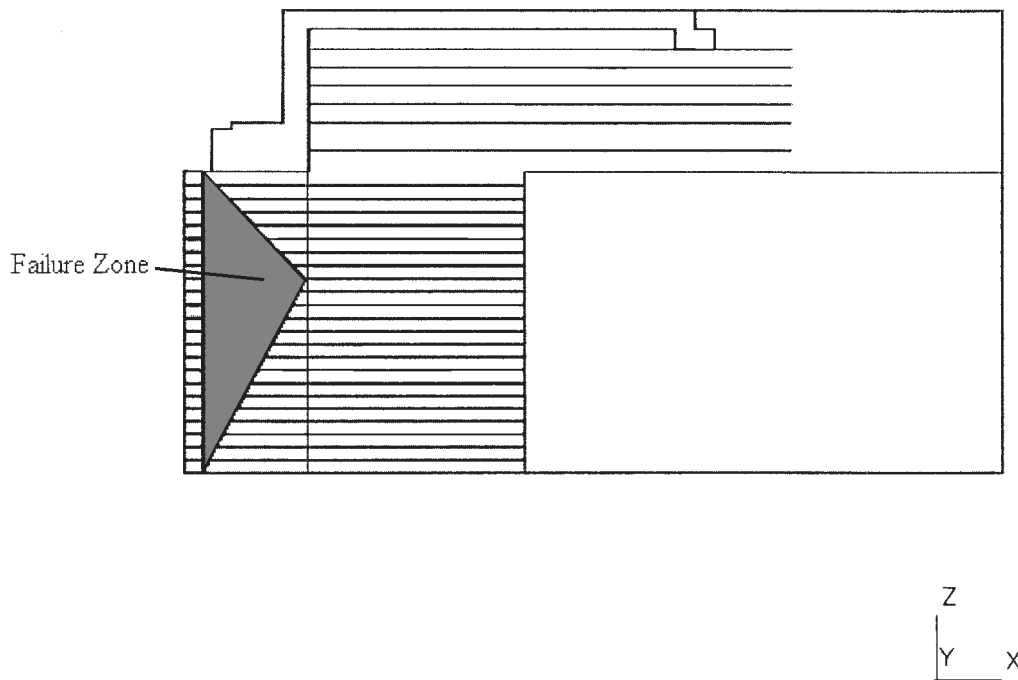


Figure 2-41. The critical shear strain distribution failure criterion.

TABLE 2-4 Allowable bearing pressures based on the critical shear strain distribution criterion

	$\phi = 34^\circ$	$\phi = 37^\circ$	$\phi = 40^\circ$
Reinforcement Spacing = 20 cm	225 kPa	280 kPa	360 kPa
Reinforcement Spacing = 40 cm	120 kPa	200 kPa	280 kPa

- Sill clear distance = 0.15 m (6 in.);
- Same backfill in the upper and lower walls;
- A conservative secant modulus for geosynthetic reinforcements = 530 kN/m; and
- Reinforcement length in lower wall = 5.0 m (0.7 * the total wall height); reinforcement length in upper wall = 7.5 m.

The case of an abutment over a rigid foundation with an integrated sill (sill width = 1.5 m) has the same configuration as the base case in the Parametric Study (see Figure 2-28).

The reinforced fill, retained earth, and the medium sand foundation were simulated by an extended two-invariant geologic cap material model. The material parameters of the geologic cap model for the three select backfills with friction angles of 34°, 37°, and 40° and the retained earth behind the reinforced soil region are summarized in Table 2-5. The medium sand foundation was assumed to have the same properties as the reinforced fill with a friction angle of 37°. Also, the same stiffness values as those used in the Parametric Study for soils with $\phi = 34^\circ$, 37°, and 40° were employed.

The sill, modular facing blocks, approach slab, and geosynthetic reinforcement were simulated by an elastic material model. The elastic material parameters are summarized in Table 2-6. The geosynthetic reinforcement in the performance analysis was assumed to have a constant stiffness ($E * t$) of 530 kN/m. The material parameters listed in Table 2-6 are of the same values as those used in the base case of the Parametric Study.

Performance Characteristics

The results of the 72 finite element analyses were summarized in 32 figures. Four performance characteristics were examined in the figures: settlement of sill, maximum lateral displacement of wall face, lateral movement of sill, and rotation of sill. Each of the 32 figures shows the relationships between the applied pressure on the sill and one of the four performance characteristics for three different sill widths (0.8 m, 1.5 m, and 2.5 m) and three soil friction angles (34°,

37°, and 40°). The conditions associated with each figure are as follows:

- The relationship between settlement of sill and applied sill pressure: Figure 2-48 ($s = 0.2$ m, integrated sill), Figure 2-49 ($s = 0.4$ m, integrated sill), Figure 2-50 ($s = 0.2$ m, isolated sill), Figure 2-51 ($s = 0.4$ m, isolated sill), all on the medium sand foundation.
- The relationship between lateral displacement of wall face and applied sill pressure: Figure 2-52 ($s = 0.2$ m, integrated sill), Figure 2-53 ($s = 0.4$ m, integrated sill), Figure 2-54 ($s = 0.2$ m, isolated sill), Figure 2-55 ($s = 0.4$ m, isolated sill), all on the medium sand foundation.
- The relationship between lateral movement of sill settlement and applied sill pressure: Figure 2-56 ($s = 0.2$ m, integrated sill), Figure 2-57 ($s = 0.4$ m, integrated sill), Figure 2-58 ($s = 0.2$ m, isolated sill), Figure 2-59 ($s = 0.4$ m, isolated sill), all on the medium sand foundation.
- The relationship between rotation of sill and applied sill pressure: Figure 2-60 ($s = 0.2$ m, integrated sill), Figure 2-61 ($s = 0.4$ m, integrated sill), Figure 2-62 ($s = 0.2$ m, isolated sill), Figure 2-63 ($s = 0.4$ m, isolated sill), all on the medium sand foundation.
- Figures 2-64 to 2-79 (16 figures) correspond to the same conditions as Figures 2-48 to 2-63 (also 16 figures), except that the abutments are situated over a rigid foundation.

The sill settlements and sill lateral movements presented in the figures have excluded the deformations caused by self-weight of the soil because those deformations in actual construction can and will be compensated for or adjusted to zero before any sill pressure is applied. On the other hand, the lateral maximum displacement of the wall face cannot be compensated for or adjusted to from the onset of construction, thus the accumulated values are reported.

General observations of the performance characteristics follow:

- For reinforcement spacing of 0.2 m, none of the abutments suffered from any stability problems up to an applied pressure of 1,000 kPa.

(text continues on page 60)

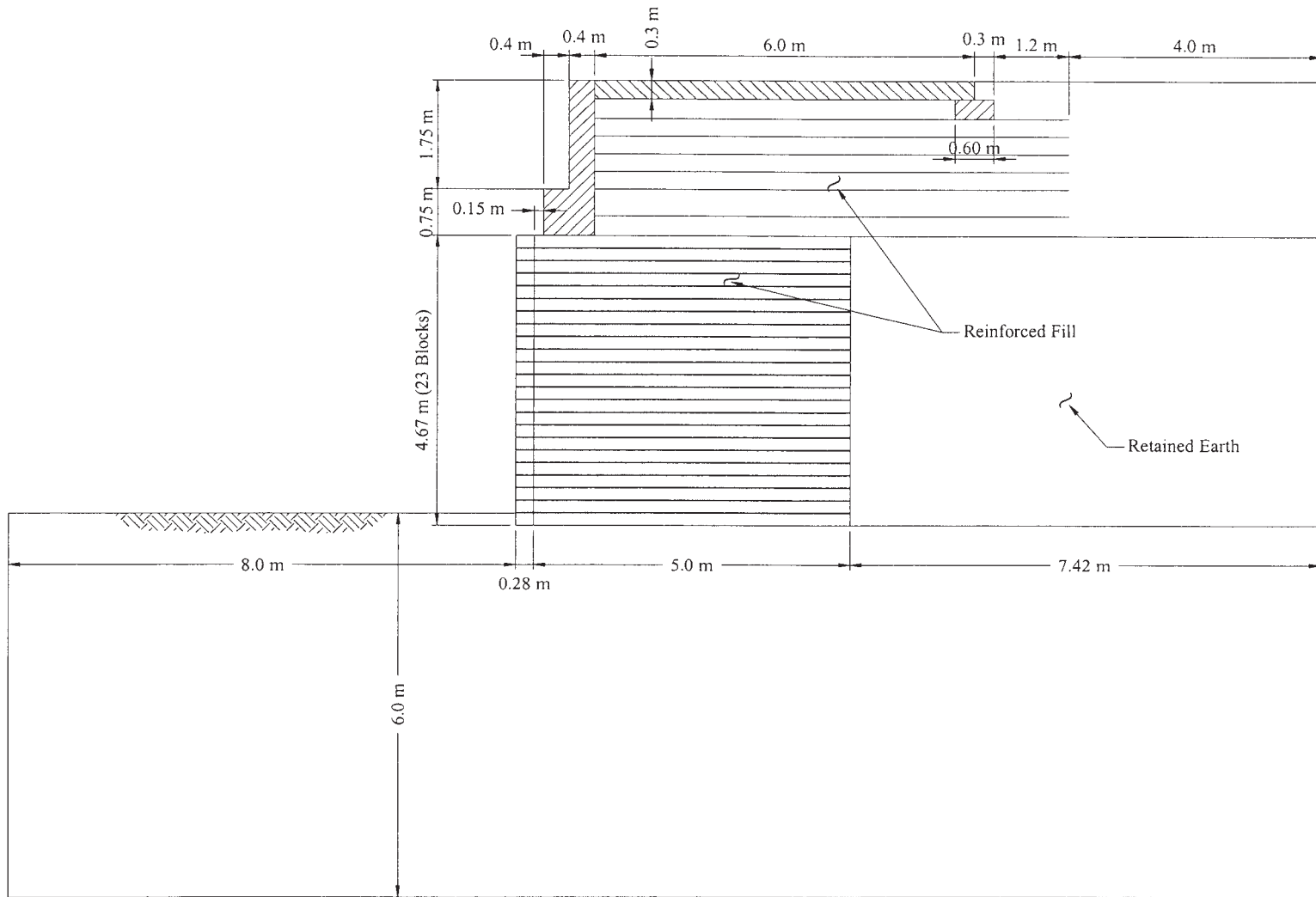


Figure 2-42. Configuration of a GRS abutment with integrated sill, sill width = 0.8 m.

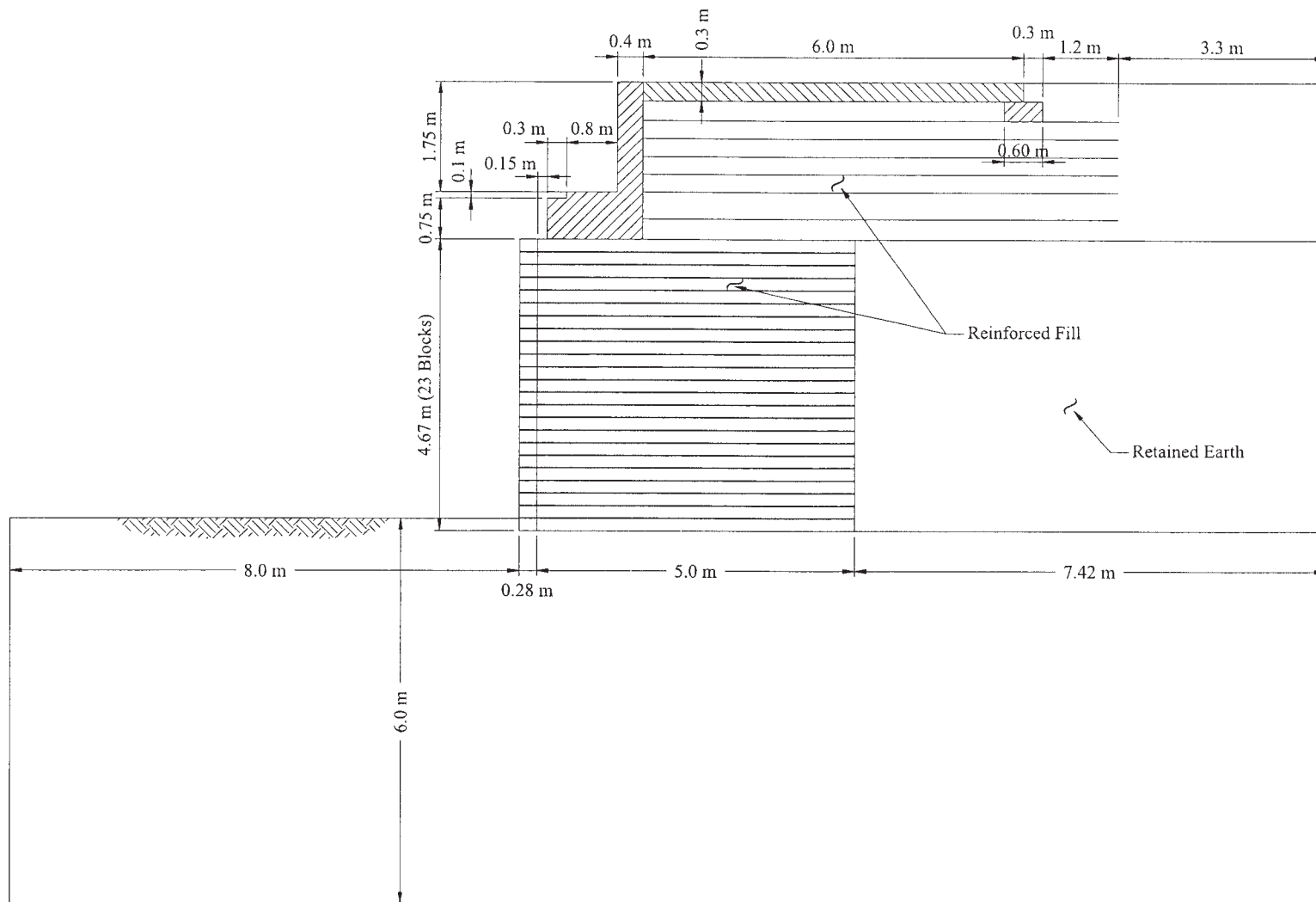


Figure 2-43. Configuration of a GRS abutment with integrated sill, sill width = 1.5 m.

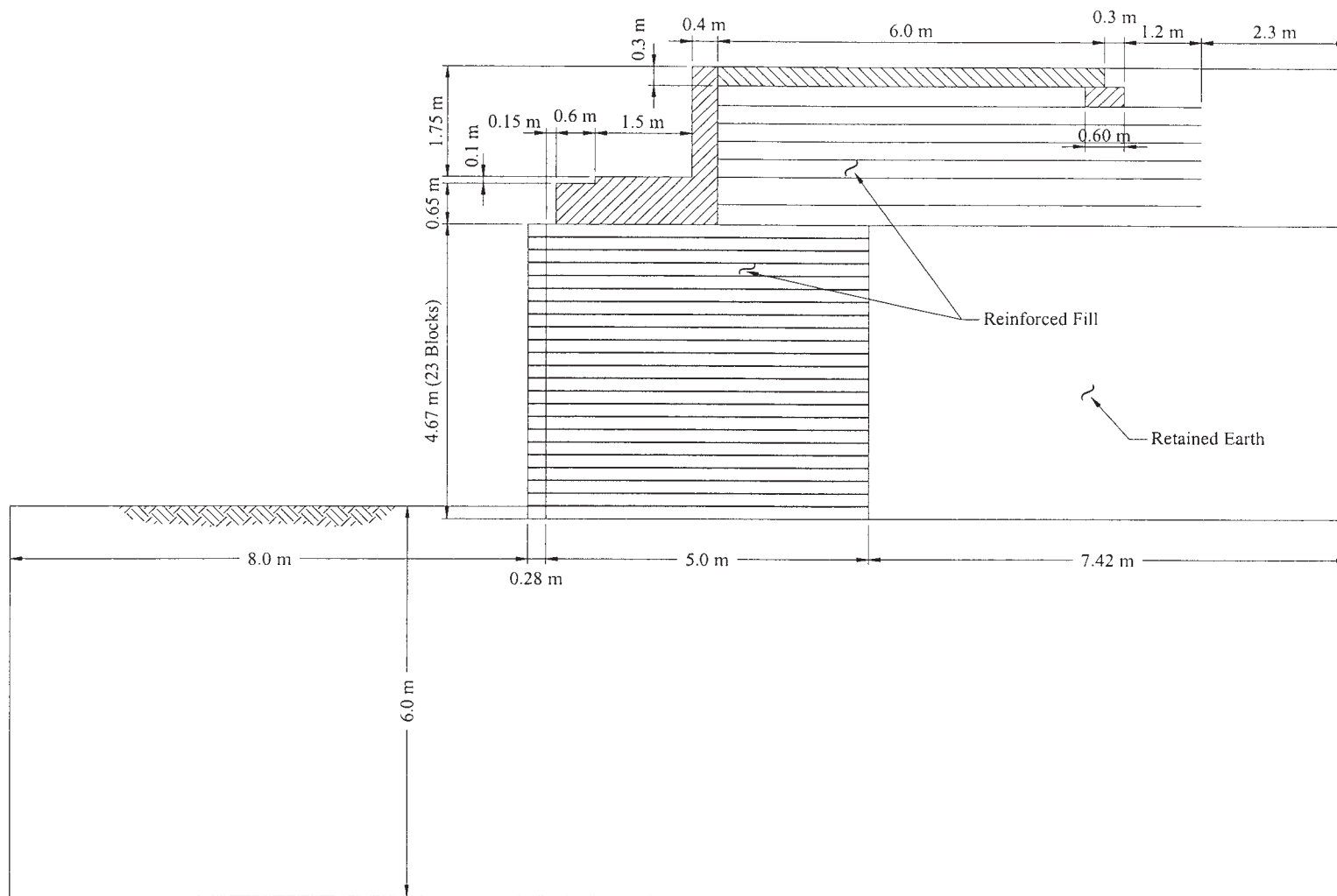


Figure 2-44. Configuration of a GRS abutment with integrated sill, sill width = 2.5 m.

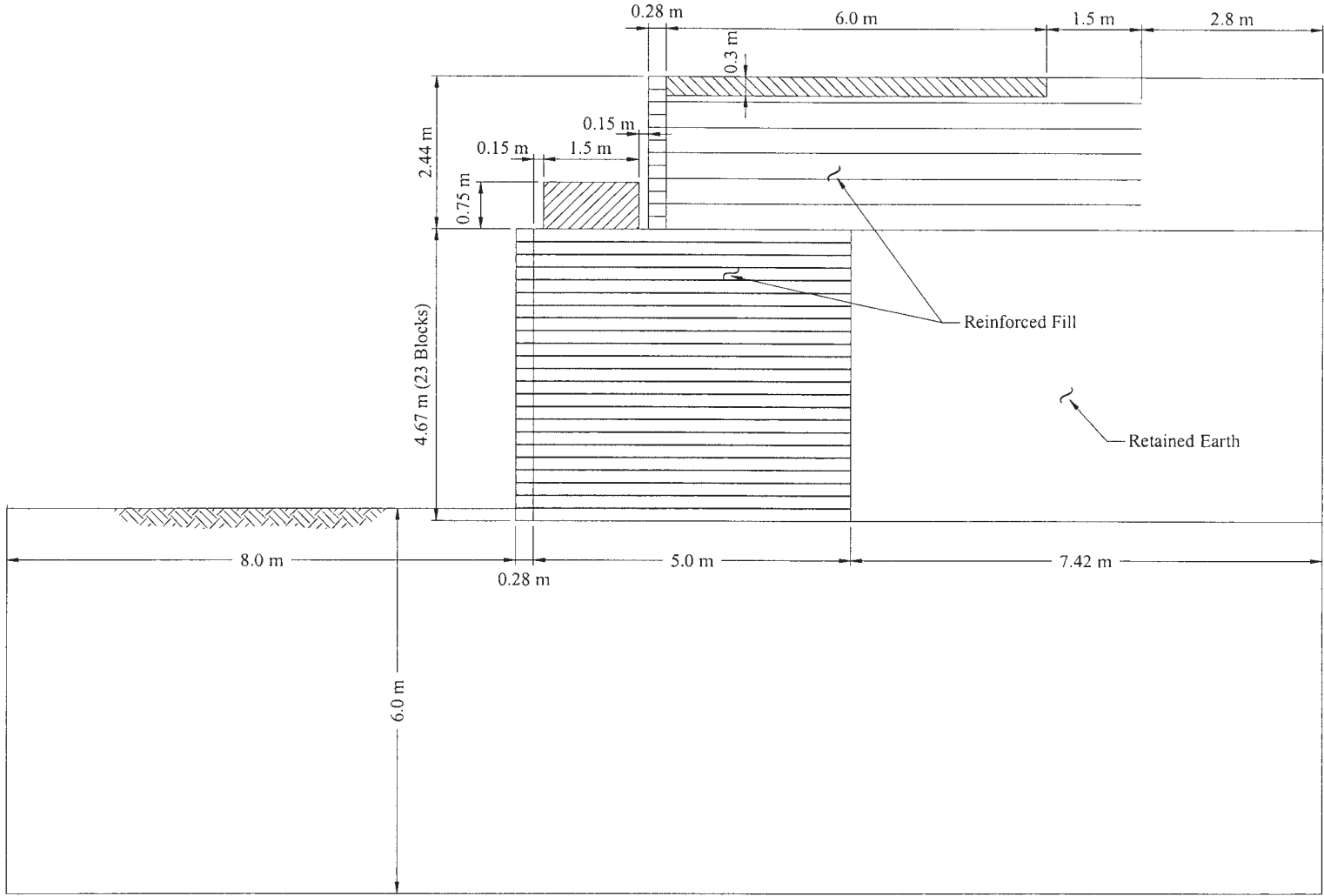


Figure 2-46. Configuration of a GRS abutment with isolated sill, sill width = 1.5 m.

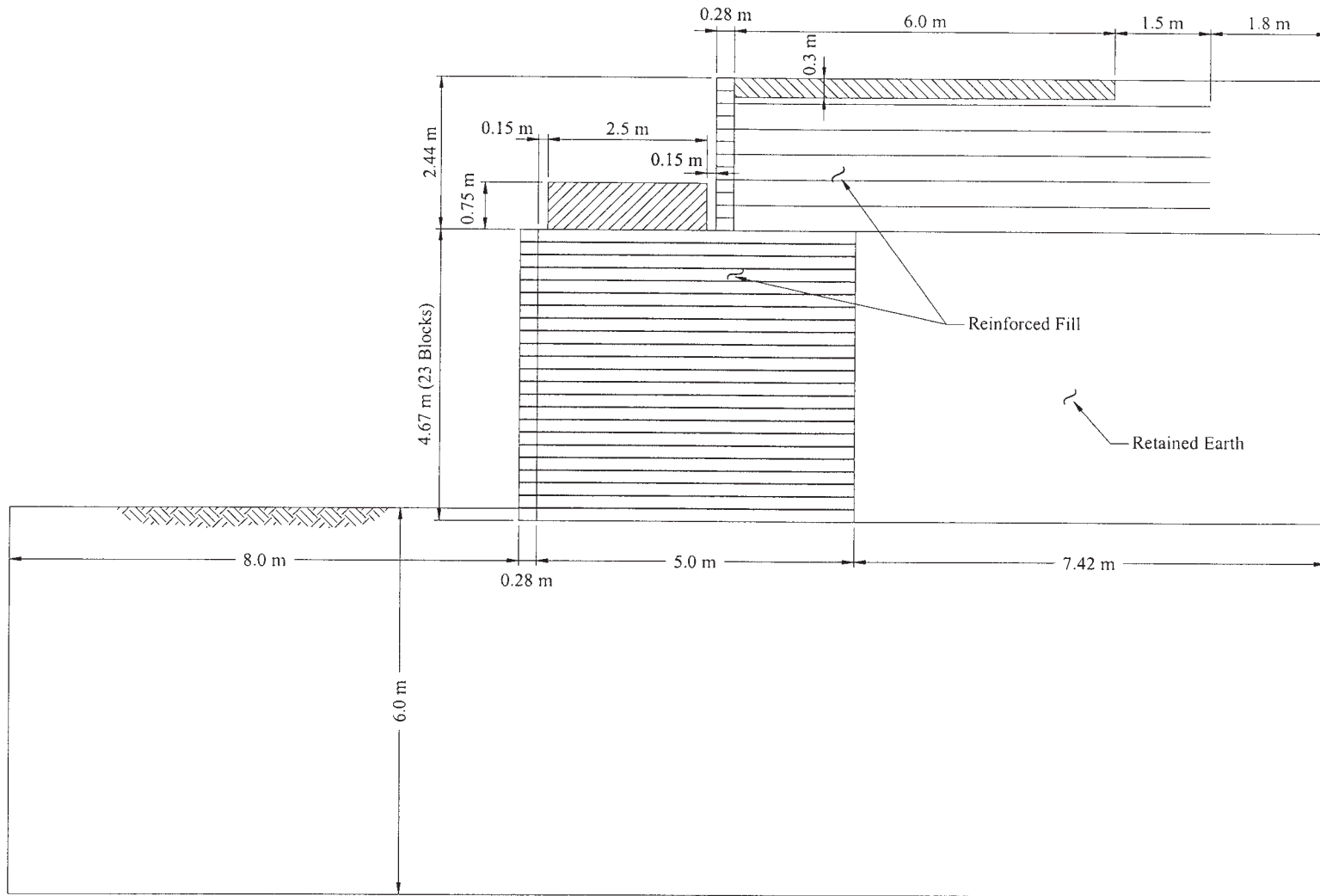


Figure 2-47. Configuration of a GRS abutment with isolated sill, sill width = 2.5 m.

TABLE 2-5 Geologic cap model material parameters

	$\phi = 34^\circ$ soil	$\phi = 37^\circ$ soil	$\phi = 40^\circ$ soil	Retained Earth ($\phi = 30^\circ$)
Initial bulk modulus, K (MPa)	16.45	24.67	32.89	16.45
Initial shear modulus, G (MPa)	7.59	11.39	15.18	7.59
Failure envelope parameter, α (kPa)	0	0	0	0
Failure envelope linear coefficient, θ	0.264	0.289	0.315	0.231
Cap surface axis ratio, R	4	4	4	4
Hardening law exponent, D (kPa) ⁻¹	7.25×10^{-6}	7.25×10^{-6}	7.25×10^{-6}	7.25×10^{-6}
Hardening law coefficient, W	2.5	1.5	1.0	2.5
Hardening law parameter, X_0 (kPa)	200	200	200	0

- For reinforcement spacing of 0.4 m, most of the abutments encountered facing failure (i.e., the top two to three courses of facing blocks “fell off” the wall face) when the applied pressure exceeded 500 kPa to 970 kPa (depending on the geometric condition and material properties of the abutment). Only those abutments with sill width = 0.8 m and soil friction angle = 37° and 40° did not encounter facing failure up to an applied pressure of 1,000 kPa. In any case, there was no catastrophic failure in any abutment up to 1,000 kPa applied pressure.
- For reinforcement spacing of 0.2 m, the rate of deformation was relatively small at an applied pressure between 0 to 100 kPa. The rate of deformation increased slightly between 100 to 200 kPa and then remained roughly constant between 200 and 1,000 kPa.
- For reinforcement spacing of 0.4 m, the rate of deformation was also relatively small at an applied pressure between 0 to 100 kPa. For applied pressure between 100 and 400 kPa, the rate of deformation increased

somewhat with increasing pressure. Once exceeding about 400 kPa, the rate of deformation was nearly constant until it approached a failure condition (facing failure).

- The settlement of sill was somewhat less for the abutments with an integrated sill than with an isolated sill; whereas the maximum lateral displacement of wall face did not differ much for the two types of sill.
- The differences in the magnitude of the performance characteristics for ϕ between 34° and 37° were generally greater than those between 37° and 40° . This suggests that increasing the soil friction angle (by selecting a better fill type and/or with better compaction efforts) to improve the performance characteristics is more efficient for soils with a lower friction angle than for soils with a higher friction angle.
- The effect of reinforcement spacing on sill settlement and maximum lateral displacement of wall face was significant, especially at applied pressure greater than 200 kPa.

(text continues on page 93)

TABLE 2-6 Elastic model material parameters

Elastic Material Parameters	Sill, Facing blocks, and Approach slab	Geosynthetic reinforcement
Young's modulus, E (kPa)	13.8×10^6	4.14×10^4
Poisson's ratio, ν	0.21	0.3

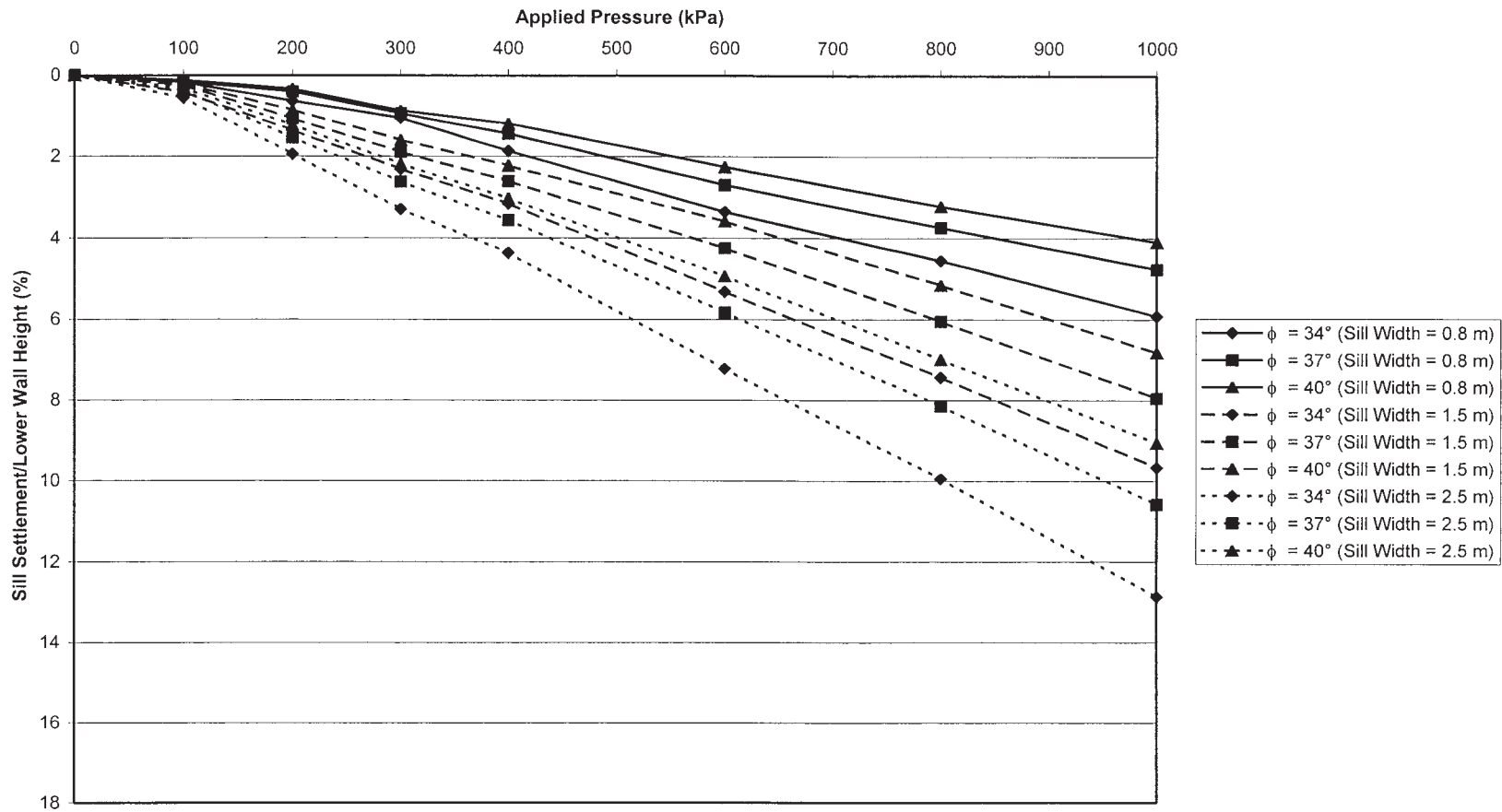


Figure 2-48. Relationship between applied pressure and sill settlement: integrated sill, $s=0.2$ m, and medium sand foundation.

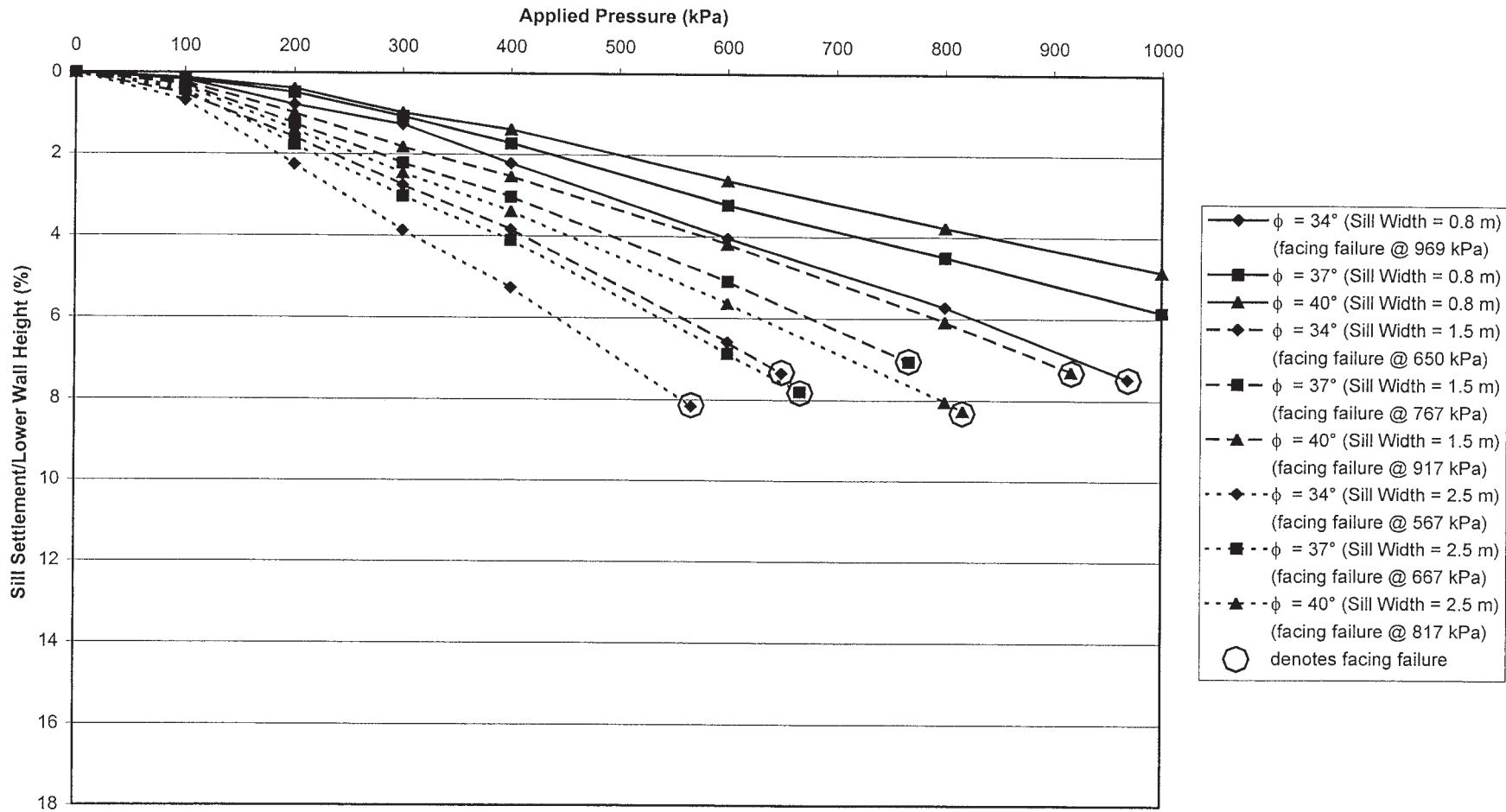


Figure 2-49. Relationship between applied pressure and sill settlement: integrated sill, $s = 0.4$ m, and medium sand foundation.

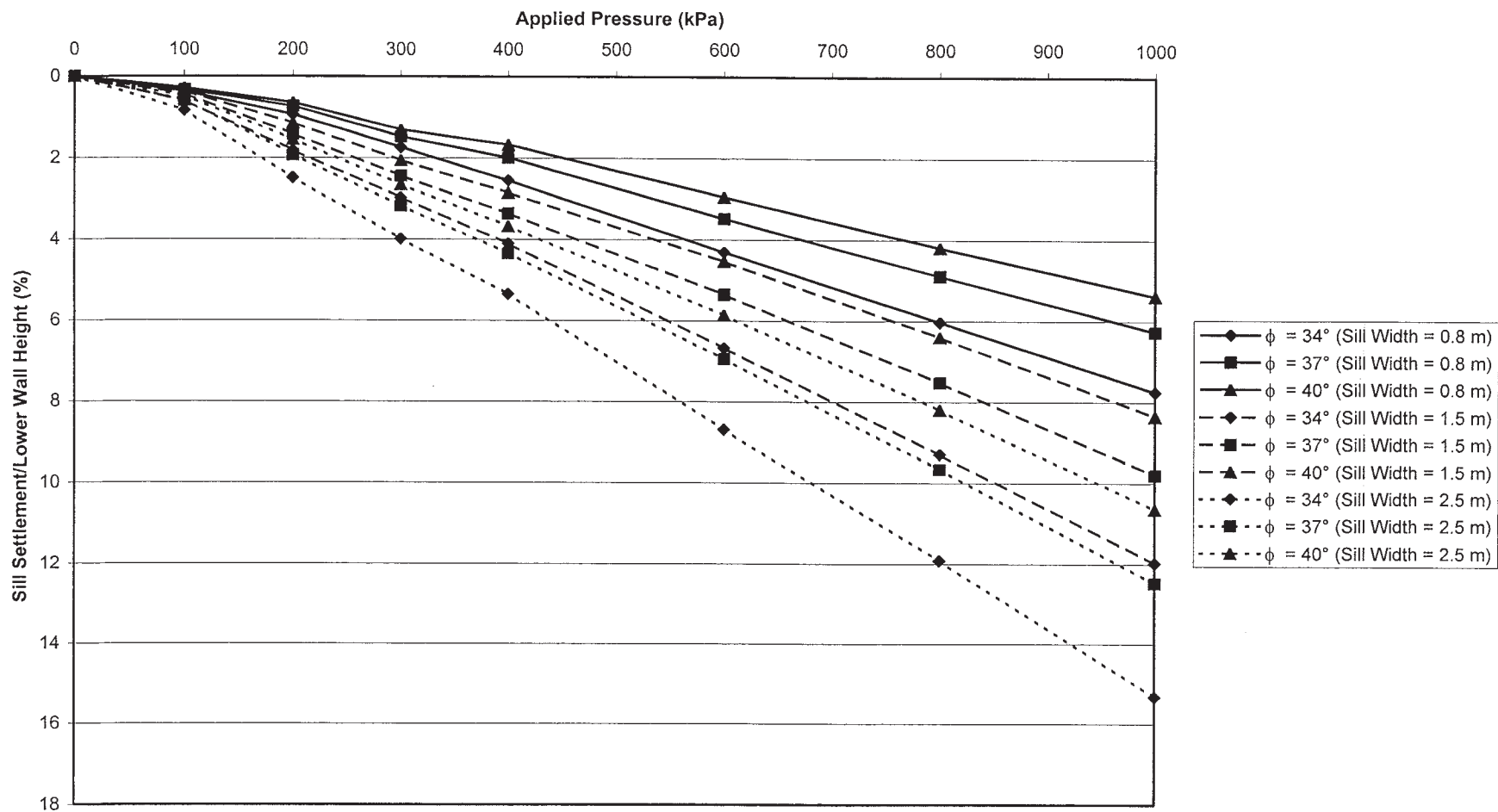


Figure 2-50. Relationship between applied pressure and sill settlement: isolated sill, $s = 0.2$ m, and medium sand foundation.

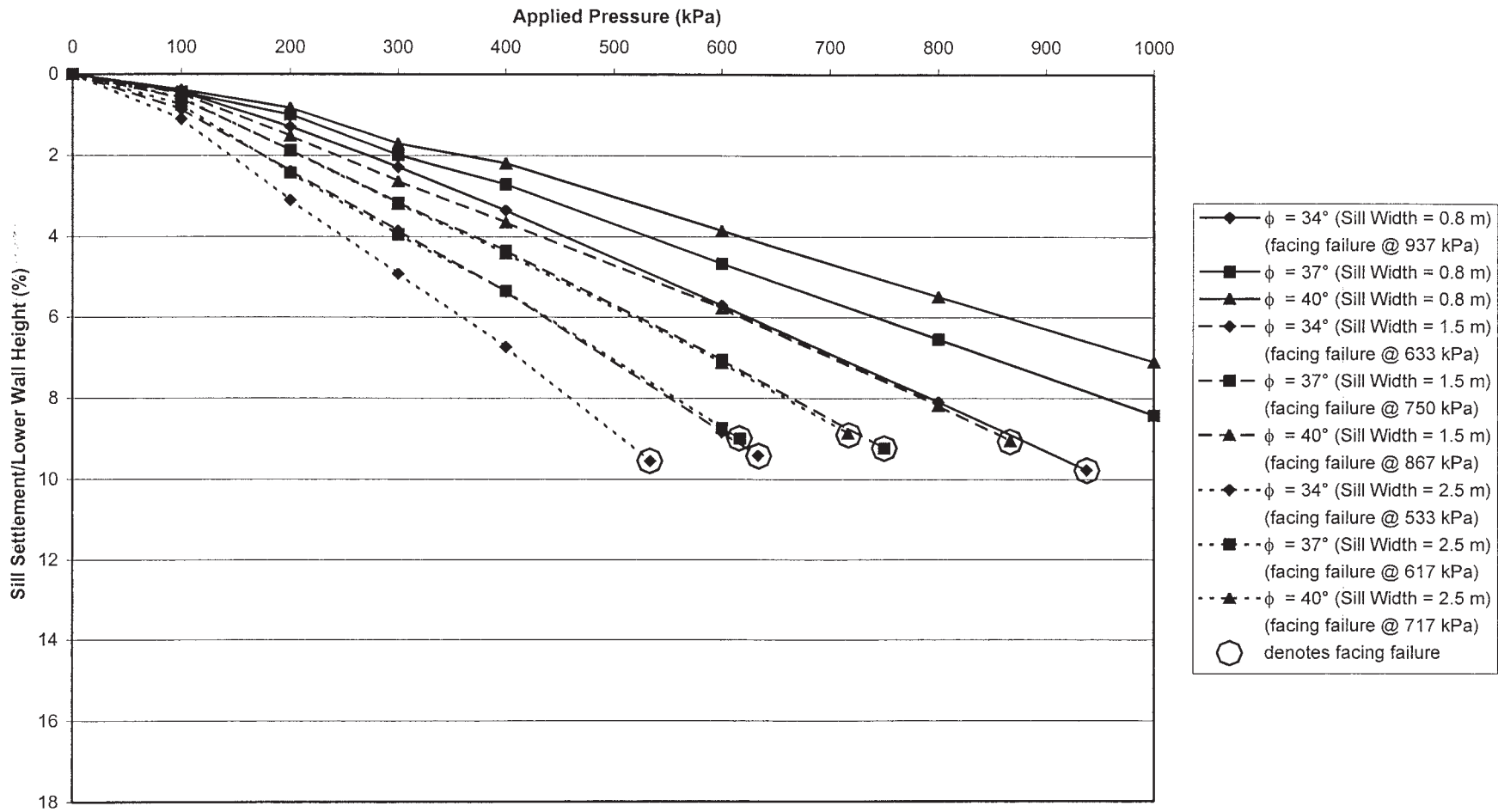


Figure 2-51. Relationship between applied pressure and sill settlement: isolated sill, $s = 0.4$ m, and medium sand foundation.

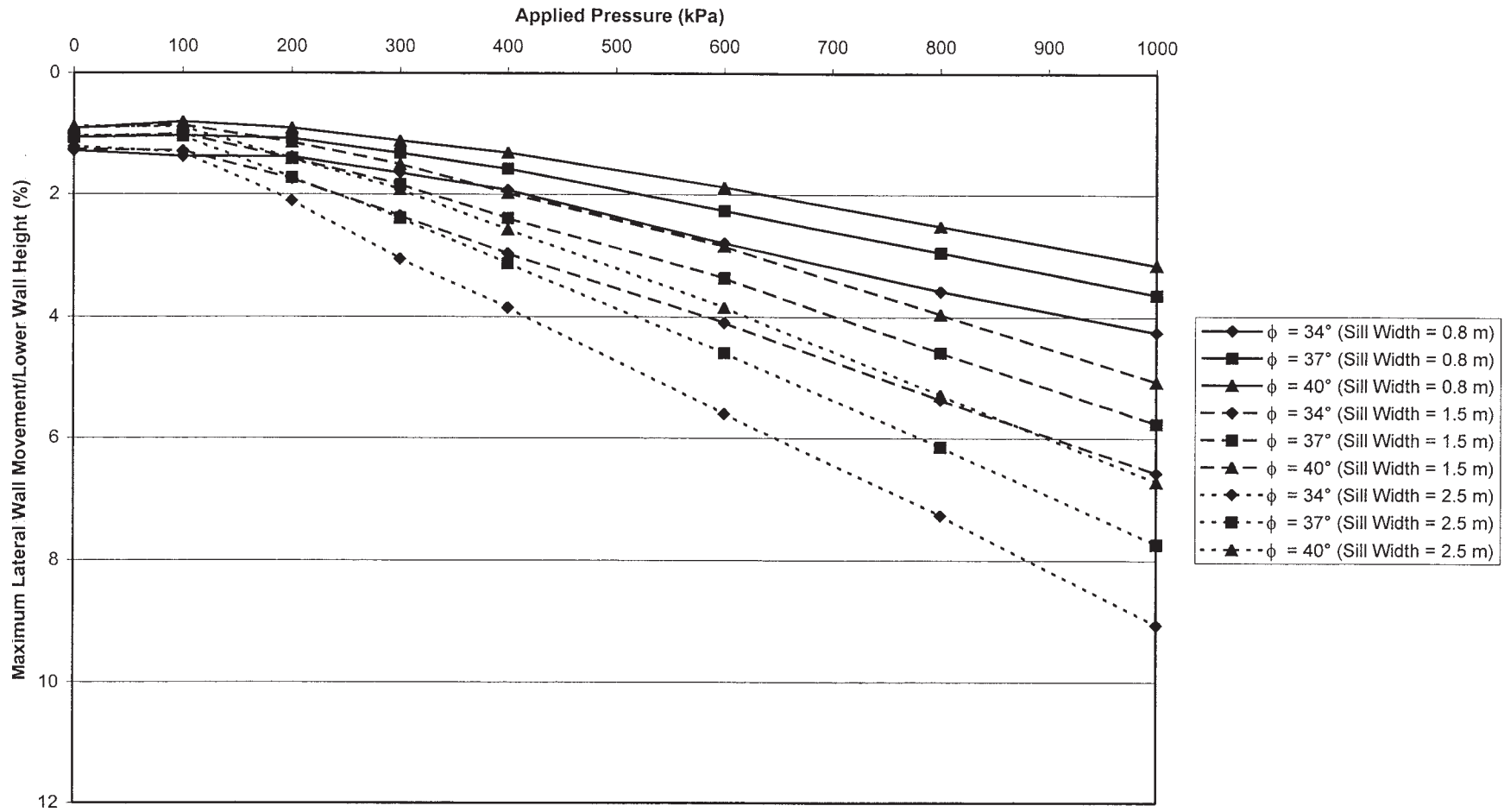


Figure 2-52. Relationship between applied pressure and maximum lateral wall displacement: integrated sill, $s = 0.2$ m, and medium sand foundation.

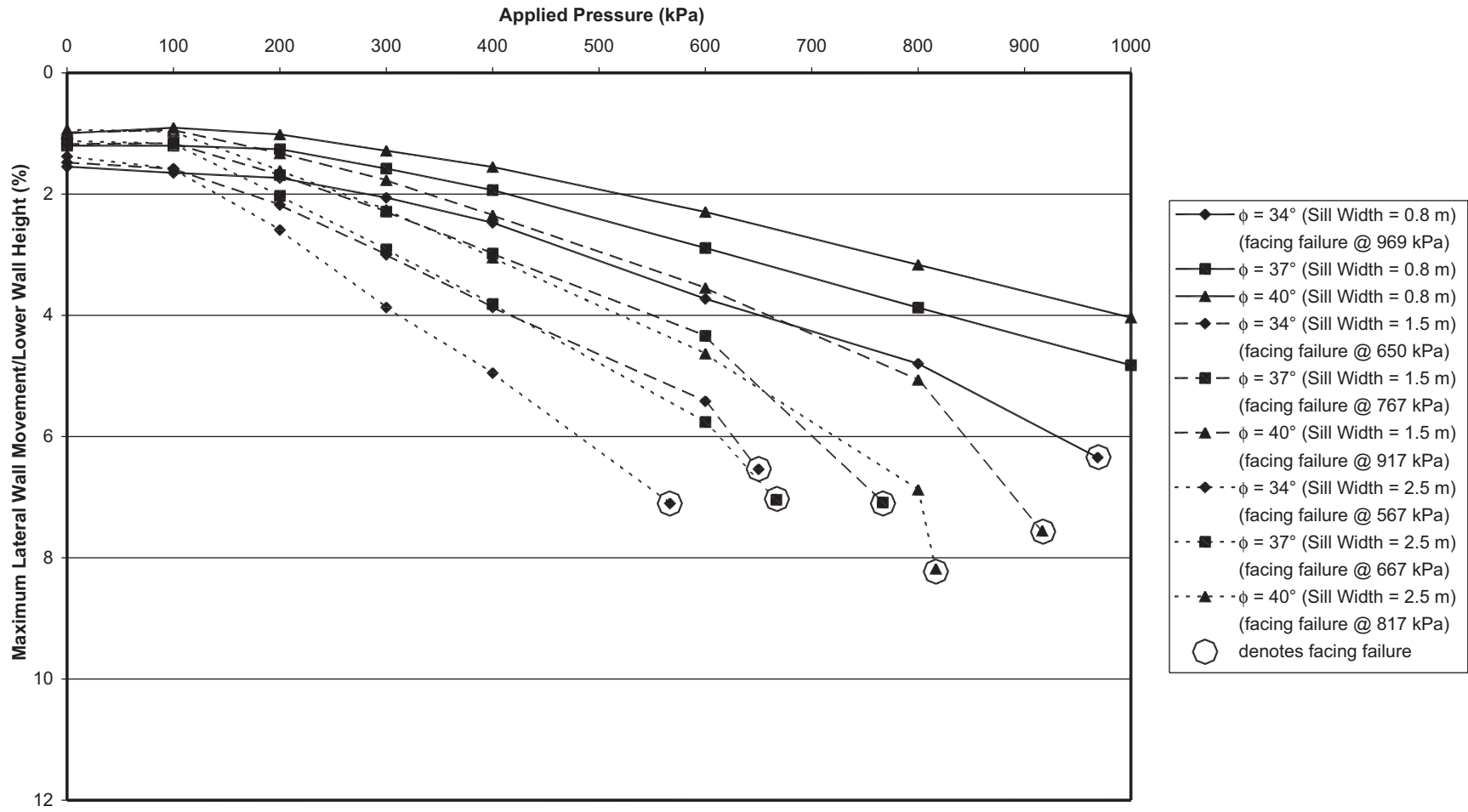


Figure 2-53. Relationship between applied pressure and maximum lateral wall displacement: integrated sill, $s = 0.4$ m, and medium sand foundation.

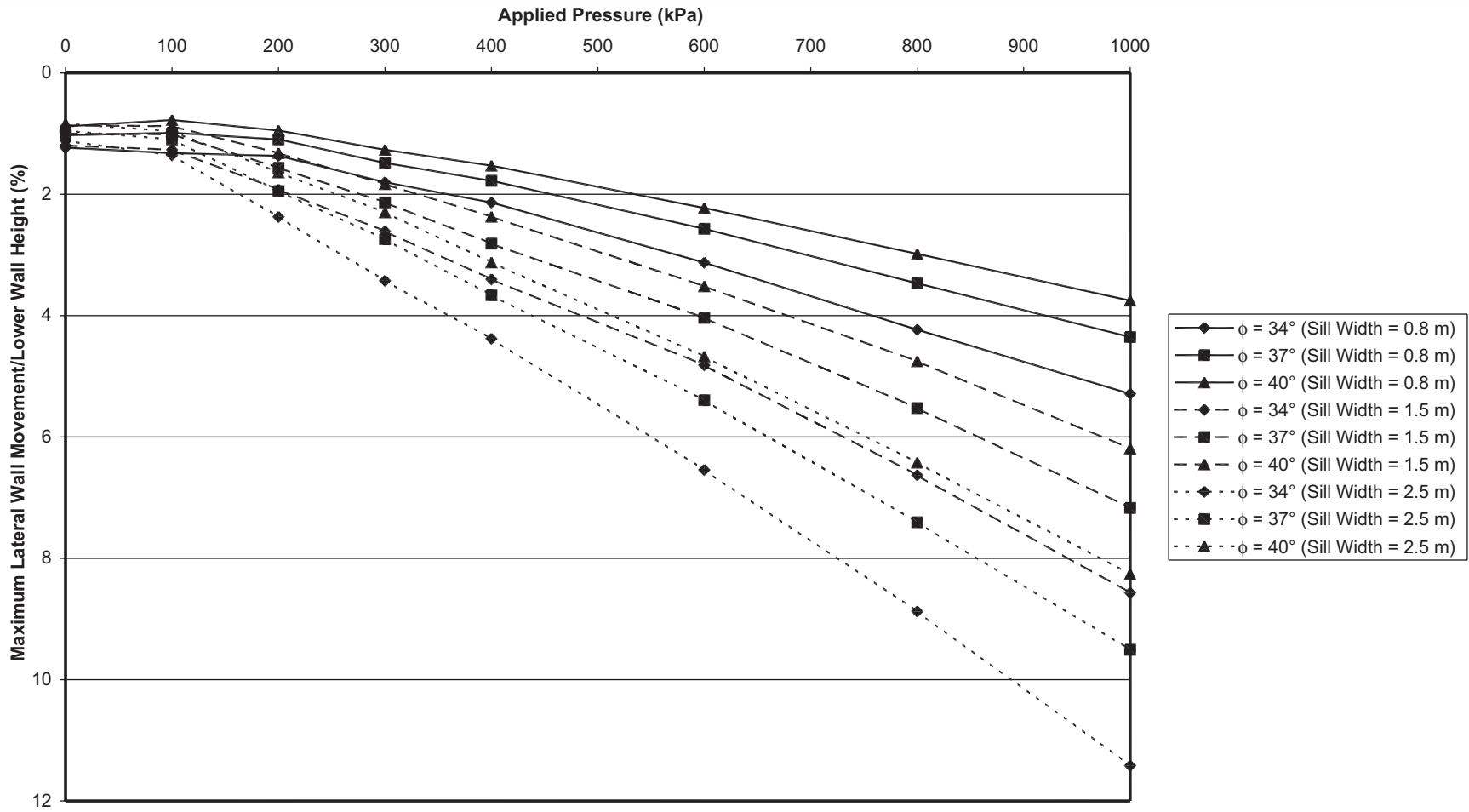


Figure 2-54. Relationship between applied pressure and maximum lateral wall displacement: isolated sill, $s = 0.2$ m, and medium sand foundation.

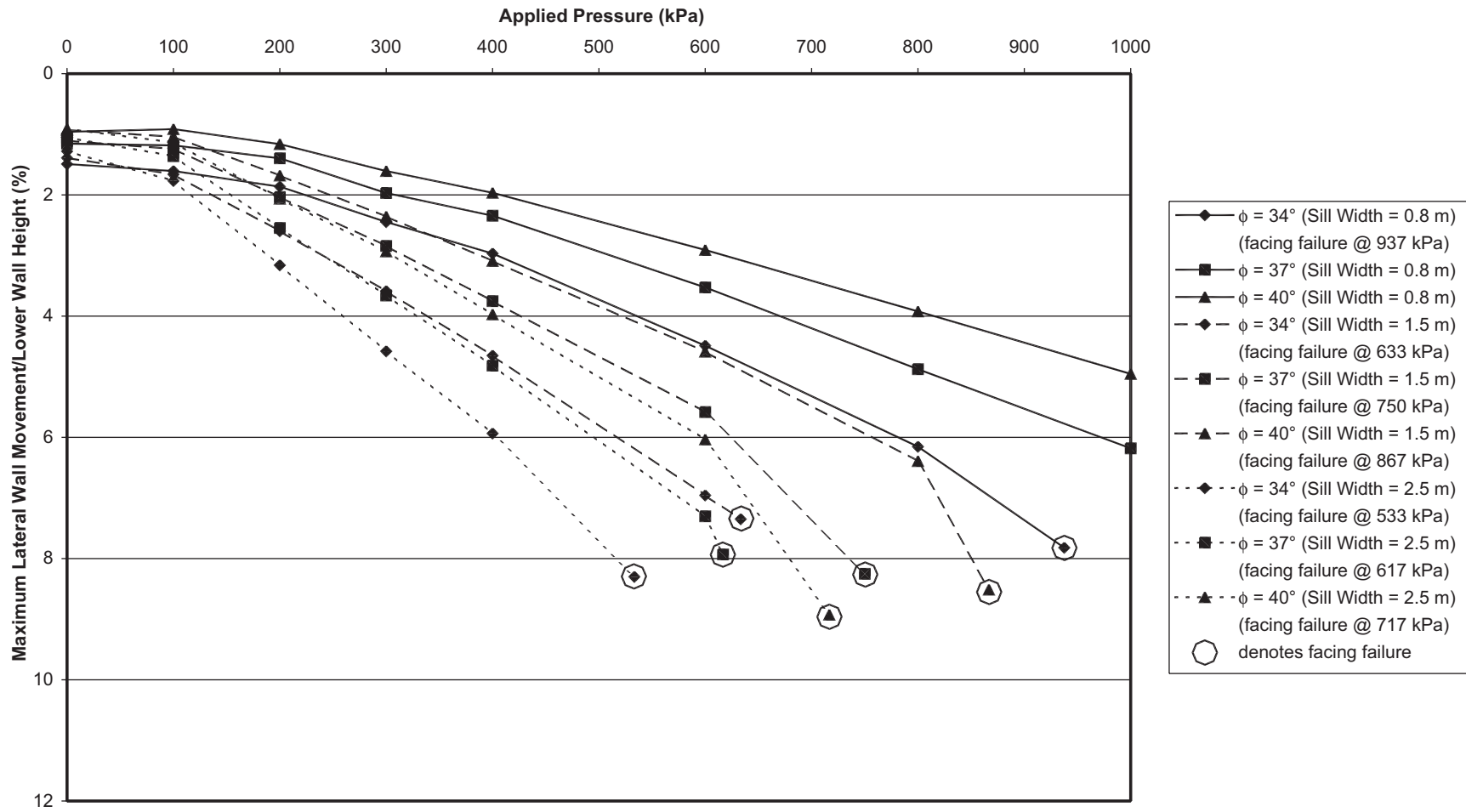


Figure 2-55. Relationship between applied pressure and maximum lateral wall displacement: isolated sill, $s = 0.4$ m, and medium sand foundation.

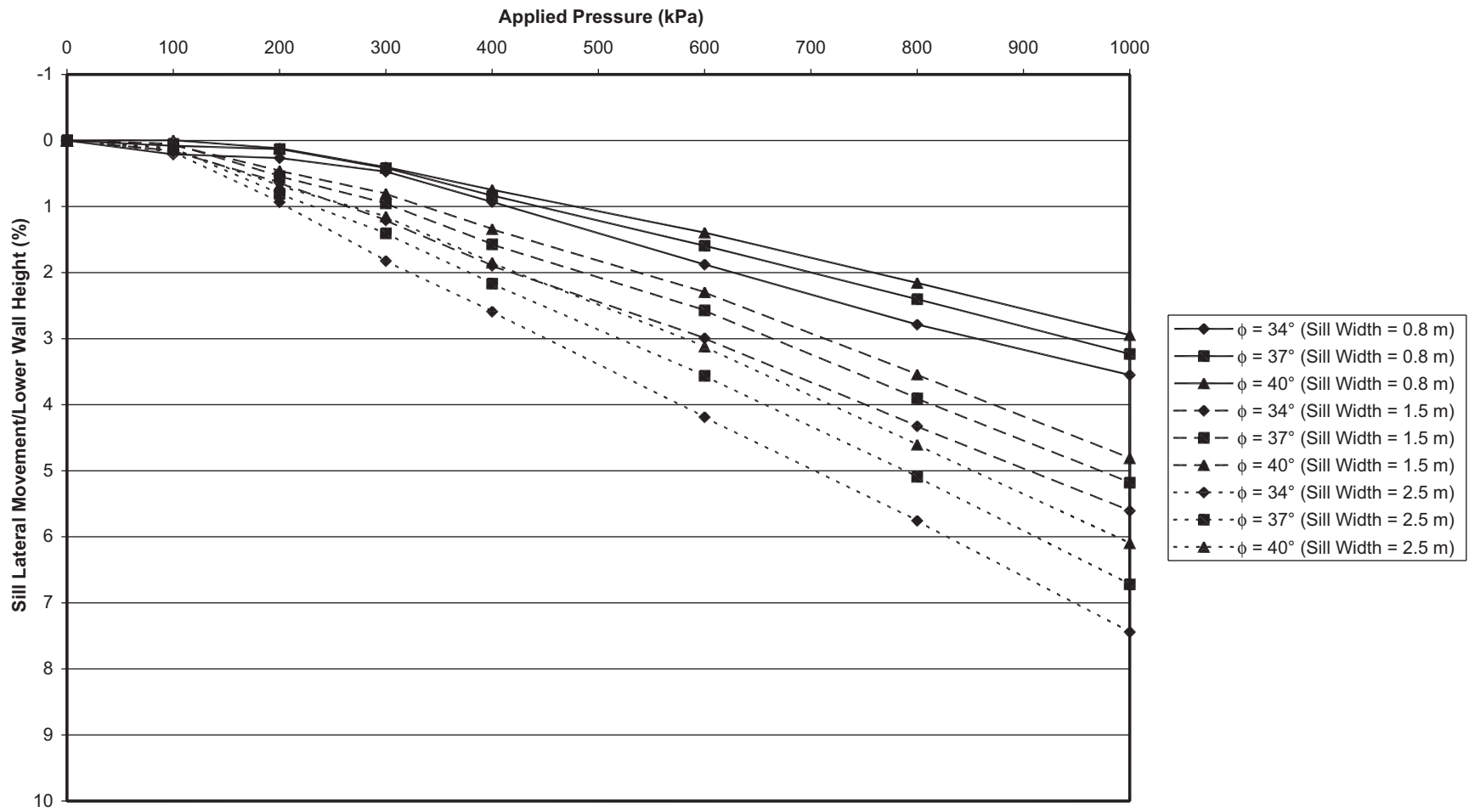


Figure 2-56. Relationship between applied pressure and sill lateral movement: integrated sill, $s = 0.2$ m, and medium sand foundation.

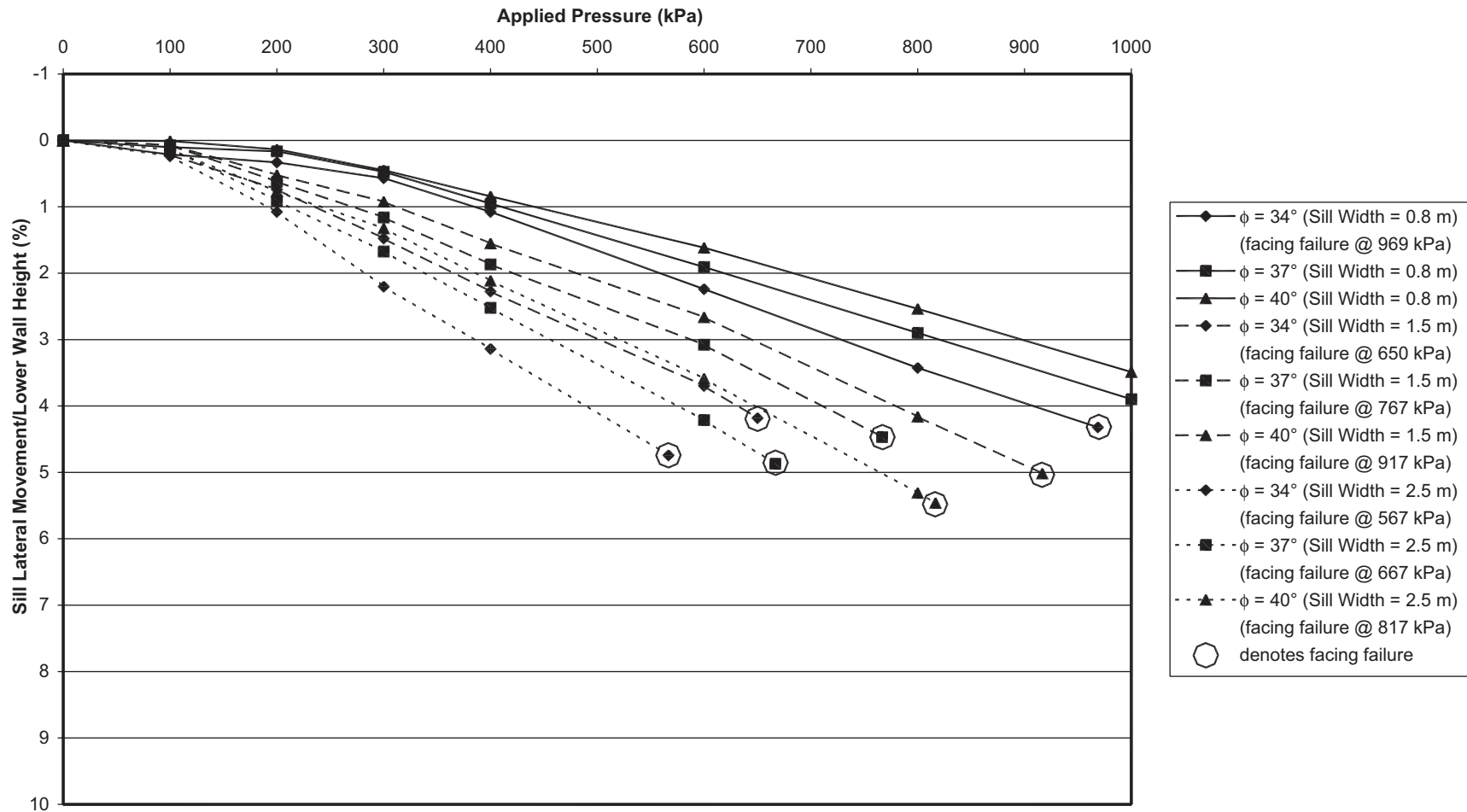


Figure 2-57. Relationship between applied pressure and sill lateral movement: integrated sill, $s = 0.4$ m, and medium sand foundation.

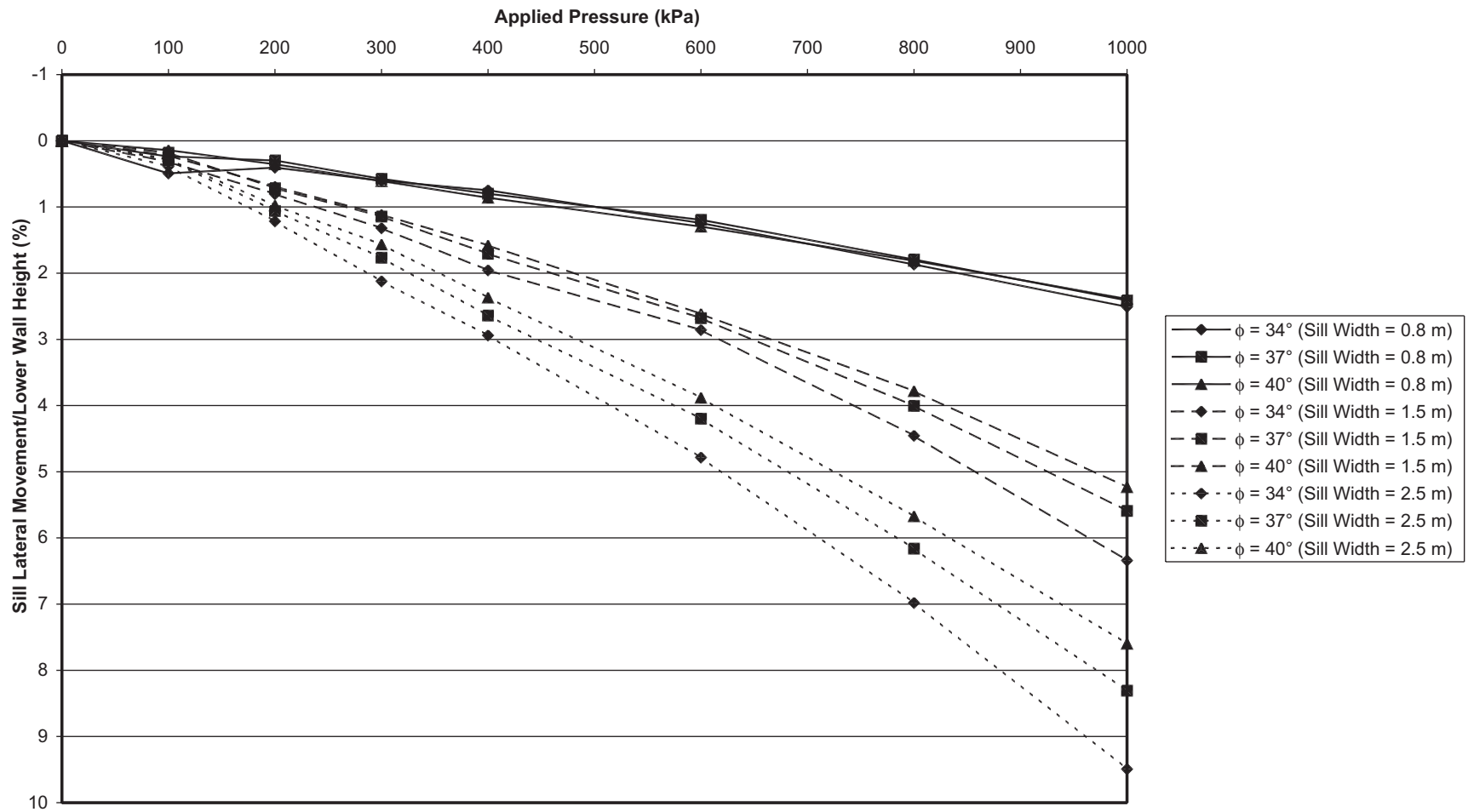


Figure 2-58. Relationship between applied pressure and sill lateral movement: isolated sill, $s = 0.2$ m, and medium sand foundation.

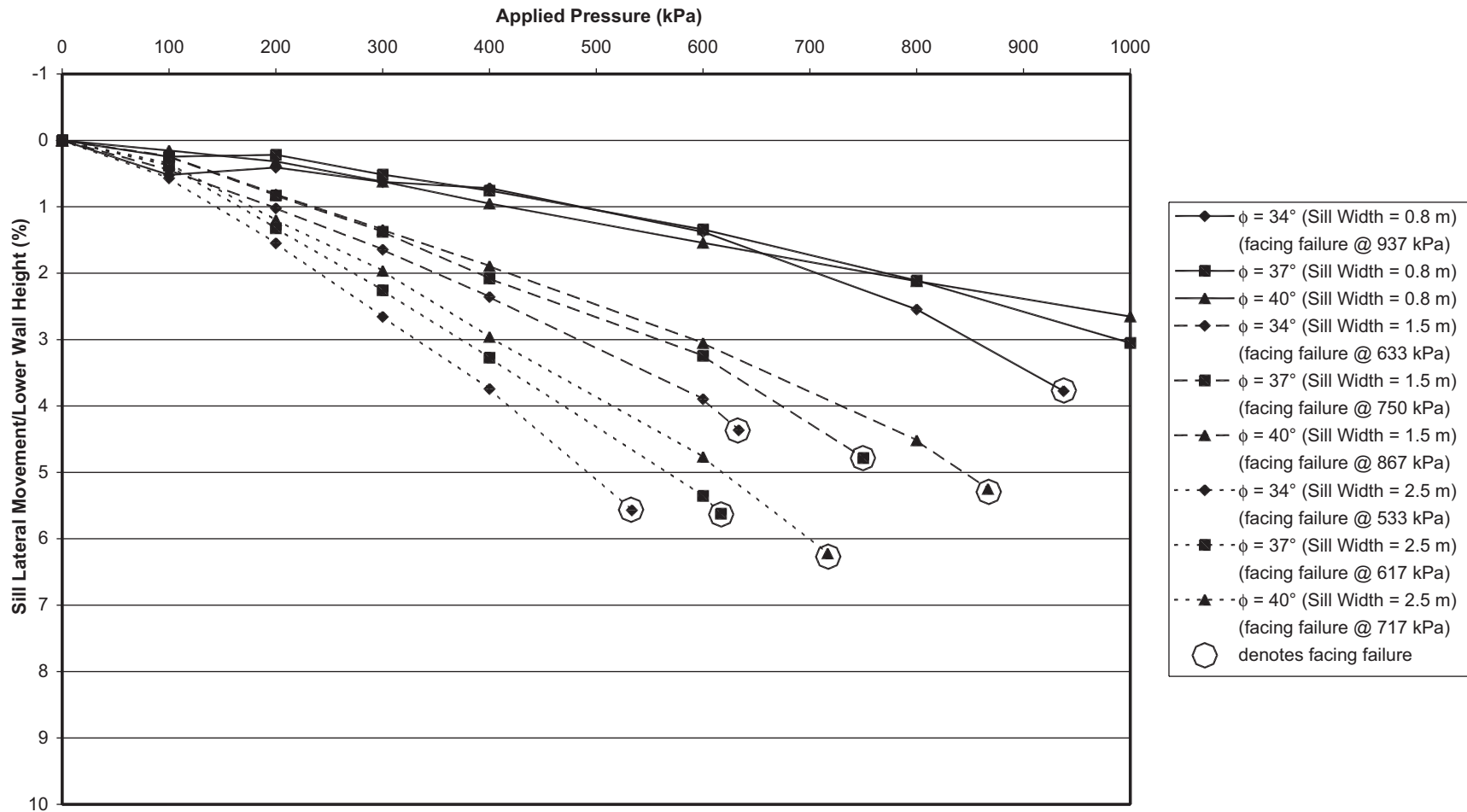


Figure 2-59. Relationship between applied pressure and sill lateral movement: isolated sill, $s = 0.4$ m, and medium sand foundation.

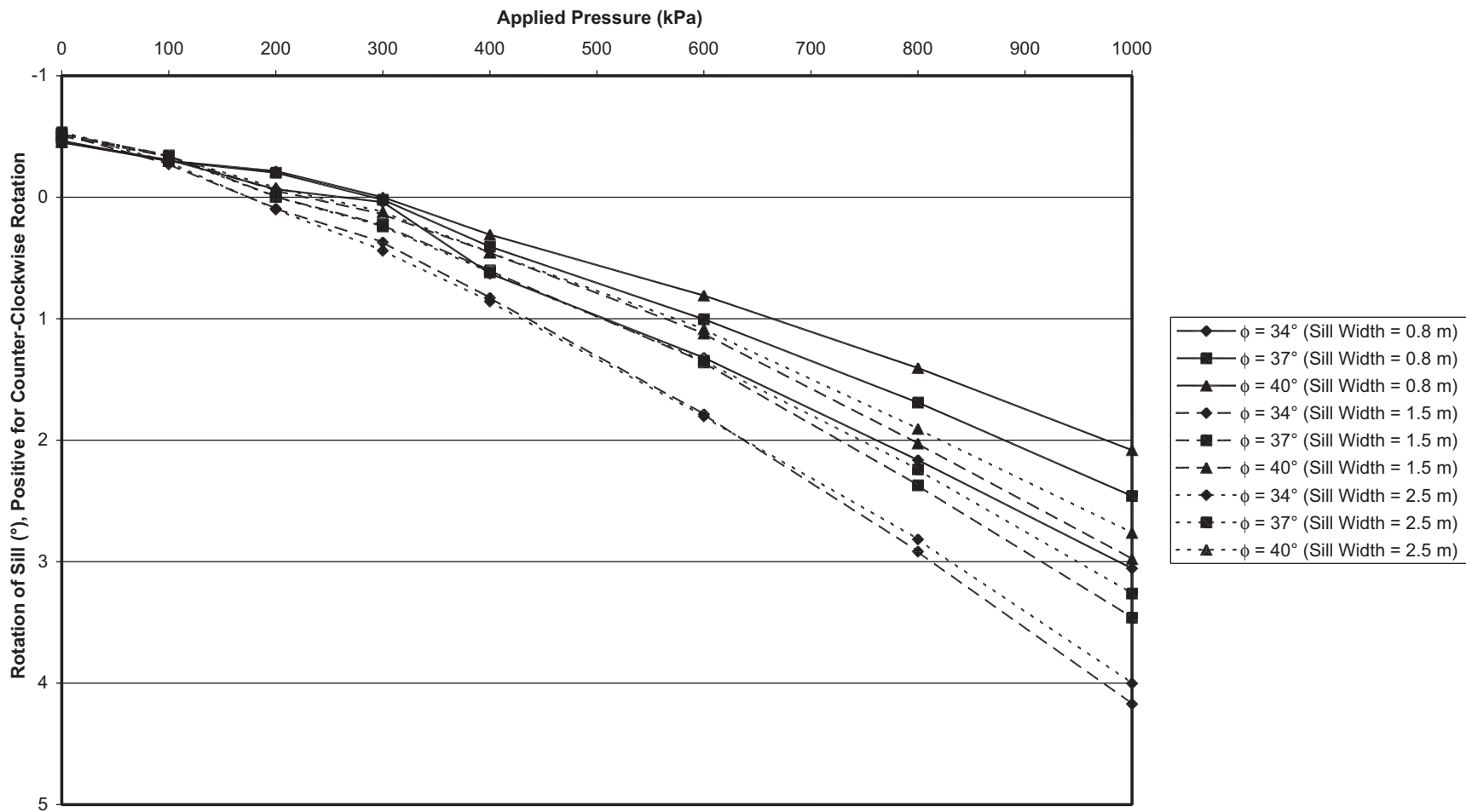


Figure 2-60. Relationship between applied pressure and rotation of sill: integrated sill, $s = 0.2$ m, and medium sand foundation.

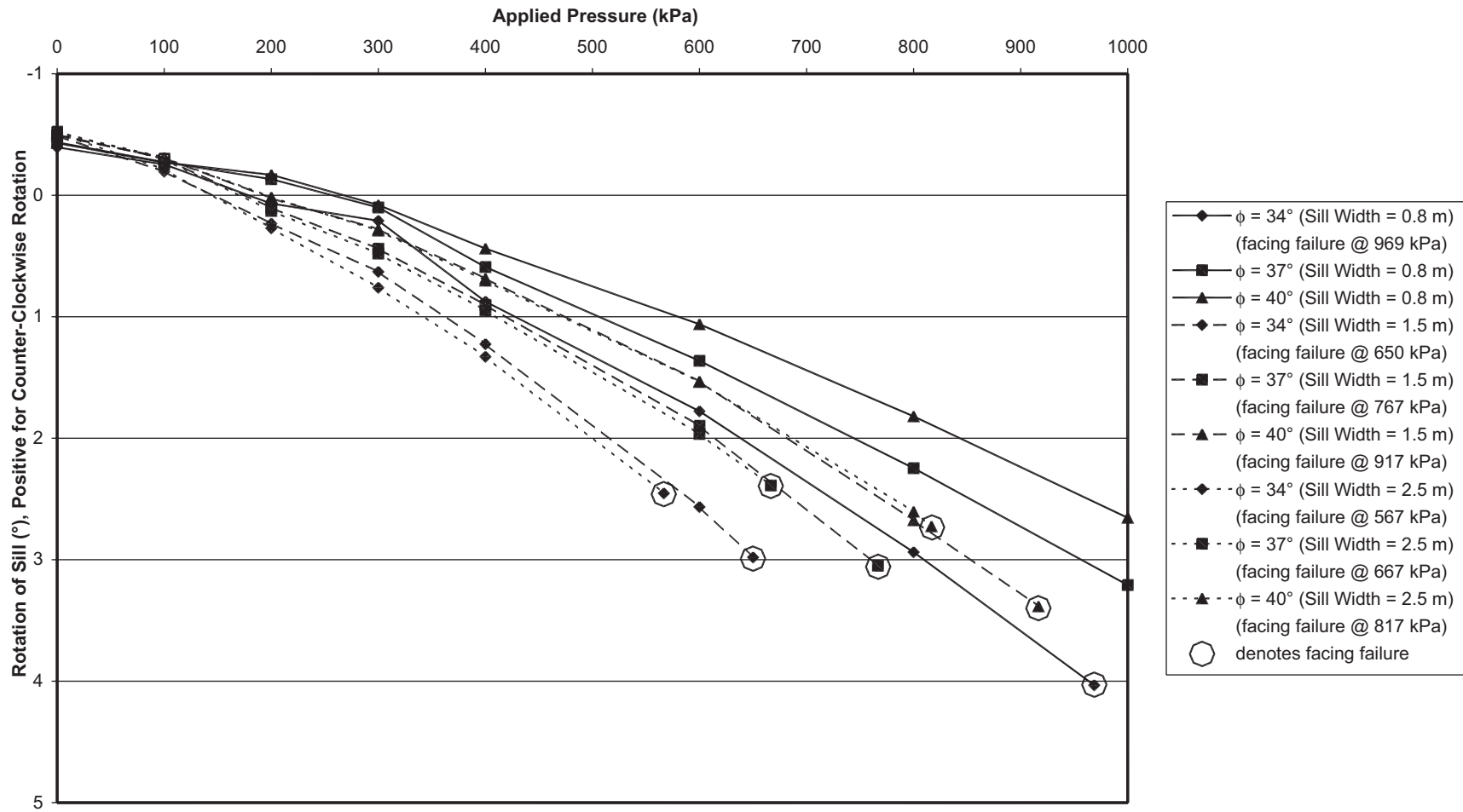


Figure 2-61. Relationship between applied pressure and rotation of sill : integrated sill, $s = 0.4$ m, and medium sand foundation.

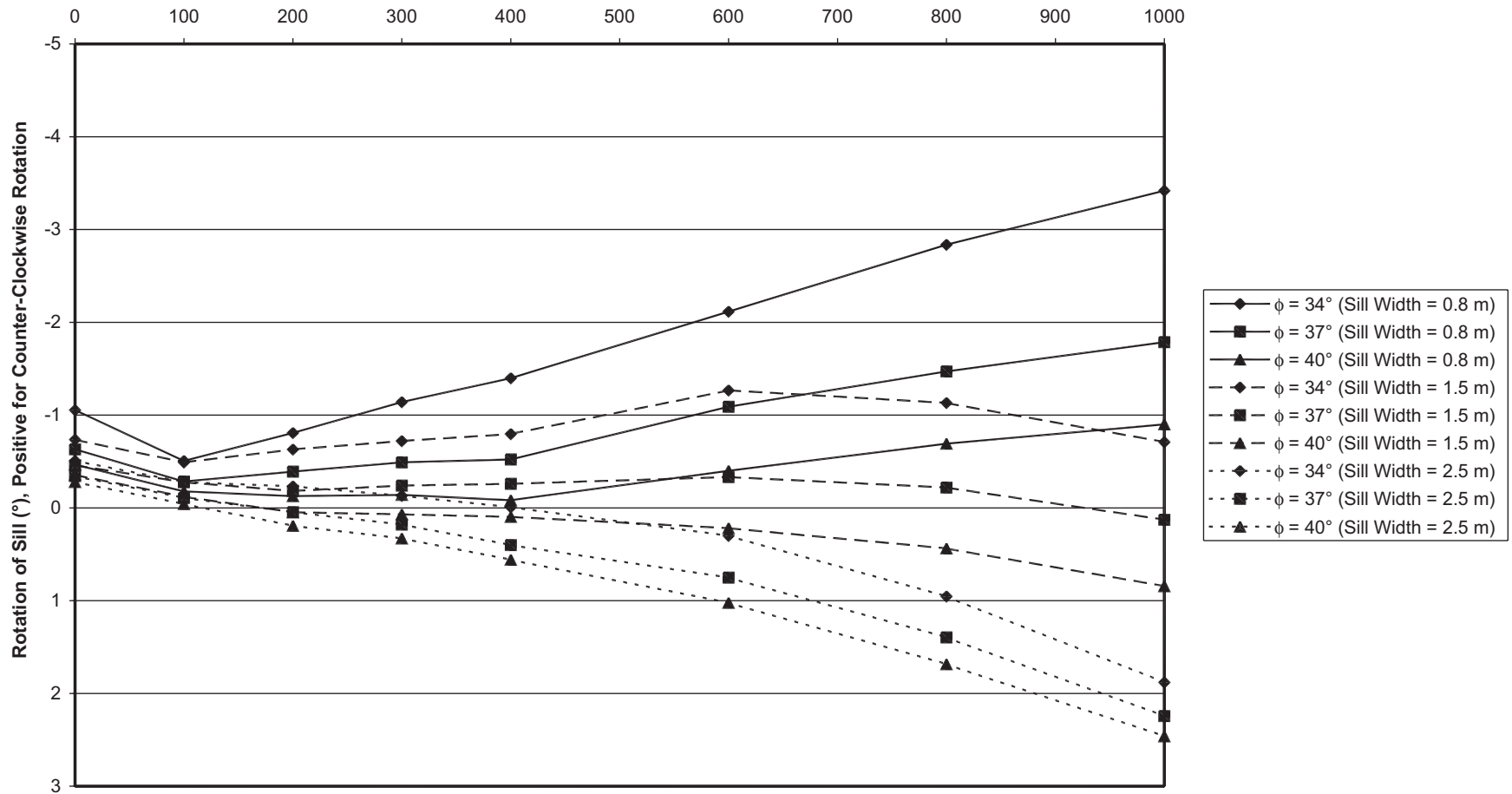


Figure 2-62. Relationship between applied pressure and rotation of sill: isolated sill, $s = 0.2$ m, and medium sand foundation.

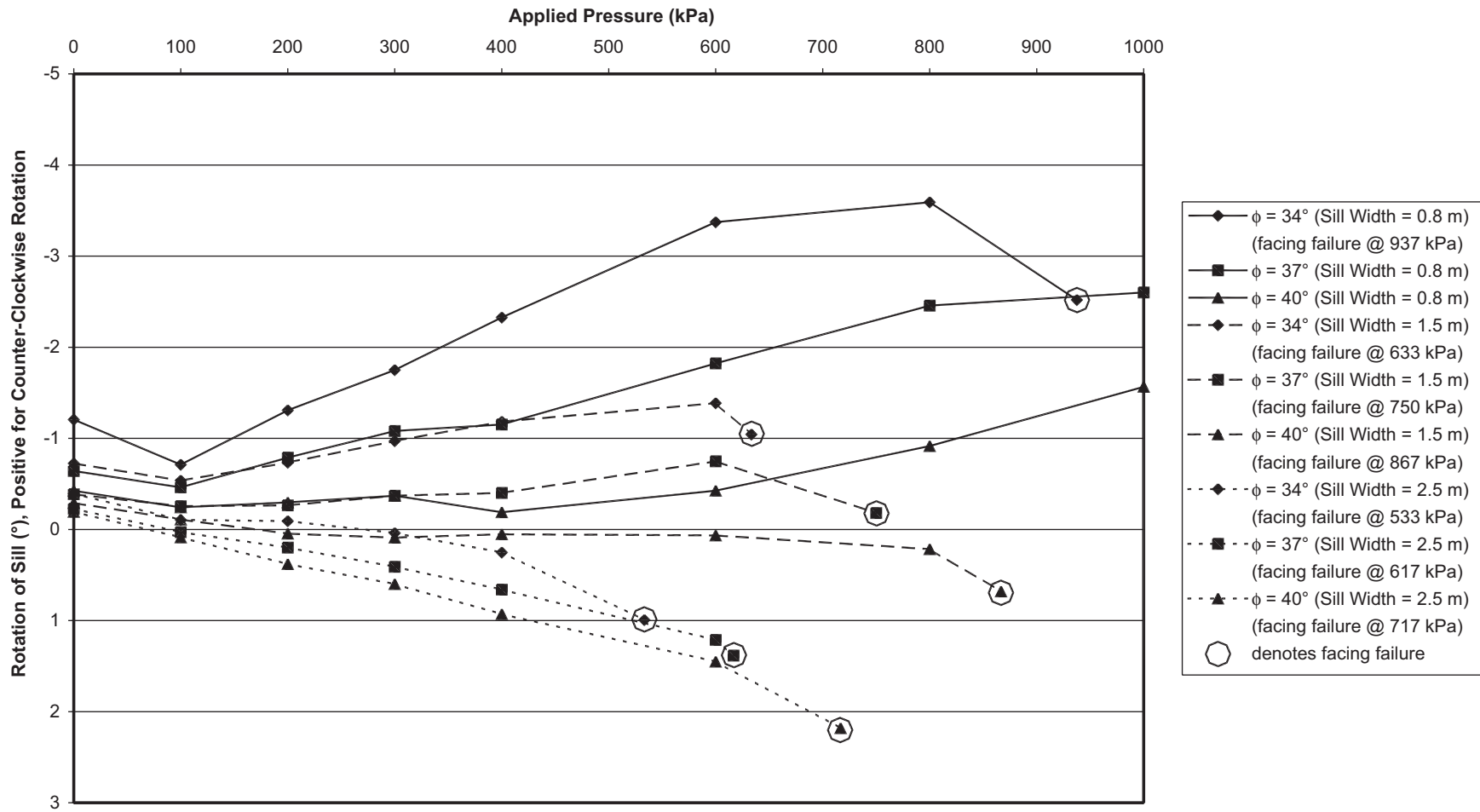


Figure 2-63. Relationship between applied pressure and rotation of sill: isolated sill, $s = 0.4$ m, and medium sand foundation.

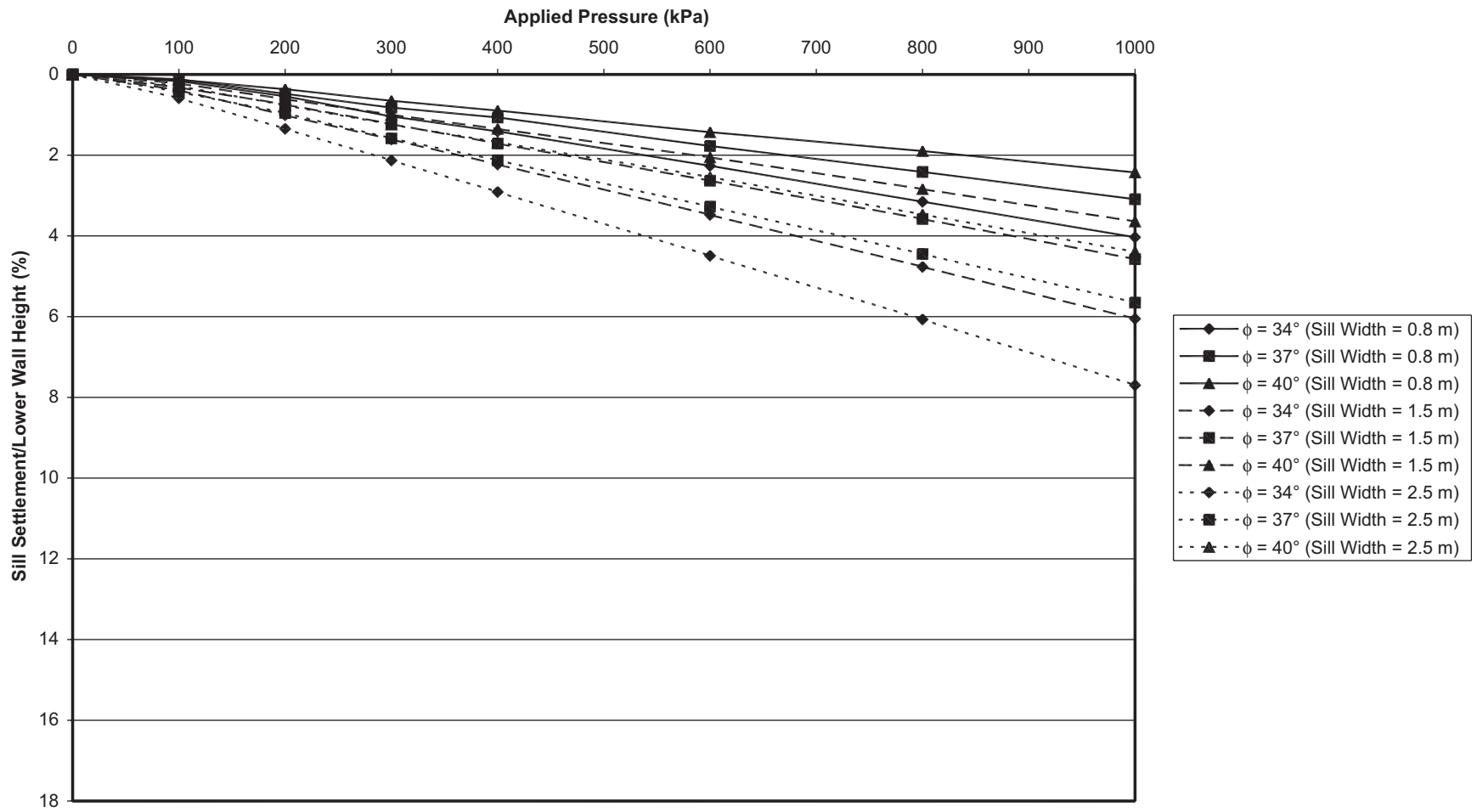


Figure 2-64. Relationship between applied pressure and sill settlement: integrated sill, $s = 0.2$ m, and rigid foundation.

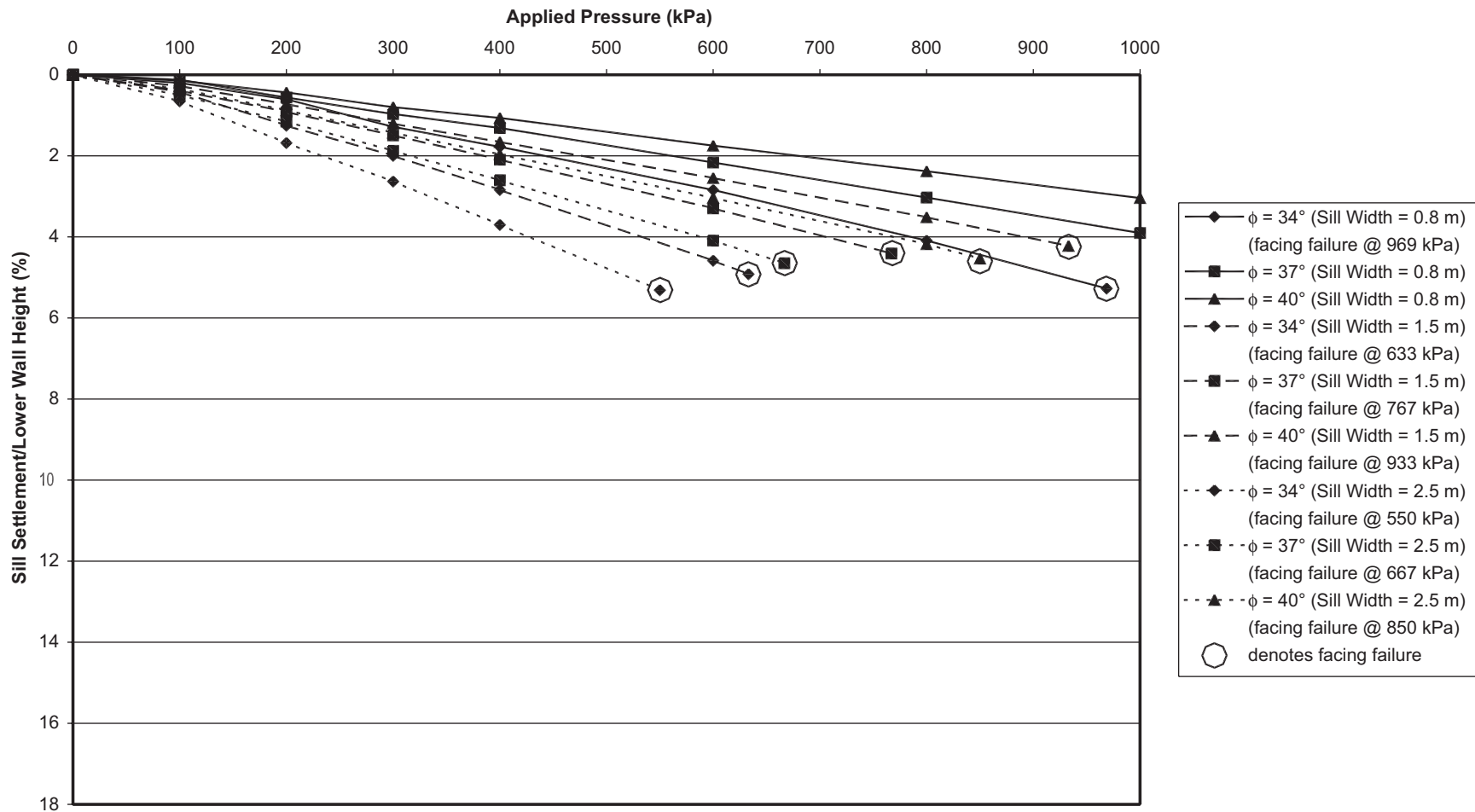


Figure 2-65. Relationship between applied pressure and sill settlement: integrated sill, $s = 0.4$ m, and rigid foundation.

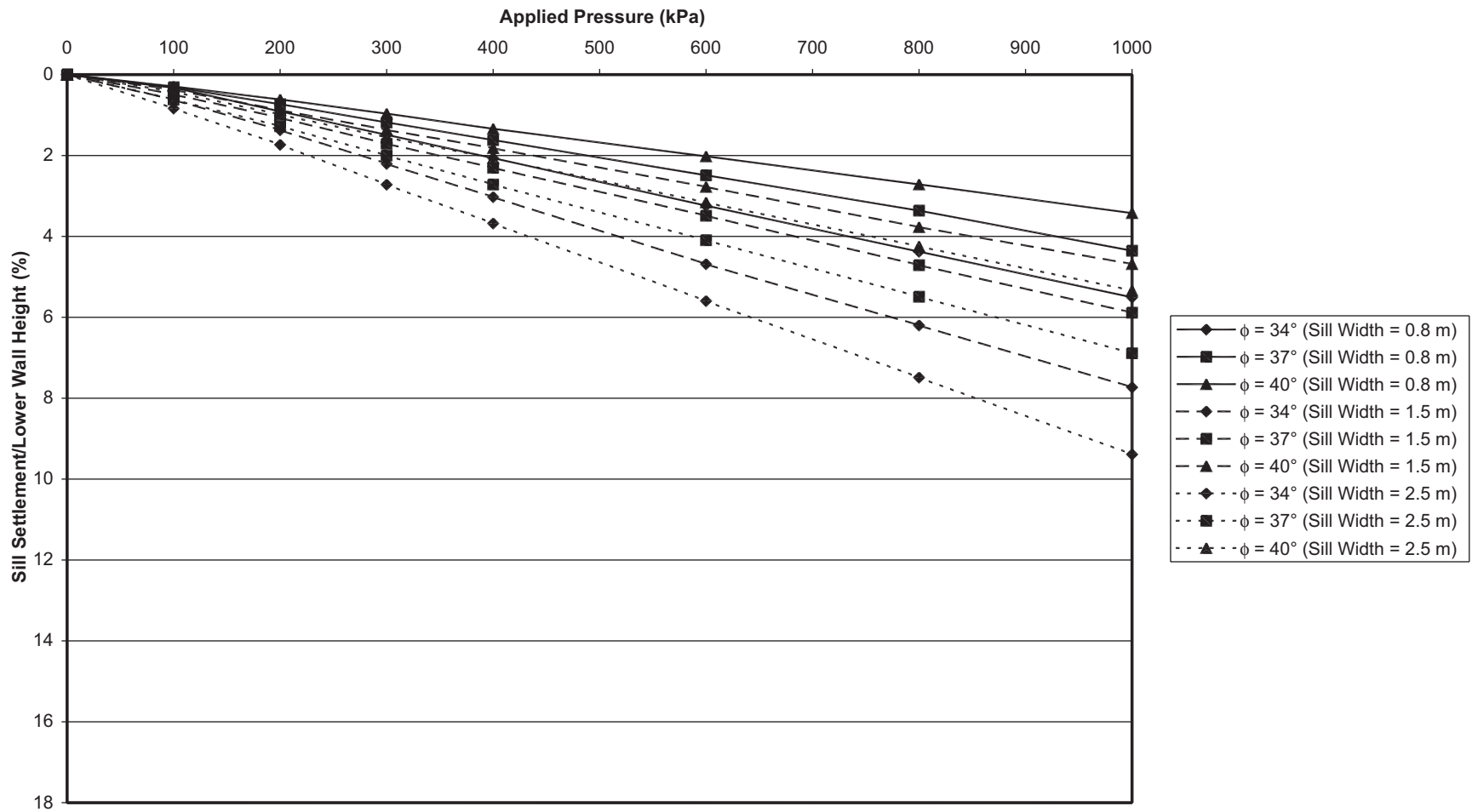


Figure 2-66. Relationship between applied pressure and sill settlement: isolated sill, $s = 0.2$ m, and rigid foundation.

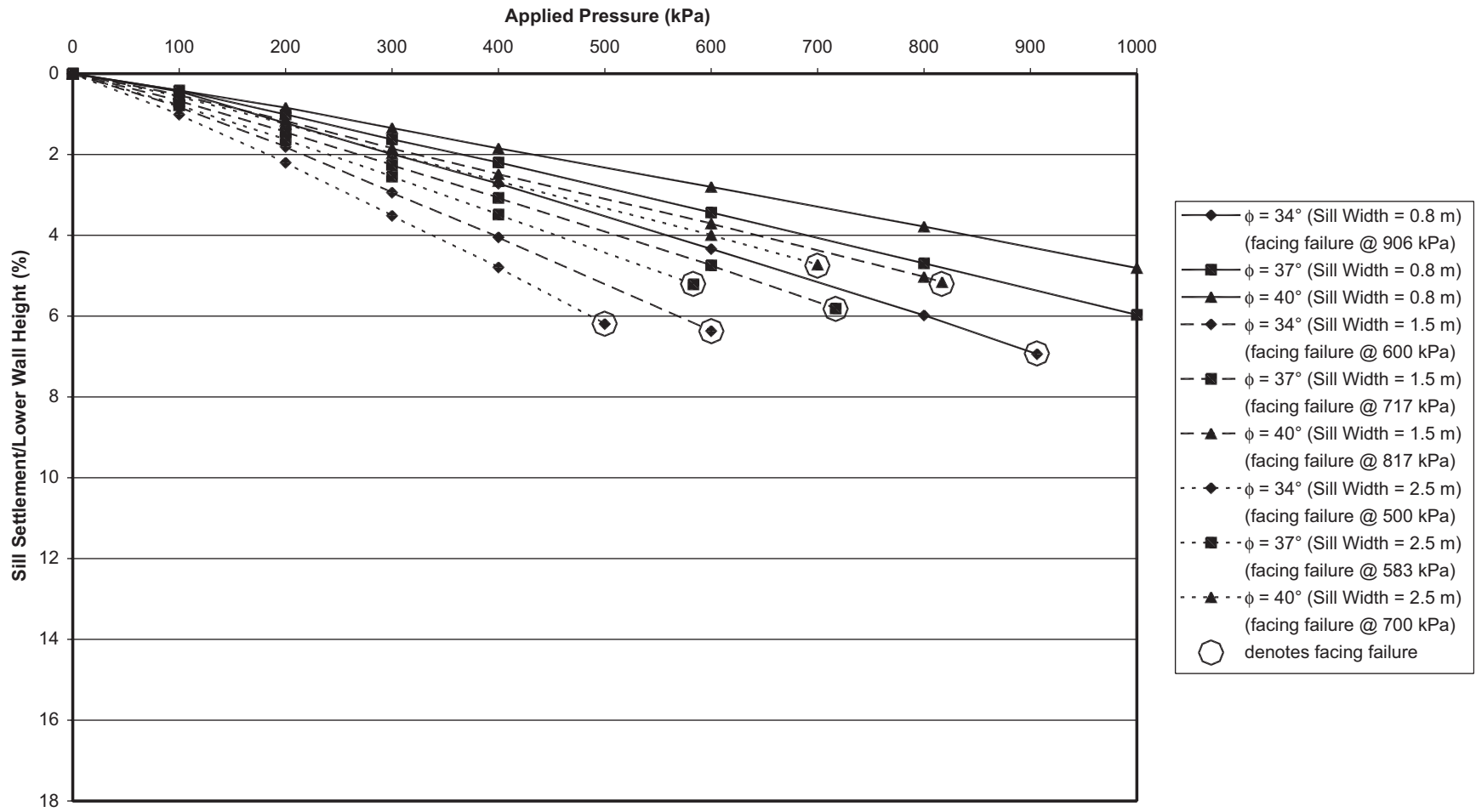


Figure 2-67. Relationship between applied pressure and sill settlement: isolated sill, s = 0.4 m, and rigid foundation.

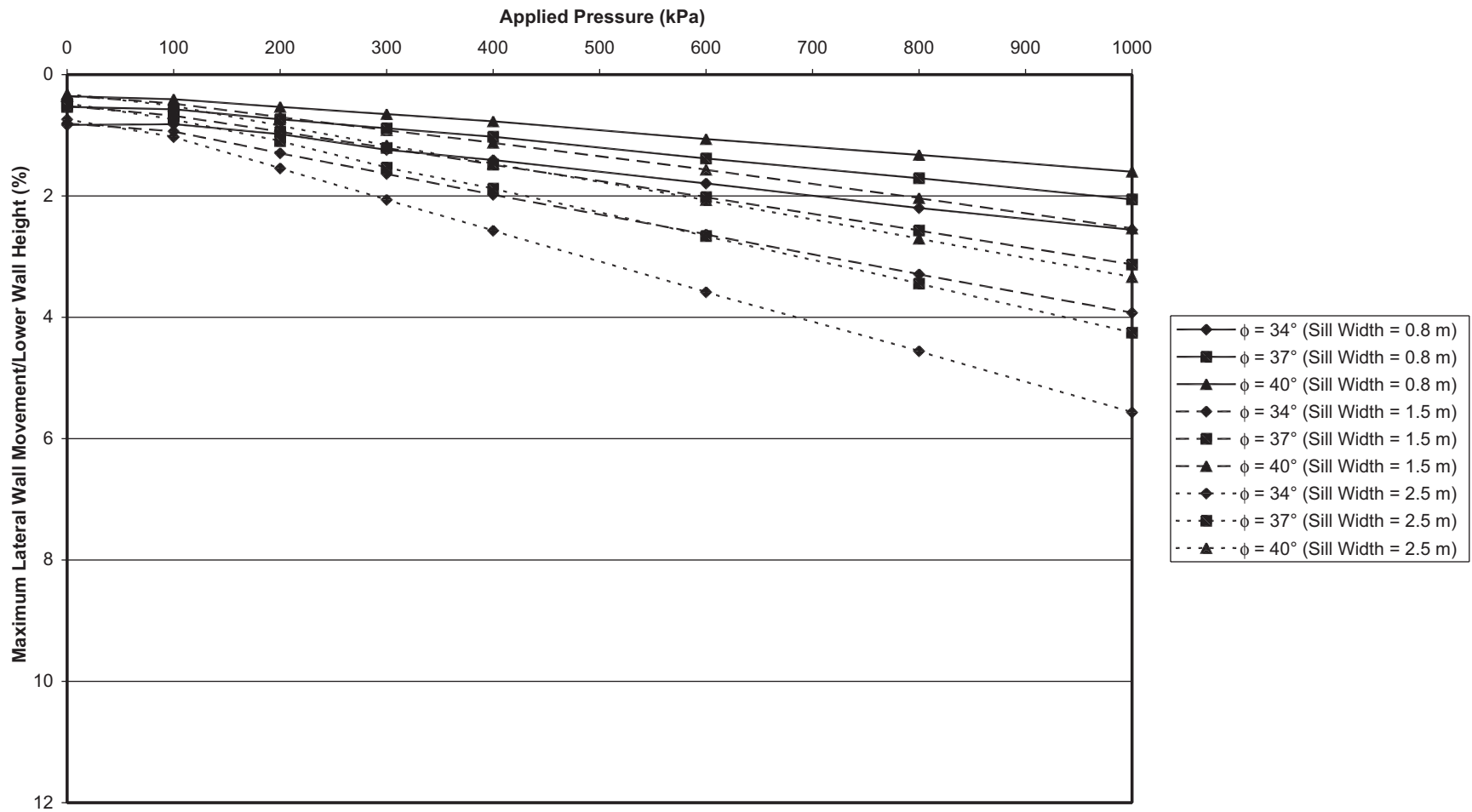


Figure 2-68. Relationship between applied pressure and maximum lateral wall displacement: integrated sill, $s = 0.2$ m, and rigid foundation.

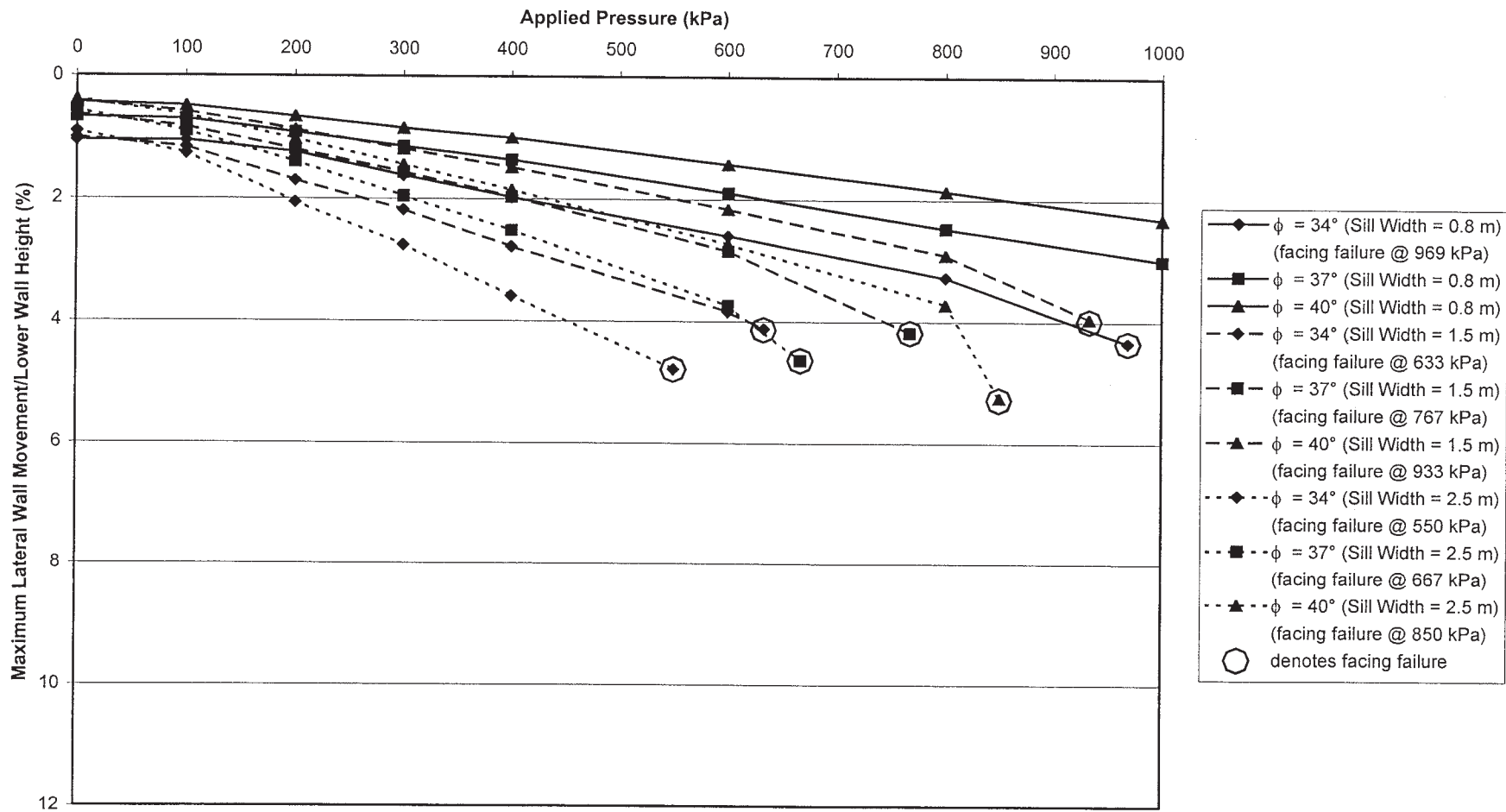


Figure 2-69. Relationship between applied pressure and maximum lateral wall displacement: integrated sill, $s = 0.4$ m, and rigid foundation.

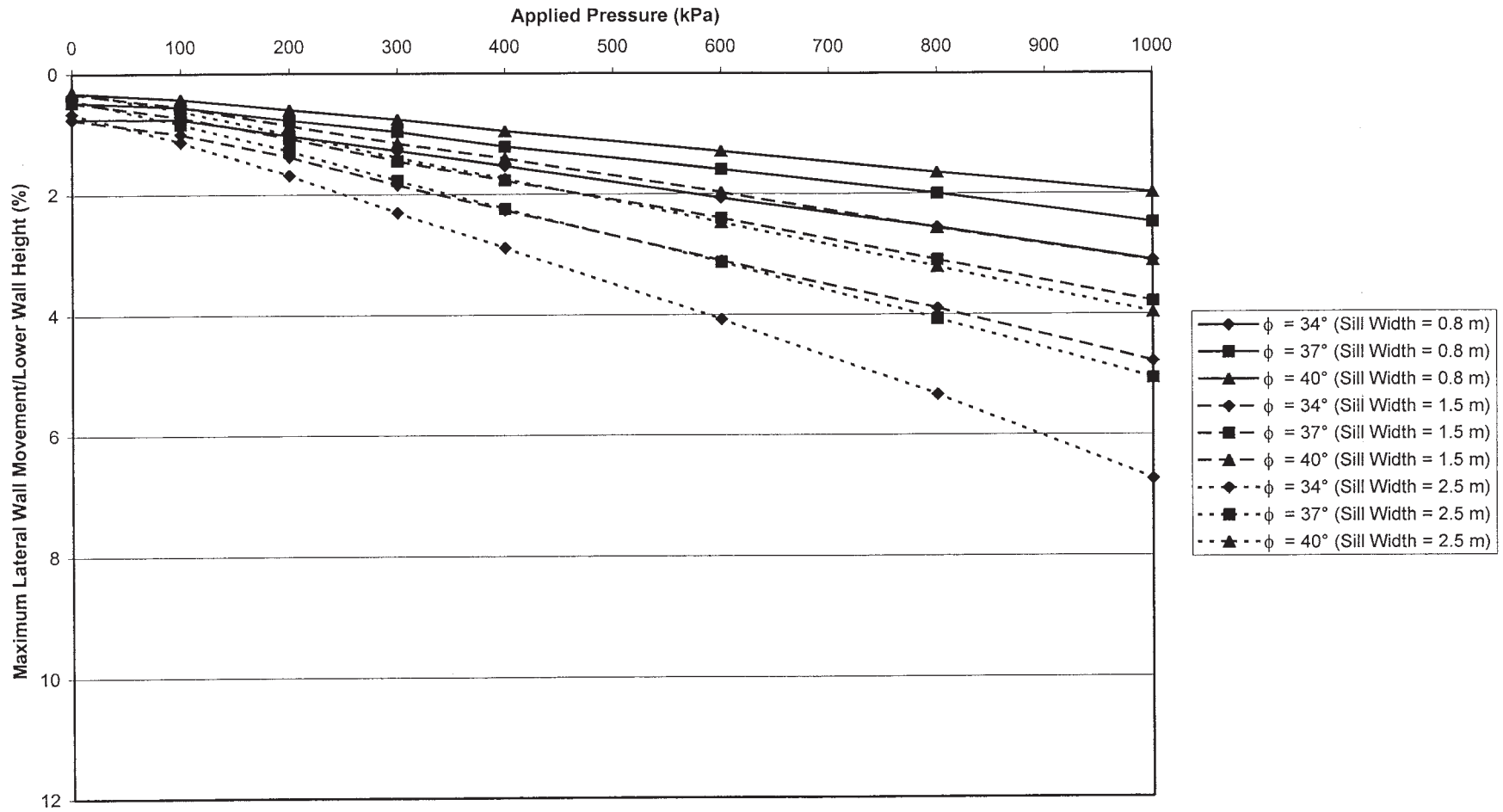


Figure 2-70. Relationship between applied pressure and maximum lateral wall displacement: isolated sill, $s = 0.2$ m, and rigid foundation.

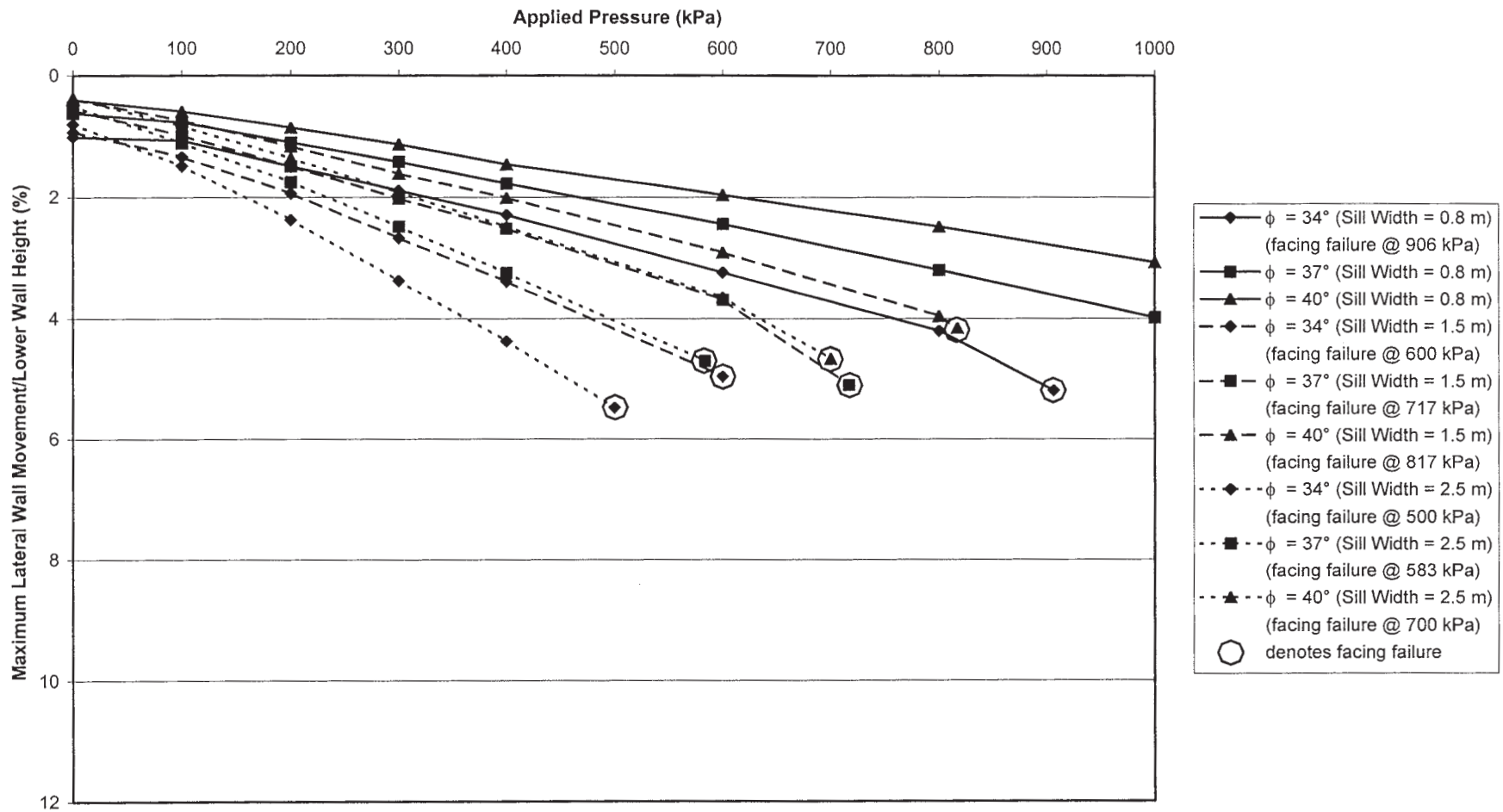


Figure 2-71. Relationship between applied pressure and maximum lateral wall displacement: isolated sill, $s = 0.4$ m, and rigid foundation.

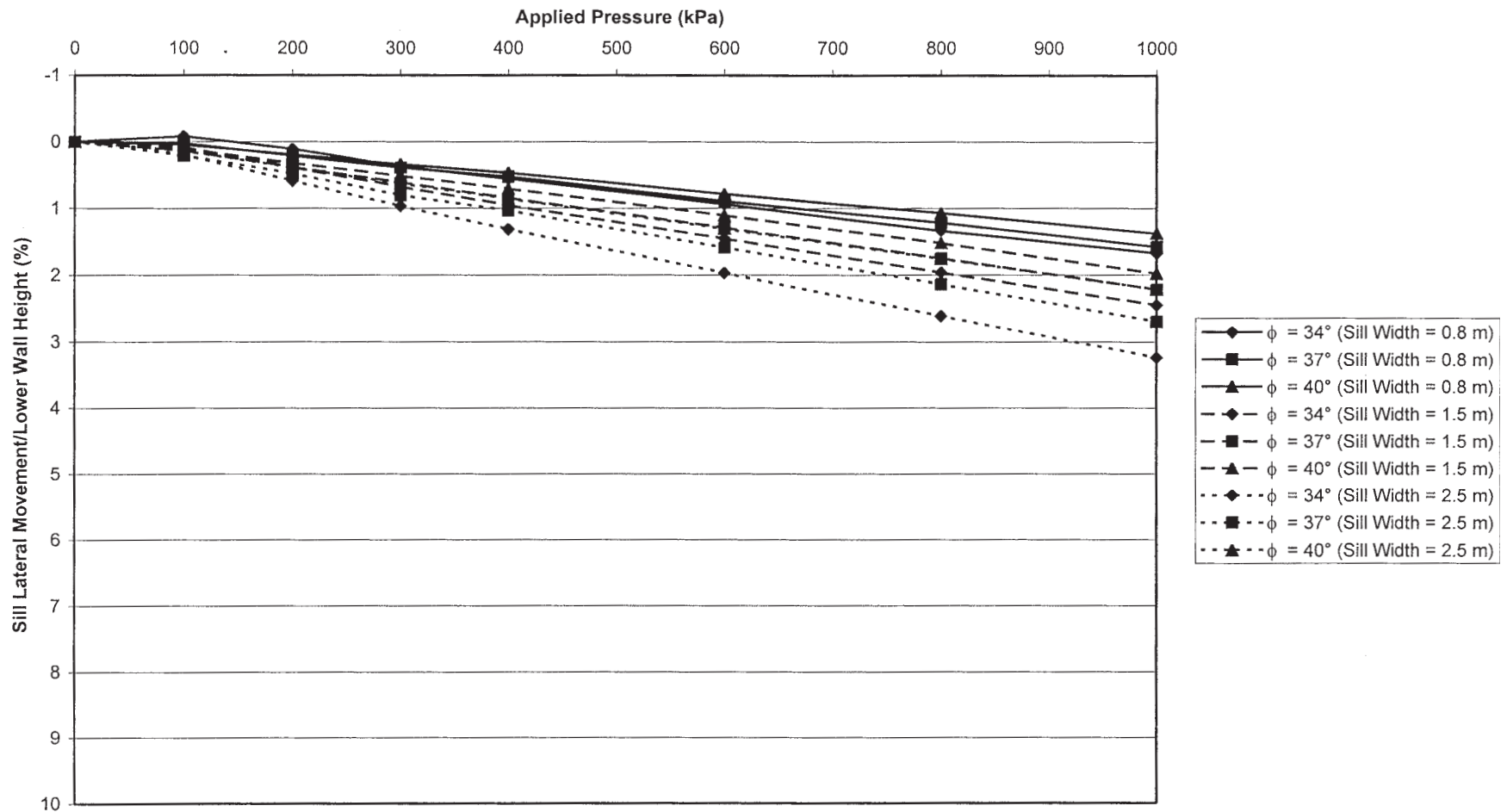


Figure 2-72. Relationship between applied pressure and sill lateral movement: integrated sill, $s = 0.2$ m, and rigid foundation.

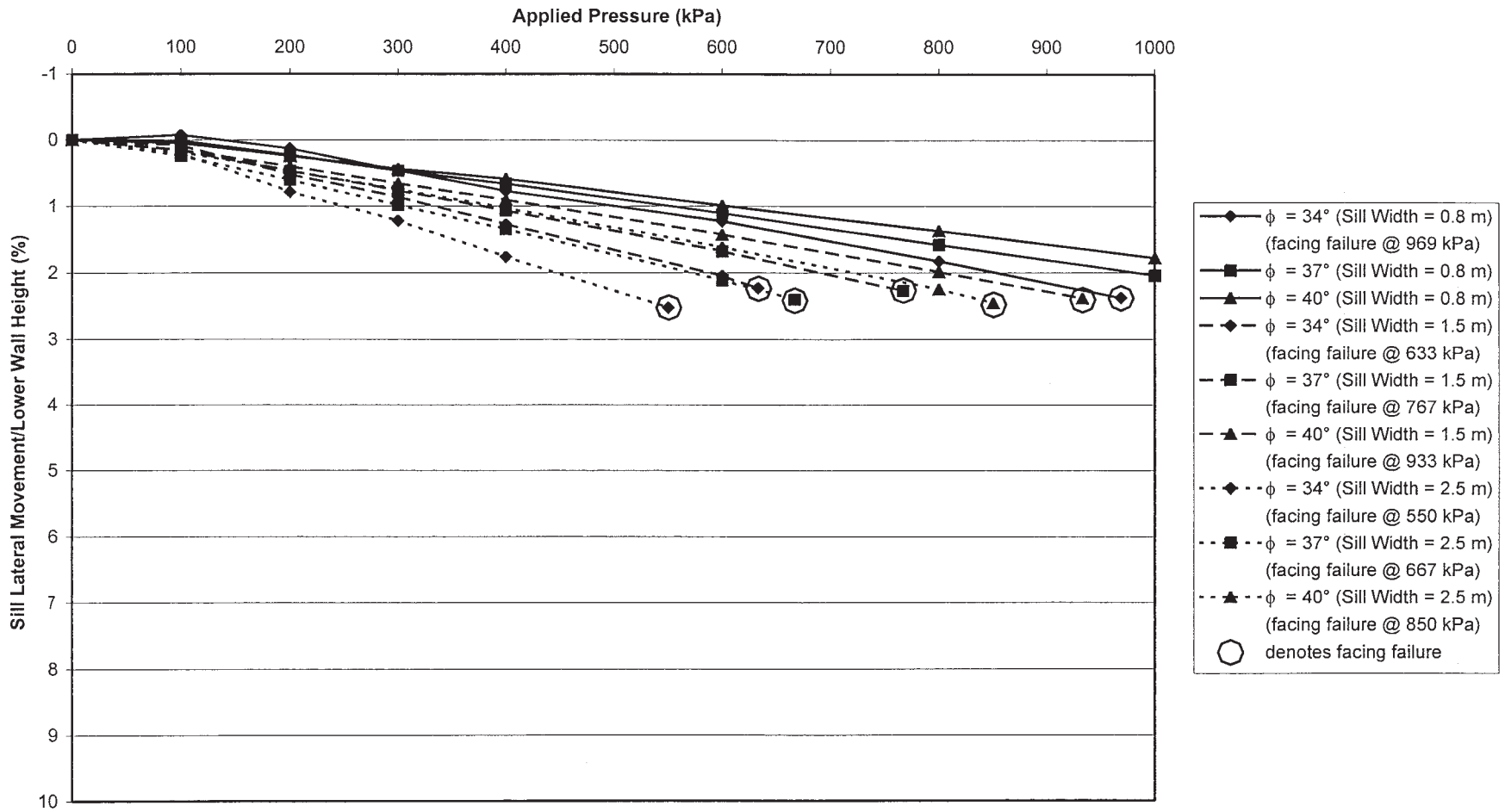


Figure 2-73. Relationship between applied pressure and sill lateral movement: integrated sill, $s = 0.4$ m, and rigid foundation.

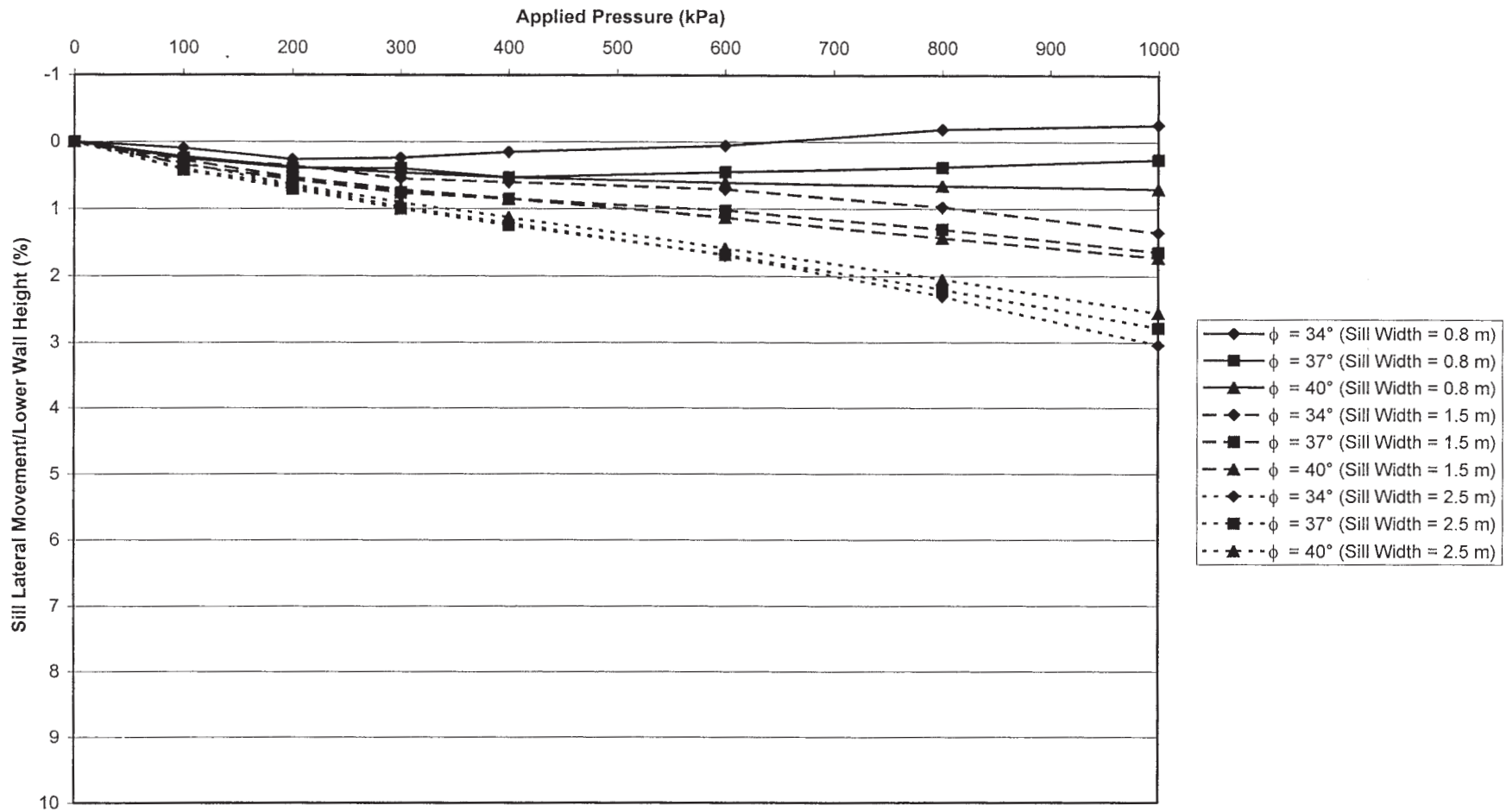


Figure 2-74. Relationship between applied pressure and sill lateral movement: isolated sill, $s = 0.2$ m, and rigid foundation.

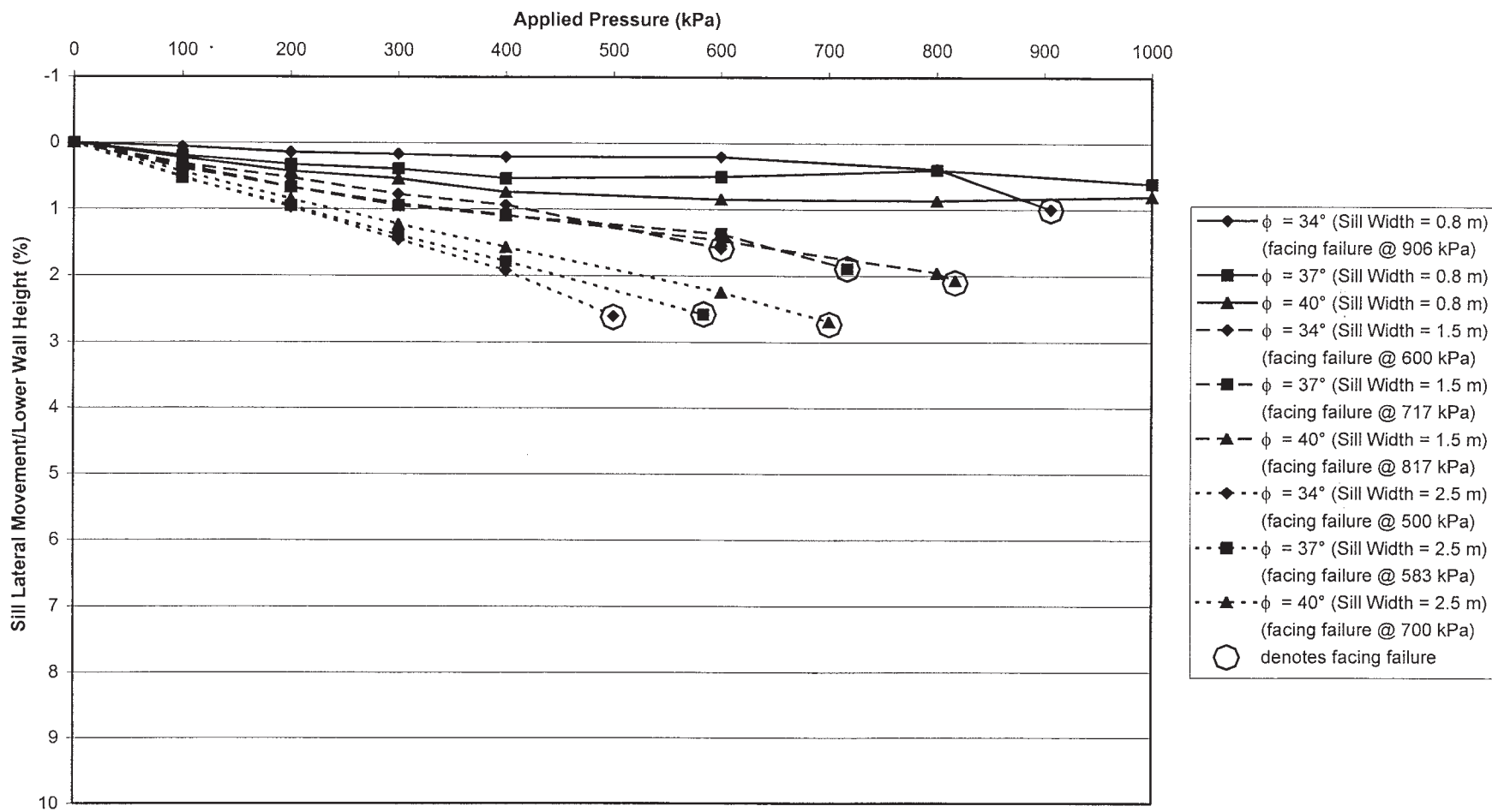


Figure 2-75. Relationship between applied pressure and sill lateral movement: isolated sill, $s = 0.4$ m, and rigid foundation.

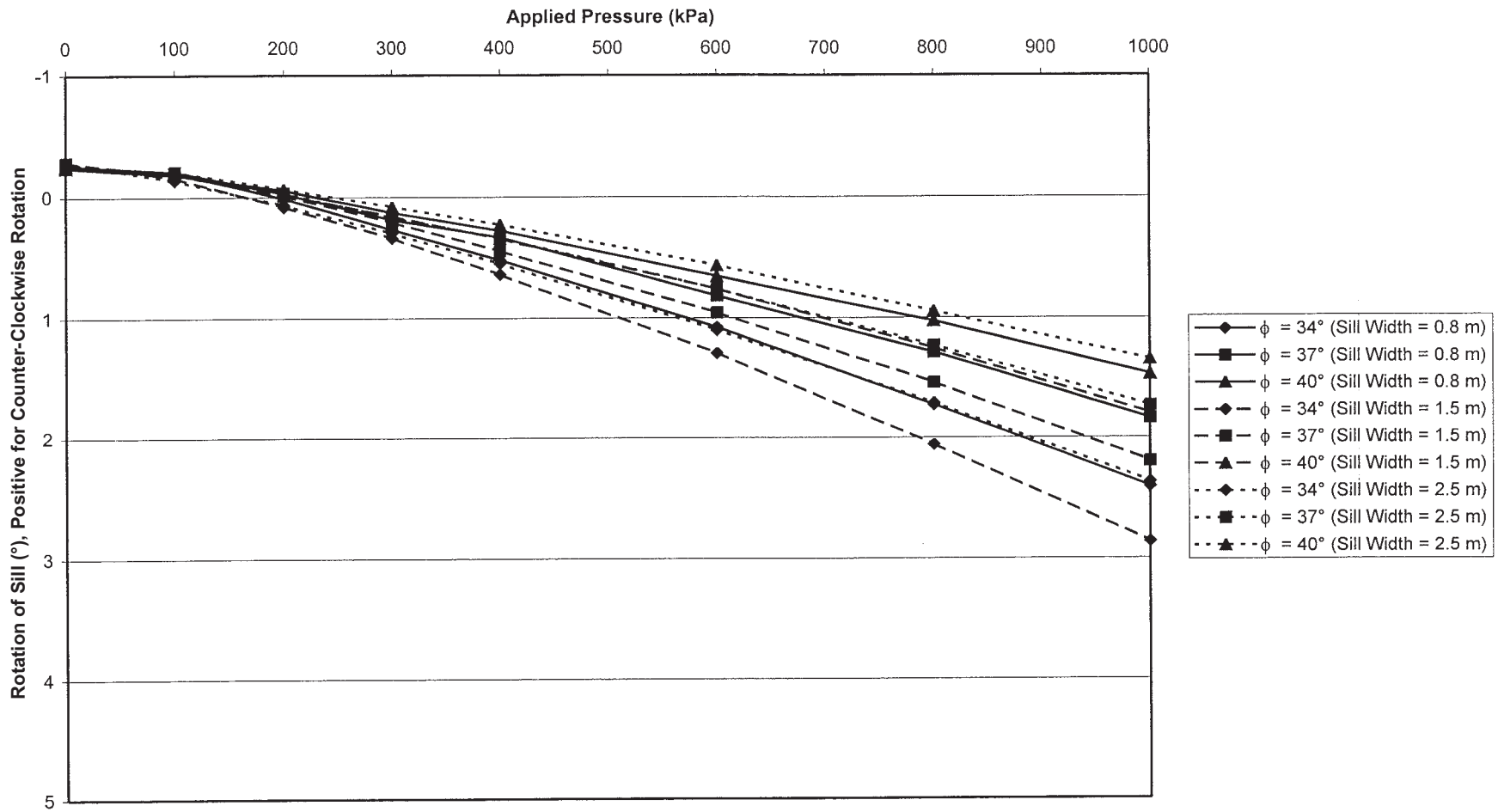


Figure 2-76. Relationship between applied pressure and rotation of sill: integrated sill, $s = 0.2$ m, and rigid foundation.

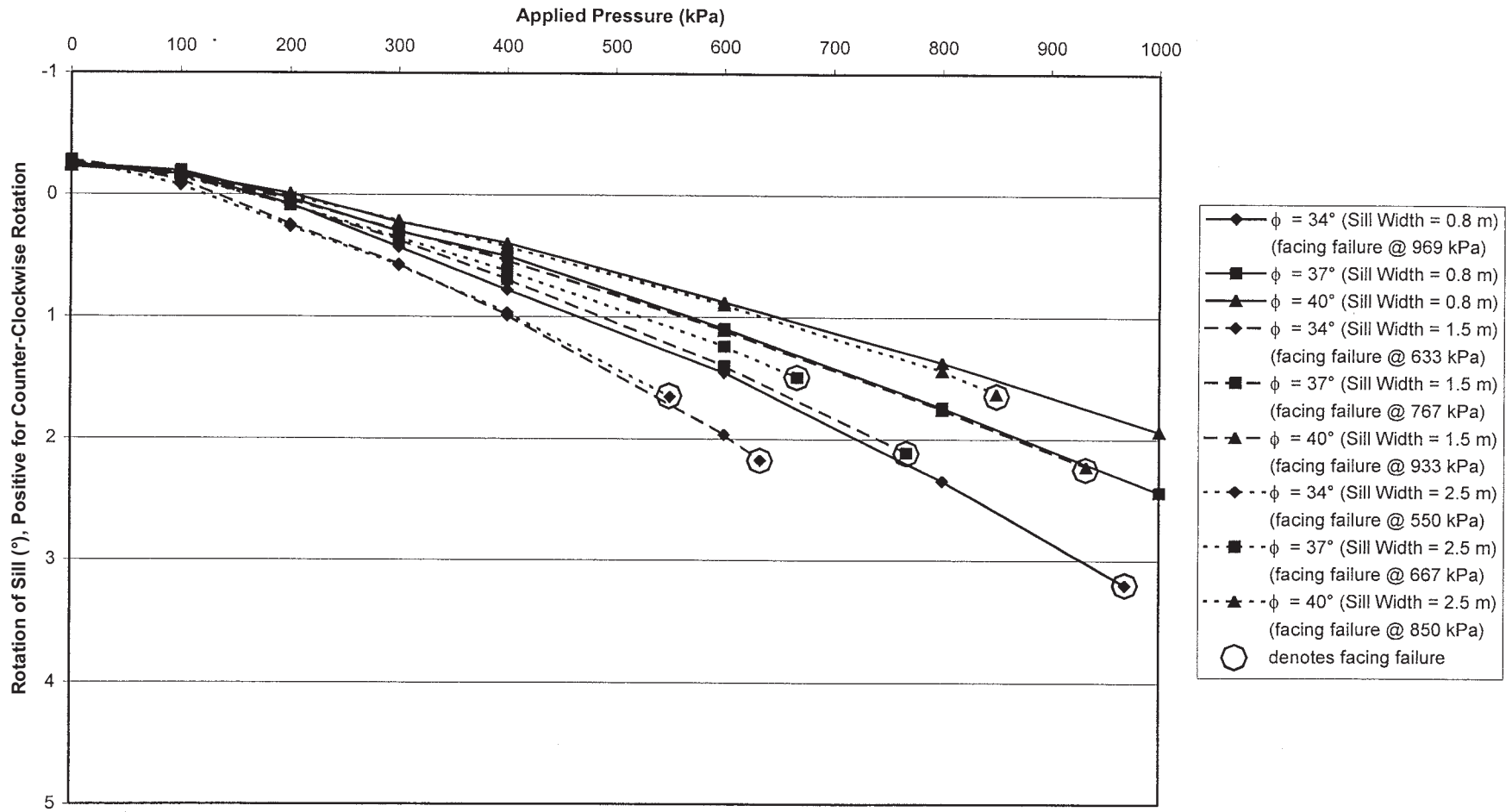


Figure 2-77. Relationship between applied pressure and rotation of sill: integrated sill, $s = 0.4$ m, and rigid foundation.

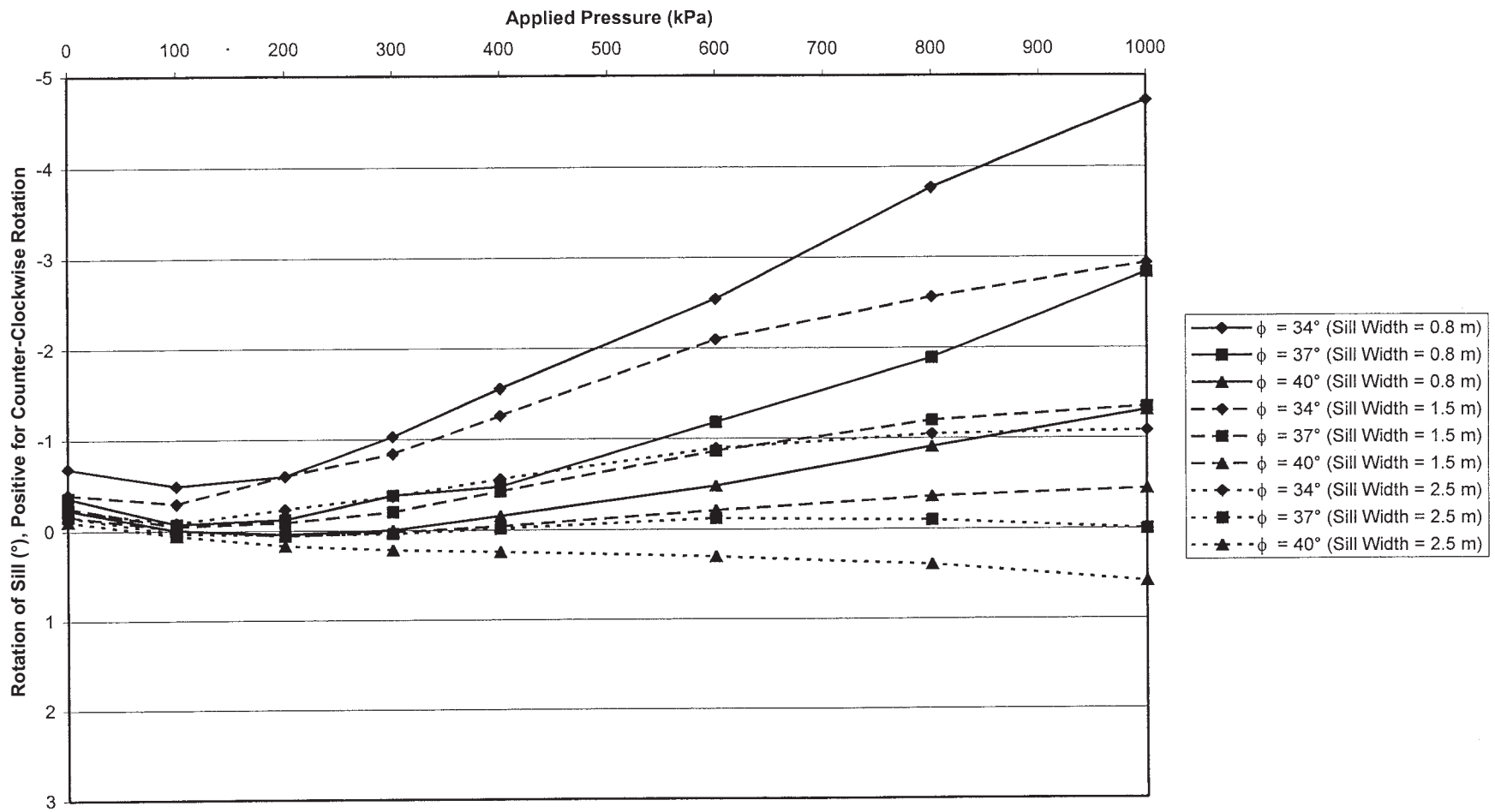


Figure 2-78. Relationship between applied pressure and rotation of sill: isolated sill, $s = 0.2$ m, and rigid foundation.

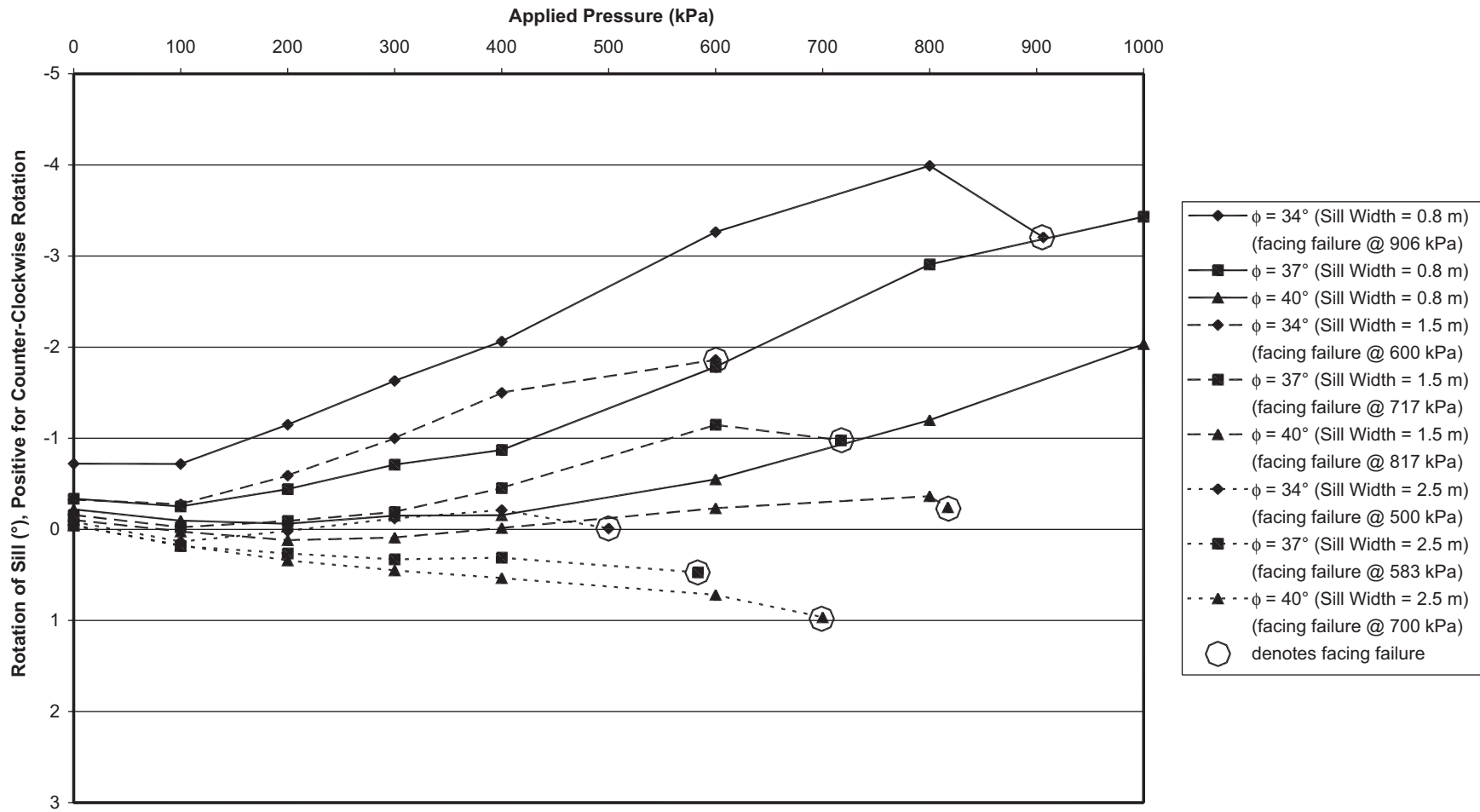


Figure 2-79. Relationship between applied pressure and rotation of sill: isolated sill, $s = 0.4$ m, and rigid foundation.

- The reinforcement spacing and sill width affects the lateral movement of the sill significantly. With an isolated sill, the lateral movement of the sill is nearly independent of soil friction angle for a small sill width (0.8 m). The effect became slightly more pronounced when sill width became larger.
- A major difference between the integrated sill and isolated sill is in the rotation of the sill. The integrated sills all experienced counter-clockwise tilting (positive values of rotation in the figures), while the isolated sills generally experienced clockwise rotation (negative values of rotation in the figures), except for sill width = 2.5 m, where the rotations were clockwise.
- With a rigid foundation, the abutments tended to have significantly smaller sill settlements, smaller maximum lateral wall displacements, smaller sill lateral movements, and smaller sill rotations (except for isolated sills) than the abutments situated over a medium sand foundation.

Allowable Bearing Pressures

The allowable bearing pressures of GRS abutments were evaluated using the results of the 36 analyses that were done with a medium sand foundation, because they offered more conservative allowable bearing pressures than those with a rigid foundation. Two performance criteria were examined. One criterion involved a limiting sill settlement, where the allowable bearing pressure corresponded to a sill settlement of 1 percent of the lower wall height (i.e., 1 percent H). The other criterion involved distribution of the critical shear strain in the reinforced soil mass, where the allowable bearing pressures corresponded to a condition in which a triangular crit-

ical shear strain distribution reached the back edge of the sill (i.e., heel of the sill). The 1 percent H criterion came from the existing maximum settlement criteria for bridge abutments proposed by Bozozuk (1978), Walkinshaw (1978), Grover (1978), and Wahls (1990). The existing settlement criteria for ride quality and structural distress range from 51 mm to 102 mm based on experience with real bridges. Given that the finite element analysis results should be regarded as short-term response, and the long-term settlement is likely to be of about the same magnitude as the short-term settlement (see “Assessment of the NCHRP Test Abutments” in Chapter 3), 1 percent H or 47 mm short-term settlement as obtained from the analysis was adopted as a criterion for evaluating the allowable bearing pressures.

The critical shear strain concept has been used in the Cam clay model, a widely used soil model developed at Cambridge University in the United Kingdom, for assessing failure of a soil mass. The critical shear strain for the three soils used in the analysis was 3.2 percent, as determined from the triaxial test results. A more detailed explanation of the critical shear strain distribution criterion is in the *parametric study* in this chapter.

Tables 2-7 and 2-8 show the values of the bearing pressures corresponding to the 1 percent H settlement criterion and the critical shear strain distribution criterion for all 36 analyses with a medium sand foundation. The critical shear strain distribution criterion generally yields a somewhat higher allowable bearing pressure for reinforcement spacing of 0.2 m than that with the 1 percent H settlement criterion. This observation, however, is less consistent for reinforcement spacing of 0.4 m. The values of bearing pressures presented in Tables 2-7 and 2-8 were used as the basis for the recommended allowable bearing pressures in the recommended design method (Chapter 3).

TABLE 2-7 Allowable bearing pressures based on the 1%H settlement criterion

Sill Type	Sill Width (m)	Reinforcement Spacing (m)	ϕ (degrees)	Applied Pressure at Settlement = 1%H (kPa)
Integrated	0.8	0.2	34	259
			37	315
			40	354
		0.4	34	231
			37	284
			40	324
	1.5	0.2	34	162
			37	192
			40	221
		0.4	34	145
			37	175
			40	202
	2.5	0.2	34	132
			37	154
			40	175
0.4		34	121	
		37	143	
		40	162	
Isolated	0.8	0.2	34	207
			37	242
			40	268
		0.4	34	166
			37	201
			40	225
	1.5	0.2	34	132
			37	157
			40	180
		0.4	34	109
			37	132
			40	150
	2.5	0.2	34	110
			37	131
			40	148
0.4		34	91	
		37	115	
		40	132	

TABLE 2-8 Allowable bearing pressures based on the critical shear strain distribution criterion

Sill Type	Sill Width (m)	Reinforcement Spacing (m)	ϕ (degrees)	Allowable Bearing Pressure ($\epsilon_{critical} = 3.2\%$) (kPa)
Integrated	0.8	0.2	34	281
			37	375
			40	500
		0.4	34	156
			37	281
			40	406
	1.5	0.2	34	167
			37	217
			40	283
		0.4	34	117
			37	167
			40	233
	2.5	0.2	34	150
			37	200
			40	267
0.4		34	100	
		37	150	
		40	217	
Isolated	0.8	0.2	34	188
			37	250
			40	313
		0.4	34	125
			37	156
			40	219
	1.5	0.2	34	150
			37	200
			40	250
		0.4	34	83
			37	133
			40	167
	2.5	0.2	34	133
			37	167
			40	233
0.4		34	67	
		37	117	
		40	150	

CHAPTER 3

INTERPRETATION, APPRAISAL, AND APPLICATIONS

ASSESSMENT OF THE NCHRP TEST ABUTMENTS

The NCHRP test abutments were assessed in two ways: (1) the measured performance and observed behavior were evaluated against existing performance criteria for bridge abutments; and (2) the safety factors and failure loads of the abutments were evaluated using the design method in the current NHI manual (Elias et al., 2001) through the computer program, MSEW.

Assessment of Measured Performance and Observed Behavior

The assessment of the measured performance and observed behavior of the two full-scale test abutments was made against performance criteria previously established based on experiences with real bridges. Load-carrying capacity and ductility, sill settlement and angular distortion, and maximum lateral movement of the abutment wall were all assessed. The performance criteria, referred to as “the existing criteria” in this chapter, are from studies conducted by Bozozuk (1978), Walkinshaw (1978), Grover (1978), Moulton et al. (1985), and Wahls (1990).

The differences in performance between the two test abutments were caused by the difference in the geosynthetic reinforcement used for the two test sections. The tensile strength of the reinforcement used was 70 kN/m for the Amoco test section and 21 kN/m for the Mirafi test section.

Load-Carrying Capacity and Ductility

- As the loading was being terminated (814 kPa for the Amoco test section and 414 kPa for the Mirafi test section), the Mirafi test section approached a bearing failure condition while the Amoco test section appeared to still be sufficiently stable. For a typical design pressure of 200 kPa, the safety margin in terms of the load-carrying capacity was “acceptable” for the Amoco test section and “marginally acceptable” for the Mirafi test section.
- With a sufficiently strong reinforcement ($T_{ult} = 70$ kN/m, per ASTM D 4595), the Amoco test section was

still exhibiting a near-linear load-settlement relationship at 814 kPa, about four times the typical design pressure of 200 kPa, although the deformation had become fairly large (average sill settlement = 163 mm, maximum lateral movement = 82 mm)—an indication of high ductility of the abutment system. With a weak reinforcement ($T_{ult} = 21$ kN/m, per ASTM D 4595), however, the ductility was significantly compromised. As the applied pressure increased beyond 200 kPa, the rate of settlement continued to increase with increasing applied pressure, and the failure state was only about twice the typical design pressure of 200 kPa.

Sill Settlement and Angular Distortion

- The settlement of the sill was much smaller in the Amoco test section than in the Mirafi test section. Under an applied pressure of 200 kPa, the average sill settlement was 40 mm and 72 mm in the Amoco test section and the Mirafi test section, respectively. As the loading was being terminated (814 kPa for the Amoco test section and 414 kPa for the Mirafi test section), the average sill settlement of the two test sections was comparable, 163 mm and 170 mm, respectively.
- The existing bridge settlement criteria for ride quality and structural distress range from 50 to 100 mm. The average sill settlement of 40 mm for the Amoco test section under a typical design pressure of 200 kPa met the settlement criterion. For the Mirafi test section, the average sill settlement of 72 mm under 200 kPa might have compromised ride quality, but was still considered “tolerable.” The performance criteria are for bridges resting on “conventional” abutments. Given that GRS abutments can provide a “smoother” transition between the approach fill and the bridge structure, the settlement criteria may be relaxed to some extent.
- The typical tolerable maximum angular distortion for single-span bridges is 1:200. For an 18-m (60-ft)-long single-span bridge, the “maximum possible” angular distortion would be 1:450 for the Amoco test section and 1:250 for the Mirafi test section—both below 1:200. The test abutments were constructed over a rigid

foundation, thus the settlement that would occur in the foundation was not accounted for.

- In the load tests, the sill was loaded in equal increments of 50 kPa average vertical pressure and maintained for about 30 minutes between increments. Maintaining each load increment for 30 minutes was intended to allow the stresses to be transferred to the entire soil mass, not to determine creep deformation. The AASHTO guideline suggests that creep tests be conducted for 10,000 hours and extrapolated for a maximum of two log cycles in time.
- Based on the soil-geosynthetic interactive performance (SGIP) tests performed on Amoco 2044 with a road base material by Ketchart and Wu (2001 and 2002), the magnitude of creep deformation over the lifetime of a GRS mass under 200 kPa (30 psi) and in an “unconfined condition” (a conservative condition) would be about the same as the magnitude of the “immediate” settlement. This means that the Amoco 2044 test under 200 kPa would settle about 80 mm and the Mirafi test section would settle about 145 mm over the design life. This would render the Amoco test section only “marginally acceptable” and the Mirafi test section “unacceptable” under a design pressure of 200 kPa. The measured data from the Founders/Meadows abutment (with a soil friction angle of 40 deg from the standard direct shear tests) showed that the sill settled 13 mm because of placement of bridge superstructure and an additional settlement of 11 mm occurred over 18 months after the bridge was opened to the traffic.
- From the standpoint of angular distortion, the maximum possible long-term angular distortion for the Amoco and Mirafi test sections would be 1:225 and 1:125, respectively, for an 18-m (60-ft)-long single-span bridge under 200 kPa pressure. Again, the Amoco test section would only be “marginally acceptable” and the Mirafi test section would be “unacceptable” under a design pressure of 200 kPa.

Lateral Movement of Abutment Wall

- In both test sections, the abutment wall moved outward with the maximum movement occurring near the top of the wall. At an average applied pressure of 200 kPa, the maximum movements in the abutment wall were 24 mm in the Amoco test section and 36 mm in the Mirafi test section. The wing-walls also moved outward with the maximum movement occurring at about H/6 from the top of the wall. At an average applied pressure of 200 kPa, the maximum movement was 18 mm in the Amoco test section and 30 mm in the Mirafi test section.
- The existing lateral movement criteria for ride quality and structural distress range from 25 to 50 mm. The maximum lateral displacements for both test sections

(24 mm and 36 mm) were somewhat below the lateral movement criterion.

- There is little information in the literature about long-term lateral movement of GRS bridge abutments. For the Founders/Meadows abutment, with a fill of 40° friction angle, the maximum outward movement of the abutment wall caused by placement of bridge superstructure was about 9 mm. The additional outward movement over 18 months after the bridge was opened to the traffic was about 13 mm. Assuming that the long-term lateral movement is about the same magnitude as the “immediate” lateral movement, the Amoco test section would be “marginally acceptable” and the Mirafi test section would be “unacceptable.”

Observed Behavior

- A tension crack was observed on the wall crest in both load test sections. The tension crack was first observed at an applied pressure of 150 to 200 kPa. The distinct tension crack was parallel to the abutment wall face and located at end of the reinforcement. The location of the tension crack suggests that the assumption of rigid reinforced soil mass in the existing design methods for evaluating external stability is a sound procedure. The tension cracks might be suppressed by lengthening the top few layers (e.g., three layers) of the reinforcement. If an upper wall had been constructed over the test abutment, as in the case of typical bridge abutments, the tension crack would not have been visible and perhaps would have been less likely to occur.
- Under higher applied loads, the facing blocks in the top three courses were pushed outward as the sill tilted forward. This suggests (1) that the sill clear distance of 0.15 m, the minimum value stipulated by the NHI manual, may be too small, and (2) that it may be beneficial to increase the connection strengthening in the top three to four courses of the facing. The authors believe that the strengthening effect will be most effective if the facing blocks are “inter-connected” after all the facing units are in place.

Assessment of Safety Factors and Failure Loads by the MSEW Program

The NCHRP test abutments were evaluated by MSEW, a computer program developed by ADAMA Engineering, Inc., for design and analysis of mechanically stabilized earth walls. The MSEW program follows the design guidelines presented in the FHWA Demo-82 manual (Elias et al., 1997) and the NHI manual (Elias et al., 2001) and is completely compatible with AASHTO Standard Specifications for Highway Bridges, 16th edition, 1996; as amended by the 1998 interim revisions.

The MSEW program has two modes of operation: design and analysis. In the design mode, the program computes the required layout (length and vertical spacing) corresponding to the user's prescribed safety factors. In the analysis mode, the program computes the factors of safety corresponding to the user's prescribed reinforcement layout. The NCHRP test abutments were evaluated using the analysis mode by Michael Adams of the FHWA.

Three loading conditions were considered: (1) soil self-weight only (i.e., no external load applied to the abutment), (2) soil self-weight plus self-weight of sill (an equivalent point load of 29 kN), and (3) loading condition of 2 plus a distributed load of 200 kPa (an equivalent point load of 866 kN).

The strength reduction factors for geosynthetic reinforcements (i.e., creep reduction factor, durability reduction factor, and installation damage reduction factor) were set equal to 1.0. The "overall factor of safety," as defined in the NHI manual, was also set to 1.0. Therefore, T_a (design long-term reinforcement tension load) = T_{al} (long-term tensile strength).

The MSEW analysis indicated that all the calculated tensile forces were less than T_a , the design long-term reinforcement tension load (i.e., the safety factors against reinforcement rupture failure were greater than 1.0 under all three loading conditions for both test sections). The MSEW analysis also indicated that all the safety factors against pullout failure were greater than 1.0 for the first two loading conditions (i.e., no external load and sill self-weight only). However, for the third loading case (i.e., with an applied pressure of 200 kPa), the pullout safety factors in the top two reinforcement layers were less than 1.0 for both test sections, with the lowest value of pullout safety factor of 0.2 occurring at the very top layer. Trial and error revealed that a pullout safety factor of 1.0 would occur at an applied pressure of 33 kPa. Therefore, the failure pressure according to the MSEW program is 33 kPa. Note that 33 kPa reflects the "true" predicted failure pressure by the MSEW program (hence by the NHI method) because all reduction factors for the reinforcements and the overall safety factor have been set equal to 1.0. The performance of the full-scale tests, however, indicated that the test abutments were far from a failure condition at 33 kPa.

LIMITATIONS OF THE DESIGN AND CONSTRUCTION GUIDELINES

The recommended design and construction guidelines presented later in this chapter apply only to GRS abutments and approaches that satisfy the following conditions:

- The total abutment height is less than 10 m.
- The facing comprises dry-stacked concrete modular blocks, timber, natural rocks, wrapped geosynthetic sheets, or gabions—with or without any mechanical connections (pins or lips) between vertically adjacent facing units.

- No prop (temporary bracing) is used in constructing the abutment wall.
- The backfill meets the following requirements: 100 percent passing 10 cm (4 in.) sieve, 0 to 60 percent passing 0.425 mm (No. 40) sieve, and 0 to 15 percent passing 0.075 mm (No. 200) sieve, free from organic material, plasticity index not greater than 6.
- The backfill has an internal friction angle not less than 34 deg, as determined by the standard direct shear test on the portion finer than 2 mm (No.10) sieve, using a sample compacted to 95 percent of AASHTO T-99, Method C or D, with oversize correction and at the optimum moisture content.
- The backfill in the construction is compacted to at least 100 percent of AASHTO T-99 (i.e., 100 percent of the standard Proctor maximum dry density) or 95 percent of AASHTO T-180 (i.e., 95 percent of the modified Proctor maximum dry density) and the placement moisture is within ± 2 percent of the optimum.
- The foundation soil is "competent," although the term "competent" is, to some extent, relative to the abutment height and the applied loads on the sill. For a medium height GRS abutment (e.g., with a total height of about 7 m) and under the maximum allowable sill pressure (see "The Recommended Design Method"), the foundation is considered "competent" if the in situ undrained shear strength is greater than about 140 kPa (3,000 lb/ft²) for a clayey foundation or the standard penetration blow count is not less than about 20 for a non-prestressed granular foundation. Specific checks of the foundation bearing pressure for a given bridge abutment are performed in Step 7 of the "The Recommended Design Method" below.

RECOMMENDED DESIGN METHOD

For ease of acceptance by the GRS design community and by AASHTO, the recommended design method adopts the format and methodology of the NHI design method. This section begins with a review of the NHI design method, followed by specific refinements and revisions to the NHI design method. Each refinement or revision is described in reference to the NHI method, and the basis for the refinement or revision is given in detail. The section ends with a complete description of the recommended design method. The design method has been established primarily for highway bridges in critical and "permanent" applications. For low-cost applications of GRS bridge abutments, the recommended design method will be rather conservative.

The NHI Design Method for MSE Abutments

The FHWA NHI reference manual, *FHWA-NHI-00-043: Mechanically Stabilized Earth Walls and Reinforced Soil*

Slopes Design and Construction Guidelines, by Elias, Christopher, and Berg (2001), formerly known as Demo 82, provides a design method for MSE bridge abutments (Section 5.1 of the NHI manual). The design method can be described as follows:

- Step 1: Establish design height and external loads.
- Step 2: Establish engineering geotechnical properties (including unit weight and internal friction angle of the reinforced fill and the retained earth and allowable bearing pressure of the foundation soil and the reinforced fill).
- Step 3: Establish design safety factors (including design life, external stability safety factors for sliding, allowable eccentricity, maximum foundation pressure, and internal pullout).
- Step 4: Choose segmental facing type and reinforcement spacing.
- Step 5: Establish preliminary reinforcement length (typically $0.7 \times$ total abutment height).
- Step 6: Size abutment footing/sill (select an initial trial size for the sill and check sliding, eccentricity, and bearing pressure).
- Step 7: Check external stability with the preliminary reinforcement selected in Step 5: (1) check eccentricity, e (e should be $\leq L/6$), (2) check bearing pressure at the foundation level by considering the effective width because of eccentricity, and (3) check safety factor against sliding.
- Step 8: Determine internal stability at each reinforcement level and required horizontal spacing (for steel strip reinforcement).
- Step 9: Determine the required reinforcement strength based on consideration of internal stability at each reinforcement level.

In addition, the NHI manual suggests that the following conditions be implemented in the design of MSE abutments:

- The tolerable angular distortions (i.e., limiting differential settlement) between abutments or between piers and abutments should be limited to 0.005 for simple-span bridges and 0.004 for continuous-span bridges.
- A minimum offset of 0.9 m (3 ft) from the front of the facing to the centerline of the bridge bearing is required.
- A clear distance of 150 mm (6 in.) between the back face of the facing units and front edge of footing is required.
- The abutment should be placed on a bed of compacted coarse aggregate 1 m (3 ft) thick where significant frost penetration is anticipated.
- The bearing capacity on the reinforced volume should be limited to 200 kPa (4,000 lb/ft²).
- The maximum horizontal force at each reinforcement level should be used for the design of connections to the facing units.

- The density, length, and cross-section of reinforcements of the abutment should be extended to wing walls for a horizontal distance of $0.5 H$ (H = height of abutment wall).
- The seismic design forces should also include seismic forces transferred from the bridge through bearing supports that do not slide freely (e.g., elastomeric bearings).

Refinements and Revisions to the NHI Design Method

The recommended design method refines and revises the NHI's bridge abutment design procedure while maintaining the format and basic methodology of the NHI design method. The refinements and revisions are based on findings of this study (including the literature study and the analytical study, both presented in Chapter 2) and the authors' experiences and knowledge. There are 14 specific refinements and revisions, as described below.

1. Refinement/Revision of Step 1

Refinement/Revision: The height of the load-bearing wall (referred to as the "facing wall height" in the NHI manual) is defined as the height measured from the base of the embedment to the top of the load-bearing wall. The embedment of a GRS abutment wall need only be a nominal depth (e.g., one block height). If the foundation soil contains frost-susceptible soils, they should be excavated to at least the maximum frost penetration line and replaced with a non-frost-susceptible soil. If the GRS abutment is in a stream environment, scour/abrasion/channel protection should also be implemented. Examples of the scour/abrasion/channel protection for GRS abutments have been described by Keller and Devin (2003).

Basis for the Refinement/Revision: Experiences from actual construction of GRS walls and bridge-supporting structures.

2. Refinement/Revision of Step 2

Refinement/Revision: The allowable bearing capacity of a bridge sill on the load-bearing wall (the lower wall) of a GRS abutment is a function of the soil stiffness/strength, reinforcement vertical spacing, sill width, sill configuration, reinforcement stiffness/strength, foundation stiffness/strength, and so forth. For an abutment founded on a "competent foundation" (as defined earlier in Limitations of the Design and Construction Guidelines) and with a sufficiently strong reinforcement (to be examined quantitatively in Step 9 of the recommended design method), the allowable bearing pressure, q_{allow} , can be determined by the three-step procedure as follows:

TABLE 3-1 Recommended allowable bearing pressures of a GRS abutment, with an integrated sill (sill width = 1.5 m), on a competent foundation

	Design Friction Angle of Fill ^{1,2}						
	$\phi = 34^\circ$	$\phi = 35^\circ$	$\phi = 36^\circ$	$\phi = 37^\circ$	$\phi = 38^\circ$	$\phi = 39^\circ$	$\phi = 40^\circ$
Reinforcement Spacing = 0.2 m (8 in.)	180 kPa (26 psi)	190 kPa (27.5 psi)	200 kPa (29 psi)	220 kPa (32 psi)	235 kPa (34 psi)	255 kPa (37 psi)	280 kPa (40.5 psi)
Reinforcement Spacing = 0.4 m (16 in.)	125 kPa (18 psi)	140 kPa (20 psi)	155 kPa (22.5 psi)	175 kPa (25 psi)	195 kPa (28 psi)	215 kPa (31 psi)	240 kPa (34.5 psi)

¹ The internal friction angle should be determined by the standard direct shear test on the portion finer than 2 mm (No. 10) sieve, using specimens compacted to 95% of AASHTO T-99, Methods C or D, at optimum moisture content.

² If multiple sets of direct shear tests are performed, the lowest friction angle should be used as the “design friction angle.” If a single set of valid shear tests is performed, the “design friction angle” will be one (1) degree lower than the value obtained from the tests.

- (1) Use Table 3-1 to determine the allowable bearing pressure under the following condition: (a) an “integrated sill” configuration, (b) sill width = 1.5 m, (c) a sufficiently strong reinforcement, and (d) a competent foundation.
- (2) Use Figure 3-1 to determine a correction factor for the selected sill width. The allowable bearing pressure for the selected sill width is equal to the allowable pressure determined in Step (1) multiplied by the

correction factor. A minimum sill width of 0.6 m is recommended.

- (3) If an “isolated sill” is used, a reduction factor of 0.75 should be applied to the corrected bearing pressure determined in Step (2). “Isolated sill” refers to an isolated footing separated from the upper wall of the abutment; whereas an “integrated sill” refers to a sill integrated with the upper wall as an integrated structure.

Correction Factor vs. Sill Width

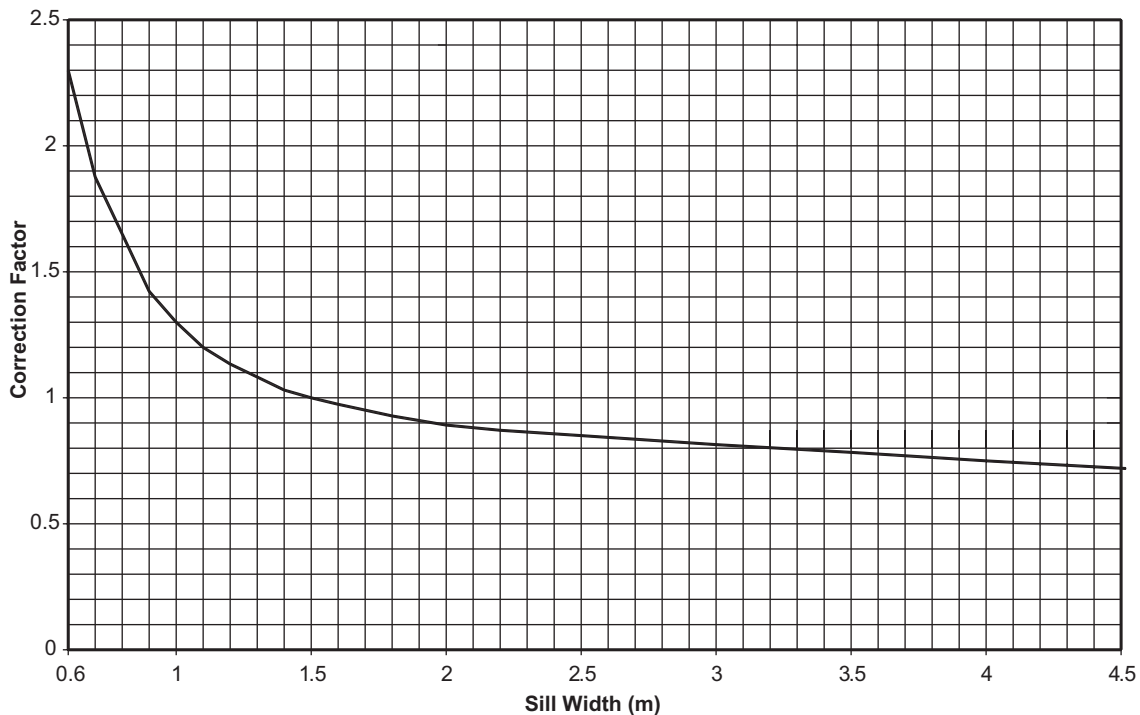


Figure 3-1. Relationship between sill width and the correction factor.

If multiple direct shear tests are performed, the lowest friction angle should be used in design. If a single set of direct shear tests is performed, the “design friction angle” should be taken as 1 degree lower than the value obtained from the tests. For instance, if a single set of tests shows that a soil has a friction angle of 35 deg, the design friction angle will be 34 deg; whereas, if two sets of tests are performed and both show a friction angle of 35 deg, then the design friction angle will be 35 deg. Standard direct shear tests performed on some presumably identical granular soil specimens have suggested that a probable variance of ± 1 degree friction angle should be used for designs of critical earth structures (Aksharadananda and Wu, 2001).

Although the soil specimens used in the tests for determining the friction angle are to be compacted to 95 percent of AASHTO T-99, it is stipulated that the fill in construction be compacted to 100 percent of AASHTO T-99. The additional 5 percent compaction is recommended to provide improved performance and an increased safety margin of a reinforced soil abutment.

Basis for the Refinement/Revision: The recommended allowable bearing pressures in Table 3-1, the correction factors in Figure 3-1, and the reduction factor for isolated sills are based on findings from the analytical study (Chapter 2), especially the analysis results of allowable bearing pressures. Special emphases have been placed on the applied pressure at short-term sill settlement = 1 percent of lower abutment wall height and on the applied pressure corresponding to the condition in which the critical shear strain has just reached a triangular distribution extending through the height of the load-bearing wall (for details, see Load-Carrying Capacity Analysis). The critical shear strain, $\gamma_{(critical)}$, is defined as: $\gamma_{(critical)} = (2/3)(\epsilon_1 - \epsilon_3)_{failure}$ and can be obtained from triaxial compression test results. The refinement/revision is also based on findings from the literature study, especially the performance characteristics of field experiments presented in Chapter 2 and the authors’ judgment of conservative, yet not overly conservative, design values and their experiences with GRS walls and bridge-supporting structures.

The fill is characterized by its friction angle in the design method. The friction angle of a soil relates directly to the “strength” of the soil but does not address its “stiffness,” which determines the deformation of a soil mass before failure. Given that different soils of a similar strength can have rather different values of stiffness, the characterization of a soil by its friction angle is generally considered inadequate in a deformation-based design method. The stiffness values used in the analyses presented in Chapter 2 had to be assumed. The assumed stiffness values are derived from the triaxial stress-strain-strength relationships of more than 120 soils for design purposes (Wong and Duncan, 1974).

3. Refinement/Revision of Step 3

Refinement/Revision: The default value for reinforcement spacing should be 0.2 m. For wrap faced geotextile walls (temporary or adding future facing), reinforcement spacing of 0.15 m is recommended. Reinforcement spacing greater than 0.4 m is not recommended under any circumstances.

Basis of Refinement/Revision: The benefits of smaller reinforcement spacing to improved performance of GRS walls and abutments (both in terms of deformation and ultimate load-carrying capacity) is shown in the analytical results presented in Chapter 2 and has been demonstrated in actual construction. The use of smaller reinforcement spacing will not only help create a more “coherent” reinforced soil mass (i.e., with greater soil-reinforcement interaction) for the abutment wall (as opposed to areas of reinforced soil sandwiched between unreinforced soil when larger reinforcement spacing is used), but will also improve the efficiency of compaction by increasing the “lock-in” lateral stresses of the soil next to the reinforcement surfaces. The finite element analysis results in Chapter 2 did not account for the lock-in lateral stress, thus the true benefits of reduced reinforcement spacing are likely to be even more pronounced than those indicated. For critical structures such as a bridge abutment, it is the authors’ view that the reinforcement spacing should be kept below 0.4 m in all cases to ensure satisfactory performance and an enhanced margin of stability.

4. Refinement/Revision of Step 4

Refinement/Revision: A minimum front batter (i.e., leaning backward from the vertical) of 1/35 to 1/40 is recommended for a segmental abutment wall facing to provide improved appearance and greater flexibility in construction. A typical minimum setback of 5 to 6 mm between successive courses of facing blocks is recommended for 200-mm-high blocks.

Basis of the Refinement/Revision: This refinement/revision is based on the findings of finite element analyses on lateral displacement of abutment wall faces. An in-depth examination of the analysis results reveals that the maximum displacement is typically about 0.03 H (H = wall height) and occurs at 0.7 to 0.8 H from the base at an applied pressure equal to two times the recommended design pressures as determined in Refinement/Revision 2, above. The typical batter needed to offset the lateral movement is calculated to be between 1/35 and 1/40. Averaging the needed batter over the distance between wall base and the point of maximum lateral movement, the setback for each course of facing block is 5 to 6 mm for a block height of 200 mm.

5. Refinement/Revision of Step 5

Refinement/Revision: The reinforcement length may be “truncated” in the bottom portion of the wall provided that the foundation is “competent” (as defined in Limitations of the Design and Construction Guidelines earlier in this Chapter). The recommended configuration of the truncation is: reinforcement length = $0.35 H'$ at the foundation level (H' = total abutment height) and increases upward at 45° angle. The allowable bearing pressure of the sill, as determined in Refinement/Revision 2, should be reduced by 10 percent for truncated-base walls. When reinforcement is truncated at the bottom portion, external stability of the wall (sliding failure, overall slope failure, and foundation bearing failure) must be checked thoroughly.

Basis of the Refinement/Revision: Finite element analysis results of walls with 0.4 m reinforcement spacing show insignificant differences in general performance characteristics between a truncated-reinforcement wall and an un-truncated-reinforcement wall, except for maximum lateral displacement at the wall face. The maximum lateral displacement of a truncated-reinforcement wall is about 10 percent higher than that of an un-truncated-reinforcement wall.

6. Refinement/Revision of Step 6

Refinement/Revision: A recommended clear distance between the back face of the facing and the front edge of sill is 0.3 m (12 in.).

Basis for the Refinement/Revision: This refinement/revision is based on the findings of the finite element analysis conducted in this study and the typical compaction operation. The analysis results were for soils with $\phi = 34^\circ$ and conservative values of soil stiffness. As the applied pressure increases beyond 100 kPa, settlement of the sill and rotation of sill tend to “increase” somewhat as the sill clear distance increases from 0 to 0.3 m. The maximum lateral displacement of the load-bearing abutment wall also increases slightly with increasing sill clear distance. To reduce the cost of bridge girder and bridge deck, the sill clear distance should also be kept to a minimum. On the other hand, the soil immediately behind the facing (within about 0.3 to 0.5 m) should not be compacted by a heavy compactor during construction. As a result, the density of the fill within 0.3 m behind the wall face is generally lower than the rest of the fill. A sill with a clear distance less than 0.3 m, therefore, may experience a larger sill settlement and larger sill rotation.

7. Refinement/Revision of Step 7

Refinement/Revision: This refinement/revision is needed only when D_1 , the “influence length” on the foundation level (note: $D_1 = d + B' + H_1/2$, see Figure 3-2) is

less than the length of the reinforcement (corrected with consideration of load eccentricity) in the load-bearing wall. In this case, the contact pressure on the foundation level, p_{contact} , should be computed as

$$p_{\text{contact}} = (p_{\text{applied}} * B / D_1) + \gamma H_1 + \gamma H_e$$

where p_{applied} is the average applied pressure on the base of the sill (including the pressures caused by the self-weight of the sill, caused by the dead load and live load applied on the sill, and caused by the traffic loads); B is the width of the sill; d is the clear distance between the back face of the facing and front edge of the sill; $B' = B - 2e'$ (e' = eccentricity of the sill load); H_1 is the height between the base of the sill and the foundation level; H_e is the “equivalent” height of the upper wall, $H_e = H_1 H_2 / (2D_1)$, in which H_2 is the height of the upper wall; and γ is the unit weight of reinforced fill. The safety factor against bearing failure is evaluated by dividing the average foundation contact pressure, p_{contact} , by the allowable bearing pressure of the foundation. The allowable bearing pressure of the foundation can be evaluated by the method described in the NHI manual.

If the reinforcements near the base of the lower wall are “truncated” (see Refinement/Revision 5), the reinforcement length at the truncated base, if it is smaller than the influence length (D_1), should be used when determining the average foundation contact pressure.

Basis of Refinement/Revision: For most bridge abutments, a relatively high-intensity bridge load is applied close to the wall face. To ensure that the foundation soil beneath the abutment will have a sufficient safety margin against bearing failure, it is important to examine the contact pressure over a more critical region (within the “influence length” D_1 measured from the wall face, provided that $D_1 <$ reinforcement length in the lower wall), as opposed to the average pressure over the entire reinforced zone (with eccentricity correction)—the procedure prescribed in the current NHI manual.

Field measurement (e.g., Founders/Meadows abutment) has suggested that the vertical stress caused by concentrated vertical loads applied on a sill can be estimated by the 2V:1H pyramidal distribution (Figure 3-2) as described in the NHI manual. The measured data of the NCHRP test abutments have also indicated that the 2V:1H pyramidal distribution yields a good average value of the measured contact pressure on the foundation level (see Assessment of the NCHRP Test Abutments in this chapter).

8. Refinement/Revision of Step 8

Refinement/Revision: If the bearing capacity of the foundation soil supporting the bridge abutment is found only marginally acceptable or somewhat unacceptable,

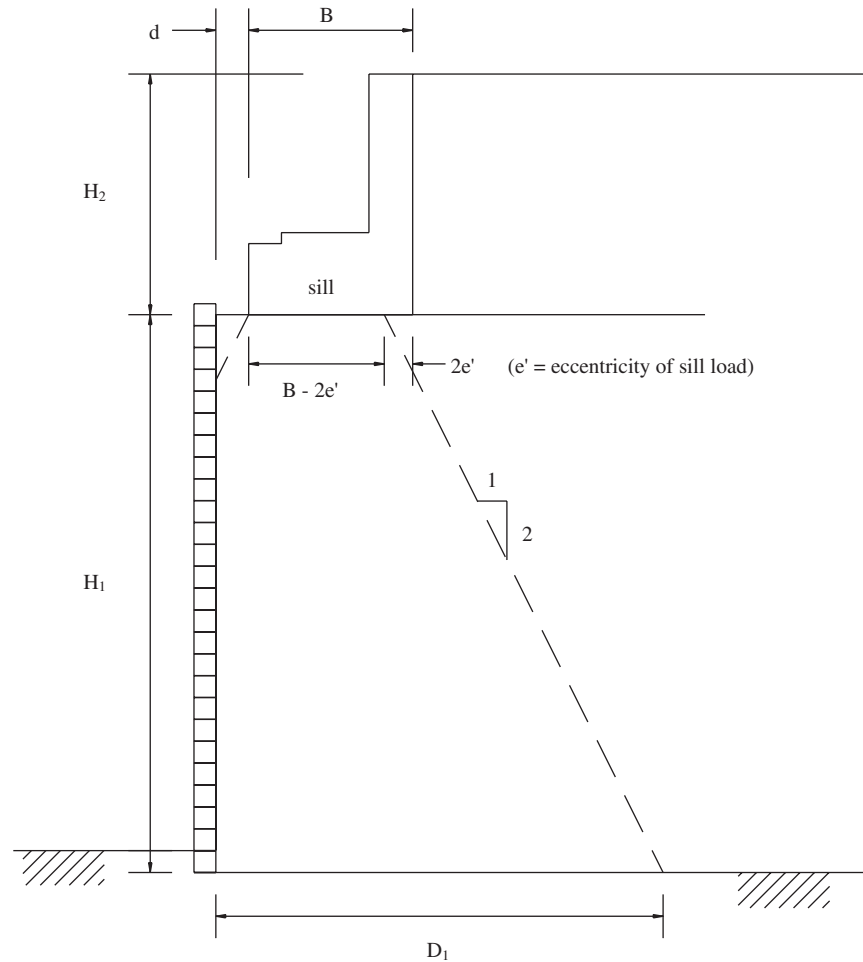


Figure 3-2. Distribution of vertical stress from sill load and definition of D_1 , the influence length.

a reinforced soil foundation (RSF) may be used to increase its bearing capacity and reduce potential settlement. A typical RSF is formed by excavating a pit that is $0.5L$ deep (L = reinforcement length) and replacing it with compacted road base material reinforced by the same reinforcement to be used in the reinforced abutment wall at 0.3 m vertical spacing. The lateral extent of the RSF should at least cover the vertical projection of the reinforced soil area and should extend no less than $0.25L$ in front of the wall face. A procedure proposed by Barreire and Wu (2001) may be used as a guide for evaluating the bearing capacity and settlement of an RSF.

Basis of the Refinement/Revision: This refinement/revision is based on full-scale experiments by Adams at the Turner-Fairbank Highway Research Center, and recent research on bearing capacity of an RSF (e.g., Huang and Tatsuoka, 1990; Omar et al., 1993; Yetimoglu et al., 1994; Adams and Collin, 1997;

Wayne et al., 1998). The use of an RSF typically adds only a small cost to the project but can produce significant benefits.

9. Refinement/Revision of Step 9

Refinement/Revision: Both a minimum ultimate tensile strength and a minimum tensile stiffness of the reinforcement should be specified to ensure sufficient tensile resistance at the service load and to ensure a sufficient safety margin against rupture failure. The tensile stiffness is defined as the tensile resistance at the working strain (i.e., the strain at the working load). The maximum reinforcement strain under the working load for an in-service GRS bridge-supporting structure typically ranges from 0.2 percent to 1.6 percent (see Chapter 2). It is recommended that the resistance at tensile strain of 1.0 percent be taken as the reference strain for specification of the required reinforcement stiffness.

The minimum required reinforcement stiffness in the direction perpendicular to the wall face, $T_{@ \epsilon = 1.0 \text{ percent}}$, should be determined by

$$T_{@ \epsilon = 1.0 \text{ percent}} \geq \sigma_{h(\text{max})} * s$$

where $\sigma_{h(\text{max})}$ is the maximum lateral stress in the reinforced fill and s is the vertical reinforcement spacing. For non-uniform reinforcement spacing, $s = (1/2 \text{ distance to reinforcement layer above}) + (1/2 \text{ distance to reinforcement layer below})$. The lateral stress in the reinforced fill, σ_h , can be calculated as $\sigma_h = K_a (\gamma Z + \Delta\sigma_v) + \Delta\sigma_h$, as suggested by the NHI Manual.

The minimum value of the ultimate reinforcement strength in the direction perpendicular to the abutment wall face, T_{ult} , should be determined by imposing a combined safety factor on $T_{@ \epsilon = 1.0 \text{ percent}}$ to ensure satisfactory long-term performance, to ensure sufficient ductility of the abutment, and to account for various uncertainties, i.e.,

$$T_{\text{ult}} \geq F_s * T_{@ \epsilon = 1.0 \text{ percent}}$$

The recommended combined safety factor is $F_s = 5.5$ for reinforcement spacing $\leq 0.2 \text{ m}$, and $F_s = 3.5$ for reinforcement spacing of 0.4 m . The combined safety factor only applies to the backfill material and placement conditions specified in Recommended Construction Guidelines in this chapter.

Basis of the Refinement/Revision: The maximum reinforcement strains measured in GRS walls, piers, and abutments under service loads typically are on the order of 0.1 percent to 2.0 percent; however, the ultimate strength of geosynthetic reinforcements typically occurs at a strain over 10 percent. Geosynthetic reinforcements of a similar strength can have rather different load-deformation relationships. In design, it will be prudent to specify the resistance required at the working load to ensure satisfactory performance under the in-service condition. In addition, a minimum value of the ultimate reinforcement strength is also needed to ensure adequate ductility and satisfactory long-term performance and to account for uncertainties. The recommended combined safety factors are derived from the cumulative long-term reduction factors for GRS mass (see Wu, 2001) in conjunction with an overall uncertainty factor of 2.5.

As an example, for a 10-m-high abutment (a 7.5-m-high lower wall plus a 2.5-m-high upper wall) with $\phi = 34^\circ$, the maximum vertical stress is about 200 kPa, and the maximum lateral stress, $\sigma_{h(\text{max})} = 56.6 \text{ kPa}$. For reinforcement spacing of 0.2 m, the minimum required tensile stiffness at 1 percent strain, $T_{@ \epsilon = 1.0 \text{ percent}} \geq \sigma_{h(\text{max})} * s = 56.6 \text{ kPa} * 0.2 \text{ m} = 11.3 \text{ kN/m}$ (or 65 lb/in.). In

other words, the reinforcement must have a minimum “working” stiffness of at least 11.3 kN/m (or 65 lb/in.). In addition, the minimum ultimate tensile strength, $T_{\text{ult}} \geq F_s * T_{@ \epsilon = 1.0 \text{ percent}} = 5.5 (11.3) = 62.1 \text{ kN/m}$ (or 357 lb/in.).

10. General Revision: If the heights of the load-bearing walls at the two ends of a bridge differ significantly, the angular distortion between the abutments may exceed 0.005 (a limiting value recommended by the NHI manual for a single-span bridge); therefore, it is a good practice to preload or even prestress the load-bearing abutment walls. The proper magnitude of preloading or prestressing and the reduction in differential settlement caused by preloading of a reinforced soil mass may be evaluated by a procedure recommended by Ketchart and Wu (2001 and 2002). Preloading typically reduces the vertical deformation of a reinforced soil mass by twofold to sixfold, depending on the field placement density, and the lateral deformation by about threefold, as evidenced by limited case histories (see Chapter 2).

Basis for the Revision: The benefits to be gained by preloading and/or prestressing a GRS bridge-supporting structure have been demonstrated in in-service bridge abutments (e.g., Black Hawk bridge abutment), in full-scale experiments of bridge supporting structures (e.g., FHWA Turner-Fairbank bridge pier), and in GRS abutment walls constructed by the Japan Railway (e.g., Tatsuoka et al., 1997; Uchimura et al., 1998). Extensive research on the subject has been conducted by Tatsuoka et al. (1997) and Ketchart and Wu (2001).

11. General Refinement: The NHI manual does not address the design of the back wall (the upper wall). The back wall should be designed in a similar manner as the load-bearing wall. In most cases, the same fill, same reinforcement, and same fill placement conditions as those of the load-bearing wall should be used, although the default reinforcement spacing in the approach fill can be increased somewhat (e.g., from 0.2 m to 0.3 or 0.4 m). The length of all the layers of reinforcement (at least in the top three layers, if there is a significant space constraint) should be about 1.5 m beyond the end of the approach slab to produce a “smoother” surface subsidence profile over the entire design life of the abutment.

Basis for the Refinement: Experiences from actual construction of GRS walls and bridge-supporting structures.

12. General Refinement: If there is no significant space constraint, it is recommended that the reinforcement length of the top three layers (all the layers, if there is

little space constraint) in the lower wall be extended to about 1.5 m beyond the end of the approach slab. Extending the reinforcement lengths beyond the approach slab tends to integrate the abutment wall with the approach embankment and the load-bearing abutment, so as to eliminate bridge “bumps”—a chronic problem in many bridges (Adams et al., 1999). The use of an integrated sill (i.e., integrating sill with the upper wall, see Refinement/Revision 2, above) is also a major part of an effective system for alleviating bridge bumps.

Basis of the Refinement: Bridge bumps typically occur over time, because of factors such as traffic loads, temperature change, and soil moisture variation. These effects cannot be examined realistically by any current analytical tools. The analytical study conducted in this study (see Chapter 2), however, did indicate that differential settlement occurring in the approach fill would be negligible under life loads. The Founders/Meadows abutment (Abu-Hejleh et al., 2000) extended the reinforcement lengths beyond the end of the approach slab in the load-bearing wall and has not experienced any noticeable bridge bumps 4 years into service. This recommended refinement is based on limited field experience. Engineering judgment, however, suggests that integrating the abutment wall, the approach fill, and the load-bearing abutment should help reduce the differential settlement.

- 13. General Revision:** Connection strength is not a design concern as long as the reinforcement spacing is kept to not more than 0.2 m, the selected fill is compacted to the specification, and the applied pressure does not exceed the recommended design pressures determined in Refinement/Revision 2, above. For reinforcement spacing of 0.4 m, long-term connection failure should be checked to ensure long-term stability. Moreover, a recommended practice that the horizontal interfaces in the top three to four courses of the facing block be strengthened to provide adequate interface shear resistance (see Recommended Construction Guidelines later in this chapter) should be observed to avoid potential facing failure. The interface strengthening effect will be more effective if the facing blocks are interconnected after all the facing units are in place.

Basis for the Revision: The revision is based primarily on field experiences of very tall GRS walls (Wu, 2001). GRS walls of a height up to 16 m have been constructed with dry-stacked split-faced concrete blocks without any interblock mechanical connections. These walls have performed satisfactorily without any sign of distress. A 15-m-high wall can be regarded as

being equivalent to a 5-m-high wall with about 200 kPa surcharge. The finite element analysis results of short-term behavior of GRS walls with a segmental facing have indicated that a GRS abutment with reinforcement spacing of 0.2 m will not suffer from any connection-related problems up to a sill pressure of 1,000 kPa. With reinforcement spacing of 0.4 m; however, connection failure may occur between 600 to 800 kPa (see Load-Carrying Capacity Analysis, Chapter 2). Also, with reinforcement spacing not greater than 0.2 m, the reinforced soil mass tends to behave as a “soil-reinforcement composite,” which will exert a far smaller lateral earth pressure against “flexible” facing (Wu, 2001).

- 14. General Refinement:** The angular distortion between abutments or between piers and abutments should be checked to ensure ride quality and structural integrity. The angular distortion = (difference in settlement between abutments or between piers and abutments)/(span between the bridge-supporting structures). The angular distortion should be limited to 0.005 (or 1:200) for simple spans and 0.004 (or 1:250) for continuous spans.

The settlement of each abutment is the sum of the foundation settlement and the abutment settlement. The foundation settlement of a GRS abutment subject to bridge loads can be estimated by using the conventional settlement computation methods found in soils engineering textbooks and reports (e.g., Terzaghi and Peck, 1967; Perloff, 1975; and Poulos, 2000). The abutment settlement with the recommended allowable bearing pressure presented in Refinement/Revision 2 (above) can be estimated conservatively as 1.5 percent of H_1 (H_1 = height of the loading bearing wall or the lower abutment wall).

Basis for the Refinement: The NHI manual stipulates the angular distortion requirement, but does not include it explicitly as part of the design procedure. This refinement makes the design method more complete. As the allowable sill bearing pressures were based in part on abutment settlement of 1.0 percent of H_1 , it is recommended that the settlement within a GRS abutment, under the allowable sill bearing pressure, be estimated conservatively to be 1.5 percent of H_1 .

The Recommended Design Method

The recommended design method for GRS bridge abutments is presented step by step. Before using the recommended design method, the limitations described earlier in this Chapter (in Limitations of the Design and Construction Guidelines) should be checked thoroughly.

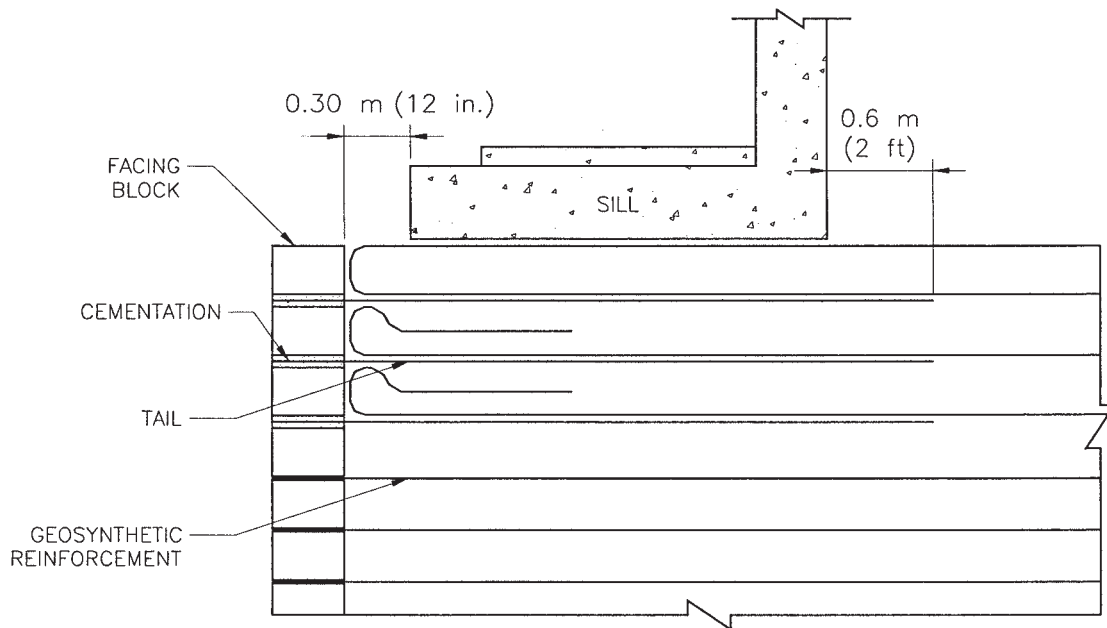


Figure 3-3. Details of reinforcement layout near the top of the load-bearing wall.

Step 1: Establish abutment geometry and external loads and trial design parameters

- Establish abutment geometry and loads (see Figure 3-4):
 - Total abutment height, H' (the sum of lower wall height and upper wall height)
 - Load-bearing wall (lower wall) height, H_1 , as measured from the base of the embedment to the top of the load-bearing wall
 - Back wall (upper wall) height, H_2
 - Traffic surcharge, q
 - Bridge vertical dead load, DL
 - Bridge vertical live load, LL
 - Bridge horizontal load
 - Bridge span and type (simple or continuous span)
 - Length of approach slab
 - The embedment of a GRS abutment wall need only be a nominal depth (e.g., one block height). If the foundation contains frost-susceptible soils, they should be excavated to at least the maximum frost penetration line and replaced with a non-frost-susceptible soil. If the GRS abutment is in a stream environment, scour/abrasion/channel protection measures should be undertaken.
- Establish trial design parameters:
 - Sill width, B (a minimum sill width of 0.6 m is recommended).
 - Clear distance between the back face of the facing and the front edge of the sill, d (the recommended clear distance is 0.3 m).
 - Sill type (integrated sill or isolated sill). “Isolated sill” refers to a sill separated from the upper wall of

the abutment; whereas “integrated sill” refers to a sill integrated with the upper wall as an integrated structure).

- Facing type (dry-stacked concrete modular blocks, timber, natural rocks, wrapped geosynthetics, or gabions) and facing block size (for concrete modular block facing).
- Batter of facing (a minimum front batter of 1/35 to 1/40 is recommended for segmental wall facing to provide improved appearance and greater flexibility in construction. A typical minimum setback of 5 to 6 mm between successive courses of facing blocks is recommended for blocks with height = 200 mm).
- Reinforcement spacing (the default value for reinforcement spacing is 0.2 m). For wrapped-faced geotextile walls, temporary walls, or walls where facing may be added in the future, a reinforcement spacing of 0.15 m is recommended. Reinforcement spacing greater than 0.4 m is not recommended under any circumstances.

Step 2: Establish soil properties

- Check to ensure that the selected fill satisfies the following criteria: 100 percent passing 100 mm (4 in.) sieve, 0-60 percent passing No. 40 (0.425 mm) sieve, and 0-15 percent passing No. 200 (0.075 mm) sieve; and plasticity index (PI) ≤ 6 .
- Establish reinforced fill parameters:
 - Wet unit weight of the reinforced fill.

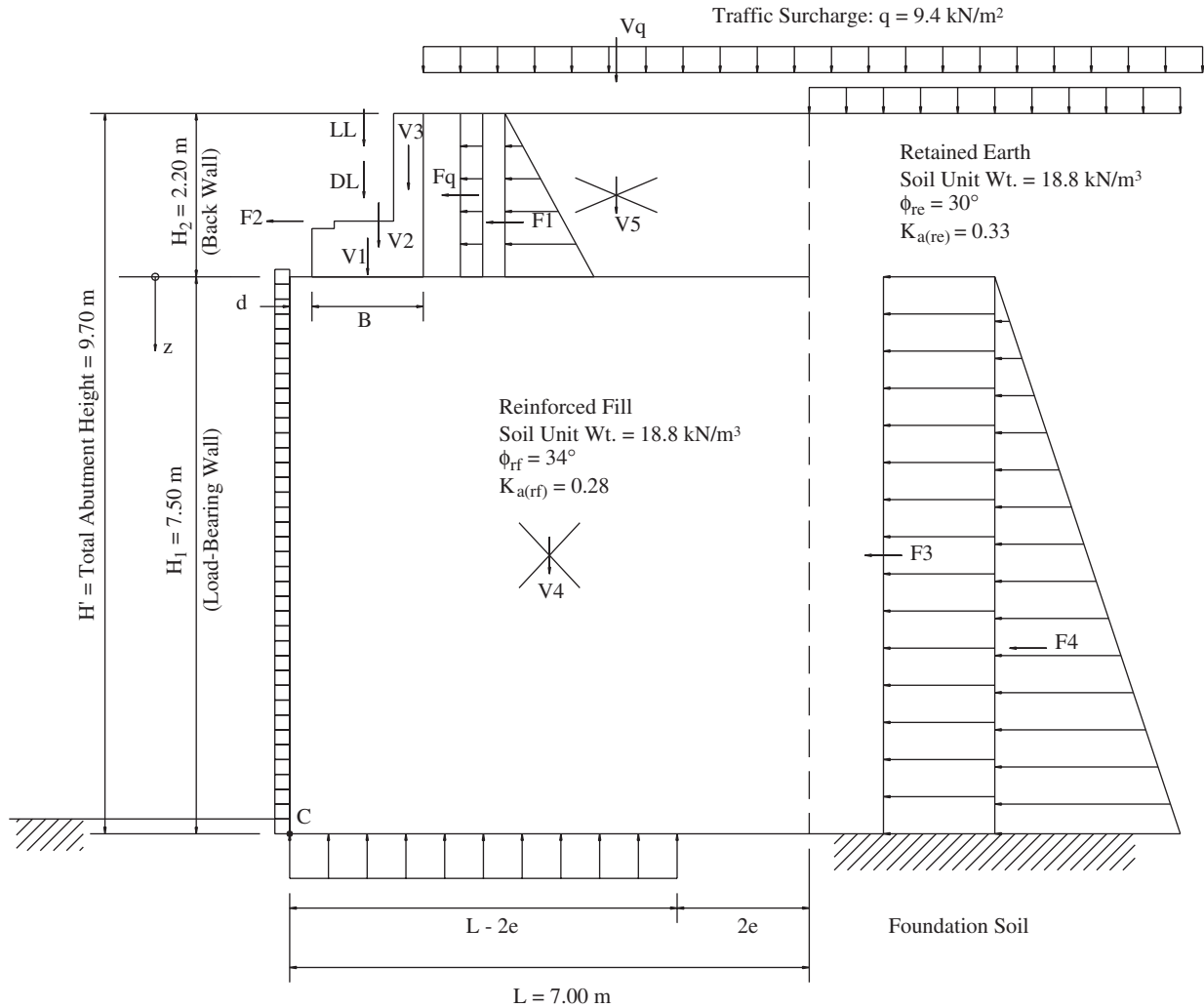


Figure 3-4. Design Example 1—configuration of the abutment.

- The “design friction angle” of the reinforced fill, ϕ_{design} , is taken as 1 degree lower than the friction angle obtained from tests, $\phi_{\text{design}} = \phi_{\text{test}} - 1^\circ$, where ϕ_{test} is determined by one set of the standard direct shear tests on portion finer than 2 mm (No. 10) sieve, using a sample compacted to 95 percent of AASHTO T-99, Methods C or D, at the optimum moisture content.
 - If multiple direct shear tests are performed, the smallest friction angle should be used in design. For instance, if two sets of tests are performed—both showing a friction angle of 35° —the “design friction angle” will be 35° . On the other hand, if a single set of tests shows that a soil has a friction angle of 35° , then the “design friction angle” will be taken as 34° .
 - Establish retained earth parameters:
 - Friction angle of the retained earth
 - Wet unit weight of the retained earth
 - Coefficient of active earth pressure of the retained earth
 - Establish foundation soil parameters:
 - Friction angle of the foundation soil
 - Wet unit weight of the foundation soil
 - Allowable bearing pressure of the foundation soil, q_{af}
- Step 3: Establish design requirements*
- Establish external stability design requirements:
 - Factor of safety against reinforced fill base sliding ≥ 1.5
 - Eccentricity $\leq L/6$ (L = length of reinforcement at base of the reinforced zone)
 - Average sill pressure \leq allowable bearing pressure of the reinforced fill, q_{allow}
 - Average contact pressure at the foundation level \leq allowable bearing pressure of the foundation soil, q_{af}

- Establish internal stability design requirements:
 - Factor of safety against reinforcement pullout, $FS_{\text{pullout}} \geq 1.5$.
 - Connection strength will not be a design concern provided that (a) the reinforcement spacing is kept no greater than 0.2 m, (b) the selected fill is compacted to the specifications in the Recommended Construction Guidelines presented later in this chapter, and (c) the average applied pressure on the sill does not exceed the recommended allowable pressure determined in Step 4, below.
 - For reinforcement spacing of 0.4 m, long-term connection failure should be checked to ensure long-term stability. Moreover, a recommended practice that “the horizontal interfaces in the top three to four courses of the facing block be strengthened to provide adequate interface shear resistance” should be observed to avoid potential facing failure (see Recommended Construction Guidelines later in this chapter). The interface strengthening effect will be even more effective if the facing blocks are interconnected “after” all the facing units are in place.

Step 4: Determine allowable bearing pressure of reinforced fill

The allowable bearing pressure of the reinforced fill, q_{allow} , can be determined by the following three-step procedure:

- (1) Use Table 3-1 to determine the allowable bearing pressure under the following conditions: (a) an “integrated sill” configuration, (b) sill width = 1.5 m, (c) a sufficiently strong reinforcement (meeting the minimum required values of stiffness and strength as defined in Step 9, below) is used, and (d) the abutment is constructed over a competent foundation (satisfying the bearing pressure requirement in Step 7, below).
- (2) Use Figure 3-1 to determine a correction factor for the selected sill width. The allowable bearing pressure for the selected sill width is equal to the allowable pressure determined in Step (1), above, multiplied by the correction factor. A minimum sill width of 0.6 m is recommended.
- (3) If an “isolated sill” is used, a reduction factor of 0.75 should be applied to the corrected allowable bearing pressure determined in Step (2), above.

The allowable bearing pressure determined by the three-step procedure is for a GRS abutment founded on a “competent” foundation and with a sufficiently strong reinforcement.

Example 1: the Founders/Meadows Abutment (see Chapter 2)

Conditions:

Fill: $\phi_{\text{design}} = 39^\circ$ (note: $\phi_{\text{test}} = 40.1^\circ$ from a single set of standard direct shear tests)
 Reinforcement spacing = 0.4 m
 Integrated sill, sill width = 3.8 m

Allowable bearing pressure:

- (1) From Table 3-1, for $\phi = 39^\circ$ and reinforcement spacing = 0.4 m, allowable pressure = 215 kPa.
- (2) Extrapolating from Figure 3-1, the correction factor for a sill width of 3.8 m = 0.77; thus, the corrected allowable bearing pressure = 215 kPa \times 0.77 = 166 kPa.
- (3) No reduction for an integrated sill. Thus, $q_{\text{allow}} = 166$ kPa.

Example 2: the NCHRP test abutments (see Chapter 2)

Conditions:

Fill: $\phi_{\text{design}} = 34^\circ$ (note: $\phi_{\text{test}} = 34.8^\circ$ from a single set of standard direct shear tests)
 Reinforcement spacing = 0.2 m
 Isolated sill, sill width = 0.9 m

Allowable bearing pressure:

- (1) From Table 3-1, for $\phi_{\text{design}} = 34^\circ$ and reinforcement spacing = 0.2 m, allowable pressure = 180 kPa.
- (2) From Figure 3-1, the correction factor for sill width of 0.9 m = 1.4; thus, the corrected allowable bearing pressure = 180 kPa \times 1.4 = 252 kPa.
- (3) Reduction factor for an isolated sill = 0.75; thus, $q_{\text{allow}} = 252 \times 0.75 = 189$ kPa.

Step 5: Establish trial reinforcement length

- A preliminary reinforcement length, L , can be taken as $0.7 \times$ total abutment wall height ($L = 0.7 \times H'$).
- The reinforcement length may be “truncated” in the bottom portion of the wall provided that the foundation is “competent” (as defined in Limitations of the Design and Construction Guidelines earlier in this chapter). The recommended configuration of the truncation is reinforcement length = $0.35H'$ at the foundation level (H' = total abutment height) and increases upward at 45° angle.
- The allowable bearing pressure of the sill, as determined in Step 4, should be reduced by 10 percent for a truncated-base wall.

- When reinforcement is truncated at the bottom portion, external stability of the wall (i.e., sliding failure, overall slope failure, and foundation bearing failure) must be examined thoroughly.

Step 6: Evaluate stability of footing/sill

- Establish trial sill configuration (e.g., establishing the magnitude of B , d , H_2 , t , b , f_w and f_h in Figure 3-5).
- Determine the forces acting on the sill (see, Figure 3-5 for example) and calculate the factor of safety against sliding, FS_{sliding} . FS_{sliding} should be ≥ 1.5 .
- Check sill eccentricity requirement: The load eccentricity at the base of the sill, e' , should be $\leq B/6$ (B = width of sill).
- Check allowable bearing pressure of the reinforced fill; the applied contact pressure on base of the sill should be $\leq q_{\text{allow}}$ determined in Step 4.

Step 7: Check external stability of reinforced fill with the preliminary reinforcement length established in Step 5

- Determine the forces needed for evaluating the external stability of the abutment (e.g., V_4 , V_5 , V_q , F_3 , F_4 , and I_1 in Figure 3-4, I_1 is the influence depth caused by the horizontal forces in the back wall, as shown in Figure 3-6).
- Check factor of safety against sliding of the reinforced volume, FS_{sliding} , should be ≥ 1.5 .

- Check eccentricity requirement for the reinforced volume, e , should be $\leq L/6$ (L = length of reinforcement).
- Check allowable bearing pressure of the foundation soil:
 - Determine the “influence length” D_1 at the foundation level ($D_1 = d + (B - 2e') + H_1/2$, see Figure 3-2) and compare it with the effective reinforcement length, $L' = L - 2e$.
 - The contact pressure on the foundation level, p_{contact} , is calculated by dividing the total vertical load in the reinforced volume by D_1 or L' , whichever is smaller.
 - p_{contact} should be $\leq q_{\text{af}}$
 If the bearing capacity of the foundation soil supporting the bridge abutment is only marginally acceptable or somewhat unacceptable, an RSF may be used to increase its bearing capacity and to reduce potential settlement. A typical RSF is founded by excavating a pit that is $0.5L$ deep (L = reinforcement length) and replacing it with compacted road base material reinforced by the same reinforcement to be used in the reinforced abutment wall at 0.3 m vertical spacing. The lateral extent of the RSF should at least cover the vertical projection of the reinforced fill and should extend no less than $0.25L$ in front of the wall face.

Step 8: Evaluate internal stability at each reinforcement level

When evaluating the internal stability, the coefficient of lateral earth pressure is assumed to be constant

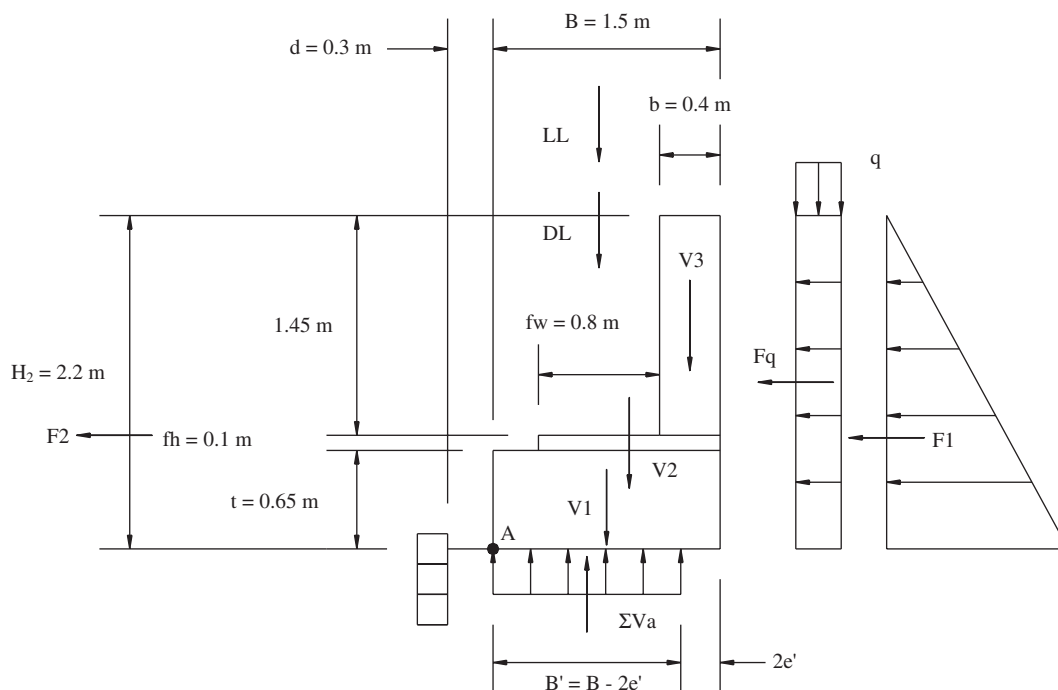


Figure 3-5. Design Example 1—dimensions and loads acting on the sill.

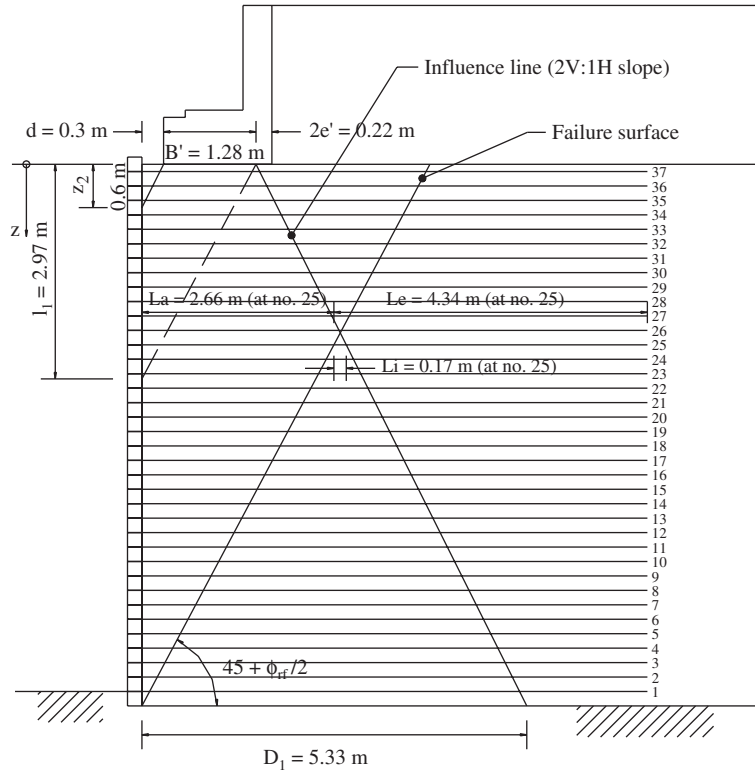


Figure 3-6. Design Example 1 - Notations of the quantities for internal stability evaluation.

throughout the entire wall height. The internal stability is evaluated by checking the factor of safety against reinforcement pullout failure at each reinforcement level.

The factor of safety against pullout failure, $FS_{pullout}$, at any given reinforcement level, is equal to pullout resistance at the reinforcement level divided by T_{max} . T_{max} is the maximum reinforcement tensile force at the reinforcement level where the pullout safety factor is being evaluated. T_{max} is calculated as the product of the average active lateral earth pressure at the reinforcement level multiplied by the reinforcement vertical spacing. The pullout resistance, on the other hand, arises from the frictional resistance at soil-reinforcement interface along the portion of reinforcement lies beyond the potential failure plane. The potential failure plane is taken as the active Rankine failure surface with a uniform vertical surcharge. $FS_{pullout}$ at all reinforcement levels should be ≥ 1.5 .

Step 9: Determine the required reinforcement stiffness and strength

Both a minimum value of ultimate tensile stiffness and a minimum value of tensile strength of the geosynthetic reinforcement should be specified to ensure sufficient tensile resistance at the service load and a sufficient safety margin against rupture failure. The tensile stiffness is

defined as the tensile resistance at the working strain. It is recommended that a tensile strain of 1.0 percent be taken as the reference working strain, and the resistance at strain = 1.0 percent be used for specification of the required reinforcement stiffness.

The minimum required reinforcement stiffness in the direction perpendicular to the wall face, $T_{@ \epsilon = 1.0 \text{ percent}}$, is to be determined as

$$T_{@ \epsilon = 1.0 \text{ percent}} \geq \sigma_{h(max)} \cdot s$$

where $\sigma_{h(max)}$ is the maximum lateral stress in the reinforced fill, and s is the vertical reinforcement spacing. For non-uniform reinforcement spacing, $s = (\frac{1}{2} \text{ distance to reinforcement layer above}) + (\frac{1}{2} \text{ distance to reinforcement layer below})$.

The required minimum value of the ultimate reinforcement strength in the direction perpendicular to the abutment wall face, T_{ult} , should be determined by imposing a combined safety factor on $T_{@ \epsilon = 1.0 \text{ percent}}$ as

$$T_{ult} \geq Fs \cdot T_{@ \epsilon = 1.0 \text{ percent}}$$

The combined safety factor is applied to ensure satisfactory long-term performance, to provide sufficient ductility of the abutment, and to account for various uncertainties. The recommended combined safety factor

is $F_s = 5.5$ for reinforcement spacing ≤ 0.2 m, and $F_s = 3.5$ for reinforcement spacing of 0.4 m. These combined safety factors only apply to the condition where the backfill material and placement conditions satisfy those in the recommended construction guidelines.

Step 10: Design the back/upper wall

If the back wall (or the upper wall) is to be a reinforced soil wall, it should be designed similarly to the load-bearing wall. In most cases, the same fill, same reinforcement, and same fill placement conditions as those of the load-bearing wall should be used, although the default reinforcement spacing in the approach fill can be increased somewhat (e.g., from 0.2 m to 0.3 m or even 0.4 m). The length of all the layers of reinforcement (at least in the top three layers, if there is a spacing constraint) should be extended about 1.5 m beyond the end of the approach slab to produce a “smoother” surface subsidence profile over the entire design life of the abutment.

If there is no significant space constraint, it is recommended that the reinforcement length of the top three layers (all the layers, if there is little space constraint) in the lower wall be also extended about 1.5 m beyond the end of the approach slab. Extending the reinforcement lengths beyond the approach slab promotes integration of the abutment wall with the approach embankment and the load-bearing abutment, so as to eliminate bridge “bumps.”

Step 11: Check angular distortion between abutments

The angular distortion between abutments or between piers and abutments should be checked to ensure ride quality and structural integrity. Angular distortion = (difference in total settlements between abutments or between piers and abutments)/(span between the bridge-supporting structures). The angular distortion should be limited to 0.005 (or 1:200) for simple spans and 0.004 (or 1:250) for continuous spans.

The total settlement of each abutment is the sum of foundation settlement (i.e., settlement occurs beneath the abut-

ment) and abutment settlement (i.e., settlement occurs within the abutment). The foundation settlement caused by the self weight of a GRS abutment and subject to bridge loads can be estimated by using the conventional settlement computation methods in soils engineering textbooks and reports (e.g., Terzaghi and Peck, 1967; Perloff, 1975; Poulos, 2000). The abutment settlement, under the recommended allowable bearing pressure determined in Step 4, can be estimated conservatively as 1.5 percent of H_1 (H_1 = height of the loading bearing wall).

In situations where the heights of the load-bearing walls at the two ends of a bridge differ significantly, it is a good practice to preload or prestress the load-bearing walls. The proper magnitude of preloading or prestressing and the probable reduction in differential settlement caused by preloading of a reinforced soil mass can be evaluated by a procedure established by Ketchart and Wu (2001 and 2002).

RECOMMENDED CONSTRUCTION GUIDELINES

Earthwork construction control for GRS abutments is essentially the same as that required for conventional bridge abutments, but with a few additional details that require special attention. Field substitutions of backfill materials or changes in construction sequence, procedures, or details should only be permitted with the express consent of the responsible geotechnical or preconstruction design engineer. The recommended construction guidelines focus on GRS abutments with a segmental concrete block facing. Only basic guidelines are given for GRS abutments with other forms of flexible facing.

Segmental Concrete Block Facing GRS Abutments

The construction guidelines presented below are established based on the guidelines for construction of segmental GRS walls provided by various agencies (including AASHTO, NCMA, FHWA, CTI, SAGP, and JR), as summarized in Appendix A, as well as the authors’ and their colleagues’ observations and experiences with construction of GRS walls and abutments.

<p>Site and Foundation Preparation</p>	<ul style="list-style-type: none"> – Before placement of the reinforcement, the ground should be graded to provide a smooth, fairly level surface. – The surface should be clear of vegetation, large rocks, stumps, and the like. Depressions may need to be filled; soft spots may need to be excavated and replaced with backfill material; and the site may need to be proof rolled. – If the foundation contains frost-susceptible soil, it should be excavated to at least the maximum frost penetration line and replaced with non-frost-susceptible soil. – If the foundation is only marginally competent, the top 1 m of the foundation should be excavated and replaced with a reinforced soil foundation (compacted granular soil
--	---

	<p>reinforced with four equally spaced layers of geosynthetic reinforcement, wide-width strength of reinforcement ≥ 70 kN/m, per ASTM D 4595).</p> <ul style="list-style-type: none"> – For abutment walls less than 10 m high, unless the ground surface is level and the foundation soil is stiff, a leveling pad should be constructed under the first course of the facing blocks. The leveling pad should be a compacted road base material of about 150 mm (6 in.) thick and 450 mm (18 in.) wide. Compaction of the leveling pad should be performed using a light-compactor to obtain a minimum of 95 percent of the maximum standard Proctor density (per ASTM D698). – If excavation is needed, it should be carried out to the lines and grades shown on the project grading plans. Over-excavation should be minimized. – In a stream environment, GRS abutments should be protected from possible scour and abrasion by using riprap or other protection measures.
Reinforcement and Reinforcement Placement	<ul style="list-style-type: none"> – Geosynthetic reinforcement should consist of high-tenacity geogrids or geotextiles manufactured for soil reinforcement applications. Geosynthetics, especially geotextiles, should not be exposed to sunlight and extreme temperatures for an extended period of time. Damaged or improperly handled geosynthetic reinforcement should be rejected. – Geosynthetic reinforcement should be installed under tension. A nominal tension shall be applied to the reinforcement and maintained by staples, stakes, or hand tensioning until the reinforcement has been covered by at least 150 mm (6 in.) of soil fill. – The geosynthetic reinforcement perpendicular to the wall face should consist of one continuous piece of material. Overlap of reinforcement in the design strength direction is not permitted. Adjacent sections of geosynthetic reinforcement should be placed so as to ensure that horizontal coverage shown on the plans is provided. – Tracked construction equipment shall not be operated directly on the geosynthetic reinforcement. A minimum backfill thickness of 150 mm (6 in.) is required before operation of tracked vehicles over the geosynthetic reinforcement. Turning of tracked vehicles should be kept to a minimum to prevent displacing the fill and damaging or moving the geosynthetic reinforcement. – Rubber-tired equipment may pass over the geosynthetic reinforcement at slow speeds less than 17 km/hr (10 miles/hr). Sudden braking and sharp turning should be avoided. – At any elevations where the facing is “rigid,” such as behind a rigid facing upper wall or the top two to three courses of the lower wall where the segmental facing blocks are interconnected, geosynthetic reinforcement should be wrapped at the wall face. The wrapped face will help reduce sloughing of fill caused by precipitation and the “gaps” that may form because of movement of the wall face. In the upper wall, the wrapped return should be extended at least 0.45 m (18 in.) in the horizontal direction and anchored in at least 0.1 m (4 in.) of fill material. The wrapped return should extend at least 1.5 m (5 ft) in the load bearing wall. The added reinforcement in the load-bearing wall will increase the safety margin of its load-carrying capacity. – It is a good practice to place a compressible layer (e.g., a low- to medium-density expanded polystyrene sheet), of about 50 mm in thickness, between the wrapped face reinforcement and the rigid abutment upper wall. Such a measure can effectively reduce lateral earth pressure and movement of the abutment wall (Monley and Wu, 1993). – A “tail” (a shortened reinforcement sheet with one end sandwiched between facing blocks) extending a minimum of 0.6 m (2 ft) beyond the heel of the sill should be used to “attach” the facing with the reinforced fill (see Figure 3-3). – The wrapped return of geosynthetic reinforcement at the top surface of each tier (top surfaces of the upper and lower walls) should extend to the full length (see Figure 3-3). – For larger reinforcement spacing (e.g., 0.4 m or larger), it is a good practice to incorporate secondary reinforcement, of length about 1 m, between full-length reinforcement.
Backfill	<ul style="list-style-type: none"> – Structure backfill material should consist of material free from organic or other unsuitable material as determined by the engineer.

	<ul style="list-style-type: none"> – Unless otherwise specified, grading of the backfill should be as follows: 100 percent passing 100 mm (4 in.) sieve, 0-60 percent passing No. 40 (0.425 mm) sieve, and 0-15 percent passing No. 200 (0.075mm) sieve; plasticity index (PI) as determined by AASHTO T90, should not exceed 6. – The backfill should exhibit an angle of internal friction of not less than 34 degrees, as determined by the standard direct shear test on the portion finer than 2 mm (No.10) sieve, using a sample compacted to 95 percent of AASHTO T-99, Methods C or D, at optimum moisture content. No testing is required for backfills where 80 percent of sizes are greater than 19 mm. – The backfill should be substantially free of shale or other soft, poor durability particles and should have an organic content not larger than 1 percent. For permanent applications, the backfill should have a pH between 4.5 and 9. The pH limits may be increased to 3 and 11 respectively for temporary applications.
Backfill Placement	<ul style="list-style-type: none"> – Reinforced fill should be placed as specified in construction plans in maximum compacted lift thickness of 250 mm (10 in.). – Reinforced fill should be placed and compacted at or within 2 percent dry of the optimum moisture content. If the reinforced fill is free draining (i.e., with less than 5 percent passing a No. 200 sieve), water content of the fill may be within ± 3 percent of the optimum. – A minimum density of 100 percent of AASHTO T-99 (or 95 percent of AASHTO T-180) is highly recommended for abutments and approaches. A procedural specification is preferable where a significant percentage of coarse material (i.e., greater than 30 percent retained on the 19 mm, or $\frac{3}{4}$ in., sieve) prevents the use of the AASHTO T-99 or T-180 test methods. For procedural specification, typically three to five passes with conventional vibratory roller compaction equipment may be adequate. The actual requirements should be determined based on field trials. – When compacting uniform medium to fine sands (in excess of 60 percent passing a No. 40 sieve), use a smooth-drum static roller or lightweight (walk-behind) vibratory roller. The use of large vibratory compaction equipment with this type of backfill material will make wall alignment control difficult. – Placement of the reinforced fill near the front should not lag behind the remainder of the structure by more than one lift. – Backfill should be placed, spread, and compacted so as to prevent the development of wrinkles or movement of the geosynthetic reinforcement and the wall facing units. – Special attention should be given to ensuring good compaction of the backfill, especially near the face of the wall. – Only hand-operated compaction equipment should be allowed within 0.5 m (1.5 ft) of the front of the wall face. Compaction within 0.5 m (1.5 ft) of the back face of the facing units should be achieved by at least three passes of a lightweight mechanical tamper, plate, or roller. Soil density in this area should not be less than 90 percent standard Proctor density. – Sheepsfoot or grid-type rollers should not be used for compacting backfill within the limits of the soil reinforcement. – Compaction control testing of the reinforced backfill should be performed regularly during the entire construction project. A minimum frequency of one test within the reinforced soil zone per 1.5 m (5 ft) of wall height for every 30 m (100 ft) of wall is recommended. – At the end of each day's operation, the last level of backfill should be sloped away from the wall facing to direct runoff of rainwater away from the wall face. In addition, surface runoff from adjacent areas to enter the wall construction site should be avoided.
Facing	<ul style="list-style-type: none"> – Masonry concrete facing should have a minimum compressive strength of 28 MPa (4,000 psi) and a water absorption limit of 5 percent. – Facing blocks used in freeze-thaw prone areas should be tested for freeze-thaw resistance and survive 300 freeze-thaw cycles without failure per ASTM C666.

	<ul style="list-style-type: none"> – Facing blocks should also meet the requirements of ASTM C90 and C140. All facing units should be sound and free of cracks or other defects that would interfere with the proper placement of the unit or significantly impair the strength or permanence of the construction. – Facing blocks directly exposed to spray from de-iced pavements should be sealed after erection with a water-resistant coating or be manufactured with a coating or additive to increase freeze-thaw resistance. – Facing blocks should be placed and supported as necessary so that their final position is vertical or battered as shown on the plans or the approved working drawings with a tolerance acceptable to the engineer. – It is recommended that the bottom of the top two to three courses of facing blocks be bonded with cement. If lightweight blocks are used, it is recommended that the three to four courses of blocks be filled with concrete mortar and reinforced with steel bars. – The cap block and/or top facing units should be bonded to the units below using cap adhesive that meets the requirements of the facing unit manufacturer. – The overall tolerance relative to the wall design verticality or batter shall not exceed ± 30 mm (1.25 in.) maximum over a 3 m (10 ft) distance; 75 mm (3 in.) maximum.
Drainage	<ul style="list-style-type: none"> – To reduce percolation of surface water into the backfill during the service life of an abutment wall, the crest should be graded to direct runoff away from the back slope. Interceptor drains on the back slope may also be used. Periodic maintenance may be necessary to minimize runoff infiltration. It is highly recommended that a combination of granular drain materials and geotextiles or a geocomposite drain be installed along the back and the base of the fill. – Geotextile reinforcement typically provides inherent drainage function; subsurface drainage at wall face is generally not needed.
Construction Sequence	<ul style="list-style-type: none"> – It is preferable to construct the upper wall and place fill behind the upper wall before placement of the bridge girder. This construction sequence tends to produce more favorable stress conditions in the load-bearing wall, increase load-carrying capacity, and reduce settlement.

Other Flexible Facings

For a flexible facing differing from the segmental concrete block facing, the following construction guidelines about the facing should be observed:

Wrapped-Faced Geotextile Facing

- If the geotextile is wide enough for the required reinforcement length, it can be unrolled parallel to the wall (i.e., in the longitudinal direction). Two rolls of geotextile can be sewn together if a single roll is not wide enough. Alternatively, the geotextile can be deployed perpendicularly to the abutment wall and adjacent sheets can be overlapped or sewn. The stronger direction of a geotextile, usually in the machine direction, should be oriented in the maximum stress direction (i.e., the direction perpendicular to the wall face).
- Compaction shall be done with equipment that will not damage the geotextile facing, and no compaction is allowed within 0.3 to 0.6 m (1 to 2 ft) from the wall face.

- Typical lift thickness ranges from 0.2 to 0.45 m (8 in. to 18 in.). Lift thickness of 0.3 m is most common.
- Reinforcement spacing of 0.15 m is recommended as it is easy to work with and it will help minimize face deformation.
- Face alignment and compaction can be greatly facilitated with the use of temporary forms, such as 50 mm x 200 mm (2 in. x 8 in.) wooden boards.
- When making a windrow, care must be exercised not to dig into the geotextile beneath or at the face of the wall.
- Before applying a coating to a vertical or near-vertical wall, a wire mesh may need to be anchored to the geotextile to keep the coating on the wall face.
- It is usually necessary to have scaffolding in front of the wall when the wall is higher than about 1.8 m (6 ft).

Timber Facing

- The timber typically has a 150 mm x 200 mm (6 in. x 8 in.) or 150 mm x 150 mm (6 in. x 6 in.) cross-sectional dimension and should be treated to an acceptable level with

copper chromate or approved equivalent preservative. The bottom row of timber should be treated for direct burial. The color may be green or brown, but not mixed.

- Forming elements in the back of the timber face may consist of wood (minimum 250 mm nominal thickness treated to an acceptable level with copper chromate or approved equivalent), fiberglass, plastic, or other approved material.
- The typical reinforcement used is a nonwoven geotextile, although other geosynthetics that satisfy the design criteria can also be used.
- Nails should be 16d galvanized ring shank nails and should be placed at the top and bottom of the timbers at 0.3 m (1 ft) intervals.
- Compaction should be consistent with project embankment specifications, except that no compaction is allowed within 0.3 to 0.6 m (1 to 2 ft) of the wall face.
- Shimming of timber to maintain verticality is permissible.
- All reinforcement overlaps should be at least 0.3 m (1 ft) wide and should be perpendicular to the wall face.
- All exposed fabric should be painted with a latex paint matching the color of the timbers.
- To improve connection strength on the top lifts, the geotextile can be wrapped around the facing timbers and then covered or protected with wooden panels. This technique has been described by Keller and Devin (2003).

Natural Rock Facing:

- Do not exceed the height and slope angles delineated in the design without evidence that higher or steeper features will be stable.
- Rocks should be placed by skilled operators and should be placed in fairly uniform lifts.
- Care should be exercised in placing the infill. The infilling should be as complete as possible.

DESIGN EXAMPLES

Two design examples are given here to illustrate the design computation procedure of the recommended design method. Design Example 1 has an integrated sill with a tall upper wall, whereas Design Example 2 has an isolated sill with a short upper wall.

Design Example 1: GRS Abutment with an Integrated Sill and a Tall Upper Wall

Step 1: Establish abutment geometry, external loads and trial design parameters

Wall heights and external loads:

Total abutment height, H'	9.7 m
Load-bearing wall height, H_1	7.5 m

Back wall height, H_2	2.2 m
Traffic surcharge, q	9.4 kN/m ²
Bridge vertical dead load, DL	45 kN/m
Bridge vertical live load, LL	50 kN/m
Bridge horizontal load, F2	2.25 kN/m
Span	24 m (simple span)
Length of concrete approach slab	4.25 m

Trial design parameters:

Sill width, B	1.5 m
Clear distance, d	0.3 m
Sill type	integrated sill
Facing	modular concrete blocks
Facing block size	200 mm x 200 mm x 400 mm
Batter of facing	1/35 (6 mm setback for each block)
Reinforcement spacing	0.2 m

Note: As the batter of 1/35 corresponds to an angle of 1.6°, less than 8°, the abutment wall is to be designed as a vertical wall, and the coefficient of earth pressure is to follow the general Rankine case, per Section 4.2d, NHI manual.

The configuration of trial design for the GRS abutment is shown in Figure 3-4.

Step 2: Establish soil properties

Reinforced fill:

The selected fill satisfies the following criteria: 100 percent passing 100 mm (4 in.) sieve, 0-60 percent passing No. 40 (0.425 mm) sieve, and 0-15 percent passing No. 200 (0.075 mm) sieve; $PI \leq 6$.

The friction angle of the fill = 35°, as determined by one set of the standard direct shear test on the portion finer than 2 mm (No. 10) sieve, using a sample compacted to 95 percent of AASHTO T-99, Methods C or D, at optimum moisture content.

$$\phi_{\text{test}} = 35^\circ, \gamma_{\text{rf}} = 18.8 \text{ kN/m}^3, K_{a(\text{rf})} = \tan^2 (45^\circ - \phi_{\text{rf}}/2) = 0.28$$

Note: The “design friction angle” is taken as one degree lower than ϕ_{test} , i.e., $\phi_{\text{design}} = \phi_{\text{rf}} = 34^\circ$ (see The Recommend Design Method Step 2).

Retained earth:

$$\phi_{\text{re}} = 30^\circ, \gamma_{\text{re}} = 18.8 \text{ kN/m}^3, K_{a(\text{re})} = \tan^2 (45^\circ - \phi_{\text{re}}/2) = 0.33$$

Foundation soil:

$$\phi_{\text{fs}} = 30^\circ, \gamma_{\text{fs}} = 20.0 \text{ kN/m}^3, q_{\text{af}} = 300 \text{ kN/m}^2$$

Step 3: Establish design requirements

External stability design requirements:

- Sliding ≥ 1.5
- Eccentricity $\leq 1/6$
- Sill pressure \leq allowable bearing of the reinforced fill
 $q_{\text{allow}} = 180 \text{ kPa}$ (as determined in Step 4 below)
- Average contact pressure at the foundation level \leq allowable bearing pressure of the foundation soil, $q_{\text{af}} = 300 \text{ kPa}$

Internal stability design requirements:

- Factor of safety against pullout $FS_{\text{pullout}} \geq 1.5$
- Facing connection strength is OK with reinforcement spacing = 0.2 m (see The Recommended Design Method, Step 3).

Step 4: Determine allowable bearing pressure of reinforced fill

Determine the allowable bearing pressure of the reinforced fill, q_{allow} , with the following conditions:

$$\phi_{\text{design}} = \phi_{\text{rf}} = 34^\circ$$

Reinforcement spacing = 0.2 m (uniform spacing with no truncation)

Integrated sill, sill width = 1.5 m

- (1) From Table 3-1, for $\phi = 34^\circ$ and reinforcement spacing = 0.2 m, allowable bearing pressure = 180 kPa.
- (2) From Figure 3-1, the correction factor for a sill width of 1.5 m is 1.0; thus the corrected allowable bearing pressure = 180 kPa \times 1.0 = 180 kPa.
- (3) No reduction for an integrated sill. Thus, $q_{\text{allow}} = 180 \text{ kPa}$.

Step 5: Establish trial reinforcement length

Select a preliminary reinforcement length = 0.7 * total abutment height

$$L = 0.7 \times H' = 0.7 \times 9.7 \text{ m} = 6.8 \text{ m (use 7.0 m)}$$

Step 6: Evaluate stability of footing/sill

The preliminary sill configuration and forces acting on the sill are shown in Figure 3-5. The dimensions of the sill are

B	1.5 m
d	0.3 m
H_2	2.2 m
t	0.65 m
b	0.4 m
fw	0.8 m
fh	0.1 m

With unit weight of concrete, $\gamma_{\text{concrete}} = 23.6 \text{ kN/m}^3$, the following forces acting on the sill are determined:

$$V1 = (B \times t) \cdot \gamma_{\text{concrete}}$$

$$V1 = (1.5 \text{ m} \times 0.65 \text{ m}) \cdot 23.6 \text{ kN/m}^3 = 23.01 \text{ kN/m}$$

$$V2 = [(fw + b) \times fh] \cdot \gamma_{\text{concrete}}$$

$$V2 = [(0.8 \text{ m} + 0.4 \text{ m}) \times 0.1 \text{ m}] \cdot 23.6 \text{ kN/m}^3 = 2.83 \text{ kN/m}$$

$$V3 = [b \times (H_2 - fh - t)] \cdot \gamma_{\text{concrete}}$$

$$V3 = [0.4 \text{ m} \times (2.2 \text{ m} - 0.1 \text{ m} - 0.65 \text{ m})] \cdot 23.6 \text{ kN/m}^3 = 13.69 \text{ kN/m}$$

$$DL = 45 \text{ kN/m (from Step 1)}$$

$$LL = 50 \text{ kN/m (from Step 1)}$$

$$Fq = K_{a(\text{rf})} \cdot q \cdot H_2$$

$$Fq = 0.28 \cdot 9.4 \text{ kN/m}^2 \cdot 2.2 \text{ m} = 5.79 \text{ kN/m}$$

$$F1 = 1/2 \cdot K_{a(\text{rf})} \cdot \gamma_{\text{rf}} \cdot H_2^2$$

$$F1 = 1/2 \cdot (0.28) \cdot 18.8 \text{ kN/m}^3 \cdot (2.2 \text{ m})^2 = 12.74 \text{ kN/m}$$

$$F2 = 2.25 \text{ kN/m (from Step 1)}$$

Check factor of safety against sliding:

ΣVa = sum of vertical forces acting on the sill

$$\Sigma Va = V1 + V2 + V3 + DL + LL$$

$$\Sigma Va = 23.01 \text{ kN/m} + 2.83 \text{ kN/m} + 13.69 \text{ kN/m} + 45 \text{ kN/m} + 50 \text{ kN/m} = 134.53 \text{ kN/m}$$

ΣFa = sum of horizontal forces acting on the sill

$$\Sigma Fa = Fq + F1 + F2$$

$$\Sigma Fa = 5.79 \text{ kN/m} + 12.74 \text{ kN/m} + 2.25 \text{ kN/m} = 20.78 \text{ kN/m}$$

$$FS_{\text{sliding}} = \frac{(\Sigma Va - LL) \tan \phi_{\text{rf}}}{\Sigma Fa}$$

$$FS_{\text{sliding}} = (134.53 \text{ kN/m} - 50 \text{ kN/m}) \cdot \tan 34^\circ / 20.78 \text{ kN/m} = 2.74 > 1.5 \text{ (OK)}$$

Check eccentricity requirement:

ΣM_{OA} = sum of overturning moments about point A

$$\Sigma M_{OA} = Fq \cdot (H_2/2) + F1 \cdot (H_2/3) + F2 \cdot (t + fh)$$

$$\Sigma M_{OA} = 5.79 \text{ kN/m} \cdot (2.2 \text{ m}/2) + 12.74 \text{ kN/m} \cdot (2.2 \text{ m}/3) + 2.25 \text{ kN/m} \cdot (0.65 \text{ m} + 0.1 \text{ m}) = 17.40 \text{ kN/m} \cdot \text{m}$$

ΣM_{RA} = sum of resisting moments about point A

$$\Sigma M_{RA} = V1 \cdot (B/2) + V2 \cdot [(fw + b)/2 + (B - b - fw)] + V3 \cdot [(b/2) + (B - b)] + (DL + LL) \cdot [(fw/2) + (B - b - fw)]$$

$$\begin{aligned}\Sigma M_{RA} &= 23.01 \text{ kN/m} \cdot (1.5 \text{ m}/2) + 2.83 \text{ kN/m} \cdot [(0.8 \text{ m} \\ &+ 0.4 \text{ m})/2 + (1.5 \text{ m} - 0.4 \text{ m} - 0.8 \text{ m})] \\ &+ 13.69 \text{ kN/m} \cdot [(0.4 \text{ m}/2) + (1.5 \text{ m} - 0.4 \text{ m})] \\ &+ (45 \text{ kN/m} + 50 \text{ kN/m}) \cdot [(0.8 \text{ m}/2) + (1.5 \text{ m} \\ &- 0.4 \text{ m} - 0.8 \text{ m})] = 104.10 \text{ kN/m} \cdot \text{m}\end{aligned}$$

e' = eccentricity at the base of the sill

$$e' = \frac{B}{2} - \frac{\Sigma M_{RA} - \Sigma M_{OA}}{\Sigma V_a}$$

$$e' = (1.5 \text{ m}/2) - (104.10 \text{ kN/m} \cdot \text{m} - 17.40 \text{ kN/m} \cdot \text{m})/134.53 \text{ kN/m} = 0.11 \text{ m}$$

$$B/6 = 1.5 \text{ m}/6 = 0.25 \text{ m}$$

$$e' < B/6 \text{ (OK)}$$

Check allowable bearing pressure of the reinforced fill:

p_{sill} = applied pressure from the sill

$$p_{\text{sill}} = \frac{\Sigma V_a}{B - 2e'}$$

$$p_{\text{sill}} = 134.53 \text{ kN/m}/[1.5 \text{ m} - (2 \cdot 0.11 \text{ m})] = 105.1 \text{ kN/m}^2$$

$$p_{\text{sill}} = 105.1 \text{ kPa} < q_{\text{allow}} = 180 \text{ kPa} \text{ (OK)}$$

Step 7: Check external stability of reinforced fill with the preliminary reinforcement length established in Step 5

The forces needed to evaluate the external stability of the abutment are shown in Figure 3-4. These forces are calculated as follows.

$$V_4 = (L \times H_1) \cdot \gamma_{\text{rf}}$$

$$V_4 = (7 \text{ m} \times 7.5 \text{ m}) \cdot 18.8 \text{ kN/m}^3 = 987 \text{ kN/m}$$

$$V_5 = [(L - d - B) \times H_2] \cdot \gamma_{\text{rf}}$$

$$V_5 = [(7 \text{ m} - 0.3 \text{ m} - 1.5 \text{ m}) \times 2.2 \text{ m}] \cdot 18.8 \text{ kN/m}^3 = 215.07 \text{ kN/m}$$

$$V_q = (L - d - B) \cdot q$$

$$V_q = (7 \text{ m} - 0.3 \text{ m} - 1.5 \text{ m}) \cdot 9.4 \text{ kN/m}^2 = 48.88 \text{ kN/m}$$

$$F_3 = [K_{a(\text{re})} \cdot (q + \gamma_{\text{re}} \cdot H_2)] \cdot H_1$$

$$F_3 = [0.33 \cdot (9.4 \text{ kN/m}^2 + 18.8 \text{ kN/m}^3 \cdot 2.2 \text{ m})] \cdot 7.5 \text{ m} = 125.63 \text{ kN/m}$$

$$F_4 = 1/2 \cdot K_{a(\text{re})} \cdot \gamma_{\text{re}} \cdot H_1^2$$

$$F_4 = 1/2 \cdot (0.33) \cdot 18.8 \text{ kN/m}^3 \cdot (7.5 \text{ m})^2 = 174.49 \text{ kN/m}$$

$$\Sigma V_a = 134.53 \text{ kN/m} \text{ (from Step 6)}$$

$$\Sigma F_a = 20.78 \text{ kN/m} \text{ (from Step 6)}$$

I_1 is the influence depth caused by the horizontal forces in the back wall (see Figure 3-6):

$$I_1 = (d + B - 2 \cdot e') \cdot \tan(45^\circ + \phi_{\text{rf}}/2)$$

$$I_1 = [0.3 \text{ m} + 1.5 \text{ m} - 2 \cdot (0.11 \text{ m})] \cdot \tan(45^\circ + 34^\circ/2) = 2.97 \text{ m}$$

Check factor of safety against sliding for the reinforced volume:

ΣV = sum of vertical forces acting on the foundation soil

$$\Sigma V = V_4 + V_5 + V_q + \Sigma V_a$$

$$\Sigma V = 987 \text{ kN/m} + 215.07 \text{ kN/m} + 48.88 \text{ kN/m} + 134.53 \text{ kN/m} = 1385.48 \text{ kN/m}$$

ΣF = sum of horizontal forces acting on the foundation soil

$$\Sigma F = F_3 + F_4 + \Sigma F_a$$

$$\Sigma F = 125.63 \text{ kN/m} + 174.49 \text{ kN/m} + 20.78 \text{ kN/m} = 320.90 \text{ kN/m}$$

$$FS_{\text{sliding}} = \frac{(\Sigma V - LL - V_q) \tan \phi_{\text{fs}}}{\Sigma F}$$

$$FS_{\text{sliding}} = (1385.48 \text{ kN/m} - 50 \text{ kN/m} - 48.88 \text{ kN/m}) \cdot \tan(30^\circ)/320.90 \text{ kN/m} = 2.31 > 1.5 \text{ (OK)}$$

Check eccentricity requirement for the reinforced volume:

ΣM_O = sum of overturning moments about point C

$$\Sigma M_O = F_3 \cdot (H_1/2) + F_4 \cdot (H_1/3) + \Sigma F_a \cdot (H_1 - I_1/3)$$

$$\Sigma M_O = 125.63 \text{ kN/m} \cdot (7.5 \text{ m}/2) + 174.49 \text{ kN/m} \cdot (7.5 \text{ m}/3) + 20.78 \text{ kN/m} \cdot [7.5 \text{ m} - (2.97 \text{ m}/3)] = 1042.62 \text{ kN/m} \cdot \text{m}$$

ΣM_R = sum of resisting moments about point C

$$\Sigma M_R = V_4 \cdot (L/2) + (V_5 + V_q) \cdot [(L - d - B)/2 + (d + B)] + (\Sigma M_{RA} + \Sigma V_a \cdot d)$$

$$\Sigma M_R = 987 \text{ kN/m} \cdot (7 \text{ m}/2) + (215.07 \text{ kN/m} + 48.88 \text{ kN/m}) \cdot [(7 \text{ m} - 0.3 \text{ m} - 1.5 \text{ m})/2 + (0.3 \text{ m} + 1.5 \text{ m})] + [104.10 \text{ kN/m} \cdot \text{m} + 134.53 \text{ kN/m} \cdot (0.3 \text{ m})] = 4760.34 \text{ kN/m} \cdot \text{m}$$

M_S = moment about point C caused by traffic surcharge

$$M_S = V_q \cdot [(L - d - B)/2 + (d + B)]$$

$$M_S = 48.88 \text{ kN/m} \cdot [(7 \text{ m} - 0.3 \text{ m} - 1.5 \text{ m})/2 + (0.3 \text{ m} + 1.5 \text{ m})] = 215.07 \text{ kN/m} \cdot \text{m}$$

e = eccentricity at the base of the reinforced volume

$$e = \frac{L}{2} - \frac{(\Sigma M_R - M_S) - \Sigma M_O}{\Sigma V - V_q}$$

$$e = (7 \text{ m}/2) - [(4760.34 \text{ kN/m} \cdot \text{m} - 215.07 \text{ kN/m} \cdot \text{m}) - 1042.62 \text{ kN/m} \cdot \text{m}]/(1385.48 \text{ kN/m} - 48.88 \text{ kN/m}) = 0.88 \text{ m}$$

$$L/6 = 7 \text{ m}/6 = 1.17 \text{ m}$$

$$e < L/6 \text{ (OK)}$$

Check allowable bearing pressure of the foundation soil:

Calculate the “influence length” D_1 at the foundation level and compare with the effective reinforcement length, L' .

$$\begin{aligned} D_1 &= d + B' + H_1/2 = d + (B - 2e') + H_1/2 \\ D_1 &= 0.3 \text{ m} + [1.5 \text{ m} - 2 \cdot (0.11 \text{ m})] + 7.5 \text{ m}/2 \\ &= 5.33 \text{ m} \end{aligned}$$

$$\begin{aligned} L' &= L - 2e \\ L' &= 7.0 \text{ m} - 2 \cdot (0.88 \text{ m}) = 5.24 \text{ m} \end{aligned}$$

Because D_1 at the foundation level is greater than L' ($L' = L - 2e$), thus the contact pressure on the foundation level, p_{contact} is calculated as follows.

$$\begin{aligned} p_{\text{contact}} &= \frac{\Sigma V}{L - 2e} \\ p_{\text{contact}} &= 1385.48 \text{ kN/m} / [7.0 \text{ m} - 2 \cdot (0.88 \text{ m})] \\ &= 264.40 \text{ kN/m}^2 \\ q_{\text{af}} &= 300 \text{ kN/m}^2 \text{ (from Step 2)} \\ p_{\text{contact}} &= 264.40 \text{ kN/m}^2 < q_{\text{af}} = 300 \text{ kN/m}^2 \text{ (OK)} \end{aligned}$$

Step 8: Evaluate internal stability at each reinforcement level

With geosynthetic reinforcement, the coefficient of lateral earth pressure is constant throughout the entire wall height, per Section 4.3b, NHI manual.

The internal stability is evaluated by checking the reinforcement pullout failure.

Check reinforcement pullout failure:

$$\begin{aligned} Pr &= \text{pullout resistance} \\ Pr &= F^* \cdot \alpha \cdot (\sigma_v \cdot Le) \cdot C \cdot Rc \end{aligned}$$

$$\begin{aligned} F^* &= \text{pullout resistance factor} \\ F^* &= 2/3 \cdot \tan \phi_{\text{rf}} \\ F^* &= 2/3 \cdot \tan(34^\circ) = 0.45 \end{aligned}$$

α = a scale effect correction factor ranging from 0.6 to 1.0 for geosynthetic reinforcement; for geotextile, α is defaulted to 0.6, per Section 3.3b, NHI manual.

$(\sigma_v \cdot Le)$ = normal force at the soil-reinforcement interface at depth z (excluding traffic surcharge)

$$(\sigma_v \cdot Le) = (\sigma_{\text{vs}} \cdot Le) + (\Delta\sigma_v \cdot Li)$$

Le = length of embedment in the resistant zone behind the failure surface at depth z

$$Le = L - La$$

La = length of embedment in the active zone at depth z
 $La = (H_1 - z) \tan(45^\circ - \phi_{\text{rf}}/2)$

Li = length of embedment within the influence area inside the resistant zone; this length can be measured directly from the design drawing.

C = reinforcement effective unit perimeter; $C = 2$ for strips, grids, and sheets.

Rc = coverage ratio; $Rc = 1.0$ for 100 percent coverage of reinforcement.

σ_h = horizontal pressure at depth z
 $\sigma_h = K_{\text{a(rf)}} \cdot (\sigma_{\text{vs}} + \Delta\sigma_v + q) + \Delta\sigma_h$

σ_{vs} = vertical soil pressure at depth z
 $\sigma_{\text{vs}} = (\gamma_{\text{rf}} \cdot H_2) + (\gamma_{\text{rf}} \cdot z)$

$\Delta\sigma_v$ = distributed vertical pressure from sill
 $\Delta\sigma_v = \Sigma Va / D$

D = effective width of applied load at depth z

For $z \leq z_2$: $D = (B - 2e') + z$

For $z > z_2$: $D = d + (B - 2e') + z/2$

$$z_2 = 2 \cdot d$$

$\Delta\sigma_h$ = supplement horizontal pressure at depth z
 For $z \leq I_1$: $\Delta\sigma_h = 2 \cdot \Sigma Fa \cdot (I_1 - z)/(I_1^2)$
 For $z > I_1$: $\Delta\sigma_h = 0$

T_{max} = maximum tensile force in the reinforcement at depth z

$$T_{\text{max}} = \sigma_h \cdot s$$

s = vertical reinforcement spacing

FS_{pullout} = factor of safety against reinforcement pullout
 $FS_{\text{pullout}} = Pr / T_{\text{max}}$

Let depth z be measured from the top of the load-bearing wall. Reinforcement no. 25 at $z = 2.5 \text{ m}$ (see Figure 3-6) would serve as an example for determining the FS_{pullout} .

$$\begin{aligned} \sigma_{\text{vs}} &= (\gamma_{\text{rf}} \cdot H_2) + (\gamma_{\text{rf}} \cdot z) \\ \sigma_{\text{vs}} &= (18.8 \text{ kN/m}^3 \cdot 2.2 \text{ m}) + (18.8 \text{ kN/m}^3 \cdot 2.5 \text{ m}) \\ &= 88.36 \text{ kN/m}^2 \end{aligned}$$

$$z_2 = 2 \cdot d = 2 \cdot (0.3 \text{ m}) = 0.6 \text{ m}$$

$$\begin{aligned} \because z = 2.5 \text{ m} > z_2 = 0.6 \text{ m}, \therefore D = d + (B - 2e') + z/2 \\ D = 0.3 \text{ m} + [1.5 \text{ m} - 2 \cdot (0.11 \text{ m})] + 2.5 \text{ m}/2 \\ = 2.83 \text{ m} \end{aligned}$$

$$\begin{aligned} \Delta\sigma_v &= \Sigma Va / D \\ \Delta\sigma_v &= 134.53 \text{ kN/m} / 2.83 \text{ m} = 47.54 \text{ kN/m}^2 \end{aligned}$$

$$\begin{aligned} \because z = 2.5 \text{ m} < I_1 = 2.97 \text{ m}, \therefore \Delta\sigma_h = 2 \cdot \Sigma Fa \cdot (I_1 - z) / (I_1^2) \\ \Delta\sigma_h = 2 \cdot (20.78 \text{ kN/m}) \cdot (2.97 \text{ m} - 2.5 \text{ m}) / (2.97 \text{ m})^2 \\ = 2.21 \text{ kN/m}^2 \end{aligned}$$

$$\begin{aligned} \sigma_h &= K_{a(\text{rf})} \cdot (\sigma_{vs} + \Delta\sigma_v + q) + \Delta\sigma_h \\ \sigma_h &= 0.28 \cdot (88.36 \text{ kN/m}^2 + 47.54 \text{ kN/m}^2 + 9.4 \text{ kN/m}^2) \\ &\quad + 2.21 \text{ kN/m}^2 = 42.89 \text{ kN/m}^2 \end{aligned}$$

$$\begin{aligned} T_{\text{max}} &= \sigma_h \cdot s \\ T_{\text{max}} &= 42.89 \text{ kN/m}^2 \cdot (0.2 \text{ m}) = 8.58 \text{ kN/m} \end{aligned}$$

$$\begin{aligned} La &= (H_1 - z) \tan(45^\circ - \phi_{\text{rf}}/2) \\ La &= (7.5 \text{ m} - 2.5 \text{ m}) \tan(45^\circ - 34^\circ/2) = 2.66 \text{ m} \end{aligned}$$

$$\begin{aligned} Le &= L - La \\ Le &= 7 \text{ m} - 2.66 \text{ m} = 4.34 \text{ m} \end{aligned}$$

Calculate the normal force at $z = 2.5 \text{ m}$:

$$\begin{aligned} (\sigma_v \cdot Le) &= (\sigma_{vs} \cdot Le) + (\Delta\sigma_v \cdot Li) \\ (\sigma_v \cdot Le) &= (88.36 \text{ kN/m}^2 \cdot 4.34 \text{ m}) + (47.54 \text{ kN/m}^2 \\ &\quad \cdot 0.17 \text{ m}) = 391.56 \text{ kN/m} \end{aligned}$$

$$\begin{aligned} Pr &= F^* \cdot \alpha \cdot (\sigma_v \cdot Le) \cdot C \cdot Rc \\ Pr &= (0.45) \cdot (0.6) \cdot 391.56 \text{ kN/m} \cdot (2) \cdot (1) \\ &= 211.44 \text{ kN/m} \end{aligned}$$

$$\begin{aligned} FS_{\text{pullout}} &= Pr / T_{\text{max}} \\ FS_{\text{pullout}} &= 211.44 \text{ kN/m} / 8.58 \text{ kN/m} = 24.64 \end{aligned}$$

$$FS_{\text{pullout}} = 24.64 > 1.5 \text{ (OK)}$$

The values of FS_{pullout} for all the reinforcements in the load-bearing wall are summarized in Table 3-2.

Step 9: Determine the required reinforcement stiffness and strength

The minimum “working” reinforcement stiffness is determined as

$$T_{@ \epsilon=1.0 \text{ percent}} \geq \sigma_{h(\text{max})} \cdot s$$

The minimum ultimate reinforcement strength is determined as

$$T_{\text{ult}} \geq Fs \cdot T_{@ \epsilon=1.0 \text{ percent}}$$

The recommended combined safety factor is $Fs = 5.5$ for reinforcement $\leq 0.2 \text{ m}$ and $Fs = 3.5$ for reinforcement spacing of 0.4 m .

From Table 3-2, $\sigma_{h(\text{max})}$ is 59.84 kN/m^2 , which occurs at reinforcement No. 1 with depth $z = 7.3 \text{ m}$ and $s = 0.2 \text{ m}$.

$$\begin{aligned} T_{@ \epsilon=1.0 \text{ percent}} &= \sigma_{h(\text{max})} \cdot s \\ T_{@ \epsilon=1.0 \text{ percent}} &= 59.84 \text{ kN/m}^2 \cdot (0.2 \text{ m}) = 11.97 \text{ kN/m} \end{aligned}$$

The uniform reinforcement spacing is 0.2 m , hence $Fs = 5.5$.

$$\begin{aligned} T_{\text{ult}} &= Fs \cdot T_{@ \epsilon=1.0 \text{ percent}} \\ T_{\text{ult}} &= 5.5 \cdot (11.97 \text{ kN/m}) = 65.84 \text{ kN/m} \end{aligned}$$

A reinforcement with minimum “working” stiffness, $T_{@ \epsilon=1.0 \text{ percent}} = 12.0 \text{ kN/m}$ and minimum ultimate strength (per ASTM D4595), $T_{\text{ult}} = 65.8 \text{ kN/m}$ is required.

Step 10: Design of back/upper wall

Reinforced fill:	Same as that of the load-bearing wall
Reinforcement:	Same as that of the load-bearing wall
Reinforcement length:	4.25 m (length of approach slab) + 1.5 m = 5.75 m (see The Recommended Design Method Step 10)
Reinforcement layout:	Vertical spacing = 0.3 m Wrapped-face with wrapped return at least 0.5 m (18 in.) in the horizontal direction and anchored in at least 100 mm of fill material.

A compressible layer of about 50 mm thick should be installed between the wrapped face and the rigid back wall.

Step 11: Check angular distortion between abutments

$$\begin{aligned} \delta_{\text{abutment}} &= \text{abutment settlement} \\ \delta_{\text{abutment}} &= 1.5 \text{ percent} \cdot H_1 \\ \delta_{\text{abutment}} &= 0.015 \cdot (7.5 \text{ m}) = 0.1125 \text{ m} \end{aligned}$$

$$\begin{aligned} \delta_{\text{foundation}} &= \text{foundation settlement (as determined by conventional settlement computation methods)} \\ Eg\delta_{\text{foundation}} &= 0.01 \text{ m} \end{aligned}$$

$$\begin{aligned} \delta_{\text{total}} &= \text{total settlement} \\ \delta_{\text{total}} &= \delta_{\text{abutment}} + \delta_{\text{foundation}} \\ \delta_{\text{total}} &= 0.1125 \text{ m} + 0.01 \text{ m} = 0.1225 \text{ m} \end{aligned}$$

TABLE 3-2 Design Example 1—tabulated results of $FS_{pullout}$ at each reinforcement level

No.	Depth z (m)	s (m)	σ_{vs} (kN/m ²)	D (m)	$\Delta\sigma_v$ (kN/m ²)	$\Delta\sigma_h$ (kN/m ²)	σ_h (kN/m ²)	T_{max} (kN/m)	La (m)	Le (m)	Li (m)	$(\sigma_v \cdot Le)$ (kN/m)	Pr (kN/m)	$FS_{pullout}$
1	7.3	0.2	178.6	5.23	25.72	0.00	59.84	11.97	0.11	6.89	5.12	1363.00	735.49	61.45
2	7.1	0.2	174.84	5.13	26.22	0.00	58.93	11.79	0.21	6.79	4.92	1315.65	709.93	60.24
3	6.9	0.2	171.08	5.03	26.75	0.00	58.02	11.60	0.32	6.68	4.71	1268.98	684.75	59.01
4	6.7	0.2	167.32	4.93	27.29	0.00	57.12	11.42	0.43	6.57	4.50	1222.99	659.93	57.76
5	6.5	0.2	163.56	4.83	27.85	0.00	56.23	11.25	0.53	6.47	4.30	1177.67	635.48	56.51
6	6.3	0.2	159.8	4.73	28.44	0.00	55.34	11.07	0.64	6.36	4.09	1133.02	611.39	55.24
7	6.1	0.2	156.04	4.63	29.06	0.00	54.46	10.89	0.74	6.26	3.89	1089.03	587.65	53.95
8	5.9	0.2	152.28	4.53	29.70	0.00	53.59	10.72	0.85	6.15	3.68	1045.68	564.25	52.65
9	5.7	0.2	148.52	4.43	30.37	0.00	52.72	10.54	0.96	6.04	3.47	1002.96	541.20	51.33
10	5.5	0.2	144.76	4.33	31.07	0.00	51.86	10.37	1.06	5.94	3.27	960.87	518.49	49.99
11	5.3	0.2	141	4.23	31.80	0.00	51.02	10.20	1.17	5.83	3.06	919.39	496.11	48.62
12	5.1	0.2	137.24	4.13	32.57	0.00	50.18	10.04	1.28	5.72	2.85	878.51	474.05	47.24
13	4.9	0.2	133.48	4.03	33.38	0.00	49.35	9.87	1.38	5.62	2.65	838.21	452.31	45.82
14	4.7	0.2	129.72	3.93	34.23	0.00	48.54	9.71	1.49	5.51	2.44	798.48	430.87	44.38
15	4.5	0.2	125.96	3.83	35.13	0.00	47.74	9.55	1.60	5.40	2.23	759.30	409.72	42.92
16	4.3	0.2	122.2	3.73	36.07	0.00	46.95	9.39	1.70	5.30	2.03	720.64	388.86	41.42
17	4.1	0.2	118.44	3.63	37.06	0.00	46.17	9.23	1.81	5.19	1.82	682.49	368.28	39.88
18	3.9	0.2	114.68	3.53	38.11	0.00	45.41	9.08	1.91	5.09	1.62	644.82	347.95	38.31
19	3.7	0.2	110.92	3.43	39.22	0.00	44.67	8.93	2.02	4.98	1.41	607.61	327.87	36.70
20	3.5	0.2	107.16	3.33	40.40	0.00	43.95	8.79	2.13	4.87	1.20	570.82	308.02	35.04
21	3.3	0.2	103.4	3.23	41.65	0.00	43.25	8.65	2.23	4.77	1.00	534.41	288.37	33.34
22	3.1	0.2	99.64	3.13	42.98	0.00	42.57	8.51	2.34	4.66	0.79	498.35	268.91	31.59
23	2.9	0.2	95.88	3.03	44.40	0.34	42.25	8.45	2.45	4.55	0.58	462.58	249.61	29.54
24	2.7	0.2	92.12	2.93	45.91	1.28	42.56	8.51	2.55	4.45	0.38	427.08	230.45	27.07
25	2.5	0.2	88.36	2.83	47.54	2.22	42.90	8.58	2.66	4.34	0.17	391.76	211.40	24.64
26	2.3	0.2	84.6	2.73	49.28	3.16	43.28	8.66	2.76	4.24	0.00	358.29	193.34	22.34
27	2.1	0.2	80.84	2.63	51.15	4.10	43.69	8.74	2.87	4.13	0.00	333.77	180.10	20.61
28	1.9	0.2	77.08	2.53	53.17	5.04	44.15	8.83	2.98	4.02	0.00	310.05	167.30	18.95
29	1.7	0.2	73.32	2.43	55.36	5.98	44.65	8.93	3.08	3.92	0.00	287.13	154.94	17.35
30	1.5	0.2	69.56	2.33	57.74	6.93	45.20	9.04	3.19	3.81	0.00	265.01	143.00	15.82
31	1.3	0.2	65.8	2.23	60.33	7.87	45.81	9.16	3.30	3.70	0.00	243.68	131.49	14.35
32	1.1	0.2	62.04	2.13	63.16	8.81	46.50	9.30	3.40	3.60	0.00	223.16	120.42	12.95
33	0.9	0.2	58.28	2.03	66.27	9.75	47.26	9.45	3.51	3.49	0.00	203.44	109.78	11.62
34	0.7	0.2	54.52	1.93	69.70	10.69	48.11	9.62	3.62	3.38	0.00	184.52	99.57	10.35
35	0.5	0.2	50.76	1.78	75.58	11.63	49.64	9.93	3.72	3.28	0.00	166.39	89.79	9.04
36	0.3	0.2	47	1.58	85.15	12.57	52.21	10.44	3.83	3.17	0.00	149.07	80.44	7.70
37	0.1	0.2	43.24	1.38	97.49	13.51	55.55	11.11	3.93	3.07	0.00	132.55	71.52	6.44

Angular distortion = $\delta_{total} / \text{span length} = 0.1225 \text{ m} / 24 \text{ m} = 0.0051$

Tolerable angular distortion for simple span = 0.005

Angular distortion = 0.0051 \approx 0.005 (OK)

Design summary:

The configuration for the trial design is shown in Figure 3-7.

Abutment configuration:

Load-bearing wall height, H_1 7.5 m

Back wall height, H_2 2.2 m
Facing modular concrete blocks (200 mm x 200 mm x 400 mm)
Front batter 1/35
Sill type integrated sill
Sill width 1.5 m
Sill clear distance 0.3 m
Embedment 200 mm (one facing block height)

Reinforcement:

Minimum stiffness at $\epsilon=1.0$ percent, $T_{@ \epsilon=1.0 \text{ percent}} = 12.0 \text{ kN/m}$
Minimum ultimate strength, $T_{ult} = 65.8 \text{ kN/m}$
Length in load-bearing wall = 7.0 m

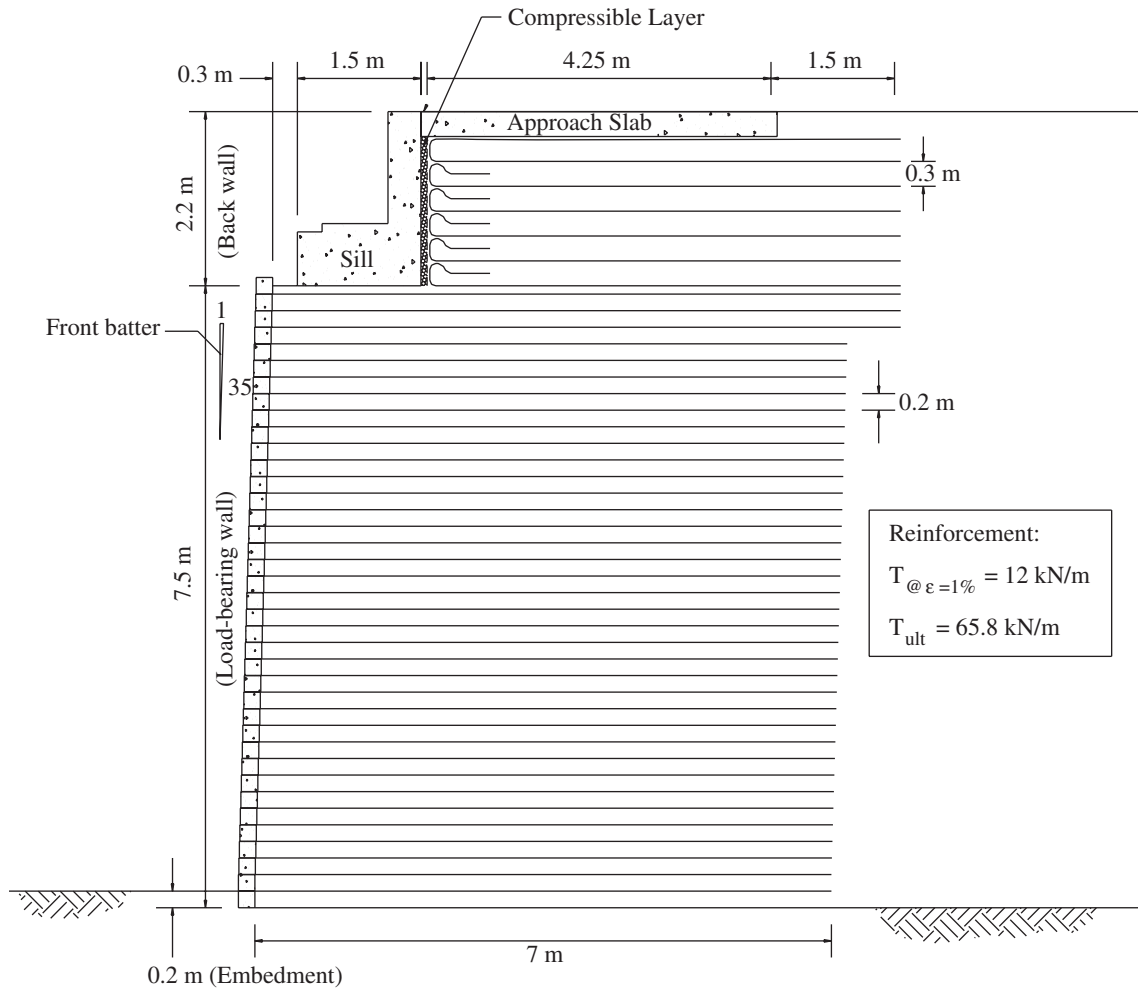


Figure 3-7. Design Example 1—configuration of the trial design.

Length of top three layers in load-bearing wall = 7.5 m
 Vertical spacing in load-bearing wall = 0.2 m
 Length in back wall = 5.75 m
 Vertical spacing in back wall = 0.3 m

Span length 10 m (simple span)
 Approach slab is not used

Trial design parameters:

Sill width, B	0.6 m
Clear distance, d	0.3 m
Sill type	isolated sill
Facing	modular concrete blocks
Facing block size	200 mm x 200 mm x 400 mm
Batter of facing	1/35 (6 mm setback for each block)
Reinforcement spacing	0.2 m

Design Example 2: A GRS Abutment with an Isolated Sill and a Short Lower Wall

Step 1: Establish abutment geometry, external loads and trial design parameters

Wall heights and external loads:

Total abutment height, H'	3.0 m
Load-bearing wall height, H_1	2.4 m
Back wall height, H_2	0.6 m
Traffic surcharge, q	9.4 kN/m ²
Bridge vertical dead load, DL	35 kN/m
Bridge vertical live load, LL	40 kN/m
Bridge horizontal load, F2	1.75 kN/m

Note: As the batter of 1/35 corresponds to an angle of 1.6°, less than 8°, the abutment wall is to be designed as a vertical wall, and the coefficient of earth pressure is to follow the general Rankine case.

The configuration of the initial trial design for the GRS abutment is shown in Figure 3-8.

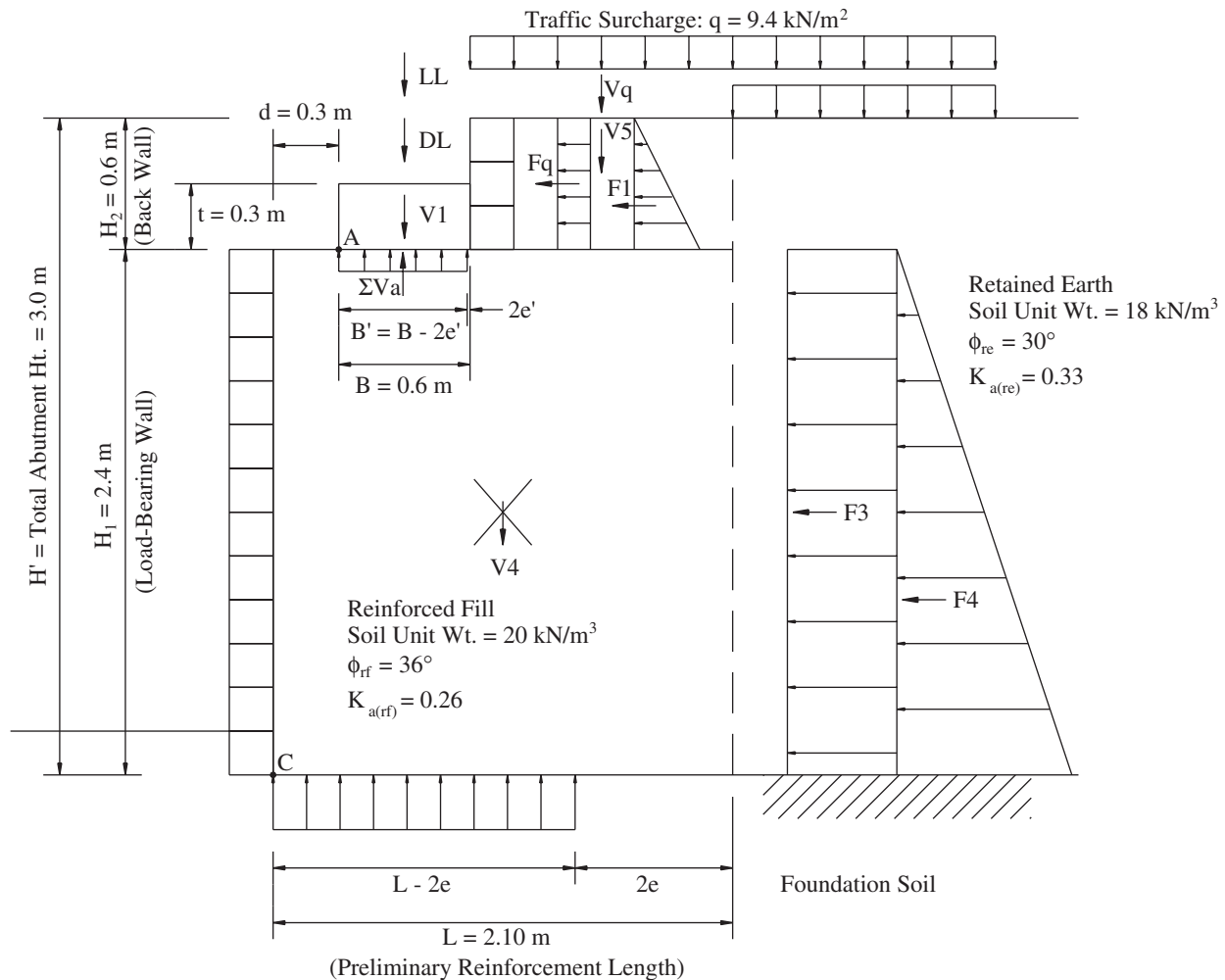


Figure 3-8. Design Example 2—configuration of the abutment.

Step 2: Establish soil properties

Reinforced fill:

The selected fill satisfies the following criteria: 100 percent passing 100 mm (4 in.) sieve, 0-60 percent passing No. 40 (0.425 mm) sieve, and 0-15 percent passing No. 200 (0.075 mm) sieve; $PI \leq 6$.

The friction angle of the fill = 37° , as determined by one set of the standard direct shear test on the portion finer than 2 mm (No. 10) sieve, using a sample compacted to 95 percent of AASHTO T-99, Methods C or D, at optimum moisture content.

$$\phi_{\text{test}} = 37^\circ, \gamma_{\text{rf}} = 20 \text{ kN/m}^3, K_{a(\text{rf})} = \tan^2 (45^\circ - \phi_{\text{rf}}/2) = 0.26$$

Note: The “design friction angle” is taken as one degree lower than ϕ_{tests} , i.e., $\phi_{\text{design}} = \phi_{\text{rf}} = 36^\circ$ (see The Recommended Design Method Step 2).

Retained earth:

$$\phi_{\text{re}} = 30^\circ, \gamma_{\text{re}} = 18 \text{ kN/m}^3, K_{a(\text{re})} = \tan^2 (45^\circ - \phi_{\text{re}}/2) = 0.33$$

Foundation soil:

$$\phi_{\text{fs}} = 30^\circ, \gamma_{\text{fs}} = 20.0 \text{ kN/m}^3, q_{\text{af}} = 300 \text{ kN/m}^2$$

Step 3: Establish design requirements

External stability design requirements:

- Sliding ≥ 1.5
- Eccentricity $\leq 1/6$
- Sill pressure \leq allowable bearing of the reinforced fill $q_{\text{allow}} = 345 \text{ kPa}$ (as determined in Step 4 below)
- Average contact pressure at the foundation level \leq allowable bearing pressure of the foundation soil, $q_{\text{af}} = 300 \text{ kPa}$

Internal stability design requirements:

- Factor of safety against pullout $FS_{\text{pullout}} \geq 1.5$
- Facing connection strength is OK with reinforcement spacing = 0.2 m (see The Recommended Design Method Step 3)

Step 4: Determine allowable bearing pressure of reinforced fill

Determine the allowable bearing pressure of the reinforced fill q_{allow} with the following conditions:

$$\phi_{\text{design}} = \phi_{\text{rf}} = 36^\circ$$

Reinforcement spacing = 0.2 m (uniform spacing with no truncation)

Isolated sill, sill width = 0.6 m

- (1) From Table 3-1, for $\phi = 36^\circ$ and reinforcement spacing = 0.2 m, allowable bearing pressure = 200 kPa.
- (2) From Figure 3-1, the correction factor for a sill width of 0.6 m is 2.3; thus the corrected allowable bearing pressure = 200 kPa \times 2.3 = 460 kPa.
- (3) Reduction factor of 0.75 applies for an isolated sill. Thus, $q_{\text{allow}} = 0.75 \times 460 \text{ kPa} = 345 \text{ kPa}$.

Step 5: Establish trial reinforcement length

Select a preliminary reinforcement length = 0.7 * total abutment height

$$L = 0.7 \times H' = 0.7 \times 3.0 \text{ m} = 2.1 \text{ m}$$

Step 6: Evaluate stability of footing/sill

The preliminary sill configuration and forces acting on the sill are shown in Figure 3-8. The dimensions of the sill are

B	0.6 m
d	0.3 m
H_2	0.6 m
t	0.3 m

With unit weight of concrete, $\gamma_{\text{concrete}} = 23.6 \text{ kN/m}^3$, the following forces acting on the sill are determined:

$$V1 = (B \times t) \cdot \gamma_{\text{concrete}}$$

$$V1 = (0.6 \text{ m} \times 0.3 \text{ m}) \cdot 23.6 \text{ kN/m}^3 = 4.25 \text{ kN/m}$$

$$DL = 35 \text{ kN/m (from Step 1)}$$

$$LL = 40 \text{ kN/m (from Step 1)}$$

F_q and $F1$ are included in this design example conservatively.

$$F_q = K_{a(\text{rf})} \cdot q \cdot H_2$$

$$F_q = 0.26 \cdot 9.4 \text{ kN/m}^2 \cdot 0.6 \text{ m} = 1.47 \text{ kN/m}$$

$$F1 = 1/2 \cdot K_{a(\text{rf})} \cdot \gamma_{\text{rf}} \cdot H_2^2$$

$$F1 = 1/2 \cdot (0.26) \cdot 20 \text{ kN/m}^3 \cdot (0.6 \text{ m})^2 = 0.94 \text{ kN/m}$$

$$F2 = 1.75 \text{ kN/m (from Step 1)}$$

Check factor of safety against sliding:

ΣV_a = sum of vertical forces acting on the sill

$$\Sigma V_a = V1 + DL + LL$$

$$\Sigma V_a = 4.25 \text{ kN/m} + 35 \text{ kN/m} + 40 \text{ kN/m} = 79.25 \text{ kN/m}$$

ΣF_a = sum of horizontal forces acting on the sill

$$\Sigma F_a = F_q + F1 + F2$$

$$\Sigma F_a = 1.47 \text{ kN/m} + 0.94 \text{ kN/m} + 1.75 \text{ kN/m} = 4.16 \text{ kN/m}$$

$$FS_{\text{sliding}} = \frac{(\Sigma V_a - LL) \tan \phi_{\text{rf}}}{\Sigma F_a}$$

$$FS_{\text{sliding}} = (79.25 \text{ kN/m} - 40 \text{ kN/m}) \cdot \tan 36^\circ / 4.16 \text{ kN/m} = 6.85 > 1.5 \text{ (OK)}$$

Check eccentricity requirement:

ΣM_{O_A} = sum of overturning moments about point A

$$\Sigma M_{O_A} = F_q \cdot (H_2/2) + F1 \cdot (H_2/3) + F2 \cdot (t)$$

$$\Sigma M_{O_A} = 1.47 \text{ kN/m} \cdot (0.6 \text{ m}/2) + 0.94 \text{ kN/m} \cdot (0.6 \text{ m}/3) + 1.75 \text{ kN/m} \cdot (0.3 \text{ m}) = 1.15 \text{ kN/m} \cdot \text{m}$$

ΣM_{R_A} = sum of resisting moments about point A

$$\Sigma M_{R_A} = V1 \cdot (B/2) + (DL + LL) \cdot (B/2)$$

$$\Sigma M_{R_A} = 4.25 \text{ kN/m} \cdot (0.6 \text{ m}/2) + (35 \text{ kN/m} + 40 \text{ kN/m}) \cdot (0.6 \text{ m}/2) = 23.78 \text{ kN/m} \cdot \text{m}$$

e' = eccentricity at the base of the sill

$$e' = \frac{B}{2} - \frac{\Sigma M_{R_A} - \Sigma M_{O_A}}{\Sigma V_a}$$

$$e' = (0.6 \text{ m}/2) - (23.78 \text{ kN/m} \cdot \text{m} - 1.15 \text{ kN/m} \cdot \text{m}) / 79.25 \text{ kN/m} = 0.01 \text{ m}$$

$$B/6 = 0.6 \text{ m}/6 = 0.10 \text{ m}$$

$$e' < B/6 \text{ (OK)}$$

Check allowable bearing pressure of the reinforced fill:

p_{sill} = applied pressure from the sill

$$p_{\text{sill}} = \frac{\Sigma V_a}{B - 2e'}$$

$$p_{sill} = 79.25 \text{ kN/m} / [0.6 \text{ m} - (2 \cdot 0.01 \text{ m})] = 136.64 \text{ kN/m}^2$$

$$p_{sill} = 136.64 \text{ kPa} < q_{allow} = 345 \text{ kPa (OK)}$$

Step 7: Check external stability of reinforced fill with the preliminary reinforcement length established in Step 5

The forces needed to evaluate the external stability of the abutment are shown in Figure 3-8. These forces are calculated as follows:

$$V4 = (L \times H_1) \cdot \gamma_{rf}$$

$$V4 = (2.1 \text{ m} \times 2.4 \text{ m}) \cdot 20 \text{ kN/m}^3 = 100.8 \text{ kN/m}$$

$$V5 = [(L - d - B) \times H_2] \cdot \gamma_{rf}$$

$$V5 = [(2.1 \text{ m} - 0.3 \text{ m} - 0.6 \text{ m}) \times 0.6 \text{ m}] \cdot 20 \text{ kN/m}^3 = 14.4 \text{ kN/m}$$

$$Vq = (L - d - B) \cdot q$$

$$Vq = (2.1 \text{ m} - 0.3 \text{ m} - 0.6 \text{ m}) \cdot 9.4 \text{ kN/m}^2 = 11.28 \text{ kN/m}$$

$$F3 = [K_{a(re)} \cdot (q + \gamma_{re} \cdot H_2)] \cdot H_1$$

$$F3 = [0.33 \cdot (9.4 \text{ kN/m}^2 + 18 \text{ kN/m}^3 \cdot 0.6 \text{ m})] \cdot 2.4 \text{ m} = 16.0 \text{ kN/m}$$

$$F4 = 1/2 \cdot K_{a(re)} \cdot \gamma_{re} \cdot H_1^2$$

$$F4 = 1/2 \cdot (0.33) \cdot 18 \text{ kN/m}^3 \cdot (2.4 \text{ m})^2 = 17.11 \text{ kN/m}$$

$$\Sigma Va = 79.25 \text{ kN/m (from Step 6)}$$

$$\Sigma Fa = 4.16 \text{ kN/m (from Step 6)}$$

I_1 is the influence depth caused by the horizontal forces in the back wall (see Figure 3-9):

$$I_1 = (d + B - 2 \cdot e') \cdot \tan(45^\circ + \phi_{rf}/2)$$

$$I_1 = [0.3 \text{ m} + 0.6 \text{ m} - 2 \cdot (0.01 \text{ m})] \cdot \tan(45^\circ + 36^\circ/2) = 1.73 \text{ m}$$

Check factor of safety against sliding for the reinforced volume:

ΣV = sum of vertical forces acting on the foundation soil

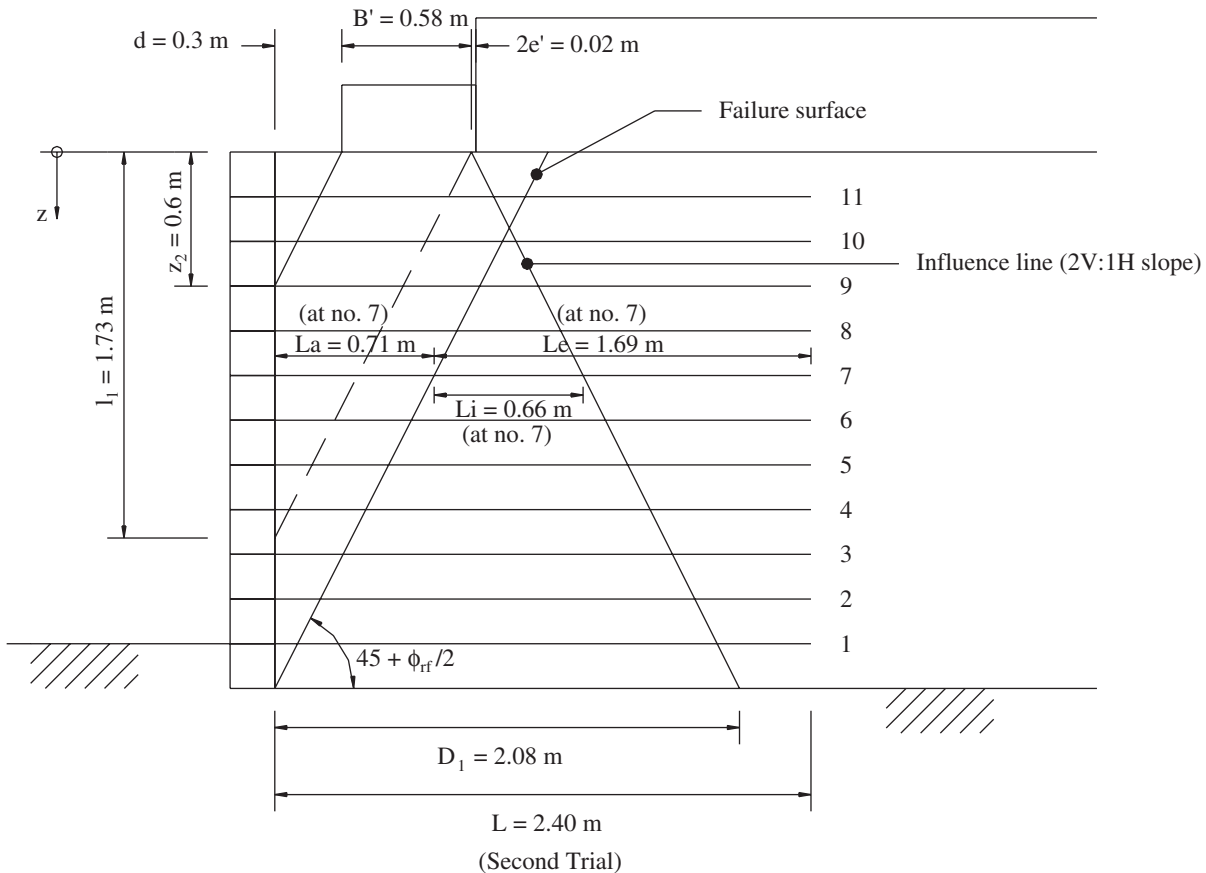


Figure 3-9. Design Example 2 - Notations of the quantities for internal stability evaluation.

$$\begin{aligned}\Sigma V &= V_4 + V_5 + V_q + \Sigma V_a \\ \Sigma V &= 100.8 \text{ kN/m} + 14.4 \text{ kN/m} + 11.28 \text{ kN/m} \\ &\quad + 79.25 \text{ kN/m} = 205.73 \text{ kN/m}\end{aligned}$$

ΣF = sum of horizontal forces acting on the foundation soil

$$\begin{aligned}\Sigma F &= F_3 + F_4 + \Sigma F_a \\ \Sigma F &= 16.0 \text{ kN/m} + 17.11 \text{ kN/m} + 4.16 \text{ kN/m} \\ &= 37.27 \text{ kN/m}\end{aligned}$$

$$FS_{\text{sliding}} = \frac{(\Sigma V - LL - V_q) \tan \phi_s}{\Sigma F}$$

$$FS_{\text{sliding}} = (205.73 \text{ kN/m} - 40 \text{ kN/m} - 11.28 \text{ kN/m}) \cdot \tan(30^\circ) / 37.27 \text{ kN/m} = 2.39 > 1.5 \text{ (OK)}$$

Check eccentricity requirement for the reinforced volume:

$$\begin{aligned}\Sigma M_O &= \text{sum of overturning moments about point C} \\ \Sigma M_O &= F_3 \cdot (H_1/2) + F_4 \cdot (H_1/3) + \Sigma F_a \cdot (H_1 - I_1/3) \\ \Sigma M_O &= 16.0 \text{ kN/m} \cdot (2.4 \text{ m}/2) + 17.11 \text{ kN/m} \cdot (2.4 \text{ m}/3) \\ &\quad + 4.16 \text{ kN/m} \cdot [2.4 \text{ m} - (1.73 \text{ m}/3)] \\ &= 40.47 \text{ kN/m} \cdot \text{m}\end{aligned}$$

$$\begin{aligned}\Sigma M_R &= \text{sum of resisting moments about point C} \\ \Sigma M_R &= V_4 \cdot (L/2) + (V_5 + V_q) \cdot [(L - d - B)/2 \\ &\quad + (d + B)] + (\Sigma M_{RA} + \Sigma V_a \cdot d) \\ \Sigma M_R &= 100.8 \text{ kN/m} \cdot (2.1 \text{ m}/2) + (14.4 \text{ kN/m} \\ &\quad + 11.28 \text{ kN/m}) \cdot [(2.1 \text{ m} - 0.3 \text{ m} - 0.6 \text{ m})/2 \\ &\quad + (0.3 \text{ m} + 0.6 \text{ m})] + [23.78 \text{ kN/m} \cdot \text{m} \\ &\quad + 79.25 \text{ kN/m} \cdot (0.3 \text{ m})] = 191.92 \text{ kN/m} \cdot \text{m}\end{aligned}$$

$$\begin{aligned}M_S &= \text{moment about point C caused by traffic surcharge} \\ M_S &= V_q \cdot [(L - d - B)/2 + (d + B)] \\ M_S &= 11.28 \text{ kN/m} \cdot [(2.1 \text{ m} - 0.3 \text{ m} - 0.6 \text{ m})/2 \\ &\quad + (0.3 \text{ m} + 0.6 \text{ m})] = 16.92 \text{ kN/m} \cdot \text{m}\end{aligned}$$

e = eccentricity at the base of the reinforced volume

$$e = \frac{L}{2} - \frac{(\Sigma M_R - M_S) - \Sigma M_O}{\Sigma V - V_q}$$

$$e = (2.1 \text{ m}/2) - [(191.92 \text{ kN/m} \cdot \text{m} - 16.92 \text{ kN/m} \cdot \text{m}) - 40.47 \text{ kN/m} \cdot \text{m}] / (205.73 \text{ kN/m} - 11.28 \text{ kN/m}) = 0.36 \text{ m}$$

$$L/6 = 2.1 \text{ m}/6 = 0.35 \text{ m}$$

$e > L/6$ (NG)

As a second trial, the length of the reinforcement was increased to 2.4 m to ensure the eccentricity requirement. The eccentricity requirement of the reinforced

volume is checked again with the new reinforcement length of 2.4 m as follows:

$$\begin{aligned}V_4 &= (L \times H_1) \cdot \gamma_{fr} \\ V_4 &= (2.4 \text{ m} \times 2.4 \text{ m}) \cdot 20 \text{ kN/m}^3 = 115.2 \text{ kN/m}\end{aligned}$$

$$\begin{aligned}V_5 &= [(L - d - B) \times H_2] \cdot \gamma_{fr} \\ V_5 &= [(2.4 \text{ m} - 0.3 \text{ m} - 0.6 \text{ m}) \times 0.6 \text{ m}] \cdot 20 \text{ kN/m}^3 \\ &= 18.0 \text{ kN/m}\end{aligned}$$

$$\begin{aligned}V_q &= (L - d - B) \cdot q \\ V_q &= (2.4 \text{ m} - 0.3 \text{ m} - 0.6 \text{ m}) \cdot 9.4 \text{ kN/m}^2 = 14.10 \text{ kN/m}\end{aligned}$$

ΣV = sum of vertical forces acting on the foundation soil

$$\begin{aligned}\Sigma V &= V_4 + V_5 + V_q + \Sigma V_a \\ \Sigma V &= 115.2 \text{ kN/m} + 18.0 \text{ kN/m} + 14.10 \text{ kN/m} \\ &\quad + 79.25 \text{ kN/m} = 226.55 \text{ kN/m}\end{aligned}$$

ΣM_R = sum of resisting moments about point C

$$\begin{aligned}\Sigma M_R &= V_4 \cdot (L/2) + (V_5 + V_q) \cdot [(L - d - B)/2 \\ &\quad + (d + B)] + (\Sigma M_{RA} + \Sigma V_a \cdot d) \\ \Sigma M_R &= 115.2 \text{ kN/m} \cdot (2.4 \text{ m}/2) + (18.0 \text{ kN/m} \\ &\quad + 14.10 \text{ kN/m}) \cdot [(2.4 \text{ m} - 0.3 \text{ m} - 0.6 \text{ m})/2 \\ &\quad + (0.3 \text{ m} + 0.6 \text{ m})] + [23.78 \text{ kN/m} \cdot \text{m} \\ &\quad + 79.25 \text{ kN/m} \cdot (0.3 \text{ m})] = 238.76 \text{ kN/m} \cdot \text{m}\end{aligned}$$

M_S = moment about point C caused by traffic surcharge

$$\begin{aligned}M_S &= V_q \cdot [(L - d - B)/2 + (d + B)] \\ M_S &= 14.10 \text{ kN/m} \cdot [(2.4 \text{ m} - 0.3 \text{ m} - 0.6 \text{ m})/2 \\ &\quad + (0.3 \text{ m} + 0.6 \text{ m})] = 23.27 \text{ kN/m} \cdot \text{m}\end{aligned}$$

e = eccentricity at the base of the reinforced volume

$$e = \frac{L}{2} - \frac{(\Sigma M_R - M_S) - \Sigma M_O}{\Sigma V - V_q}$$

$$e = (2.4 \text{ m}/2) - [(238.76 \text{ kN/m} \cdot \text{m} - 23.27 \text{ kN/m} \cdot \text{m}) - 40.47 \text{ kN/m} \cdot \text{m}] / (226.55 \text{ kN/m} - 14.10 \text{ kN/m}) = 0.38 \text{ m}$$

$$L/6 = 2.4 \text{ m}/6 = 0.4 \text{ m}$$

$e < L/6$ (OK)

Check allowable bearing pressure of the foundation soil:

Calculate the “influence length” D_1 at the foundation level and compare with the effective reinforcement length, L' .

$$\begin{aligned}D_1 &= d + B' + H_1/2 = d + (B - 2e') + H_1/2 \\ D_1 &= 0.3 \text{ m} + [0.6 \text{ m} - 2 \cdot (0.01 \text{ m})] + 2.4 \text{ m}/2 = 2.08 \text{ m}\end{aligned}$$

$$L' = L - 2e$$

$$L' = 2.4 \text{ m} - 2 \cdot (0.38 \text{ m}) = 1.64 \text{ m}$$

Because D_1 at the foundation level is greater than L' ($L' = L - 2e$), the contact pressure on the foundation level, p_{contact} , is calculated as follows:

$$p_{\text{contact}} = \frac{\Sigma V}{L - 2e}$$

$$p_{\text{contact}} = 226.55 \text{ kN/m} / [2.4 \text{ m} - 2 \cdot (0.38 \text{ m})]$$

$$= 138.14 \text{ kN/m}^2$$

$$q_{\text{af}} = 300 \text{ kN/m}^2 \text{ (from Step 2)}$$

$$p_{\text{contact}} = 138.14 \text{ kN/m}^2 < q_{\text{af}} = 300 \text{ kN/m}^2 \text{ (OK)}$$

Step 8: Evaluate internal stability at each reinforcement level

With geosynthetic reinforcement, the coefficient of lateral earth pressure is constant throughout the entire wall height, per Section 4.3b, NHI manual.

The internal stability is evaluated by checking the reinforcement pullout failure.

Check reinforcement pullout failure:

$$Pr = \text{pullout resistance}$$

$$Pr = F^* \cdot \alpha \cdot (\sigma_v \cdot Le) \cdot C \cdot Rc$$

$$F^* = \text{pullout resistance factor}$$

$$F^* = 2/3 \cdot \tan \phi_{\text{rf}}$$

$$F^* = 2/3 \cdot \tan(36^\circ) = 0.48$$

α = a scale effect correction factor ranging from 0.6 to 1.0 for geosynthetic reinforcement; for geotextile, α is defaulted to 0.6, per Section 3.3b, NHI manual.

$(\sigma_v \cdot Le)$ = normal force at the soil-reinforcement interface at depth z (excluding traffic surcharge)

$$(\sigma_v \cdot Le) = (\sigma_{\text{vs}} \cdot Le) + (\Delta\sigma_v \cdot Li)$$

Le = length of embedment in the resistant zone behind the failure surface at depth z

$$Le = L - La$$

La = length of embedment in the active zone at depth z

$$La = (H_1 - z) \tan(45^\circ - \phi_{\text{rf}}/2)$$

Li = length of embedment within the influence area inside the resistant zone; this length can be measured directly from the design drawing.

C = reinforcement effective unit perimeter; $C = 2$ for strips, grids, and sheets

Rc = coverage ratio; $Rc = 1.0$ for 100 percent coverage of reinforcement

σ_h = horizontal pressure at depth z

$$\sigma_h = K_{\text{a(rf)}} \cdot (\sigma_{\text{vs}} + \Delta\sigma_v + q) + \Delta\sigma_h$$

σ_{vs} = vertical soil pressure at depth z

$$\sigma_{\text{vs}} = (\gamma_{\text{rf}} \cdot H_2) + (\gamma_{\text{rf}} \cdot z)$$

$\Delta\sigma_v$ = distributed vertical pressure from sill

$$\Delta\sigma_v = \Sigma Va / D$$

D = effective width of applied load at depth z

For $z \leq z_2$: $D = (B - 2e') + z$

For $z > z_2$: $D = d + (B - 2e') + z/2$

$$z_2 = 2 \cdot d$$

$\Delta\sigma_h$ = supplement horizontal pressure at depth z

For $z \leq I_1$: $\Delta\sigma_h = 2 \cdot \Sigma Fa \cdot (I_1 - z)/(I_1^2)$

For $z > I_1$: $\Delta\sigma_h = 0$

T_{max} = maximum tensile force in the reinforcement at depth z

$$T_{\text{max}} = \sigma_h \cdot s$$

s = vertical reinforcement spacing

FS_{pullout} = factor of safety against reinforcement pullout

$$FS_{\text{pullout}} = Pr / T_{\text{max}}$$

Let depth z be measured from the top of the load-bearing wall. Reinforcement no. 7 at $z = 1.0 \text{ m}$ (see Figure 3-9) would serve as an example for determining the FS_{pullout} .

$$\sigma_{\text{vs}} = (\gamma_{\text{rf}} \cdot H_2) + (\gamma_{\text{rf}} \cdot z)$$

$$\sigma_{\text{vs}} = (20 \text{ kN/m}^3 \cdot 0.6 \text{ m}) + (20 \text{ kN/m}^3 \cdot 1.0 \text{ m})$$

$$= 32.0 \text{ kN/m}^2$$

$$z_2 = 2 \cdot d = 2 \cdot (0.3 \text{ m}) = 0.6 \text{ m}$$

$$\because z = 1.0 \text{ m} > z_2 = 0.6 \text{ m}, D = d + (B - 2e') + z/2$$

$$D = 0.3 \text{ m} + [0.6 \text{ m} - 2 \cdot (0.01 \text{ m})] + 1.0 \text{ m}/2 = 1.38 \text{ m}$$

$$\Delta\sigma_v = \Sigma Va / D$$

$$\Delta\sigma_v = 79.25 \text{ kN/m} / 1.38 \text{ m} = 57.43 \text{ kN/m}^2$$

$$\because z = 1.0 \text{ m} < I_1 = 1.73 \text{ m}, \therefore \Delta\sigma_h = 2 \cdot \Sigma Fa \cdot (I_1 - z)/(I_1^2)$$

$$\Delta\sigma_h = 2 \cdot (4.16 \text{ kN/m}) \cdot (1.73 \text{ m} - 1.0 \text{ m})/(1.73 \text{ m})^2$$

$$= 2.03 \text{ kN/m}^2$$

$$\sigma_h = K_{\text{a(rf)}} \cdot (\sigma_{\text{vs}} + \Delta\sigma_v + q) + \Delta\sigma_h$$

$$\sigma_h = 0.26 \cdot (32.0 \text{ kN/m}^2 + 57.43 \text{ kN/m}^2 + 9.4 \text{ kN/m}^2) + 2.03 \text{ kN/m}^2 = 27.73 \text{ kN/m}^2$$

$$T_{\max} = \sigma_h \cdot s$$

$$T_{\max} = 27.73 \text{ kN/m}^2 \cdot (0.2 \text{ m}) = 5.55 \text{ kN/m}$$

$$L_a = (H_1 - z) \tan(45^\circ - \phi_{rt}/2)$$

$$L_a = (2.4 \text{ m} - 1.0 \text{ m}) \tan(45^\circ - 36^\circ/2) = 0.71 \text{ m}$$

$$L_e = L - L_a$$

$$L_e = 2.4 \text{ m} - 0.71 \text{ m} = 1.69 \text{ m}$$

Calculate the normal force at $z = 1.0 \text{ m}$:

$$(\sigma_v \cdot L_e) = (\sigma_{vs} \cdot L_e) + (\Delta\sigma_v \cdot L_i)$$

$$(\sigma_v \cdot L_e) = (32.0 \text{ kN/m}^2 \cdot 1.69 \text{ m}) + (57.43 \text{ kN/m}^2 \cdot 0.66 \text{ m}) = 91.98 \text{ kN/m}$$

$$Pr = F^* \cdot \alpha \cdot (\sigma_v \cdot L_e) \cdot C \cdot Rc$$

$$Pr = (0.48) \cdot (0.6) \cdot 91.98 \text{ kN/m} \cdot (2) \cdot (1) = 52.98 \text{ kN/m}$$

$$FS_{\text{pullout}} = Pr / T_{\max}$$

$$FS_{\text{pullout}} = 52.98 \text{ kN/m} / 5.55 \text{ kN/m} = 9.55$$

$$FS_{\text{pullout}} = 9.55 > 1.5 \text{ (OK)}$$

The values of FS_{pullout} for all the reinforcements in the load-bearing wall are summarized in Table 3-3.

Step 9: Determine the required reinforcement stiffness and strength

The minimum “working” reinforcement stiffness is determined as

$$T_{@ \epsilon=1.0 \text{ percent}} \geq \sigma_{h(\max)} \cdot s$$

The minimum ultimate reinforcement strength is determined as

$$T_{\text{ult}} \geq F_s \cdot T_{@ \epsilon=1.0 \text{ percent}}$$

The recommended combined safety factor is $F_s = 5.5$ for reinforcement $\leq 0.2 \text{ m}$, and $F_s = 3.5$ for reinforcement spacing of 0.4 m .

From Table 3-3, $\sigma_{h(\max)}$ is 37.57 kN/m^2 , which occurs at reinforcement no. 11 with depth $z = 0.2 \text{ m}$ and $s = 0.2 \text{ m}$.

$$T_{@ \epsilon=1.0 \text{ percent}} = \sigma_{h(\max)} \cdot s$$

$$T_{@ \epsilon=1.0 \text{ percent}} = 37.57 \text{ kN/m}^2 \cdot (0.2 \text{ m}) = 7.51 \text{ kN/m}$$

The uniform reinforcement spacing is 0.2 m , hence $F_s = 5.5$.

$$T_{\text{ult}} = F_s \cdot T_{@ \epsilon=1.0 \text{ percent}}$$

$$T_{\text{ult}} = 5.5 \cdot (7.51 \text{ kN/m}) = 41.31 \text{ kN/m}$$

A reinforcement with minimum “working” stiffness, $T_{@ \epsilon=1.0 \text{ percent}} = 7.5 \text{ kN/m}$ and minimum ultimate strength (per ASTM D4595), $T_{\text{ult}} = 41.3 \text{ kN/m}$ is required.

Step 10: Design of back/upper wall

Reinforced fill:	Same as that of the load-bearing wall
Reinforcement:	Same as that of the load-bearing wall
Reinforcement length:	1.3 m (without an approach slab, the back wall reinforcement length is to be flush with the reinforcement in the load-bearing wall)
Reinforcement layout:	Vertical spacing = 0.2 m

TABLE 3-3 Design Example 2—tabulated results of FS_{pullout} at each reinforcement level

No.	Depth z (m)	s (m)	σ_{vs} (kN/m ²)	D (m)	$\Delta\sigma_v$ (kN/m ²)	$\Delta\sigma_h$ (kN/m ²)	σ_h (kN/m ²)	T_{\max} (kN/m)	L_a (m)	L_e (m)	L_i (m)	$(\sigma_v \cdot L_e)$ (kN/m)	Pr (kN/m)	FS_{pullout}
1	2.2	0.2	56.0	1.97	40.21	0.00	27.42	5.48	0.10	2.30	1.87	203.84	118.48	21.61
2	2.0	0.2	52.0	1.87	42.36	0.00	26.94	5.39	0.20	2.20	1.67	184.82	107.42	19.94
3	1.8	0.2	48.0	1.77	44.75	0.00	26.52	5.30	0.31	2.09	1.47	166.09	96.54	18.20
4	1.6	0.2	44.0	1.67	47.43	0.31	26.49	5.30	0.41	1.99	1.26	147.58	85.78	16.19
5	1.4	0.2	40.0	1.57	50.45	0.88	26.80	5.36	0.51	1.89	1.06	129.16	75.07	14.01
6	1.2	0.2	36.0	1.47	53.88	1.45	27.22	5.44	0.61	1.79	0.86	110.70	64.34	11.82
7	1.0	0.2	32.0	1.37	57.81	2.01	27.77	5.55	0.71	1.69	0.66	91.99	53.47	9.63
8	0.8	0.2	28.0	1.27	62.35	2.58	28.48	5.70	0.82	1.58	0.46	72.79	42.31	7.43
9	0.6	0.2	24.0	1.17	67.68	3.15	29.39	5.88	0.92	1.48	0.25	52.77	30.67	5.22
10	0.4	0.2	20.0	0.97	81.62	3.72	32.54	6.51	1.02	1.38	0.05	31.85	18.52	2.84
11	0.2	0.2	16.0	0.77	102.79	4.29	37.57	7.51	1.12	1.28	0.00	20.46	11.89	1.58

Step 11: Check angular distortion between abutments

$$\delta_{\text{abutment}} = \text{abutment settlement}$$

$$\delta_{\text{abutment}} = 1.5 \text{ percent} \cdot H_1$$

$$\delta_{\text{abutment}} = 0.015 \cdot (2.4 \text{ m}) = 0.036 \text{ m}$$

$$\delta_{\text{foundation}} = \text{foundation settlement (as determined by conventional settlement computation methods)}$$

$$\text{Eg} \delta_{\text{foundation}} = 0.01 \text{ m}$$

$$\delta_{\text{total}} = \text{total settlement}$$

$$\delta_{\text{total}} = \delta_{\text{abutment}} + \delta_{\text{foundation}}$$

$$\delta_{\text{total}} = 0.036 \text{ m} + 0.01 \text{ m} = 0.046 \text{ m}$$

$$\text{Angular distortion} = \delta_{\text{total}} / \text{span length} = 0.046 \text{ m} / 10 \text{ m} = 0.0046$$

Tolerable angular distortion for simple span = 0.005

Angular distortion = 0.0046 < 0.005 (OK)

Design summary:

The configuration for the trial design is shown in Figure 3-10.

Abutment configuration:

Load-bearing wall	
height, H_1	2.4 m
Back wall	
height, H_2	0.6 m
Facing	modular concrete blocks (200 mm x 200 mm x 400 mm)
Front batter	1/35
Sill type	isolated sill
Sill width	0.6 m
Sill clear distance	0.3 m
Embedment	200 mm (one facing block height)

Reinforcement:

Minimum stiffness at $\epsilon = 1.0$ percent, $T_{@ \epsilon = 1.0 \text{ percent}} = 7.5 \text{ kN/m}$
 Minimum ultimate strength, $T_{\text{ult}} = 41.3 \text{ kN/m}$
 Length in load-bearing wall = 2.4 m
 Vertical spacing in load-bearing wall = 0.2 m
 Length in back wall = 1.3 m
 Vertical spacing in back wall = 0.2 m

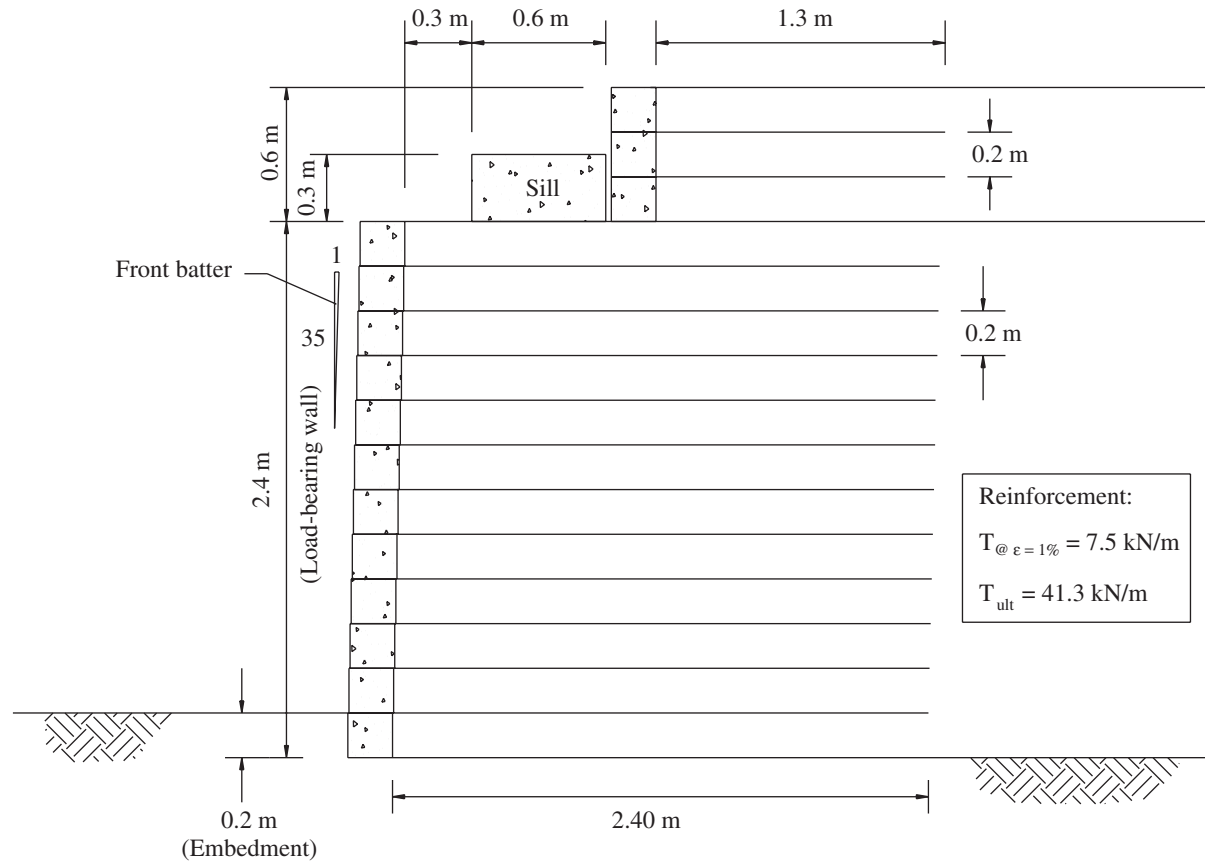


Figure 3-10. Design Example 2—configuration of the trial design.

CHAPTER 4

CONCLUSIONS AND SUGGESTED RESEARCH

CONCLUSIONS

A design method and construction guidelines for GRS abutments with a flexible facing have been developed in the course of this study. The design method adopted the format and methodology of the NHI manual for the design of MSE bridge abutments. Fourteen specific refinements and revisions of the NHI design method are presented, and the basis for each refinement and revision is provided. The refinements and revisions are based on findings from previous case histories, full-scale loading experiments, and finite element analysis of GRS abutments, as well as the authors' experiences and knowledge on GRS structures in general and GRS abutments in particular.

The construction guidelines were established based on the guidelines for segmental GRS walls as provided by various agencies (including AASHTO, NCMA, FHWA, CTI, SAGP, and JR) as well as the authors' observations and experiences with the construction of GRS walls and abutments. The construction guidelines focus on GRS abutments with a segmental concrete block facing. As the literature on construction of GRS abutments with other forms of flexible facing is rather limited, only the basic construction guidelines for three types of flexible facing—geotextile-wrapped, timber, and natural rock—are presented.

The major refinements and revisions to the NHI design method are as follows:

- The allowable bearing pressure of a bridge sill on the load-bearing wall (the lower wall) of a GRS abutment is determined as a function of the friction angle of the fill, reinforcement vertical spacing, sill width, and sill type (isolated sill or integrated sill). A simple three-step procedure is provided for determination of the allowable bearing pressures under various design conditions.
- The default value for reinforcement vertical spacing is set at 0.2 m. To ensure satisfactory performance and an adequate margin of stability, reinforcement spacing greater than 0.4 m is not recommended for GRS abutments under any conditions.
- To provide improved appearance and greater flexibility in construction, a front batter of 1/35 to 1/40 from the vertical is recommended for a segmental abutment wall facing. A typical setback of 5 to 6 mm between successive courses of facing blocks is recommended for 200 mm (8 in.) height blocks.
- The reinforcement length may be “truncated” in the bottom portion of the wall provided that the foundation is “competent.” The recommended configuration of the truncation is: reinforcement length = 0.35 H at the foundation level (H = total height of the abutment wall) and increases upward at a 45 deg angle. The allowable bearing pressure of the sill, as determined in the three-step procedure, should be reduced by 10 percent for truncated-base walls. Permitting truncated reinforcement typically will translate into significant savings when excavation is involved in the construction of the load-bearing wall of a bridge abutment.
- A recommended “sill clear distance” between the back face of the facing and the front edge of the sill is 0.3 m (12 in.). The recommended clear distance is a result of finite element analysis with the consideration that the soil immediately behind the facing is usually of a lower compacted density because a heavy compactor is not permitted close to the wall face.
- For most bridge abutments, a relatively high-intensity load is applied close to the wall face. To ensure that the foundation soil beneath the abutment will have a sufficient safety margin against bearing failure, a revision is made to check the contact pressure over a more critical region – within the “influence length” D_1 (as defined in Chapter 3) behind the wall face or the reinforcement length in the lower wall, whichever is smaller. In the current NHI manual, the contact pressure is the average pressure over the entire reinforced zone (with eccentricity correction).
- If the bearing capacity of the foundation soil supporting the bridge abutment is found only marginally acceptable or somewhat unacceptable, it is recommended that a reinforced soil foundation (RSF) be used to increase bearing capacity and reduce potential settlement. A typical RSF is formed by excavating a pit $0.5 * L$ deep (L = reinforcement length in the load-bearing wall) and replacing it with compacted road base material reinforced by the same reinforcement to

be used in the load-bearing wall at 0.3-m vertical spacing.

- Both a minimum ultimate tensile strength and a minimum tensile stiffness of the reinforcement should be specified to ensure sufficient tensile resistance at the service loads, to provide adequate ductility, and to ensure a sufficient safety margin against rupture failure. A recommended procedure for determining the required minimum tensile stiffness (at 1.0 percent strain) and the minimum ultimate tensile strength are stipulated.
- It is recommended to extend the reinforcement lengths in both the upper and lower walls, at least the top three layers of each wall, to about 1.5 m beyond the end of the approach slab to promote integration of the abutment walls with the approach embankment and the load-bearing abutment, so as to eliminate the bridge “bumps”—a chronic problem in many bridges.
- Connection strength is not a design concern as long as the reinforcement spacing is kept not more than 0.2 m, the selected fill is compacted to meet the specification stipulated in the recommended construction guidelines, and the applied pressure does not exceed the recommended design pressures in the recommended design method.

SUGGESTED RESEARCH

It is suggested that a series of full-scale experiments of GRS bridge abutments be conducted to confirm the overall validity of the recommended design and construction

guidelines. The most important features to be confirmed by the experiments follow:

- Allowable design pressure. The allowable design sill pressure as affected by sill width, sill clear distance, soil friction angle, reinforcement spacing, truncated base, and sill type (especially an integrated sill) should be confirmed. Some attention should also be given to the effect of construction sequence (i.e., the potential benefits of constructing the upper wall before placing the bridge superstructure).
 - Long-term performance of GRS bridge abutments in the in-service condition. It is suggested that the design method and construction guidelines be implemented in bridges on secondary roads with simple (yet reliable) instruments to monitor their long-term performance.
 - Offset between the facing blocks and the centerline of bridge bearings. The analysis conducted in this study has indicated that an offset less than 0.9 m (3 ft) (as suggested by the NHI manual) would not cause any adverse effects. The effect of an offset of 0.8 m (e.g., 0.2 m of block depth + 0.3 m of clear distance + 0.3 m of half-sill-width) may be selected for testing.
 - Preloading and/or pre-stressing of GRS abutments. Simple measures of preloading and/or prestressing has been shown effective at increasing significantly the load-carrying capacity of a GRS abutment and reducing the sill settlement from two- to fivefold (depending on the fill placement condition) and the lateral movement by about threefold. A cost-effective procedure and proper specifications for preloading and/or prestressing have not been established.
-

REFERENCES

- AASHTO, "Interims to Standard Specifications for Highway Bridges." 16th Edition, AASHTO, Washington, D.C. (1998).
- Abu-Hejleh, N., Wang, T., and Zornberg, J.G., "Performance of Geosynthetic-Reinforced Walls Supporting Bridge and Approaching Roadway Structures." *ASCE Geotechnical Special Publication No. 103, Advances in Transportation and Geoenvironmental Systems Using Geosynthetics* (2000) pp. 218–243.
- Abu-Hejleh, N., Zornberg, J.G., Wang, T., and Watcharamonthein, J., "Monitored Displacements of Unique Geosynthetic-Reinforced Soil Bridge Abutments." *Geosynthetics International*, Vol. 9, No. 1 (2002) pp. 71–95.
- Abu-Hejleh, N., Zornberg, J.G., Elias, V., and Watcharamonthein, J., "Design Assessment of the Founders/Meadows GRS Abutment Structure." Transportation Research Board 82nd Annual Meeting Compendium of Papers CD-ROM, Washington, D.C. (2003).
- Adams, M.T., "Performance of a Prestained Geosynthetic Reinforced Soil Bridge Pier." *Mechanically Stabilized Backfill*, Wu, editor, A. A. Balkema Publishers, Rotterdam, The Netherlands, (1997) pp. 35–53.
- Adams, M.T., and Collin, J.G. "Large Model Spread Footing Tests on Geosynthetic Reinforced Soil Foundations." *ASCE Journal of Geotechnical and Geoenvironmental Engineering*, Vol. 123, No. 1 (1997) pp. 66–72.
- Adams, M.T., Ketchart, K., Ruckman, A., DiMillio, A.F., Wu, J.T.H., and Satyanarayana, R., *Transportation Research Record 1652: Reinforced Soil for Bridge Support Applications on Low-Volume Roads*, Transportation Research Board, National Research Council, Washington, D.C. (1999) pp. 150–160.
- Aksharadananda, T. and Wu, J.T.H., "Strength Parameters of Backfills for Design and Construction of Retaining Walls." *Report No. 2001-07*, Colorado DOT (2001) 125 pp.
- Baladi, G.Y. and Rohani, B., "An Elastic-Plastic Constitutive Model for Saturated Sand Subjected to Monotonic and/or Cyclic Loadings." 3rd International Conference on Numerical Methods in Geomechanics, University of Aachen, Aachen, West Germany (1979) pp. 389–404.
- Barreire, W. and Wu, J.T.H., "Guidelines for Design and Construction of Reinforced Soil Foundations." Research Report, Department of Civil Engineering, University of Colorado at Denver (2001) 109 pp.
- Benigni, C., Bosco, G., Cazzuffi, D., and Col, R.D., "Construction and Performance of an Experimental Large-Scale Wall Reinforced with Geosynthetics." *Earth Reinforcement* (Ochiai, Yasufuku, and Omine, editors) Vol. 1, A. A. Balkema Publishers, Rotterdam, The Netherlands (1996) pp. 315–320.
- Bozozuk, M., "Bridge Foundations Move." *Transportation Research Record 678: Tolerable Movements of Bridge Foundations, Sand Drains, K-Test, Slopes, and Culverts*, Transportation Research Board, National Research Council, Washington, D.C. (1978) pp. 17–21.
- Briaud, J.L., and Gibbens, R.M., editors, "Predicted and Measured Behavior of Five Spread Footings on Sand." ASCE, New York (1994).
- Chen, W.F. and McCarron, W.O., "Modeling of Soils and Rocks Based on Concept of Plasticity." Proceedings, Symposium on Recent Developments in Laboratory and Field Tests and Analysis of Geotechnical Problems, Asian Institute of Technology, Bangkok, Thailand (1983) pp. 467–510.
- Daddazio, R.P., Ettouney, M.M., and Sandler, I.S., "Nonlinear Dynamic Slope Stability Analysis." *ASCE Journal of Geotechnical Engineering*, Vol. 113, No. 4 (1987) pp. 285–298.
- DiMaggio, F.L. and Sandler, I.S., "Material Model for Granular Soils." *ASCE Journal of Engineering Mechanics Division*, Vol. 97, No. 3 (1971) pp. 935–950.
- Drucker, D.C. and Prager, W., "Soil Mechanics and Plasticity Analysis or Limit Design." *Quarterly Applied Mathematics*, Vol. 10, No. 2 (1952) pp. 157–165.
- Duncan, J.M., Byrne, P.M., Wong, K.S. and Mabry, P., "Strength, Stress-Strain and Bulk Modulus Parameters for Finite Element Analyses of Stresses and Movements in Soil Masses." *Report No. UCB/GT/80-01*, University of California, Berkeley (1980).
- Elias, V. and Christopher, B.R., "Mechanically Stabilized Earth Walls and Reinforced Soil Slopes, Design and Construction Guidelines." *FHWA-SA-96-071*, FHWA (1997) 371 pp.
- Elias, V., Christopher, B. R., and Berg, R.R., "Mechanically Stabilized Earth Walls and Reinforced Soil Slopes Design and Construction Guidelines." NHI Course 132042, FHWA NHI-00-043 (2001) 394 pp.
- Gotteland, P., Gourc, J.P., and Villard, P., "Geosynthetics Reinforced Structures as Bridge Abutments: Full Scale Experimentation and Comparison with Modelisations." *Mechanically Stabilized Backfill* (Wu, editor) A. A. Balkema Publishers, Rotterdam, The Netherlands (1997) pp. 25–34.
- Grover, R.A., "Movements of Bridge Abutments and Settlements of Approach Slabs in Ohio." *Transportation Research Record 678: Tolerable Movements of Bridge Foundations, Sand Drains, K-Test, Slopes, and Culverts*, Transportation Research Board, National Research Council, Washington, D.C. (1978) pp. 12–17.
- Hallquist, J.O. and Whirley, R.G., "dyna3d USER'S MANUAL: Nonlinear Dynamic Analysis of Structures in Three Dimensions." University of California, Lawrence Livermore National Laboratory, *Report UCID-19592*, Rev. 5 (1989).
- Huang, T.K. and Chen, W.F., "Simple Procedure for Determining Cap-Plasticity-Model Parameters." *ASCE Journal of Geotechnical Engineering*, Vol. 116, No. 3 (1990) pp. 492–513.
- Huang, C.C. and Tatsuoka, F., "Bearing Capacity of Reinforced Horizontal Sand Ground," *Geotextiles and Geomembranes* Vol. 9 (1990) pp. 51–82.
- Japan Railway (JR) Technical Research Institute, "Manual on Design and Construction of Geosynthetic-Reinforced Soil Retaining Wall." (1998) 118 pp.
- Kanazawa, Y., Ikeda, K., Murata, O., Tateyama, M, and Tatsuoka, F., "Geosynthetic-Reinforced Soil Retaining Walls for Reconstructing Railway Embankment at Amagasaki." *Recent Case Histories of Permanent Geosynthetic-Reinforced Soil Retaining Wall* (Tatsuoka and Leshchinsky, editors) A. A. Balkema Publishers, Rotterdam, The Netherlands (1994) pp. 233–242.
- Keller, G. R. and Devin, S.C., "Geosynthetic-Reinforced Soil Bridge Abutments." *Transportation Research Record* 1819, Vol. 2 (2003) pp. 362–368.
- Ketchart, K. and Wu, J.T.H., "Performance of Geosynthetic-Reinforced Soil Bridge Pier and Abutment." *Mechanically Sta-*

- bilized Backfill* (Wu, editor) A. A. Balkema Publishers, Rotterdam, The Netherlands (1997) pp. 101–116.
- Ketchart, K. and Wu, J.T.H., “Performance Test for Geosynthetic-Reinforced Soil Including Effects of Preloading,” *FHWA-RD-01-018* (2001) 270 pp.
- Ketchart, K. and Wu, J.T.H., “A Modified Soil-Geosynthetic Interactive Performance Test for Evaluating Deformation Behavior of GRS Structures.” *ASTM Geotechnical Testing Journal, American Society of Testing and Materials*, Vol. 25, No. 4. (2002) pp. 405–413.
- Mannsbart, G. and Kropik, O., “Nonwoven Geotextile Used for Temporary Reinforcement of a Retaining Structure under a Railroad Track.” *Geosynthetics: Applications, Design and Construction* (DeGroot, Hoedt, and Termaat, editors) A. A. Balkema Publishers, Rotterdam, The Netherlands (1996) pp. 121–124.
- Mayne, P., “Stress-Strain-Strength Parameters from Enhanced In-Situ Tests.” Proceedings, In-Situ 2001, Bali, Indonesia (May 2001).
- McCarron, W.O. and Chen, W.F., “A Capped Plasticity Model Applied to Boston Blue Clay.” *Canadian Geotechnical Journal*, Vol. 24, No. 4 (1987) pp. 630–644.
- Miyata, K. and Kawasaki, H., “Reinforced Soil Retaining Walls by FRP Geogrid.” *Recent Case Histories of Permanent Geosynthetic-Reinforced Soil Retaining Wall* (Tatsuoka and Leshchinsky, editors), A. A. Balkema Publishers, Rotterdam, The Netherlands (1994) pp. 253–257.
- Minuzo, E. and Chen, W.F., “Plasticity Modeling and its Application to Geomechanics.” Proc., Symposium on Recent Developments in Laboratory and Field Tests and Analysis of Geotechnical Problems, Rotterdam, The Netherlands (1984) pp. 391–426.
- Monley, G.J. and Wu, J.T.H., “Tensile Reinforcement Effects on Bridge-Approach Settlement.” *ASCE Journal of Geotechnical Engineering*, Vol. 119, No. 4 (1993) pp. 749–762.
- Moulton, L. K., GangaRao, H. V. S., and Halvorsen, G. T., “Tolerable Movement Criteria for Highway Bridges.” *FHWA/RD-85/107*, FHWA, Washington, D.C. (1985) 118 pp.
- National Concrete Masonry Association (NCMA), “Design Manual for Segmental Retaining Walls.” 2nd Edition, NCMA, Herndon, Virginia (1997).
- Nelson, I. and Baladi, G.Y., “Outrunning Ground Shock Computed with Different Methods.” *ASCE Journal of Engineering Mechanics Division*, Vol. 103, No. 3 (1977) pp. 377–393.
- Omar, M.T., Das, B.M., Yen, S.C., Puri, V.K., and Cook, E.E., “Ultimate Bearing Capacity of Rectangular Foundations on Geogrid-Reinforced Sand.” *ASTM Geotechnical Testing Journal*, Vol. 16, No. 2 (1993) pp. 246–252.
- Perloff, W. H., “Pressure Distribution and Settlement,” Chapter 4, *Foundation Engineering Handbook* (Winterkorn and Fang, editors) Van Nostrand Reinhold, New York (1975) pp. 148–196.
- Poulos, H.G., “Foundation Settlement Analysis—Practice Versus Research,” The Eighth Spencer J. Buchanan Lecture, Texas A&M University (2000).
- Sandler, I.S., and Rubin, D., “An Algorithm and Modular Subroutine for the Cap Model.” *International Journal of Numerical and Analytical Methods in Geomechanics*, Vol. 3 (1979) pp. 173–186.
- Swiss Association of Geotextile Professionals (SAGP), *The Geotextile Handbook*. Translations by U.S. Bureau of Reclamation, Denver, Colorado (1981) 411 pp.
- Tateyama, M., Murata, O., Watanabe, K., and Tatsuoka, F., “Geosynthetic-Reinforced Retaining Walls for Bullet Train Yard in Nagoya.” *Recent Case Histories of Permanent Geosynthetic-Reinforced Soil Retaining Wall* (Tatsuoka and Leshchinsky, editors) A. A. Balkema Publishers, Rotterdam, The Netherlands (1994) pp. 141–150.
- Tatsuoka, F., Uchimura, T., and Tateyama, M., “Preloaded and Prestressed Reinforced Soil.” *Soils and Foundations*, Vol. 37, No. 3 (1997) pp. 79–94.
- Tatsuoka, F., Uchimura, T., Tateyama, M., and Koseki, J., “Geosynthetic-Reinforcement Soil Retaining Walls as Important Permanent Structures.” *Mechanically Stabilized Backfill* (Wu, editor) A. A. Balkema Publishers, Rotterdam, The Netherlands (1997) pp. 3–24.
- Terzaghi, K. and Peck, R.B., “Soil Mechanics in Engineering Practice,” 2nd edition. John Wiley and Sons, New York (1967).
- Uchimura, T., Tatsuoka, F., Tateyama, M., and Koga, T., “Preloaded-Prestressed Geogrid-Reinforced Soil Bridge Pier.” Proceedings 6th International Conference on Geosynthetics, Atlanta, Georgia, Vol. 2 (1998) pp. 565–572.
- Wahls, H. E., *National Cooperative Highway Research Program Synthesis of Highway Practice 159: Design and Construction of Bridge Approaches*, Transportation Research Board, National Research Council, Washington, D.C. (1990) 51 pp.
- Walkinshaw, J. L., “Survey of Bridge Movements in the Western United States.” *Transportation Research Record 678: Tolerable Movements of Bridge Foundations, Sand Drains, K-Test, Slopes, and Culverts*, Transportation Research Board, National Research Council, Washington, D.C. (1978) pp. 6–12.
- Wayne, M.H., Han, J., and Akins, K., “The Design of Geosynthetic Reinforced Foundations.” ASCE Annual Convention and Exposition, Boston, Massachusetts (1998) pp. 18–21.
- Werner, G. and Resl, S., “Stability Mechanisms in Geotextile Reinforced Earth-Structures.” III International Conference on Geotextiles, Vienna, Austria, Vol. 4 (1986) pp. 1131–1135.
- Won, G.W., Hull, T., and De Ambrosis, L., “Performance of a Geosynthetic Segmental Block Wall Structure to Support Bridge Abutments.” *Earth Reinforcement* (Ochiai, Yasufuku, and Omine, editors) A. A. Balkema Publishers, Rotterdam, The Netherlands, Vol. 1 (1996) pp. 543–548.
- Wong, K. S. and Duncan, J.M., “Hyperbolic Stress-Strain Parameters for Nonlinear Finite Element Analysis of Stresses and Movements in Soil Masses.” Department of Civil Engineering, University of California at Berkeley (1974) 90 pp.
- Wu, J.T.H., “Design and Construction of Low Cost Retaining Walls: The Next Generation in Technology.” *Report No. CTI-UCD-1-94*, Colorado Transportation Institute (1994) 152 pp.
- Wu, J.T.H., “Revising the AASHTO Guidelines for Design and Construction of GRS Walls,” *Report No. CDOT-DTD-R-2001-16*, Colorado DOT (2001) 148 pp.
- Wu, J. T. H., Ketchart, K., and Adams, M. T., “GRS Bridge Piers and Abutments.” *Report FHWA-RD-00-038*, FHWA, U.S. DOT (2001) 136 pp.
- Yetimoglu, T., Wu, J.T.H., and Saglamer, A., “Bearing Capacity of Rectangular Footings on Geogrid-Reinforced Sand,” *ASCE Journal of Geotechnical Engineering*, Vol. 120, No. 12 (1994) pp. 2083–2099.

APPENDIX A

Review of Construction Guidelines for GRS Walls [Note: This appendix has not been edited by TRB.]

The guidelines for construction of segmental Geosynthetic Reinforced Soil (GRS) walls have been provided by various agencies. Most of these guidelines should be equally applicable to segmental GRS abutments. This Chapter summarizes the construction guidelines provided by: (1) American Association of State Highway and Transportation Officials,

AASHTO (1998), (2) National Concrete Masonry Association, NCMA (1997), (3) Federal Highway Administration, FHWA (Elias and Christopher, 1997), (4) Colorado Transportation Institute, CTI (Wu, 1994), (5) Swiss Association of Geotextile Professionals, SAGP (1981), and (6) Japan Railways, JR (1998).

American Association of State Highway and Transportation Officials, AASHTO (1997)

Reinforcement and Reinforcement Placement	<ul style="list-style-type: none"> – Geosynthetic reinforcement and connection hardware shall be of the type and size designated on the plan or the approved working drawings and shall conform to the specified material and manufacturing requirements. – All geosynthetic reinforcement shall be uniformly tensioned to remove any slack during placement.
Backfill	<ul style="list-style-type: none"> – Structure backfill material shall consist of material free from organic material or other unsuitable material as determined by the engineer. – Grading shall be as follows unless otherwise specified: 100% passing 100 mm (4 in.) sieve, 0-60% passing No. 40 (0.42 mm) sieve, and 0-15% passing No. 200 (0.074mm) sieve; plasticity index (PI) as determined by AASHTO T90, shall not exceed 6. The maximum soil particle size shall generally be 20 mm (0.75 in.). – The backfill shall exhibit an angle of internal friction of not less than 34 degrees, as determined by the standard direct shear test on the portion finer than 2 mm (No.10) sieve, using a sample compacted to 95% of AASHTO T-99 at optimum moisture content. – The backfill shall be substantially free of shale or other soft, poor durability particles, and shall have an organic content not larger than 1%. For permanent applications, the backfill shall have a pH between 4.5 and 9. The pH limits may be increased to 3 to 11 for temporary applications.
Backfill Placement	<ul style="list-style-type: none"> – Backfill shall be placed and compacted simultaneously with the placement of facing and soil reinforcement. – Placement and compaction of backfill shall be accomplished without distortion or displacement of the facing or soil reinforcement. – Sheepsfoot or grid-type rollers shall not be used for compacting backfill within the limits of the soil reinforcement. – At each level of soil reinforcement the backfill material shall be roughly leveled to an elevation approximately 30 mm (0.2 ft) above the level of connection at the facing before placing the soil reinforcement.
Facing	<ul style="list-style-type: none"> – Masonry concrete blocks used as wall facing elements should have a minimum compressive strength of 28 MPa (4,000 psi) and a water absorption limit of 5%. – Facing blocks may be tested for freeze-thaw resistance and survive 300 freeze-thaw cycles without failure per ASTM C666. – Facing blocks should also meet the requirements of ASTM C90 and C140. – Facing blocks directly exposed to spray from deiced pavements shall be sealed after erection with a water resistance coating or be manufactured with a coating or additive to increase freeze-thaw resistance. – Facing blocks shall be placed and supported as necessary so that their final position is vertical or battered as shown on the plans or the approved working drawings with a tolerance acceptable to the engineer.

Others	<ul style="list-style-type: none"> – A minimum bench width of 4 ft is recommended at the base of walls constructed on slopes. – When required, a cast-in-place or precast reinforced concrete leveling pad shall be provided at the foundation level. Prior to placing the leveling pads, the foundation material shall be properly treated.
--------	--

National Concrete Masonry Association, NCMA (1997)

Site Preparation	<ul style="list-style-type: none"> – Excavation shall be carried out to the lines and grades shown on the project grading plans. Over-excavation shall be minimized. – A minimum 0.5 m of wall embedment is required. – Foundation soils not meeting the required strength should be removed and replaced with soil meeting the design criteria. – A minimum 6 in. thick layer of compacted granular material shall be placed for use as a leveling pad. The granular base shall be compacted to provide a firm and level bearing pad on which to place the first course of facing blocks. Compaction should be performed using a light-compacto to obtain a minimum of 95% of the maximum standard Proctor density (per ASTM D698).
Reinforcement and Reinforcement Placement	<ul style="list-style-type: none"> – Geosynthetic reinforcement shall consist of high tenacity geogrids or geotextiles manufactured for soil reinforcement applications. – Geosynthetic reinforcement should be installed under tension. A nominal tension shall be applied to the reinforcement and maintained by staples, stakes or hand tensioning until the reinforcement has been covered by at least 6 in. of soil fill. – The geosynthetic reinforcement perpendicular to the wall face should consist of one continuous piece of material. Overlap of reinforcement in the design strength direction shall not be permitted. Adjacent sections of geosynthetic should be placed in a manner to assure that horizontal coverage shown on the plans is provided. – Tracked construction equipment shall not be operated directly on the geosynthetic reinforcement. A minimum backfill thickness of 6 in. is required prior to operation of tracked vehicles over the geosynthetic reinforcement. Turning of tracked vehicles should be kept to a minimum to prevent displacing the fill and damaging or moving the geosynthetic reinforcement. – Rubber-tired equipment may pass over the geosynthetic reinforcement at slow speeds less than 10 mph. Sudden braking and sharp turning should be avoided.
Backfill	<ul style="list-style-type: none"> – Reinforced backfill shall be free of debris and consist of one of the following inorganic USCS soil types: GP, GW, SW, SP, SM, meeting the following gradation: 75% to 100% passing 4 in. sieve, 20% to 100% passing No. 4 sieve, 0 to 60% passing No. 40 sieve, and 0 to 35% passing No. 200 sieve. The maximum size shall generally be limited to ¾ in. – The plasticity of the fine fraction of the reinforced backfill shall be less than 20. – The pH of the backfill material shall be between 3 and 9 (per ASTM G 51).
Backfill Placement	<ul style="list-style-type: none"> – Reinforced backfill shall be placed as shown in construction plans in maximum compacted lift thickness of 10 in. – Reinforced backfill shall be compacted to a minimum 95% of standard Proctor density at a moisture content within 2% of optimum. – Backfill shall be placed, spread and compacted in such a manner that eliminates the development of wrinkles or movement of the geosynthetic reinforcement and the wall facing units. – Only hand-operated compaction equipment shall be allowed within 3 ft of the front of the wall face. Compaction within 3 ft of the back face of the facing units shall be achieved by at least three passes of a lightweight mechanical tamper, plate or roller. Soil density in this area should not be less than 90% standard Proctor density. – At the end of each day’s operation, the last level of backfill should be sloped away from the wall facing to direct runoff of rainwater away from the wall face. In addition, surface runoff from adjacent areas to enter the wall construction site should be avoided.

Facing	<ul style="list-style-type: none"> – Concrete segmental units shall have a minimum 28 days compressive strength of 3,000 psi and a maximum absorption of 10 pcf per ASTM C140. For areas subject to detrimental freeze-thaw cycles, the concrete shall have adequate freeze-thaw protection. – All facing units shall be sound and free of cracks or other defects that would interfere with the proper placement of the unit or significantly impair the strength or permanence of the construction. – Facing units dimensions shall not differ more than $\pm 1/8$ in., except height which shall not differ more than $\pm 1/16$ in. – If pins are used to interconnect the facing units, they shall consist of a non-degrading polymer or galvanized steel and be made for the expressed use with the facing units. – The cap block and/or top facing units should be bonded to the units below using cap adhesive that meets the requirements of the facing unit manufacturer. – The overall tolerance relative to the wall design verticality or batter shall not exceed ± 1.25 in. maximum over a 10 ft distance; 3 in. maximum.
Drainage	<ul style="list-style-type: none"> – Drainage aggregates shall be a clean crushed stone or granular fill meeting the following gradation criteria: 100% passing 1 in. sieve, 75% to 100% passing $3/4$ in. sieve, 0 to 60% passing No. 4 sieve, 0 to 50% passing No. 40 sieve, and 0 to 5% passing No. 200 sieve. – Drainage collection pipes shall be perforated or slotted, PVC or corrugated HDPE pipe. – Drainage collection pipes shall be installed to maintain gravity flow of water outside of the reinforced soil zone. The pipe should daylight into a storm sewer manhole or along a slope that an elevation smaller than the lowest point of the pipe within the aggregate drain. – The main collection drain pipe, just behind the block facing, shall be a minimum of 3 in. in diameter. The secondary collection drain pipes should be sloped a minimum of 2% to provide gravity flow into the main collection drain pipe. Drainage laterals shall be spaced at a maximum of 50 ft spacing along the wall face. – Drainage pipes and drainage aggregates may be wrapped with a geotextile that will function as a filter.

Federal Highway Administration, FHWA (Elias et al. 2001)

Site Preparation	<ul style="list-style-type: none"> – Foundation should be prepared by removal of unsuitable materials from the area to be occupied by the retaining structure, including all organic matter, vegetation, and slide debris, if any. – Where construction of reinforced fill will require a side slope cut, a temporary earth support system may be required to maintain stability. Cautions should be exercised for excavation of utilities or removal of temporary bracing or sheeting in front of completed MSE structures. – Construction dewatering operations should be required for any excavations performed below the water table to prevent a reduction in shear strength due to hydrostatic water pressure. – A concrete leveling pad should have minimum dimensions of 150mm thick by 300mm wide and should have a minimum 13.8 MPa (3,000 psi) compressive strength. Cast-in-place pads should cure a minimum of 12 hours before facing panels are placed. A vertical tolerance of 3 mm (1/8 in.) to the design elevation is recommended for the leveling pad. Gravel pads of suitable dimensions may be used with modular block wall construction.
Reinforcement Placement	<ul style="list-style-type: none"> – Reinforcements should generally be placed perpendicular to the back of the facing panel. In specific situations, e.g., abutments and curved walls, it may be permissible to skew the reinforcements from their design location in either the horizontal or vertical direction. – Overlapping layers of reinforcements should be separated by a 75mm (3 in.) minimum thickness of fill. – Flexible reinforcements, such as geotextiles and geogrids, usually require pre-tensioning to remove any slack in the reinforcement or in the panel. The tension is then maintained by staking or by placing fill during tensioning.

<p>Backfill and Backfill Placement</p>	<ul style="list-style-type: none"> – Backfill material should be reasonably free from organic or otherwise deleterious materials and should conform to the following gradation limits: 100 % passing 102 mm sieve, 0-60% passing No. 40 sieve, and 1-15% passing No. 200 sieve. The plasticity index should not exceed 6. – Backfill material should exhibit an angle of internal friction of not less than 34 degrees, as determined by the standard direct shear test AASHTO T-236 on the portion finer than the No. 10 sieve, using a sample compacted to 95% of AASHTO T-99, Methods C or D. No testing is required for backfills where 80% of sizes are greater than 19 mm. – The backfill shall be substantially free of shale or other soft, poor durability particles, and shall have an organic content less than 1%, and a pH between 5 and 10. – Reinforced wall fill material should be placed and compacted at or within 2% dry of the optimum moisture content. If the reinforced fill is free draining with less than 5% passing a No. 200 sieve, water content of the fill may be within $\pm 3\%$ of the optimum. – A density of 95% of AASHTO T-99 maximum value is recommended for retaining walls and slopes, and 100% of AASHTO T-99 is recommended for abutments and walls or slopes supporting structural foundations abutments. A procedural specification is preferable where a significant percentage of coarse material, generally $\geq 30\%$ retained on the 19 mm (3/4 in.) sieve, prevents the use of the AASHTO T-99 or T-180 test methods. For procedural specification, typically three to five passes with conventional vibratory roller compaction equipment is adequate. The actual requirements should be determined based on field trials. – Reinforced backfill should be dumped onto or parallel to the rear and middle of the reinforcements and bladed toward the front face. At no time should any construction equipment be in direct contact with the reinforcements. – Soil layers should be compacted up to or even slightly above the elevation of each level of reinforcement connections prior to placing that layer of reinforcing elements. – With the exception of the 1-m zone directly behind the facing elements or slope face, large, smooth-drum, vibratory rollers should generally be used to obtain the desired compaction. Sheepfoot rollers should not be permitted. When compacting uniform medium to fine sands (in excess of 60% passing a No. 40 sieve) use a smooth-drum static roller or lightweight (walk behind) vibratory roller. The use of large vibratory compaction equipment with this type of backfill material will make wall alignment control difficult. – Within 1 m (3 ft) of the wall or slope face, use small single or double drum, walk-behind vibratory rollers or vibratory plate compactors. – Placement of the reinforced fill near the front should not lag behind the remainder of the structure by more than one lift. – Within 1 m (3 ft) of the wall, quality control should be maintained by a methods specification such as three passes of a light drum compactor. High quality fill is sometimes used in this zone so that the desired properties can be achieved with less compactive effort. – Flooding of the backfill to facilitate compaction is not permitted. – Compaction control testing of the reinforced backfill should be performed on a regular basis during the entire construction project. A minimum frequency of one test within the reinforced soil zone per 1.5 m (5 ft) of wall height for every 30 m (100 ft) of wall is recommended.
<p>Facing</p>	<ul style="list-style-type: none"> – The compressive strength for facing units should be 28 MPa (4,000 psi) and the water absorption should be $\leq 5\%$ after 24 hours. – The compressive strengths and water absorption of dry-cast modular blocks should be carefully checked on a lot basis. – Dimensional tolerances of the blocks are typically ± 3.2 mm (1/8 in.) for overall dimensions and ± 1.6 mm (1/16 in.) for block height.
<p>Drainage</p>	<ul style="list-style-type: none"> – MSE structures should be designed to permit drainage of any seepage or trapped groundwater in the retained soil. If water levels intersect the structure, it is also likely that a drainage structure behind and beneath the wall will be required. Surface water infiltration into the retained fill and reinforced fill should be minimized by providing an impermeable cap and adequate slopes to nearby surface drain pipes or paved ditches with outlets to storm sewers or to natural drains.

	<ul style="list-style-type: none"> – Internal drainage of the reinforced fill can be attained by use of a free-draining granular material that is free of fines (less than 5% passing No. 200 sieve). Arrangement should be provided for drainage to the base of the fill to prevent water exiting the wall face and causing erosion and/or face stains. The drains should have suitable outlets for discharge of seepage away from the reinforced soil structure. Care should be taken to avoid creating planes of weakness within the structure with drainage layers.
--	--

Colorado Transportation Institute, CTI (Wu 1994)

Site Preparation	<ul style="list-style-type: none"> – Before placement of the reinforcement, the ground should be graded to provide a smooth, fairly level surface. – The surface should be clear of vegetation, large rocks, stumps, and the like. Depressions may need to be filled; soft spots may need to be excavated and replaced with backfill material; and the site may need to be proof rolled. – It is usually not necessary to sub-excavate the ground for embedment and frost heave protection, as is commonly done in the construction of conventional reinforced concrete walls. – If site preparation involves excavation, the construction site should be excavated to the limits shown in the construction plans. The excavation width at any depth should be at least equal to the length of the reinforcement layer designed for that elevation. – A nominal thickness (about 4 in. to 6 in.) of granular soil should be placed at the base of the wall for drainage and leveling purposes.
Reinforcement and Reinforcement Placement	<ul style="list-style-type: none"> – Geosynthetics, especially geotextiles, should not be exposed to sunlight and extreme temperatures for an extended period of time. Damaged or improperly handled geosynthetic reinforcement should be rejected. – After the reinforcement is in place, it should be examined carefully. Damaged or torn materials should be replaced or repaired as prescribed in the specifications. – In no case should construction equipment be allowed to operate directly on any geosynthetic reinforcement before fill is placed. When using geotextile reinforcement, a minimum backfill cover of 6 in. should always be maintained between the geotextile and moderate size construction equipment (e.g., Caterpillar D6 or 955). – Geosynthetic reinforcement should be unrolled in the direction perpendicular to the wall face whenever feasible. In which case, overlapping of adjacent geosynthetic sheets should be at least 12 in., and sewing or other connections are usually not necessary. If the reinforcement is not unrolled perpendicular to the wall face, joining adjacent geosynthetic sheets should be performed strictly according to the plan and specifications. Generally, overlapping the layers should be of a minimum of 3 ft; sewing of layers should be made on a minimum of 4 in. overlaps. – Wrinkles and folds in the geosynthetic reinforcement prior to placement of fill should be kept to a minimum. Slight pre-tension of geosynthetic reinforcement (e.g., by stretching) is beneficial.
Backfill Placement	<ul style="list-style-type: none"> – Backfill should be progressively dumped and spread toward the back of the wall to ensure that little or no slack is left in the reinforcement. – Special attention should be given to ensuring good compaction of the backfill, especially near the face of the wall. Otherwise detrimental settlements behind the face may cause a downward drag on the reinforcement, which might induce excessive tensile stress at locations where the reinforcement is attached to the facing. – Care should be taken not to allow heavy construction equipment to operate too close (within 1 ft to 2 ft) to the wall face. Otherwise undesirable bulging of face may result. – Each lift should not exceed 12 in. in loose thickness and should be compacted to achieve a minimum of 95% of the maximum dry density according to ASTM D698 or AASHTO T-99. It is recommended that the placement moisture content for a granular fill be $\pm 2\%$ of the optimum, and within 4% wet of optimum (i.e., between the optimum and 4% wet-of-optimum) for a cohesive fill.

	<ul style="list-style-type: none"> – Care should be exercised when placing backfill over geosynthetic reinforcement. The backfill should be emplaced from the wall face to the back of the wall to ensure that no slack is left in the reinforcement. – At the end of each day's backfilling operation, the last lift of fill should be sloped away from the wall facing to direct any possible runoff away from the wall face.
Facing	<ul style="list-style-type: none"> – For modular block faced walls, the alignment of the first few courses of blocks is critical to the alignment of the wall face. – The concrete leveling pad under the first course of modular blocks can be replaced with a leveling pad of compacted gravel (or compacted in-situ soil). However, the use of a concrete leveling pad is recommended when the foundation soil is relatively incompressible and not susceptible to significant shrinkage and swell due to moisture changes. A properly poured and leveled concrete pad will speed up construction, ease the leveling process, and facilitate the construction of a straighter wall. – Walls with curves along their length require that the leveling pad be poured to the proper radius. In general, a curve radius of 10 ft or greater is not a problem; however, tight curves of 3 ft to 6 ft radius require special consideration (Moreno, et al., 1993). In some cases, field modification of the blocks may be necessary for tight curves. – The blocks should be laid from one end of the wall to the other to preclude laborious block cutting and fitting in the middle. When curves are involved in a wall, the blocks on the curves should be laid first, as their alignment is more critical and less forgiving. Tight curves often require cutting blocks to fit or breaking off the block tail. A diamond-tipped blade saw is recommended for the cutting. – When shear pins are used, they should be tapped into well-seated position immediately after setting each block to avoid getting fill into the block's pin holes. – Leveling of the first course of blocks is especially important for wall alignment. A string line set over the pins from one end of the wall to the other will help leveling the blocks. – Geosynthetic reinforcement should be placed up to front face of the blocks to ensure maximum interface contact with the blocks. – After front of the geosynthetic reinforcement is properly secured (i.e., after the hollow cores of the next course is filled and compacted), the reinforcement should be pulled tight and pre-tensioned while the backfill is being placed. – To avoid movement of blocks during construction, a hand-operated tamper should be used to compact the soil within 3 ft of the wall face, and no construction vehicles are allowed within the 1 m (3 ft) region.
Control of Water during Construction	<ul style="list-style-type: none"> – Surface runoff should be directed away from the site during construction. Also, surface runoff from adjacent areas should be prevented from encroaching on the site. – The simplest way to control surface water is to excavate a trench or construct a dike or curb around the perimeter of the site, and disposal of the water by gravity or by pumping from sumps. – For walls constructed below the ground water table, dewatering may be required to provide a working platform. Although there are many methods available for this purpose (e.g., well points, horizontal drains, etc.), the simplest technique is to construct perimeter trenches and connect them to sumps. This method is most effective when the excavation is in cohesive material and the ground water is not too high. The trench should be installed as far from the location of the wall base as practical to prevent disturbance due to ground water seepage. In certain cases, impermeable barrier to reduce or eliminate the inflow of ground water into the work site may be more effective than dewatering. Usually the selection of the method is left to the contractor.
Control of Water throughout Service Life	<ul style="list-style-type: none"> – To reduce percolation of surface water into the backfill during the service life of a wall, the crest should be graded to direct runoff away from the back slope. Sometimes interceptor drains on the back slope can be used. Periodic maintenance is also necessary to minimize runoff infiltration.

	<ul style="list-style-type: none"> – Geosynthetic reinforcement provides inherent drain capability at their face. Therefore, subsurface drainage at wall face is generally not necessary. However, when a cohesive backfill is used, measures should be taken to minimize wetting of the cohesive soil. This can be achieved by providing a combination of granular drain materials and geotextiles, or a geocomposite drain along the top, the back, and the base of the cohesive backfill.
--	---

Swiss Association of Geotextile Professionals, SAGP (1981)

Site Selection	<ul style="list-style-type: none"> – A uniform subsoil constitutes an important factor for the durability of the GRS retaining wall.
Reinforcement Placement	<ul style="list-style-type: none"> – The geotextile reinforcement must be placed exclusively in the direction of the primary load. Joints in the direction of the load are unacceptable. – The wrapped return must be extended at least 0.3 m in the horizontal direction and anchored in at least 10 cm of fill material, which is usually half the thickness of a layer. Folding back the geotextile and placing the next sheet of geotextile directly on top of it is unacceptable, since this will create a greater risk of sliding. – The overlapping of geotextile in the longitudinal direction of the wall must be at least 0.3 m, or even 0.5 m if there are large surface irregularities. – The top layer of geotextile reinforcement must not be placed directly below the ballast of a railway. It must be covered with a layer of sand or gravel at least 10 cm thick. – The top two uppermost sheets of geotextile should be made of a continuous strip to avoid any problem due to an inadequate anchoring of the top fold.
Backfill Placement	<ul style="list-style-type: none"> – Fill material and those next to the covering of the face must be laid and compacted according to professional standards in layers not exceeding 0.40 m. This means that layers 0.5 m to 0.6 m thick must be laid in two stages. – Compacted lifts, not exceeding a thickness of 0.4 m, are built up between layers of reinforcement. – The required compaction of the fill material is 97% Proctor, or $M_E = 6 \text{ MN/m} = 600 \text{ kg/cm}$, thus, a 5-ton vibrating roller is necessary.
Drainage	<ul style="list-style-type: none"> – Care must be taken to collect and evacuate water on the upside (road, railway, storage space, etc.). When this is not feasible, a drainage system must be installed behind the geosynthetic-reinforced soil wall. – Drainage is also necessary when there is slope water. – When there is a possibility of large quantities of water, or even of liquid chemicals flowing through the top of the soil wall, a waterproof liner must be provided above the top geotextile bed, with a 2% to 3% downslope towards the upside, in order to collect and evacuate the liquid. A drain pipe must also be provided in a channel leading towards a hydrocarbon separator.

Japan Railways, JR (1998)

Site Preparation	<ul style="list-style-type: none"> – On-site surveying for confirmation of site conditions should be made. – Any buried structures and existing structures should be identified and removed if necessary. If the existing structure is located along the slope of excavation, its stability should be evaluated. – Plants and remains of trees, etc. if located at the foundation should be removed prior to construction. The ground should be cleared by digging about 0.3 m into the subsoil. – The ground surface of the foundations should be leveled for ease of geotextile installation. For foundation soils of low strength and high compressibility, such as peat, the soils should be replaced by the backfill soil up to a required depth so that subsequent unnecessary settlement and lateral flow will not occur. If the subsoil foundation is composed of undulating rocks or gravels, the backfill soil should be used to level off the foundation. The undulating ground surface may damage the geosynthetic reinforcement and lead to unwanted sagging during installation.
------------------	--

	<ul style="list-style-type: none"> – If the water table is close to the ground surface or if outflow is detected, drainage channels or blankets should be installed. – Any rocks extruding through the ground surface should be removed since they may damage geosynthetic reinforcement. – For rock foundation, concrete should be used to level the ground surface.
Reinforcement Placement	<ul style="list-style-type: none"> – Geosynthetic reinforcement must be placed flat without slack. – The strong axis of geosynthetic reinforcement should be aligned perpendicular to the wall face. – Overlapping of geosynthetic reinforcement in the direction parallel to the wall face should be avoided whenever possible. Otherwise, a 50 cm overlapping is required. The overlapped portion should be tied using wires or strings. – Overlapping of geosynthetic reinforcement in the direction perpendicular to the wall face is permitted. A 0.1 m overlapping is recommended. – Geosynthetic reinforcement should be secured using sand bags or pins until backfill is placed so that they will not be blown away or torn by strong wind. – During installation, the folding-back portion of geosynthetic layer should be laid to the outside of the wall. After placing the gabions (formwork for facing), this portion should be folded back/wrapped to give a fold-back length of 0.3 m. The overlapped portion should be tied using wires or string. – Geosynthetic layers should be cut into appropriate length at the construction site. A proper cutting tool should be used. – A layer of backfill over the foundation surface may be necessary to protect the geosynthetic from being damaged and to provide a flat surface.
Backfill Placement	<ul style="list-style-type: none"> – The machinery and construction procedure should be properly arranged so that geosynthetic reinforcement will not sag during soil spreading. The main reasons leading to sagging of geosynthetic reinforcement during soil spreading are the high water content and the use of improper machinery, among other factors. – Backfill soil should render stability to the wall by allowing good compaction, giving little residual settlement, and exhibiting essentially elastic response. – For construction using heavy machinery, the backfill soil must be spread parallel to the wall face. The soil spreading should start from the wall face and proceed inward to avoid sagging of geosynthetic reinforcement and bulging of the wall face. It is recommended that soil spreading within a distance of 1 m from the wall face should be performed manually. – Sudden stopping or turning of heavy machinery should be avoided. – A “trial construction” involving less than 30,000 m³ of soil should normally be conducted to evaluate compaction characteristics of the backfill. The specified degree of compaction should be obtained in the field and should be uniform throughout each wall construction. – Compaction within 1 m from the wall face should normally be conducted using a light compaction plant. – Compaction should be completed within each day. If the work is terminated after soil spreading, precipitation overnight may soften the soil and thus affect compaction in the following day. If precipitation is anticipated, the top surface of the compacted soil should be covered with water proof sheets. Drain channels should be provided so that precipitation will not percolate into the backfill. – The construction should not proceed during rainy days. During precipitation the soil will be under-compacted. The presence of high water content will be a source of future settlement.
Facing	<ul style="list-style-type: none"> – Gabions should be used to ensure stability of the wall face during construction. The gabions function as a drainage layer after completion of construction and also as a buffer at the interface between the highly rigid concrete facing and the deformable backfill. – Gabions should not be simply placed on the wall face. A vibratory compactor should be used so that voids in the gabions will be minimized. – Alignment of the gabions should be checked, but strict enforcement is not required since a cast-in-place concrete facing will be installed over it. Priority should be given to good compaction of the gabions.

APPENDIX B

A Brief Description of DYNA3D and LS-DYNA [Note: This appendix has not been edited by TRB.]

The computer codes DYNA3D (Hallquist and Whirley 1989) and LS-DYNA, a PC-version of DYNA3D, are employed for the analysis of GRS bridge abutments. The reasons for choosing DYNA3D/LS-DYNA are twofold. Firstly, the code has soil models (two- and three-invariant models) with large deformation formulation that are capable of analyzing the behavior of compacted fill in a bridge abutment and the approach fill, under both service-state and ultimate-state loading conditions (hence capable of predicting failure conditions). Secondly, the reliability of the code has been well documented and the code has been accepted by the California Department of Transportation as well as other DOTs.

Description of DYNA3D

DYNA3D is a finite element code for analyzing the dynamic response of three-dimensional solids and structures. DYNA3D is based on a finite element discretization of the three spatial dimensions and a finite difference discretization of time. The explicit central difference method is used to integrate the equations of motion in time. The element formulations available include one-dimensional truss and beam elements, two-dimensional quadrilateral and triangular shell elements, and three-dimensional continuum elements. Many material models are available to represent a wide range of material behavior, including elasticity, plasticity, thermal effects, and rate dependence. In addition, DYNA3D has a sophisticated contact interface capability, including frictional sliding and single surface contact, to handle a range of mechanical interactions between independent bodies. This capability is essential for the analyses of segmental walls. DYNA3D has been used extensively at Lawrence Livermore National Laboratory and in industry. It has been applied to a wide spectrum of problems, many involving large inelastic deformations and contact.

The following models, suitable for simulation of soil and concrete, are available in DYNA3D:

- An elastic-plastic model with the Mohr-Coulomb yield surface and a Tresca limit: a simple model suitable for soil.
- An extended two invariant geologic cap model suited for soils: In this model, volumetric response is elastic until the stress point hits the cap surface. Thereafter, plastic volumetric strain (compaction) is generated at a rate controlled by the hardening law. Thus, in addition to controlling the amount of dilatancy, the introduction of the cap surface adds more experimentally observed

response characteristic of geological materials into the model.

- A three-invariant viscoplastic cap model: The model is similar to the extended two invariant geologic cap model, briefly described above, but is more suited for soils exhibiting time-dependent behavior.
- Elastic-plastic with damage and failure: a simple model for plain concrete.
- Isotropic elastic-plastic with oriented cracks model: suited for porous brittle materials such as the concrete used for segmental facings where pressure-hardening effects are not significant.

The Elasto-Plastic Soil Model

The cap plasticity model has been widely used in finite element analysis programs for a variety of geotechnical engineering applications (Nelson and Baladi 1977, Baladi and Rohani 1979, Chen and McCarron 1983, Minuzo and Chen 1984, Daddazio et al. 1987, McCarron and Chen 1987). The cap model is very appropriate to soil behavior because it is capable of considering the effect of stress history, stress path, dilatancy, and the effect of the intermediate principal stress (Huang and Chen 1990).

The failure function used in the cap model (see Figure B-1) is of the Drucker-Prager type (Drucker and Prager 1952)

$$f_1 = \theta J_1 - \sqrt{J_{2D}} + \alpha \quad \text{Equation B-1}$$

where J_1 is the first invariant of the effective stress tensor; J_{2D} is the second invariant of the deviatoric stress tensor; and θ and α are material constants related to the friction and cohesion of the soil through

$$\theta = \frac{2 \sin \phi}{\sqrt{3}(3 - \sin \phi)} \quad \text{Equation B-2}$$

$$\alpha = \frac{6 c \cos \phi}{\sqrt{3}(3 - \sin \phi)} \quad \text{Equation B-3}$$

where ϕ is the internal friction angle of the soil and c is the cohesion intercept of the soil. Both ϕ and c are determined from conventional triaxial compression test results.

The strain-hardening elliptic cap function (see Figure B-1) is of the form

$$f_2 = (J_1 - L)^2 + R^2 J_{2D} - (X - L)^2 = 0 \quad \text{Equation B-4}$$

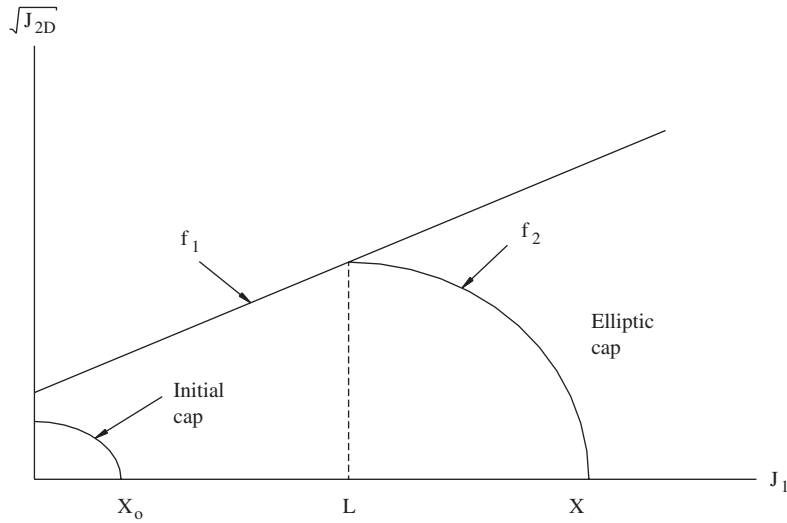


Figure B-1. The cap model.

where R is the ratio of the major to minor axis of the elliptic cap, X and L define the J_1 value at the intersections of the ellipse cap with the J_1 axis and the failure function, respectively.

The cap model uses the hardening function proposed by Dimaggio and Sandler (1971)

$$X = -\frac{1}{D} \ln\left(1 - \frac{\epsilon_v^p}{W}\right) + X_0 \tag{Equation B-5}$$

where D , W and X_0 are material constants, and ϵ_v^p is the plastic volumetric strain.

The results of one hydrostatic compression test can be used to evaluate the parameters D and W . A plastic volumetric strain versus pressure curve can be obtained from the total volumetric strain curve by subtracting the elastic strains

from the latter. The parameter W represents the asymptote value of the plastic volumetric strain curve. The parameter D can be obtained by trial-and-error until a best fit of the plastic volumetric strain versus pressure curve is achieved.

The parameter X_0 is the first invariant of the effective stress tensor corresponding to the initial yield cap (see Figure B-1). This parameter can be used to account for backfill pre-stress caused by compaction. The calculated vertical stress, σ_v , due to the compaction machine can be used to estimate the at-rest lateral stress of the soil. The parameter X_0 is then calculated by adding the three principal stresses, i.e., the vertical stress and the two at-rest lateral stresses [$X_0 = \sigma_v(1 + 2K_0)$, where σ_v is the vertical stress and K_0 is the coefficient of lateral earth pressure at rest].

Abbreviations used without definitions in TRB publications:

AASHO	American Association of State Highway Officials
AASHTO	American Association of State Highway and Transportation Officials
ADA	Americans with Disabilities Act
APTA	American Public Transportation Association
ASCE	American Society of Civil Engineers
ASME	American Society of Mechanical Engineers
ASTM	American Society for Testing and Materials
ATA	American Trucking Associations
CTAA	Community Transportation Association of America
CTBSSP	Commercial Truck and Bus Safety Synthesis Program
DHS	Department of Homeland Security
DOE	Department of Energy
EPA	Environmental Protection Agency
FAA	Federal Aviation Administration
FHWA	Federal Highway Administration
FMCSA	Federal Motor Carrier Safety Administration
FRA	Federal Railroad Administration
FTA	Federal Transit Administration
IEEE	Institute of Electrical and Electronics Engineers
ISTEA	Intermodal Surface Transportation Efficiency Act of 1991
ITE	Institute of Transportation Engineers
NASA	National Aeronautics and Space Administration
NCHRP	National Cooperative Highway Research Program
NCTRP	National Cooperative Transit Research and Development Program
NHTSA	National Highway Traffic Safety Administration
NTSB	National Transportation Safety Board
SAE	Society of Automotive Engineers
SAFETEA-LU	Safe, Accountable, Flexible, Efficient Transportation Equity Act: A Legacy for Users (2005)
TCRP	Transit Cooperative Research Program
TEA-21	Transportation Equity Act for the 21st Century (1998)
TRB	Transportation Research Board
TSA	Transportation Security Administration
U.S.DOT	United States Department of Transportation